THREE DIMENSIONAL LINEAR-ELASTIC FRACTURE MECHANICS ANALYSIS OF THICK-WALLED PRESSURE VESSEL COMPONENTS

by

Manuel Frederico Oom de SEABRA PEREIRA, Dipl.Eng. (I.S.T.)

A thesis submitted for the degree of Doctor of Philosophy of the University of London and for the Diploma of Imperial College.

Mechanical Engineering Department
Imperial College of Science and Technology
University of London

February 1977

ABSTRACT

The present work deals with the evaluation of Fracture Mechanics parameters in some pressure vessel components, viz. corner cracks in the inside transition of a junction of thick-walled cylinders.

This study is confined to elastic, isotropic and homogeneous materials. No temperature effects have been considered.

Such crack configurations, because of their particular geometry and loading conditions, are fully three dimensional in nature and consequently have been dealt with as such. Moreover these configurations are geometrically too complicated to be treated analytically and for this reason finite element methods have been applied.

A three dimensional finite element computer program using brick type elements has been brought into use and mesh generation, plotting routines and computational procedures, including substructuring schemes are described in detail.

Special "crack tip elements" have been introduced to model the singularity in stress and strain fields near the crack tips.

The effectiveness of such elements is demonstrated by performing analyses of Compact Tension Specimens, Corner and Part-through crack configurations and Semi-circular cracks emanating from the inner surface of thick-walled cylinders subjected to internal pressure.

Finally, stress intensity factors have been obtained for some hypothetical cracks of different sizes situated in

the plane of highest nominal stresses near the intersection regions of a T-junction of thick walled cylinders.

Consideration is given to the application of these results to a fracture safety analysis of this particular component.

Throughout the present work the variation of stress intensity factor along the crack fronts of the various configurations is discussed along with the general stress behaviour of the cracked and uncracked geometries.

ERRATA

Page	Line or Expr.	Should read
3	13	.. hazards is particularly relevant was ...
6	6	in the y direction
8	6	plane stress
31	17	$Ni = (1 + \xi_o)(1 + \eta_o)(1 + \zeta_o)(\xi_o + \eta_o + \xi_o - 2)/8$
37	1	... Poisson's ratio
43	3	... semi-bandwidth
45	23	and their derivatives
50	2	BACWD is described
53	25	these types of
61	22	$\sum_{n=\ell}^{m}$
63	exp. (3.10), (3.11)	$\left.\frac{\partial P}{\partial a}\right\|_f$
66	8	... thus equation (2.7)
74	exp. (3.43)	.. + ½ $(1 - \eta)(Y_2 + Y_6)$
76	exp. (3.46a)	$p_1 = 3/4 + 1/4\eta$
76	exp. (3.46b)	$p_2 = 3/4 + 1/4\xi$
76	exp. (3.47a)	$x = 1/4(3 + \eta + 4\xi + \xi^2 - \eta\xi^2)$
76	exp. (3.47b)	$x = 1/4(3 + \xi + 4\eta + \eta^2 - \xi\eta^2)$
77	22	to the mesh
	6	in the y direction
	6	plane stress
	1	.. Poisson's ratio ..
	3	.. semi-band width ...
	23	and their derivations
	2	BACWD is described

Page	Line or Expr.	Should read
77	25	.. these types of ..
78	9	.. a microfilm plotter
79	17	length a
80	10	the remaining nodes in the free surface
81	9	Levy et al
89	15	of structure
92	18	
141	foot note	$\Sigma \Delta u_i / \Sigma u_i$
145	4	so has the number
146	7	this section describes
148	1	[KEL]
148	10	conditions according
148	18	largest nodal number
157	28	MATN,E(MATN)
144	12	node k as it is indicated in Figure A1.1
159	8	.. be replaced by ..
175	11	.. The four angles ..
175	26	.. to all ..
180	8	.. Poisson's Ratio ..
250	2	P_s across

ACKNOWLEDGEMENTS

I would like to express my sincere gratitude to Dr. J.L. Head for all his help, invaluable guidance and encouragement throughout the course of this project.

I would like also to record my special thanks to my former research supervisor Professor C.E. Turner whose advice and help I have found extremely valuable.

Many thanks are also due to the Instituto de Alta Cultura, Ministry of Education and Scientific Research, Lisbon, Portugal for their financial support during the course of this work. My leave of absence from the Lisbon Institute of Technology is also gratefully acknowledged. I would particularly like to acknowledge Professor Luciano de Faria of the Mechanical Engineering Department for his constant encouragement during the course of this work.

I would like to extend my gratitude to Mr. D.J.F. Slater who helped me in coming to terms with the DIM3B code and Mr. J.D. Silva who fully participated in the development of the program FRONT.

Thanks are due to Madeleine Field for typing the manuscript.

Finally, I wish to acknowledge the debt I owe to my parents who, in every way, made this possible.

To my wife João

To my son Tiago

TABLE OF CONTENTS

NOMENCLATURE

a	Crack length; axis of an ellipse
A	Crack area
A_i	Coefficients of the Williams stress function
b	Axis of an ellipse
B	Thickness
B_i	Coefficients of the Williams stress function, $B_i = B_i(\theta,\nu)$
$[B]$	Matrix of shape function derivatives
C	Compliance of a test specimen (Reciprocal of stiffness)
C_i, C_j, C_m	Weight Coefficients in the Gaussian quadrature formaulae
$[D]$	Elasticity matrix
E	Young's Modulus
$E' = E$	for plane stress conditions
$= E/(1-\nu^2)$	for plane strain conditions
$E(k)$	complete elliptical integral of the second kind
	$k = \sqrt{1-(b/a)^2}$
$f_{ij}(\theta,\nu)$	Functions of θ and ν in the Westergaard expressions
F	Externally applied generalized nodal forces
F_g	Nodal equivalent point forces in a 3D element
$g(x,y,z)$	Function representing the applied loads in the FEM
G_I	Mode I strain energy release rate
G_c	Critical strain energy release rate (at onset of fracture)
$[J]$	Jacobian of tranformation of coordinates
k	Stiffness matrix

k_{ij}	Stiffness coefficients
K	Stiffness matrix; stress intensity factor (assumed to be mode I)
K_I, K_{II}, K_{III}	Mode I, Mode II, Mode III Stress intensity factors
K_o	Stress intensity factors of cracks in infinite medium $K_o = \sigma \sqrt{\pi a}$ for a crack of length 2a in an infinite plate $K_o = 2\sigma \frac{a}{\pi}$ for a penny shaped crack of radii a in an infinite solid
K*	Stress intensity factors obtained from the displacement or stress method
[M]	Matrix describing the terms of a polimonial
M_f	Magnifaction factor
M_{UN}, M_{KN}, M_U	Submatrices of the general body stiffness matrix K
[N]	Shape function matrix
N_i	Nodal shape functions
p	Parameter defining the intermediate nodal position in the second order elements
p_i	Parameter defining the intermediate nodal positions in the third or higher order elements
P	Load, internal pressure
P_i	Nodal point forces
P_s	Parameter defining the condition of place stress or plane strain
q=u/v	Parameter describing a slope boundary condition
Q	Working variable in Gaussian elimination
r	Radial coordinate in a system of polar coordinates r,θ or in a system of cylindrical coordinates r,θ,z
r_y	Distance from the crack tip where the stress is equal to the yield strength
R	Radius of curved crack fronts in CTS specimens.

R_1	Internal radius of a cylinder
R_2	External radius of a cylinder
R_s	External forces
R_{bs}	Forces statically equivalent to body forces
$R_{\varepsilon s}$	Forces to suppress initial strains
S_{ij}	Stiffness coefficients
T	Thickness
u	Displacement component in the x direction or r direction
u_i	Nodal displacement component
U	Strain energy
v	Displacement component in the y direction
v_i	Nodal displacement component
w	Displacement component in the z direction
w_i	Nodal displacement component
x	Coordinate in x,y,z system
$\hat{x}$	Cartesian unit vector in the x direction
x_i	Nodal coordinate in the x direction
x'	Coordinate in a transformed x',y',z' system
y	Coordinate in a x,y,z system
$\hat{y}$	Cartesian unit vector in the y direction
y_i	Nodal coordinate in the y direction
y'	Coordinate in a transformed x',y',z' system
Y	Magnification factor or "calibration factor"
z	Coordinate in x,y,z or r,θ,z system
$\hat{z}$	Cartesian unit vector in the z direction
z_i	Nodal Coordinate in the z direction
z'	Coordinate in a transformed x',y',z' system

α	Angle measured from the major axis in the plane of an ellipse
$\{\alpha\}$	Vector of generalized nodal coordinates in a finite element
β	Angle defining radial planes in the T-junction
γ	Specific surface energy (Griffith's theory)
γ_p	Plastic work (Energy balance approach)
$\delta=\delta(x,y,z)$ $\delta=\delta(\xi,\eta,\zeta)$	Displacement field within a finite element
δ_i	Nodal displacement components
δ_{KN}, δ_{UN}	Suvectors of the general displacement solution vector in the FEM
Δ	Displacement solution vector or finite difference
$\{\varepsilon\}$	Strain vector in a finite element formulation
ε_i	i=1,3 corresponds to $\varepsilon_x, \varepsilon_y, \varepsilon_z$
ε_{ij}	i,j=1,3 corresponds to $\varepsilon_{xy}, \varepsilon_{yz}, \varepsilon_{zx}$
ζ	Coordinate in a system ξ,η,ζ of local curvilinear coordinates
η	Coordinate in a system ξ,η,ζ of local curvilinear coordinates
θ	Coordinate in a r,θ or r,θ,z system of coordinates
θ_x, θ_z	Rotation of the x and z axis in program DRAW
$\kappa=3-4\nu$ $=(3-\nu)/(1+\nu)$	for plane strain for plane stress
μ	Shear Modulus
ν	Poisson's Ratio
ξ	Coordinate in a system ξ,η,ζ of local curvilinear coordinates
ρ	Radius of curvature at one end of an ellipse
σ	Stress level or remote stress applied in a cracked body

$\{\sigma\}$	Stress vector in the finite element formulation
σ_{cr}	Critical stress at the onset of fracture
σ_m	Membrane stress
σ_y, σ_{yy}	Stress in the y direction
σ_{ys}	Yield strength of the material
$\phi=\phi(x,y,z)$	Field variable within a finite element
ϕ_i	Nodal values of the field variable.

ABREVIATIONS

AGARD	Advisory Group for Aerospace Research and Development (NATO)
ASME	American Society of Mechanical Engineers
ASKA	Automatic System for Kinematic Analysis (ISD-Institut fuer static und Dynamik der Luft - und Raumfahrtkonstruktionen der Universitaet Stuttgart)
ASTM	American Society for Testing and Materials
BERSAFE	Berkeley Stress Analysis by Finite Elements (CEGB BNL, Berkeley, Gloucestershire)
CDC	Control Data Corporation (computers available at ICCC and ULCC)
CEGB	Central Electricity Generating Board
CM	Central Memory (computers)
CPU	Central Processor Unit (computers)
CTS	Compact tension specimen
CYL1,CYL2	Cracked cylinders test cases (Section 3.4.6)
DIMDIM	Computer program for "dynamic operation" with DIM3B
DIM3B	Three dimensional finite element computer program Version B.
DRAW	Computer program for graphic mesh visualization
FEM	Finite Element Method
FMS	Frontal Method of Solution
FRONT	Two dimensional axi-symmetric finite element program using the FMS

ICCC	Imperial College Computer Centre
LEFM	Linear Elastic Fracture Mechanics
PP	Peripheral Processor (computers)
SCF	Stress concentration factor
TJUN1	Finite element mesh idealization of a "T-piece" with 32 node hexahedron elements
TJUN2	Finite element mesh idealization of a "T-piece" with 20 node hexahedron elements (equivalent to two diametrically opposed "T-pieces")
TJUN3	Finite element mesh idealization of a "T-piece" with 20 node hexahedron elements
ULCC	University of London Computer Centre
2D	Two-dimensional
3D	Three-dimensional

C H A P T E R 1

INTRODUCTION TO THE PROBLEM

1.1 Definition

Thick walled pressure vessels occur in many engineering installations and modern technology requires these components to work under increasingly severe conditions. The utilization of new materials, the introduction of new fabrication techniques, the requirements either to work under extremely high or low temperatures such as in the cases that occur in boilers and reactors, or to work under adverse environmental conditions, impose new demands on methods of design and analysis.

It is well known that a problem of stress concentration arises in the regions of intersections or changes in geometry, therefore knowledge of the stress distribution in these areas is important to ensure proper and safer designs.

Furthermore, the existence of crack starting tendencies, cracks or crack like flaws in the structure can eventually lead to failures at loads well below the ones specified by the conventional strength of structures.

On the other hand, the science of Fracture Mechanics can be used, providing the designer with an approach to safe design, even if components have crack-like defects.

Figure 1.1 a) shows a typical construction of a pressure vessel used in Nuclear Reactor Technology. As can be seen,

these vessels normally have cylindrical and/or spherical shapes with several discontinuities like nozzles, and the supports of the vessel. During the last five years some attempts have been made (1)(*), (2), (3), (4), (5) to access the severity of cracks in those nozzles.

Figure 1.1 b) shows a typical component of the piping system associated with those vessels, they differ substantially in geometry (diameter ratio and size) from the vessel nozzles but no reports on Fracture studies of these configurations could be found in recent literature. Such a study was carried out by the author on a main steam vent pipe "T" junction of a C.E.G.B. power station.

Such components seem to be too compact to be treated analytically and for this reason recourse is to be made to the Finite Element Method already adopted by other workers in this field of studies.

Chapters 2 and 3 describe the Finite Element Method, its computer implementation and relative merits for the evaluation of Fracture Mechanics parameters. Finally, Chapter 4 presents results for some crack configurations in the considered "T" piece.

In the next three sections, design criteria for pressure vessels are outlined followed by a brief review of Linear Elastic Fracture Mechanics (LEFM) with some reference to three dimensional crack problems.

(*) - Numerals in round brackets indicate references described in Appendix 5 of this thesis.

1.2 Design Criteria, The Role of Fracture Mechanics

The design of pressure vessel components has in the past received considerable attention and a comprehensive report on its developments can be found elsewhere in the literature, (6), (7).

In the late fifties, as a result of the accumulated experience the basic philosophy of design was mainly governed by two general rules, first, keeping overall stress levels at low values and second, requiring ductile materials to safely tolerate local peak stresses and discontinuity stresses.

The development of Nuclear Power Technology, where concern for safety and possible serious hazards was a clear stimulus for further research in this area.

The simultaneous development of electronic digital computers made possible more thorough structural analysis and improvement on the existing evaluation methods.

A better knowledge of material behaviour beyond the elastic limit lead to a more accurate elastic plastic analysis of pressure vessels with the use of numerical methods and of the equivalent plastic stress-strain curve of the material.

Pressure vessels are often subjected to cyclic loading systems either due to flow induced vibrations or cyclic stresses generated by major pressure changes and thermal gradients due to start up and shut down conditions. Although for the best part of this century fatigue has been recognised as a potential threat to safety and reliability

of engineering structures, it was only in the fifties that this type of failure was explicitly recognized in pressure vessels and specific procedures and criteria were developed for evaluating fatigue damage.

We have seen so far, a first group of engineering situations where the successful application of the outlined design criteria did not take into account the service life expected. Moreover, many structures in the past, have experienced brittle fracture by application of a small number of loading cycles or even failures at proof test stages which were directly attributable to pre-existing defects. Reports on spectacular brittle failures of pressure vessels are well known in the literature of which some examples are given in Refs. (8), (9) and (10).

The necessity to assume the existence of cracks in structures becomes evident. However, at the time it was felt to be impossible to evaluate fast failure in terms of stresses. This fact justified the use of the temperature transition approach described by Pellini et al(11), based on information obtained from notched impact tests. This method of selection of materials provided and still provides helpful information to the non fracture specialist, but it cannot be applied directly to assess the resistance of a piece in service.

The relationships between crack instability, the surrounding stress fields and the critical flaw sizes, forming no part of traditional design methods, remained unsolved. It was only in the late forties, that Irwin

and Orowan laid the foundation of Fracture Mechanics, and more recently, in the sixties that its principles were applied providing then, the continuity between the design method for flawed and unflawed structures.

During the last decade Fracture Mechanics and particularly the concepts of stress intensity factor and critical stress intensity factor have advanced to the stage where it is of direct value for the prevention of brittle fracture in thick walled pressure vessels, and efforts are being made to include these concepts in standards and codes of practice.

An excellent compilation of papers on the developments of the art in the 1960 - 70 period and onwards can be found in ASME publications (12), (13) and in a recent Conference on Reactor Technology (14).

1.3 Review on the Linear Elastic Fracture Mechanics

1.3.1 Introduction

The main objective of Fracture Mechanics is to study in a macroscopic manner the fracture phenomenon as a function of the applied loads. Such a study, in the absence of large plastically yielded areas surrounding the cracks or flaws, is referred to as Linear Elastic Fracture Mechanics (LEFM).

Provided fracture occurs prior to large-scale yielding of the structural member LEFM can be extended to study fracture problems involving moderate plastic yielding by incorporating various plasticity correction factors.

The classical stress function method of solving elasticity problems described by Timoshenko et al. (15) was first used by Inglis (16) to derive an equation (1.1) for the maximum stresses at the tip of an elliptical notch with major axis a on the x direction and minor axis b subjected to a remote stress σ on the y direction.

$$(\sigma_y)_{max} = \sigma \left(1 + \frac{2a}{b}\right) \qquad (1.1)$$

The ellipse degenerates to a crack when $a >> b$ and again the methods of elasticity can be used (17), to calculate the stresses in the vicinity of the crack. The maximum tensile stress occurs at the end of the crack, $(\sigma_y)_{max}$, and is given approximately by

$$(\sigma_y)_{max} \simeq 2\sigma\sqrt{\frac{a}{\rho}} \quad \text{for } a >> \rho \qquad (1.2)$$

where ρ is the radius of curvature at one end of the ellipse and is given by $\rho = b^2/a$.

1.3.2 The Energy Balance Approach to Fracture

The energy balance approach to fracture was first proposed by Griffith (18) based on the Inglis' solutions.

The basic idea in his theory is that a crack will begin to propagate if the elastic energy released by its growth is greater than the energy required to create the fractured surfaces. The main value of this thermodynamic approach is that by considering the changes in energy as the crack grows, it can ignore the details of the fracture

process at the crack tip.

For a problem of a crack of length 2a in a plate under remote tension σ, Griffith then found that the critical stress, σ_{cr}, required for crack growth is given by the following expressions

$$\sigma_{cr}\sqrt{a} = \sqrt{\frac{2E\gamma}{\pi}} \quad \text{in plane stress conditions} \qquad (1.3.a)$$

$$\sigma_{cr}\sqrt{a} = \sqrt{\frac{2E\gamma}{\pi(1-\nu^2)}} \quad \text{in plane strain conditions} \qquad (1.3.b)$$

where E is the Young's Modulus

γ is the specific surface energy

ν is the Poisson's ratio

Since the terms on the right hand side of expressions (1.3) are only material constants the factor $\sigma_{cr}\sqrt{a}$ should be an intrinsic material parameter. The experiments Griffith performed on glass have shown encouraging results, in fact at the instance of fracture a constant value of $\sigma_{cr}\sqrt{a}$ was obtained over a wide range of crack lengths.

However, Griffith's work could not be applied to materials which did not behave in a pure elastic manner, thus virtually ruling out consideration of any engineering problem.

Some twenty five years later Irwin, (19), and Orowan, (20), in their analysis of fracture suggested that the energy released in the fracture process was mainly dissipated by producing plastic flow around the crack tip. A quantity γ_p

called plastic work was then introduced and was estimated to be on the order 10^3 times greater than Griffith's surface energy 2γ which enabled Orowan to re-write equations (1.3) in the following manner by simply neglecting the Griffith term 2γ

$$\sigma_{cr}\sqrt{a} = \sqrt{\frac{E\gamma_p}{\pi}} \quad \text{in plane strain conditions} \qquad (1.4.a)$$

$$\sigma_{cr}\sqrt{a} = \sqrt{\frac{E\gamma_p}{\pi(1-\nu^2)}} \quad \text{in plane strain conditions} \qquad (1.4.b)$$

Surprisingly enough this new quantity γ_p appeared to be independent of the initial crack length, hence could still be regarded as a material property. Furthermore, if the plastic zone was small enough, all the merits in Griffith's idea were still safeguarded and a theory correlating fracture behaviour could still be substantiated. In Irwin's view the modified theory consisted of evaluating the strain energy release rate with respect to crack extension at the point of fracture. If the fracture process were essentially the same, regardless of the loading conditions and geometry, the fracture event would occur when the strain energy release rate reached a critical value, G_c, and this value would be a material property.

As stated by Irwin, the G_c concept plays a similar role in relation to fracture as the yield strength to plastic deformation. As in the case of design methods based on the knowledge of the stress-strain curve of the material, experiments on cracked specimens enable the onset of fracture

to be predicted in real structures and this ability is sufficient justification for utilizing the concept as an engineering approach.

1.3.3 The Stress Intensity Factor Approach to Fracture

In Griffith's theory of brittle fracture a critical stress-crack size relation was derived from an energy postulate. An alternative interpretation of the fracture phenomenon leads to stress-crack size relations by focussing attention on the elastic stresses close to the tip of the crack.

Based on the method of Westergaard (24), Irwin (19), (22), (23), derived a general solution for the stress system at the tip of an ideally plane sharp ended crack in an isotropic elastic body. Referring to Figure 1.3, a local coordinate system is chosen so that the z-axis is parallel with the leading edge of the crack, the y-direction is perpendicular to the plane of the crack and the x-axis is such that the plane (xy) is normal to the crack front line.

If in the case of a straight front crack the z-dimension of the body is large or small, plane strain or plane stress will exist respectively. More realistically, in all but thin plate-like geometries a mixed plane stress plane-strain situation will exist across the z direction varying from plane stress at the surface to plane strain at the central area. Any plastic deformation which may occur at the crack borders is neglected in a first approximation and will be subsequently treated as a minor correction to the elastic analysis.

Three basic modes (I, II, III) of crack surface displacements which can lead to crack extension are shown in Figure 1.2. During the course of this work attention will be confined only to the opening mode of separation, mode I.

Corresponding to opening mode conditions, the stresses and displacements at points close to the crack front can be shown (25) to have the form (see Figure 1.3)

$$\sigma_x = \frac{K_I}{\sqrt{2\pi r}} \cos\frac{\theta}{2}\left(1-\sin\frac{\theta}{2}\sin\frac{3\theta}{2}\right) + \ldots \qquad (1.5.a)$$

$$\sigma_y = \frac{K_I}{\sqrt{2\pi r}} \cos\frac{\theta}{2}\left(1+\sin\frac{\theta}{2}\sin\frac{3\theta}{2}\right) + \ldots \qquad (1.5.b)$$

$$\sigma_{xy} = \frac{K_I}{\sqrt{2\pi r}} \sin\frac{\theta}{2}\cos\frac{\theta}{2}\cos\frac{3\theta}{2} + \ldots \qquad (1.5.c)$$

$$\sigma_z = \nu(\sigma_x + \sigma_y) \quad \text{for plane strain}$$

$$= 0 \quad \text{for plane stress} \qquad (1.5.d)$$

$$u_x = \frac{K_I}{8\mu}\sqrt{\frac{2r}{\pi}}\left[(2\kappa-1)\cos\frac{\theta}{2} - \cos\frac{3\theta}{2}\right] + \ldots \qquad (1.6.a)$$

$$u_y = \frac{K_I}{8\mu}\sqrt{\frac{2r}{\pi}}\left[(2\kappa+1)\sin\frac{\theta}{2} - \sin\frac{3\theta}{2}\right] + \ldots \qquad (1.6.b)$$

$$u_z = 0 \quad \text{for plane strain}$$

where $\kappa = 3-4\nu$ for plane strain

$= \frac{3-\nu}{1+\nu}$ for plane stress

The omitted terms of these series expansions involve increasing half powers of the ratio of r divided by the crack length and consequently are important only at large distances from the crack tip.

Results similar to expressions (1.5) and (1.6) can be obtained for the edge sliding mode II and the tearing Mode III.

The K term in these equations is independent of the polar coordinates r and θ, and serves only as a positive multiplying factor which can be shown to depend on the applied boundary load and the crack size. In Fracture Mechanics terminology, K is referred to as the "stress intensity factor" (SIF).

The significance of the above expressions is due to their generality since they hold for any plane crack, thus the elastic stresses and displacements around the crack tip are entirely characterized by the stress intensity factor K. Hence it must be expected that fracture will occur when K reaches a critical K_c.

The K_c concept should indeed be expected to be equivalent to the G_c concept already described. In fact Irwin (19), (22), using virtual work arguments has shown that the strain energy release rate could be identified with K according to the following expression:

$$G_I = K_I^2/E' \qquad (1.7)$$

where E' = E(Young's Modulus) for plane stress conditions

or $E' = E/(1-\nu^2)$ for plane strain conditions.

It was mentioned early in this section that LEFM should take into account a plasticity correction factor.

In fact the stress solutions (1.5) predict infinite values of stress at the crack tip (r=0) which cannot occur in practice of course. Plastic flow will therefore take place in areas of small r values. The approximate extent of the region of plastic flow can be estimated by substituting a yield criterion into the stress field equation, leading to

$$r_y = \frac{1}{2\pi} \left(\frac{K_I}{\sigma_{ys}}\right)^2 \qquad \text{for plane stress conditions} \qquad (1.8)$$

r_y is the distance ahead of the crack tip where σ_y reaches the yield strength of the material.

For plane strain conditions, due to the triaxialaty effects (see Figure 1.4) allowance must be made for the elevation of yield stress ahead of the crack and this is normally done (26) by substituting $\sqrt{3}\ \sigma_{ys}$ for σ_y, leading to

$$r_{Iy} = \frac{1}{6\pi} \left(\frac{K_I}{\sigma_{ys}}\right)^2 \qquad \text{for plane strain conditions} \qquad (1.9)$$

Current test specimen dimensional specifications (21) (56) in order to ensure proper determination of K_{Ic} values(*) require that the crack length a, the specimen thickness B the uncracked ligament w-a should all exceed $2.5(K_{Ic}/\sigma_{ys})^2$.

(*) - In K_{Ic}, I denotes opening mode I

c denotes critical for onset of fracture under plane strain conditions.

This limit should be proportional to the plastic zone size r_{Iy} (e.g. 1.9), (25)

$$\frac{r_{Iy}}{2.5(K_{Ic}/\sigma_{ys})^2} \simeq 0.02 \qquad (1.10)$$

Therefore the range of applicability of LEFM is limited in principle by the existance of a plastic zone size at the crack tip which cannot be greater than 2% of, for instance, the crack length a.

Finally, reference to methods of obtaining K for different loading conditions and geometries are outlined.

In general, mode I stress intensity factors may be written in the form

$$K_I = Y\sigma\sqrt{\pi a} \qquad (1.11)$$

The term $\sigma\sqrt{\pi a}$ represents the SIF of a crack of length 2a in an infinite sheet subjected to a remote tensile stress perpendicular to the plane of the crack. Y is a nondimensional magnification factor which is a funtion of the relevant geometric parameters and loading conditions(*).

A great variety of K_I determination methods is already available: analytical methods using complex stress funtions, alternating techniques or integral transforms: numerical methods using conformal mapping techniques, boundary collocation and finite element methods.

(*) - The evaluation of this factor Y is sometimes called "K calibration".

The principle of superposition (29) also enables the calculation of solutions with different boundary conditions to be combined to produce solutions for more complex problems.

A comprehensive review of this subject was made by Cartwright and Rooke (27) and Sih (28) and Cartwright and Rooke(30) compiled a wide variety of solutions in a "Compendium of Stress Intensity Factors".

Experimental methods have been also used to obtain K values, amongst these the more relevant are: Compliance Methods, also used for determination of K_{1c} values for different materials, Photoelasticity techniques and fatigue tests where the K variations in the loading cycles can be related to the crack growth rate using some fatigue crack propagation law.

1.3.4 The Three Dimensional Crack Problem.

In real heavy-section structures, for example pressure vessel components, cracks will often be initiated in areas of high nominal strain. Normally these cracks will not be through- cracks, but surface flaws or more commonly known as part-through cracks or corner cracks. These cases, because of their particular geometry and/or loading conditions are fully three dimensional in nature and consequently should be dealt with as such. Moreover, these cracks will normally advance in a curved front and the stress intensity factor may vary along the periphery of the crack. The analysis of

this type of flaw usually requires the assumption that fracture will occur when somewhere along the crack front the SIF exceeds the critical value K_{Ic}.

However, two major difficulties arise when dealing with such problems. First, as pointed out by Hartranft and Sih (31), an agreement amongst the theoreticians has not yet been reached as regards stress and displacement fields as well as K values in areas where the crack meets the free surface. In their studies of a part-through semi-circular crack, using an alternating method, they found that a drastic drop in values of K will occur in a small area near the surface. Benthem (33) on the other hand, has shown that the degree of singularity in those areas is no longer constant and equal to the well known $-\frac{1}{2}$ (for stresses) suggested by Westergaard, but strongly dependant on the Poisson's ratio. For the case where the Poisson's ratio is equal to 0.3 he indicates a value of about .45 for the degree of singularity, thus ruling out the usage of the stress intensity factor concept, which has lost its meaning.

However, if this boundary layer effect is restricted to very small areas near the free surface, as it appears to be, it may yield only a minor contribution to the overall distribution of K values in the more central portions of the crack and the discrepancies introduced by neglecting it, will be, hopefully, irrelevant for engineering purposes.

The second difficulty concerned with the surface flaw is related to the crack front shape and the local variations

of K along the crack front.

Such crack configurations are normally characterized by a length and a depth, but these two geometric parameters are obviously insufficient to define the crack front, thus allowing an infinity of possible shapes, (see Figure 1.5 for some examples), each one with its own K calibration and with its own local variation of K values.

This complexity, however, may be irrelevant as stated by Swedlow et al. (35), following R.A. Westman's reasoning (. . . we expect, perhaps merely hope, that most of the contours . . . will grow in a slow manner to a common shape before rapid fracture ensues . . . The point is that irregularities in crack shape may be expected to be smoothed out somewhat and that the range of shapes that one might be obliged to deal with is relatively modest . . . .).

These assumptions are widely supported by post-mortem observations of various thick walled pressure vessels, and a typical example, which was taken from (6), is given in Figure 1.6.

Since the famous papers by Sneddon (36) and Green et al. (37) on the penny shaped and elliptical cracks in an infinite solid, a good number of workers have devoted themselves to studies involving circular and elliptical cracks, fully imbedd with different loading and/or geometric conditions.

The only exact opening mode solutions are for infinite regions. For the planar case of crack of length 2a the SIF is given by:

$$K = \sigma \sqrt{\pi a} \tag{1.12}$$

and for the circular crack of radius a the SIF is given by

$$K = 2\sigma \sqrt{\frac{a}{\pi}} \tag{1.13}$$

where σ in both cases is the remote applied stress perpendicular to the plane of the crack.

For the more general case of an elliptical crack Irwin (38) derived an expression for the SIF which is given by

$$K = \frac{\sigma}{E(k)} \left(\frac{b}{a}\right)^{\frac{1}{2}} \left(a^2 \sin^2\alpha + b^2 \cos^2\alpha\right)^{\frac{1}{4}} \tag{1.14}$$

where $E(k)$ is the complete elliptical integral of the second kind with the argument $k = \sqrt{1-\left(\frac{b}{a}\right)^2}$

$a,b,$ are the major and minor semi-axis of the ellipse

α is the angle measured from the major axis in the plane of the crack.

Paris and Sih (25) have shown that the problem of a crack in an infinite solid subjected to remote tension can be replaced by a pressurized crack in an infinite solid.

Kobayashi (42) using a stress function method evaluated the SIF for an elliptical crack in a solid subjected to an internal varying pressure distibution which was represented by a double-Fourrier series expansion.

He then, based on Paris' (25) ideas, extended his studies to elliptical cracks subjected to uniaxial tension, pure bending and transient heating, using suitable pressure distributions on the faces of the crack. For the case of

uniaxial tension, he eventually arrived at the same expression as Irwin (1.14).

The semi-elliptical surface flaw has been initially studied by Irwin (38) based on the Green-Sneddon results. His expression including a plasticity correction factor, evaluates the SIF for the deepest point of a shallow crack(*) as follows:

$$K = \sqrt{\frac{1.2\sigma^2 b}{E(K) - .212\left(\frac{\sigma}{\sigma_{ys}}\right)^2}} \qquad (1.15)$$

later Kobayashi et al. (39) have modified Irwin's expression by introducing another magnification factor, M_f, as follows

$$K = 1.12 M_f \sigma \sqrt{\frac{\pi b}{E(K)^2 - .212\left(\frac{\sigma}{\sigma_{ys}}\right)^2}} \qquad (1.16)$$

This factor, being a funtion of the ratio b/a and b/B where B is the thickness of the plate and accounts for the proximity of the back free surface for the case when the crack penetrates deeply inwards.

Smith et al. (32) have obtained the SIFs for semi-circular surface flaws at its deepest points in a beam in bending. From their results they show that the SIF does not vanish when these points are at the neutral axis of the beam. This means that the crack tip can penetrate further

---

(*) - Shallow crack means the crack depth being less than half of the plate thickness (see Ref. (41)).

into the compression region before it can no longer open.

The quarter elliptical corner crack bearing great resemblance to the semi-elliptical configurations was studied by Broek (40) by applying the expressions (1.15) and (1.16) to particular problems such as radial corner cracks emanating from holes in plates.

Among the several other studies on the surface flaw problem which have been published to date, the more accurate analytical solutions have been obtained using the alternating method which basically combines analytical results of two auxiliary problems with numerical techniques (31).

The method has been used extensively by Smith et al. (43), (44), who determined the SIF for part-circular cracks in different loading conditions and by Shah and Kobayashi (41), (45), for elliptical cracks, including also cracks under uniform and non-uniform internal pressure.

Quite recently Sih (28) has introduced an entirely new approach to LEFM based on the field strength of the local strain energy density.

In this new theory a fundamental "strain energy density factor", S, is derived which not only measures the amplitude of local stresses (like K and G) but is also direction sensitive. In his paper, Sih gives an example of the application of these concepts in a three dimensional crack problem yet no results have been presented at this time.

However, a three-dimensional analysis for predicting the growth of an embedded elliptical crack subjected to general loadings was carried out by Sih and Cha (58) in which fracture is assumed to initiate in the direction of minimum strain energy density factor.

The principles of the Compliance test(*) used in the experimental determinations of SIFs, have also been applied to 3D crack problems. Sih and Hartranft (57) generalized this approach to study various elliptical surface flaw configurations. They computed the compliance changes for several possible extensions of the crack front, and indicate how this method is applied to cracks in pressure vessels subjected to internal pressure.

The main advantage of this method lies in the fact that values of G derived from compliance changes ignores the complex local stress field analyses of 3D crack problems.

However, the evaluation of local values of G using this method, is strongly dependant on the local variation of the crack front. The necessity to assume a particular shape for the extended crack front may yield doubtful results.

The use of Finite Element Methods in the solution of 3D crack problems has been limited in the past due to its inaccuracy as compared to the more rigorous analytical and numerical methods.

(*) The strain energy release rate G can be obtained experimentally using the following expression

$$G = \tfrac{1}{2}P^2\left(\frac{\partial C}{\partial a}\right)/B$$

Where C is the so called "compliance" or the reciprocal of the load (P) - deflection curve of a test specimen with thickness B. (see Ref.(26)).

However, when a real problem becomes three dimensional most of the conventional methods can no longer be applied.

The application of the Finite Element Methods to Fracture Mechanics will be discussed in Chapter 3.

Experimental Methods have also been studied recently to determine the SIFs for 3D crack configurations.

Broekhoven and Ruijtenbeek (59) carried out some experiments by monitoring crack growth rates (da/dN) under uniaxial fatigue loading of precracked nozzle-on-plate specimens. They then converted the resulting (da/dN) measurements into ΔK values with the use of a suitable fatigue crack propagation law for the same material of the nozzle specimens. This method has the advantage that SIFs are determined under conditions very similar to those in reality.

Fatigue crack growth behaviour is strongly dependant amongst other factors (61) on loading history, mean stress specimen thickness and environmental conditions, therefore the accuracy in the simple application of fatigue crack growth laws to evaluate K values is yet to be demonstrated.

Sommer et al. (60) investigated the growth characteristics of part-through cracks in thick walled plates and tubes under fatigue loading.

They have shown that (verbatim) (. . . Although . . the results cannot provide a refined failure analysis . . they indicate which parameters are of importance for crack extension and explain some general tendencies of crack growth in thick walled plates and tubes).

A consise review on the various analytical methods used in 3D crack studies as well as some solutions can be found in Refs. (31) and (41) and a reasonable collection of practical results in this family of crack problems is given in Refs. (25) and (42).

C H A P T E R 2

THREE-DIMENSIONAL FINITE ELEMENT ANALYSIS

2.1 Introduction

2.1.1 General

The Finite Element Method (FEM) is a very powerful technique for numerically solving many complex field problems.

This method which was introduced in the fifties has been successfully applied to the solution of a great number of problems in stress analysis.

The basic idea of the FEM is that a structure can be represented by an idealized discrete analogue made up of relatively small standard subregions, called elements, with a number of nodal points related to them.

The energetic assumptions behind the Finite Element theory allows the overall behaviour of the model to be obtained as the sum of the contributions of all of its elements. At the same time the characteristic behaviour of each element can be developed based only upon its geometry and material properties.

There exists a great number of excellent texts for example Ref. (46) which covers the details of this method. Refs. (47) and (48) give a good description of a wide range of types of element which have been introduced during the past twenty years.

Much has been published to date about the FEM. It has reached such a stage where it has become a common tool in a great number of research institutions and some industrial organisations. Therefore a complete review of this subject will not be given here.

One of the main features of the FEM and particularly the displacement (stiffness) method, as compared to others, is the ease involved in the handling of geometric shapes, and the specification of boundary conditions of real engineering structures.

This particular advantage was a governing aspect on the choice of the FEM to perform the stress analysis of the rather complex "T-junction" geometries and the subsequent LEFM studies of some three-dimensional crack configurations in those structures. The displacement method was adopted in this work and will be briefly outlined and followed by some considerations of the Finite Elements which have been used.

2.1.2 The Displacement Method

In the displacement method, as opposed to the force or equilibrium method, the displacement field within each element is defined in terms of various functions ϕ (usually simple polynomials).

$$\{\delta\} = [\phi(x,y,z)] \{\alpha\} \qquad (2.1)$$

where

$$\{\delta\} = \begin{Bmatrix} u(x,y,z) \\ v(x,y,z) \\ w(x,y,z) \end{Bmatrix} \quad , \{\alpha\} = \begin{Bmatrix} \alpha_1 \\ \alpha_2 \\ \vdots \\ \alpha_n \end{Bmatrix}$$

and n is the number of generalized coordinates (α) which is equal to the number of degrees of freedom of the element. The x,y and z coordinates are not necessarily the global coordinates.

Equation (2.1) can be solved for the generalized coordinates, α , in terms of generalized nodal displacements.

By using the strain-displacements relationships and the constitutive law, the stresses and strains within the element can be evaluated in terms of nodal displacements. The strain energy of the entire structure is then obtained by adding the contributions of all its elements. Applying the principle of minimum potential energy leads to a set of linear equations relating the externally applied generalized nodal forces F to the generalized nodal displacements, Δ ,

$$k\,\Delta = F \qquad (2.2)$$

where k is the stiffness matrix of the entire system.

It can be shown through the principle of minimum potential energy, (see (48)), that this method provides a lower bound for the displacement solution Δ.

Criteria for convergence to the true solution by finer mesh subdivision must be met (48), which imposes two well-known conditions on the choice of the displacement functions:

1. The displacement field should include "constant strain" states and "rigid body" movements.

2. Continuity of the displacement field must be ensured within the element and at interelement boundaries.

A wide range of functions ϕ can be found to meet these requirements. However a proper selection of these functions is essential to ensure good rates of convergence.

Some detailed considerations of this method, as applied to the three dimensional elements used, will be made later on this Chapter.

2.1.3 The Choice of Elements, the Computer Program

Finite Element Programs, in general, are bound to require large spaces of computer memory and this problem is obviously more relevant in the case of three-dimensional applications, and the use of more sophisticated programming techniques such as the "Front Method", to be described later, becomes compulsory.

Several powerful and elaborate systems do exist in the United Kingdom (ASKA, BERSAFE, etc.) in which libraries of

various finite elements are used together. However at the time this work was started, none of these systems were available at Imperial College. It was only quite recently (1974) that the ASKA system was implemented at Imperial College Computer Centre and later on at the University of London Computer Centre.

In view of the foregoing, a computer code initially developed by Alujevic (DIM3) Ref.(50) based on a shell program (NAMAIN) developed by Natarajan Ref.(49) under the supervision of Dr. J.A. Blomfield* was brought into use.

The present version of the code, now called DIM3B, uses two different brick-based elements: 20 and 32 node hexahedrons using second and third order displacement functions respectively. However only one type of these elements is used at a time in one computer run.

The choice of these elements was based on past experience with Finite Element applications (see Refs.(1)-(5)), Refs.(46) and (52)). Problems of idealizing second order curved boundaries (viz. cylinders) are eased by using these higher order curved elements. Moreover, these particular elements have proven to be extremely useful when dealing with cracked structures.

Bearing in mind the forseeable large costs involved in running the DIM3B code, an attempt was made to model a "T-junction" piece by a two-dimensional axisymetric simulation of the real problem.

---

* formerly Lecturer, Mechanical Engineering Department, Imperial College.

For this purpose a Finite Element program using triangular axisymetric elements was developed (FRONT) using a simplified version of the "Frontal Method".

This study was carried out in the early stages of this work, simultaneously with the debugging process of the DIM3B code. This analysis will be omitted for no conclusive results nave been reached. However, in order to provide a permanent record of the program FRONT a description and listing are given in Appendix 1 of this thesis.

2.2 Mathematical Theory of Three Dimensional Finite Elements.

2.2.1 General

This section describes the mathematical theory involved in the calculation of the individual matrices of the two element types available.

Although a fairly general formulation of the FEM using these elements is known (48), a brief sketch of this theory is presented here for the sake of completness and also to introduce the notation which will be used later.

2.2.2 Isoparametric Concept, Shape Functions

In a typical three-dimensional isoparametric finite element with n nodes the coordinates or any field variable are given by, for example

$$\phi = \alpha_1 + \alpha_2 x + \alpha_3 y + \alpha_4 z + \ldots + \alpha_n x^p y^q z^r \qquad (2.3)$$

or

$$\phi(x,y,z) = [M(x,y,z)] \begin{Bmatrix} \alpha_1 \\ \alpha_2 \\ \vdots \\ \alpha_n \end{Bmatrix} \tag{2.4}$$

where $M = [1,x,y, \ldots .]$

$$\{\alpha\}^T = [\alpha_1, \alpha_2, \ldots , \alpha_n]$$

by substituting the coordinates at each node

$$\phi_i = [1,x_i,y_i, \ldots .] \{\alpha\} \tag{2.5}$$

and for all nodes

$$\begin{Bmatrix} \phi_1 \\ \phi_2 \\ \cdot \\ \cdot \\ \cdot \\ \phi_n \end{Bmatrix} = \begin{bmatrix} 1 & x_1 & y_1 & \cdot & \cdot & \cdot \\ 1 & x_2 & y_2 & \cdot & \cdot & \cdot \\ & & & & & \\ \cdot & \cdot & \cdot & \cdot & \cdot & \cdot \\ 1 & x_n & y_n & \cdot & \cdot & \cdot \end{bmatrix} \begin{Bmatrix} \alpha_1 \\ \alpha_2 \\ \cdot \\ \cdot \\ \cdot \\ \alpha_n \end{Bmatrix} \tag{2.6}$$

$$= [C]\{\alpha\} \tag{2.7}$$

where $[C]$ is a square matrix of constant terms. The coeficients α can be calculated as follows

$$\{\alpha\} = [C]^{-1} \{\phi_i\} \tag{2.8}$$

then from expression (2.4) and substituting {α} calculated in (2.8)

$$\phi\ (x,y,z) = \left[M(x,y,z)\right]\left[C\right]^{-1}\ \{\phi_i\} \tag{2.9}$$

or

$$\phi\ (x,y,z) = \sum_{i}^{n} N_i \phi_i \tag{2.10}$$

where N_i are called the shape functions and ϕ_i are the nodal values of the field variable.

It is convenient to stress that the shape functions N_i, so far, are funtions of the general coordinates x, y and z.

The isoparametric concept is based on the fact that the same interpolation functions are used for defining any field variable, namely, in this case, coordinates and displacements within the element.

2.2.3 Local Curvilinear Coordinates

Let us consider curvilinear coordinates ξ, η, ζ varying between -1, +1 so that in the space (ξ,η,ζ) the hexahedron (20 or 32 node 3D finite elements, see figure 2.1) becomes a cube with side length of two units.

Following expression (2.10), the relationship between the cartesian and the curvilinear coordinates will be

$$x_i = \sum_{i=1}^{n} N_i\ \xi_i \tag{2.11}$$

and displacements within the element will be defined as follows

$$\{\delta\} = \sum_{i=1}^{n} N_i \{\delta_i\} \qquad (2.12)$$

where

$$\{\delta\}^T = [u,v,w] \quad \text{and}$$

$$\{\delta_i\}^T = [u_i,v_i,w_i]$$

$n = 20$ or 32

Once the local coordinates have been defined, the shape functions N_i can be expressed in terms of the local coordinates and they become independant of the element shape, therefore the same for all the elements. From now on they will be considered as

$$N_i = N_i(\xi,\eta,\zeta). \qquad (2.13a)$$

For these elements the shape functions N_i, i=1,2, . .20/32 defined in terms of local coordinates are, using the notation

$$\xi_o = \xi\xi_i \ , \ \eta_o = \eta\eta_i \ , \ \zeta_o = \zeta\zeta_i$$

Quadratic element (20 node):

Corner nodes

$$N_i = (1+\xi_o)(1+\eta_o)(\xi_o+\eta_o+\zeta_o-2)/8 \qquad (2.13b)$$

Mid-side nodes

$$\xi_i=0, \ \eta_i=\pm 1, \ \zeta_i=\pm 1 \quad N_i=(1-\xi^2)(1+\eta_o)(1+\zeta_o)/4 \qquad (2.13c)$$

$\eta_i=0,\ \zeta_i=\pm 1,\ \xi_i=\pm 1 \qquad N_i(1+\xi_o)(1-\eta^2)(1+\zeta_o)/4 \qquad (2.13d)$

$\zeta_i=0,\ \xi_i=\pm 1,\ \eta_i=\pm 1 \qquad N_i(1+\xi_o)(1+\eta_o)(1-\zeta^2)/4 \qquad (2.13e)$

Cubic element (32 node):

Corner nodes

$$N_i=(1+\xi_o)(1+\eta_o)(1+\zeta_o)\left[9(\xi^2+\eta^2+\zeta^2)-19\right]/64 \qquad (2.13f)$$

Typical third side node

$\xi_i=\pm\frac{1}{3},\ \eta_i=\pm 1,\ \zeta_i=\pm 1 \qquad N_i=(1-\xi^2)(1+9\xi_o)(1+\eta_o)(1+\zeta_o)9/64 \qquad (2.13g)$

The main advantage of this formulation is that the numerical procedures involved with the element will always be the same regardless of their particular distorted shape they will assume in the idealized mesh.

2.2.4 General Steps of Finite Element Formulation

Following the basic finite element formulation described elsewhere, Ref.(47), a list of wanted relationships is described below.

i) $\{\delta\}=[N]\{\delta\}_e \qquad (2.14)$

ii) $\{\varepsilon\}=[B]\{\delta\}_e \qquad (2.15)$

iii) $\{\sigma\}=[D]\{\varepsilon\}=[D]\,B\{\delta\}_e \qquad (2.16)$

iv) $[K]_e=\int_{vol_e}[B]^T[D][B]\ d\ vol \qquad (2.17)$

where

$[N]$ is called the shape function matrix

$\{\varepsilon\}$ are the strains $\{\varepsilon\}^T=\{\varepsilon_x,\varepsilon_y,\varepsilon_z,\varepsilon_{xy},\ \ldots\}$

$\{\delta\}_e$ are the nodal displacements for each element

$[D]$ is the elasticity matrix

$[B]$ is the displacement/strain transformation matrix

$[K]_e$ is the stiffness matrix for each element.

2.2.5 Strains; Derivation of Expression (2.15)

To calculate strains, derivatives of displacements with respect to x,y,z are needed. Bearing in mind expressions (2.13) and (2.14).

$$\begin{Bmatrix} \frac{\partial \delta}{\partial \xi} \\ \frac{\partial \delta}{\partial \eta} \\ \frac{\partial \delta}{\partial \zeta} \end{Bmatrix} = \begin{bmatrix} \frac{\partial N_1}{\partial \xi} & \frac{\partial N_2}{\partial \xi} & \cdots \\ \frac{\partial N_1}{\partial \eta} & \frac{\partial N_2}{\partial \eta} & \cdots \\ \frac{\partial N_1}{\partial \zeta} & \frac{\partial N_2}{\partial \zeta} & \cdots \end{bmatrix} \begin{Bmatrix} \delta_1 \\ \delta_2 \\ \cdot \\ \cdot \\ \cdot \\ \delta_n \end{Bmatrix} \tag{2.18}$$

$$= [DE] \begin{Bmatrix} \delta_1 \\ \delta_2 \\ \cdot \\ \cdot \\ \delta_n \end{Bmatrix} \tag{2.19}$$

Looking at expression (2.19) $[DE]$ can be considered as a derivative operator so the same principle is also applied to the coordinates as follows

$$[DE] \begin{bmatrix} x_1 & y_1 & z_1 \\ x_2 & y_2 & z_2 \\ \cdot & \cdot & \cdot \\ x_n & y_n & z_n \end{bmatrix} = \begin{bmatrix} \frac{\partial x}{\partial \xi} & \frac{\partial y}{\partial \xi} & \frac{\partial z}{\partial \xi} \\ \frac{\partial x}{\partial \eta} & \frac{\partial y}{\partial \eta} & \frac{\partial z}{\partial \eta} \\ \frac{\partial x}{\partial \zeta} & \frac{\partial y}{\partial \zeta} & \frac{\partial z}{\partial \zeta} \end{bmatrix} = [J] \tag{2.20}$$

where $[J]$ is obviously the Jacobian of transformation of general coordinates x,y,z to the local ones ξ, η, ζ.

Using now chain rule relationships of the type

$$\frac{\partial \phi}{\partial \xi} = \frac{\partial \phi}{\partial x}\ \frac{\partial x}{\partial \xi} + \frac{\partial \phi}{\partial y}\ \frac{\partial y}{\partial \xi} + \frac{\partial \phi}{\partial z}\ \frac{\partial z}{\partial \xi} \tag{2.21}$$

$$= \begin{bmatrix} \frac{\partial x}{\partial \xi} & \frac{\partial y}{\partial \xi} & \frac{\partial z}{\partial \xi} \end{bmatrix} \begin{Bmatrix} \frac{\partial \phi}{\partial x} \\ \frac{\partial \phi}{\partial y} \\ \frac{\partial \phi}{\partial z} \end{Bmatrix} \tag{2.22}$$

Generalizing for the rest of the coordinates and having now the displacement as field variable

$$\begin{Bmatrix} \frac{\partial \delta}{\partial \xi} \\ \frac{\partial \delta}{\partial \eta} \\ \frac{\partial \delta}{\partial \zeta} \end{Bmatrix} = [J] \begin{Bmatrix} \frac{\partial \delta}{\partial x} \\ \frac{\partial \delta}{\partial y} \\ \frac{\partial \delta}{\partial z} \end{Bmatrix} \tag{2.23}$$

inverting this equation

$$\begin{bmatrix} \frac{\partial \delta}{\partial x} & \frac{\partial \delta}{\partial y} & \frac{\partial \delta}{\partial z} \end{bmatrix}^T = [J]^{-1} \begin{bmatrix} \frac{\partial \delta}{\partial \xi} & \frac{\partial \delta}{\partial \eta} & \frac{\partial \delta}{\partial \zeta} \end{bmatrix}^T \tag{2.24}$$

Substituting the right hand side of expression (2.18) into expression (2.24) we obtain

$$\begin{bmatrix} \frac{\partial \delta}{\partial x} & \frac{\partial \delta}{\partial y} & \frac{\partial \delta}{\partial z} \end{bmatrix}^T = [J]^{-1} [DE] [\delta_1 \delta_2 \ \cdots \ \delta_n]^T \tag{2.25}$$

$$= [DEXYZ] \ [\delta_1 \delta_2 \ \cdots \ \delta_n]^T \tag{2.26}$$

The matrix [DEXYZ] can be suitably changed in order to accommodate the derivatives for the several components of the engineering strains

$$\{\varepsilon\} = \begin{Bmatrix} \varepsilon_x \\ \varepsilon_y \\ \varepsilon_z \\ \varepsilon_{xy} \\ \varepsilon_{yz} \\ \varepsilon_{zx} \end{Bmatrix} = \begin{Bmatrix} \partial u/\partial x \\ \partial v/\partial y \\ \partial w/\partial z \\ \partial u/\partial y + \partial v/\partial x \\ \partial v/\partial z + \partial w/\partial y \\ \partial w/\partial x + \partial u/\partial z \end{Bmatrix} \tag{2.27}$$

as follows : if[DEXYZ] is given by

$$[\,DEXYZ\,] = \begin{bmatrix} d_{11} & d_{12} & \cdots & d_{1n} \\ d_{21} & d_{22} & \cdots & d_{2n} \\ d_{31} & d_{32} & \cdots & d_{3n} \end{bmatrix} \tag{2.28}$$

hence

$$\{\varepsilon\} = \begin{bmatrix} d_{11} & 0 & 0 & d_{12} & 0 & 0 & \cdots & d_{1n} & 0 & 0 \\ 0 & d_{21} & 0 & 0 & d_{22} & 0 & \cdots & 0 & d_{2n} & 0 \\ 0 & 0 & d_{31} & 0 & 0 & d_{32} & \cdots & 0 & 0 & d_{32} \\ d_{21} & d_{11} & 0 & d_{22} & d_{12} & 0 & \cdots & d_{2n} & d_{1n} & 0 \\ \cdots & \cdots & \cdots & \cdots & \cdots & \cdots & \cdots & \cdots & \cdots & \cdots \end{bmatrix} \begin{Bmatrix} \delta_1 \\ \delta_2 \\ \vdots \\ \delta_n \end{Bmatrix} \tag{2.29}$$

$$= [\,B\,]\,[\,\delta_1\ \delta_2\ \cdots\ \delta_n\,]^T \tag{2.30}$$

as it was required in expression (2.15)

2.2.6 Stiffness matrix $[K]_e$

Remembering the basic theory Ref.(48), the stiffness matrix of an element is defined as follows

$$[K]_e = \int_{vol_e} [\,B\,]^T [\,D\,]\,[\,B\,]\ \ dvol_e \tag{2.31}$$

where B was defined in expression (2.29), D is the elasticity matrix to be defined, and vol_e is the volume of

the element.

Remembering that $[B]$ is a funtion of ξ,η and ζ so the element volume dvol must be transformed as

$$dxdydz = |J|\, d\xi d\eta d\zeta \tag{2.32}$$

Taking into account the definition of the local coordinates (ξ,η,ζ) given in 2.2.3 the integral (2.31) becomes

$$[k]_e = \int_{-1}^{+1}\int_{-1}^{+1}\int_{-1}^{+1} [B]^T[D][B]\,|J|\, d\xi\ d\eta\ d\zeta \tag{2.33}$$

2.2.6.1 Numerical Integration of Expression (2.33)

The element stiffness matrix is assembled by numerical integration of the expression (2.33). Using the Gaussian Quadrature formula Ref.(51) as a definite integral, $\int_{-1}^{+1} f(x)dx$ is replaced by a summation $\sum_{j=1}^{n} C_j f(a_i)$ where C_j are the weight coefficients, a_i are the Gauss abcissae and n the number of Gauss points.

To evaluate the integral (2.33) over the volume of the element the summation referred above will be used three times,

$$[K]_e = \sum_{m=1}^{n}\sum_{j=1}^{n}\sum_{i=1}^{n} C_m\, C_j\, C_i f(\xi_i,\eta_j,\zeta_m) \tag{2.34}$$

where f in this case is the function $[B]^T[D][B]|J|$.

2.2.6.2 Elasticity Matrix and its Economical Use.

The elasticity matrix for isotropic materials (52) will be defined as follows

$$[D] = \frac{E}{(1+\nu)(1-2\nu)} \begin{bmatrix} 1-\nu & \nu & \nu & 0 & 0 & 0 \\ & 1-\nu & \nu & 0 & 0 & 0 \\ & & 1-\nu & 0 & 0 & 0 \\ & & & \frac{1}{2}-\nu & 0 & 0 \\ & \text{symmetric} & & & \frac{1}{2}-\nu & 0 \\ & & & & & \frac{1}{2}-\nu \end{bmatrix} \tag{2.35}$$

where E is the Young's modulus and ν the Poisson's ration.

The multiplication of the three matrices of (2.33) involves a very large number of arithmetic operations.

Owing to the presence of a large number of zero elements in these matrices Irons suggested a method which improves the matrix forms and reduces the number of operations considerably. This feature which was inherited from the initial version of the DIM3B code is described in detail in Ref.(53) and, therefore, will not be included here.

2.2.7 Equivalent Nodal Forces

In general a structure is loaded by surface forces acting on finite areas. For the FEM this loads must be converted into consistant nodal forces by the use of the expression

$$\{F_g\}_e = \int [N]^T \{g\} \, dA \tag{2.36}$$

where $\{g(x,y,z)\}$ is a vector representing the applied load and $[N]$ the shape function matrix.

Assume the pressurized face is $\zeta = \pm 1$, an element of area δA in this face will be

$$\delta A = \delta\xi\delta\eta \tag{2.37}$$

or in vector notation

$$\delta\vec{A} = \delta\vec{\xi} \times \delta\vec{\eta} \tag{2.38}$$

where the product is a vector product, and the direction of $\delta\vec{A}$ is normal to the surface $\zeta=\pm 1$.

Expression (2.38) can be written also as

$$\delta\vec{A} = \begin{Bmatrix} \delta A_x \\ \delta A_y \\ \delta A_z \end{Bmatrix} = \begin{Bmatrix} \frac{\partial x}{\partial \xi} \\ \frac{\partial y}{\partial \xi} \\ \frac{\partial z}{\partial \xi} \end{Bmatrix} \times \begin{Bmatrix} \frac{\partial x}{\partial \eta} \\ \frac{\partial y}{\partial \eta} \\ \frac{\partial z}{\partial \eta} \end{Bmatrix} d\xi d\eta \tag{2.39}$$

$$= \text{Det} \begin{bmatrix} \hat{x} & \hat{y} & \hat{z} \\ \frac{\partial x}{\partial \xi} & \frac{\partial y}{\partial \xi} & \frac{\partial z}{\partial \xi} \\ \frac{\partial x}{\partial \eta} & \frac{\partial y}{\partial \eta} & \frac{\partial z}{\partial \eta} \end{bmatrix} d\xi d\eta \tag{2.40}$$

where $\hat{x}$, $\hat{y}$, and $\hat{z}$ are cartesian unit vectors.

The jacobian matrix $[J]$ (see expression (2.20)) has an adjoint

$$\text{adj}\,[J] = \begin{bmatrix} J_{11} & J_{21} & J_{31} \\ J_{12} & J_{22} & J_{32} \\ J_{13} & J_{23} & J_{33} \end{bmatrix} \tag{2.41}$$

where, for instance, J_{21} is the cofactor of the (2,1) term in the expression above.

$$J_{21} = \begin{vmatrix} \frac{\partial y}{\partial \xi} & \frac{\partial z}{\partial \xi} \\ \frac{\partial y}{\partial \zeta} & \frac{\partial z}{\partial \zeta} \end{vmatrix} \tag{2.42}$$

Thus expression (2.40) is re-written as follows

$$\delta\vec{A} = (J_{31}\,\hat{x} + J_{32}\,\hat{y} + J_{33}\,\hat{z}) \tag{2.43}$$

In general, if the pressure is applied in face i where i=1 for $\xi=\pm 1$, i=2 for $\eta=\pm 1$, i=3 for $\zeta=\pm 1$

$$\delta\vec{A} = (J_{i1}\,\hat{x} + J_{i2}\,\hat{y} + J_{i3}\,\hat{z})\;\; d\alpha\, d\beta \tag{2.44}$$

where α,β are the two coordinates of ξ,η,ζ parallel to the loaded face.

Expression (2.36) may now be written as

$$\{F_g\}_e = \int [N]^T \begin{bmatrix} g_x & 0 & 0 \\ 0 & g_y & 0 \\ 0 & 0 & g_z \end{bmatrix} \begin{Bmatrix} dA_x \\ dA_y \\ dA_z \end{Bmatrix} \tag{2.45}$$

$$= \int [N]^T \begin{Bmatrix} J_{i1} & g_x \\ J_{i2} & g_y \\ J_{i3} & g_z \end{Bmatrix} \quad d\alpha\, d\beta \tag{2.46}$$

The integration is performed numerically using again the Gaussian Quadrature formulae.

2.2.8 Evaluation of Stresses

Once the nodal displacements have been calculated by the overall solution of equation (2.2), the stresses are calculated at node points. At node i the stress vector is given by

$$\{\sigma\} = [D][B]\{\delta\}_e \tag{2.47}$$

where [B] is calculated using values of the shape functions at node i.

2.3 Description of the code DIM3B

2.3.1 Introduction

In the previous programs, NAMAIN Ref.(49) and DIM3 Ref.(50), special subroutines were developed to perform the initialization work and carry out the book-keeping procedures before entering the actual solution stages. These subroutines generate the necessary data to perform the analysis of the particular problems being studied, with the use of very small sets of input data.

Although it is recognised that manually assembled programs may be advantageous for research purposes, any potential user of these codes would have to face enormous difficulties if a new class of problems is to be studied.

The idea to create a general purpose 3D finite element program was the main reason for the development of the DIM3B code.

One disadvantage, of course, is that the potential user of such a program is faced with the tedious and sometimes difficult task of producing large amounts of input data.

However, he will be strictly concerned with his particular problem without being involved in the more difficult and complicated programming aspects of the code.

The problem of producing this type of data can be eased with the use of automatic data generation techniques, and this method has been adopted throughout the work

reported in this thesis.

2.3.2 The Solution Technique of Equation (2.2)

Remembering equation (2.2), the stiffness matrix of the overall assemblage relates the nodal forces F acting on the structure to the corresponding nodal displacements δ.

The stiffness matrix may be characterized in general as symmetric, banded, positive definite and sparsely populated.

Prescribed displacements, which are physically required to preserve equilibrium as well as to specify initial displacements at certain nodes, are accommodated in the solution technique. A suitable partitioning of the equation (2.2) is performed as

$$\begin{bmatrix} M_{KN} & M_U \\ M_U^T & M_{UN} \end{bmatrix} \begin{bmatrix} \delta_{KN} \\ \delta_{UN} \end{bmatrix} = \begin{bmatrix} F_{UN} \\ F_{KN} \end{bmatrix} \tag{2.48}$$

where δ_{KN} and δ_{UN} are known (prescribed) and unknown nodal displacements respectively. The corresponding unknown and known generalized forces are F_{UN} and F_{KN}.

The expansion of equation (2.48) yields

$$M_{KN}\,\delta_{KN} + M_U\,\delta_{UN} = F_{UN} \tag{2.49}$$

$$M_U^T\,\delta_{KN} + M_{UN}\delta_{UN} = F_{KN} \tag{2.50}$$

or

$$M_{UN}\delta_{UN} = F_{KN} - M_U^T\delta_{KN} \tag{2.51}$$

$$F_{UN} = M_U\delta_{UN} + M_{KN}\delta_{KN} \tag{2.52}$$

From equation (2.51) the unknown nodal variables can be calculated by an extension of the Gaussian elimination process. In the backward substitution stages, as the elements of δ_{UN} are explicitly known, the unknown reactions F_{UN} can also be found.

2.3.3 Frontal Method of Solution (FMS)

The use of these three dimensional elements with 3x20 or 3x32 degrees of freedom implies large dimensions of the stiffness matrix k, which is equal to the number of degrees of freedom in the structure. Normally these matrices cannot be fully assembled and stored in fast core.

The FMS is suitable for such cases and is used in this program with the Gaussian Elimination technique.

This method was first introduced by Irons (54) and is based on the fact that only a small amount of the banded matrix has to be processed before forward elimination of a variable corresponding to a row. After the elimination process, data pertaining to the variable is stored on a disk file and the row is freed. Thus a variable becomes active on its first appearance and is eliminated immediately after its last.

Due to this method the total number of equations (one per variable) is not anymore the limiting factor, rather it is the semi-band with in the case of the matrix k.

A simplified version of this method is described in detail in Appendix 1 as used in the FRONT code.

2.3.4 Program Breakdown

This section describes the general layout of the program and gives a survey of each subroutine included in the program.

An User's Guide of DIM3B code is given in Appendix 2, which contains a definition of the relevant program variables which will be mentioned in this section. A quick reading of that Appendix may be useful if difficulties are encountered in reading this section.

The DIM3B code consists of four main parts

A - Initializations

B - Determination of forces; evaluation of coefficients for assemblage of stiffness matrices by numerical integration.

C - Solution of the overall stiffness matrix; determination of displacements

D - Backward substitution; stress determination.

Some of the initialization procedures and parts B and C are performed in a general DO LOOP element by element as is shown on a primary flow chart in Fig. 2.2. A more

detailed flow chart of DIM3B code is shown in figure 2.3.

A - Initializations

In this initial part, the program reads the input data concerned with the description of the two basic systems (basic and global) as well as numerical data for the Gaussian integration procedures, all these data correspond to the first five input data cards.

After checking these data, the matrix TP relating the two basic systems is evaluated. The elasticity matrix EI is calculated and then the P matrix is formed.

The subroutine INIAL is now called and the resulting integer values NUNKVA, NKNVA, NCELNO, NCELN1, NT, NTOTAL, NUNVA1 and NKNVA1 are calculated and printed out.

The subroutine NODE is called by INIAL and forms the ELNODE and PRENIC arrays which describe the topology of the structure including the last appearances adding a minus sign to the respective nicknames.

The ELNODE matrix is stored in a random access file using non-standard subroutines available in the CDC system at ICCC and ULCC.

The matrix UNKMAT, UNKNIC, UNCLE, KNOMAT, KNONIC, KNORHS and UNRHS are reset to zero and the dimensionless local coordinates are defined depending on the type of element (20 or 32 node).

Finally the global coordinates are fed into the program together with nodal point forces RHSI. If the global system for input is cylindrical or spherical the subroutine GTRANS is called from the main program and transforms the coordinates into cartesian coordinates.

B - Determination of forces, stiffness matrices

From now on the program proceeds within a general DO LOOP until all finite elements have been processed.

Firstly, stress data are fed into the program and the equivalent nodal forces RHSL are calculated in subroutine LOAD called by the main program.

Prior to this, subroutine COORD is called and sets up nodal matrices TR which are going to be used in subroutine LOAD to transform the local components RHSL into new components TRHSL, referred to the main problem system.

The subroutine COORD also stores the nodal coordinates in a random access file no.2.

The equivalent nodal point forces TRHSL are added to the initial prescribed nodal point forces RHSI and the sum RHSRED of the components of these forces will be used on the right hand side of the stiffness equations. These values eventually can be printed out.

In the subroutine LOAD, numerical integrations are performed (see section 2.2.7) using the shape funtions DE and their partial derivatives with respect to the local coordinates.

The subroutines SHAP2O and SHAP32 containing these functions and its derivatives are called when necessary, one or the other according to the elements in use.

The main program now calls the subroutine FEM from which the components SK of the stiffness matrix are evaluated (see section 2.2.6).

The subroutine STFTR is called next, and distributes the SK coeficients over the UNKMAT, KNOMAT and UNCLE matrices. According to equation (2.48) KNOMAT, UNKMAT and UNCLE correspond to the partial matrices M_{KN}, M_{UN} and M_U respectively.

In fact

UNKMAT = Submatrix corresponding to nodes with unknown displacements

KNOMAT = Submatrix corresponding to PRENIC

UNCLE = Off diagonal submatrix of [k]

KNORHS = Known submatrix of load vector

UNRHS = Unknown submatrix of load vector

KNONIC = Addresses of known subvector of displacements

UNKNIC = Addresses of unknown subvector of displacements

The distribution of these matrices is shown again as they are kept in the program.

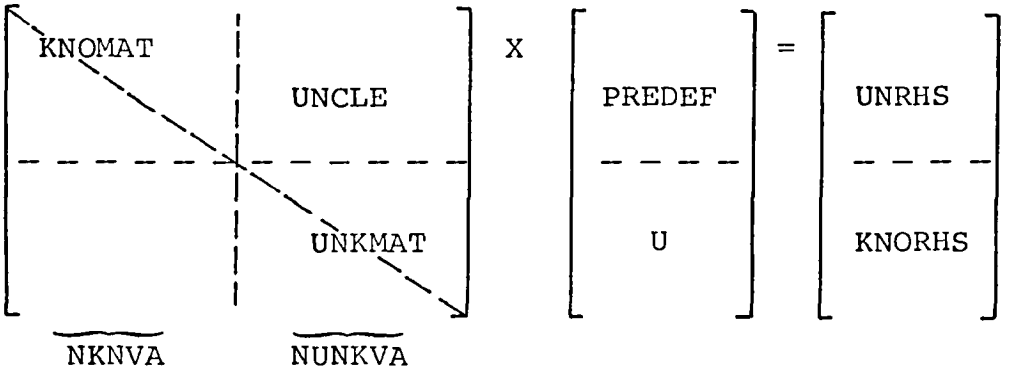

Due to symmetry of this matrix only the upper triangles and leading diagonals are kept in the computer.

In terms of computer variables expressions (2.51) and (2.52) will become

UNKMAT * U = KNORHS - UNCLE^T * PREDEF

UNRHS = KNOMAT * PREDEF + UNCLE * U

where

PREDEF = Submatrix containing the known displacements (boundary conditions)

U = Submatrix where the vector solution will be stored.

C - Solution of the overall stiffness matrix

The forward elimination process for each frontal position is performed in subroutines FORWD and BUFFER. During the forward elimination process the system of equations (2.51) and (2.52) is solved by the Gaussian Elimination Method as follows.

Suppose the set of equations is

$$\begin{array}{ll} (e_1) & S_{11}\delta_1 + S_{12}\delta_2 + \ldots + S_{1n}\delta_n = F_1 \\ (e_2) & S_{21}\delta_1 + S_{22}\delta_2 + \ldots + S_{2n}\delta_n = F_2 \\ & \cdots \\ (e_n) & S_{n1}\delta_1 + S_{n2}\delta_2 + \ldots + S_{nn}\delta_n = F_n \end{array} \qquad (2.53)$$

and when δ_s is eliminated with the use of equation e_s one obtains

$$S_{ij}^* = S_{ij} - (S_{is}S_{sj}/S_{ss}) \qquad (2.54)$$

$$i=1,2 \ldots n, (i \neq s)$$

or

$$S_{ij}^* = S_{ij} - Q^*S_{sj} \qquad (2.55)$$

where $Q = S_{is}/S_{ss}$

and the modified right hand side

$$F_i^* = F_i - Q\,F_s \qquad (2.56)$$

$$i=1,2,\ldots n$$

These elimination procedures are performed in subroutine FORWD in the following manner. A completed row composed of NUNKVA coefficients retrieved from UNKMAT and NKNVA coefficients retrieved from UNCLE is stored in an auxiliary array COMP and the factor Q (see exp. (2.55)) is evaluated.

The submatrices KNOMAT, UNCLE and UNKMAT are modified according to expression (2.55).

The stored equation space is released and the data contained in COMP is transferred to a buffer area. Also the known and unknown righthand sides are calculated according to expression (2.56) and then placed in a buffer area. Finally, all the working variables used are reset for the next forward elminiation.

Writing on a diskfile takes place in blocs for all the eliminated nodes, in order to reduce the number of tape operations, this is done using subroutine BUFFER which is called from subroutine FORWD where all the data already stored in a buffer area are to be tranferrred for a random access file.

D - Backward substitution, Evaluation of stresses

When the general DO LOOP in the main program has processed all the elements, all the evaluated upper triangular overall matrix, including the leading diagonal, is stored on disk.

The main program calls subroutine BACKWD to calculate the nodal displacements.

This subroutine firstly reads back from the random access file the stored data in blocks in a reversed order.

Starting with the last eliminated node the unknown displacements are now obtained directly.

$$\delta_n = F_n^* / S_{nn}^* \tag{2.56}$$

and the rest are obtained from the formula

$$\delta_s = (F_s^* - \sum_{i=s+1}^{n} S_{si}^* \delta_i) / S_{ss}^* \tag{2.57}$$

where s = n-1, n-2, ... 2,1

In terms of program variables the above expression, using the same index notation, will be written as follows:

$$U_s = (KNORHS_s - \sum_{i=s+1}^{n} UNCLE_{si}^T * PREDEF_i) / UNKMAT_{ss} \tag{2.58}$$

If the index s corresponds to a prescribed deflection, the respective unknown reaction is computed using the already calculated unknown displacements U_{s+1}, U_{s+2} . . . in the following manner.

$$UNRHS_s = KNOMAT*PREDEF + UNCLE * U \tag{2.59}$$

The unknown reactions and the displacement solution eventually can be printed out using subroutine DEFOUT.

A brief summary of the procedures involved in subroutines FORWAD and BACKWD are described below.

Subroutine FORWAD

If in presence of an unknown displacement

(i) Storing completed row in a row matrix COMP

(ii) Modify KNOMAT, UNCLE, UNKMAT and RHS matrices

(iii) Release the stored equation space

(iv) Storing required data in buffer area (sub.BUFFER)

(v) Reset for the next element.

If in presence of a prescribed deflection

(i) Storing completed row terms of KNOMAT and column terms of UNCLE in COMP

(ii) Modify the unknown right hand side RHS

(iii) Storing required data in buffer area (sub.Buffer)

(iv) Reset for the next element.

Subroutine BACKWD

(i) Initialization (reset KNONIC, UNKNIC, KNORS)

(ii) Read back stored data in blocks in reversed order.

If in presence of an unknown displacement

(iii) UNCLE is multiplied with known displacements

(iv) UNKMAT is multiplied with known displacements except the diagonal term

If in presence of a prescribed deflection

(iii) Multiply KNOMAT with PREDEF

(iv) Multiply UNCLE with UNKDEF now stored in RHS

(v) Evaluate the corresponding unknown reactions.

If stresses are required by specifying the control parameter IOUT=2, the subroutine STRESS is called by the main program. The output results for the displacements are used here to compute nodal stresses using expression (2.16) described in section 2.2.4.

The matrix product $[D][B]$ (sometimes is referred to as "stress" matrix) is evaluated in subroutine FEM2 using again the shape functions DE stored in subroutines SHAP20 and SHAP32.

The stresses referred to the main problem system are calculated using TR matrix already described.

$$[\sigma]_{MP} = [TR]^T [\sigma]_{L\ C} [TR] \qquad (2.60)$$

where $[\sigma]_{MP}$ are the stresses referred to the main problem system which are obtained from the stresses, $[\sigma]_{LC}$, obtained from expression (2.16) and are referred to the local system of coordinates (ξ,η,ζ).

If various elements meet at one node, the stresses are averaged, i.e., the final result will be the mean of values obtained for that particular node from each element.

The nodal stresses, if so desired, are printed out by calling subroutine STROUT.

As it can be seen from figure 2.3, the main program although spread in the central column from the top to the bottom of the page, is indeed, a relatively small and simple routine. Its basic function is to call the various modules in an appropriate manner.

2.3.5 Program Environment

The DIM3B code is a program written in FORTRAN IV language.

One of the main features of this program as compared to its predecessors (NAMAIN and DIM3) is related to the transfer of data into back-up store files. In the previous versions these operations have been made with the use of the standard READ and WRITE Fortran statements, (see Ref.(55)).

The physical time involved in these operations has been drastically reduced by the implementation of special subroutines READMS and WRITMS which are presently available in the CDC machines at ICCC and ULCC. These subroutines transfer large amounts of data to random access files with the use of mass storage devices.

Several other technical aspects regarding the operation with this program are described in more detail in Appendix 2.

C H A P T E R 3

THE FINITE ELEMENT METHOD APPLIED TO LINEAR ELASTIC FRACTURE MECHANICS

3.1 Introduction

A number of solutions for SIFs and strain energy release rates, G, have been obtained using the more accurate methods which have already been outlined in Chapter 1.

Unfortunately these solutions have been limited in the past, to idealized and relatively simple-shaped configurations and, in several cases, these solutions are far from providing the engineer with good estimates of SIFs for the more complex configurations of actual problems.

The FEM, which was originaly designed as a versatile tool to solve general problems in structural analysis, has become also a useful method when dealing with such complex LEFM applications.

The next section will review the various finite element techniques used for calculating SIFs and strain energy release rates for cracked bodies.

It has been shown (section 2.2.3, Chapter 2) that the displacement fields within the element (expressions 2.12 and 2.13) are described by continuous polynomials (shape functions) of the second and third order depending on the type of the element used.

These elements, having these type of shape functions, are obviously unable to describe in an adequate manner the

square root behaviour of the displacement components and the subsequent singularity fields in stresses and strains near the crack tip. Moreover, the deteriorated solutions obtained in those areas with the use of conventional elements may eventually cause the propagation of errors into larger regions away from the crack tip.

The need to use relatively coarse meshes in 3D finite element analysis, due to the limitations of present generation computers, leads to the compulsory use of special elements with embedded singularity fields modelled by the introduction of a square root term in their displacement functions.

Various planar elements of this type have been developed and have been reviewed by Rice and Tracey (65), Jerram and Hellen (66) and Atluri et al. (67).

In the three dimensional family of elements Blackburn (68) introduced an element containing an $r^{\frac{1}{2}}$ displacement function which was implemented in the BERSAFE system in the CEGB Research Department. Tracey also developed a wedge-shaped element which is described in Ref. (69). The former is compatible with the 20-node isoparametric elements whereas the latter can be used with 8-node linear isoparametric brick-type elements.

Although these elements have been used successfully by Hellen and Dowling (2) and Schmit et al.(4), they have specific stiffness formulations and differ from their related conventional elements. Therefore the implementation of these elements has the disadvantage of requiring major

alterations in the initial standard computer programs.

In section 3.3 of this Chapter, it is shown how a "crack tip element" can be derived from the isoparametric elements previously described in Chapter 2 without requiring specific changes in the standard computer program DIM3B.

The final sections of this Chapter will describe the results obtained in several tests which have been carried out to assess these "crack tip elements".

3.2 Finite Element Techniques in LEFM

3.2.1 - Introduction

The various techniques for determining SIFs using finite element methods can be divided into three groups. Firstly, those utilizing directly the computed stresses and displacements obtained from standard finite element programs. Secondly, those in which the rate of reduction of potential energy of the body with respect to increasing crack length, G, is calculated, hence K.

A third group of techniques involves a simultaneous use of the FEM and the analytical near tip expansions.

In this third method, which was developed by Wilson (62), a displacement pattern associated with the leading terms of the Williams stress function (64) is imposed in a small circular area(*) (for 2D problems) near the crack tip. This region is then coupled with the more conventional finite elements in order to model the areas away from the crack tip.

(*) This circular region can be eventually regarded as another special crack tip element.

This method was well described by Hilton and Sih in Ref.(63) in which results are given for some planar cases.

3.2.2 - The Direct Method

3.2.2.1 - The Stress Method

One of the more straightforward methods of calculating the SIFs of cracked bodies is to correlate the stresses at nodal points of the finite element mesh with those of the near tip stress field which are given for the opening mode I by

$$\sigma_{ij}(r,\theta) = \frac{K_1}{\sqrt{2\pi r}} f_{ij}(\theta) \qquad (3.1)$$

where r, θ are the polar coordinates centred at the crack tip, and $f_{ij}(\theta)$ is a known function of θ (see expression 1.5, Chapter 1).

Earlier work using this method has been done by Chan et al.(70). They applied this approach to a compact tension test piece, symmetric about the crack, and found that good results could be obtained by substituting the σ_y (y being normal to the crack line) stress components ahead of the crack (θ=0), and the distance, r, of the node from the crack tip into equation (3.1).

A discrepancy of about 10% in relation to a collocation method(*) was reached at the cost of a highly refined mesh.

(*) The collocation solution is believed to be accurate within 0.5% (see Ref(63)).

In the stiffness formulation of the FEM it is well known that the computed stresses are directly obtained through the strains by differentiating the displacement fields which means that the functions which model the stress fields within the elements are of one order lower than the displacement functions.

In fact Chan et al.(70) confirmed that a better estimate of the SIFs could be obtained with the use of the computed displacements rather than the stresses.

3.2.2.2 - The Displacement Method

Similarly to the stress method, the displacement technique requires a correlation of the finite element nodal point displacements with the known crack tip displacement field solutions (see section 1.3.3). For plane strain opening mode I, these solutions are:

$$u_i = \frac{K_1}{\mu} \sqrt{\frac{r}{2\pi}} \quad f_i(\theta,\nu) \tag{3.2}$$

where $u_1 = u, \quad u_2 = v$

$$f_1(\theta,\nu) = \cos\left(\frac{\theta}{2}\right) \left[1 - 2\nu + \sin^2\left(\frac{\theta}{2}\right) \right]$$

$$f_2(\theta,\nu) = \sin\left(\frac{\theta}{2}\right) \left[2 - 2\nu - \cos^2\left(\frac{\theta}{2}\right) \right]$$

By substituting the computed displacements u_i^* and the respective distances r_i^* into expression (3.2) the SIF will be obtained by extrapolating the curve

$$K^* = \frac{\mu u_i^*}{f_i(\theta,\nu)} \sqrt{\frac{2\pi}{r_i^*}} \qquad (3.3)$$

towards the line r*=0.

It should be remembered that expression (3.2) describes only the first term of the Westergaard solution, and it is only valid for regions very close to the crack tip. On the other hand the computed values u_i^*, are normally less relaible in that area, thus the need to extrapolate values of K* from regions far away from the crack tip and using large values of r*.

Some improvements of the extrapolation procedures can be obtained either by retaining higher order terms in expression (3.2) or by acquiring, at least, some knowledge of the K* curve in regions away from the crack tip.

The displacement expansions for the case of plane strain conditions can be derived from the Williams stress function (71) as follows

$$2\mu v = A_1 B_1 r^{\frac{1}{2}} - A_2 B_2 r - A_3 B_3 r^{3/2} + \ . \ . \ . \qquad (3.4)$$

where $A_1 = - \frac{K_1}{\sqrt{2\pi}}$

μ is the shear modulus

$B_i = B_i(\theta,\nu)$ similarly to $f_{ij}(\theta,\nu)$ (*)

By substituting the value of A_1, expression (3.4)

(*) These coefficients as described by Williams in Ref(64) contain some typographical mistakes which have been corrected by Rook and Cartwright(27) and Ewing et al.(71)

becomes

$$K^* = K_1 - \frac{\sqrt{2\pi}}{B_1} \left(- A_2 B_2 r^{\frac{1}{2}} - A_3 B_3 r + \quad \right) \qquad (3.5)$$

where $K^* = - \frac{2\mu v}{B_1} \sqrt{\frac{2\pi}{r}}$ similarly to expression (3.3).

By inspection of the functions B_i it can be shown that $B_2=0$ when $\theta=\pi$ thus expression (3.5) becomes

$$K^* = K_1 + \frac{\sqrt{2\pi}}{B_1} (A_3 B_3 r + \ . \ . \ .) \qquad (3.6)$$

Therefore a plot of values of K* vs. r should be expected to behave in a linear manner up to relatively large values of r.

The first seven coefficients A_i have been obtained by Leevers (72) using a variational method as it applies to the Williams series solution to the crack problem in a single edge notch geometry under plain strain conditions.

The various K* curves for various ratios a/w represented in Figure 3.1 show that for this type of configurations the variations found in the evaluated coefficients A_2, A_3.. ..A_7, have a very small effect on the overall behaviour of those curves regarding their linearity or otherwise.

It is clear from this figure 3.1(*) that in the case of $\theta = \pi$ the influence of the square and higher order terms is

---

(*) The squares and circles in this figure will be referred to later on.

practically negligible over a range of r values up to about 80% of the crack length. However the use of the extrapolation method in the direction $\theta=\pi/2$ becomes much less reliable due to the strong influence of the square root term in expression (3.5), and in this case the extrapolated SIFs are bound to overestimate the true solution.

3.2.3 - Energy Methods

Finite element techniques using the energy method are based on the LEFM relation

$$P_i \frac{d\Delta_i}{dA} - \frac{dU}{dA} = G = \frac{K^2(1-\nu^2)}{E} \qquad (3.7)$$

for plane strain conditions, where A is the area of the crack surface. The energy available for an increment of crack area dA is provided from the work done by the forces P_i when displaced in the direction of its application of an amount $d\Delta_i$, and the release - dU of the total strain energy U, stored in the cracked body.

In fact the terms in the left-hand side of expression (3.7) account for the well known "constant load" and/or "fixed grip" conditions.

The strain energy due to the highly localized crack tip stress fields should be small compared with the total energy of the body, also the overall deflection of the body is only slightly affected by these stress fields. Thus the need to use either special tip elements or highly refined meshes, is not so critical as in the case when the direct methods are applied.

For planar cases the direct application of expression (3.7) obliges the finite element analysis to be performed twice, as described by Dixon and Strannigan (73), thus increasing considerably the computing costs of such an analysis.

In three dimensional applications the problem is complicated many-fold. If localized SIFs are to be evaluated, a set of successive runs must be carried out and small and localized extensions of the crack front must be assumed.

A variety of techniques have been put forward to simplify and improve the efficiency of these energy methods.

Jerram (74) suggested that the strain energy release rates, G=dU/dA, could be obtained by evaluating the amount of work required to close successive nodal intervals along a crack. This procedure is illustrated in Figure 3.2 and is particularly useful when the plane of the crack is a plane of symmetry of the body.

For this case Broekhoven and Spaas (75) have shown that the associated change of strain energy with successive crack extensions (modelled by unpinning successive nodes) can be written as

$$\Delta U_{i \to i+1} = \sum_{l=n}^{m} \frac{1}{2} P_{n_i} u_{n_{i+1}} \qquad (3.8)$$

where $\Delta U_{i \to i+1}$ is the change in strain energy due to extension from crack front i to crack front i+1

$n = 1,2 \ldots m$, is the number of node released

P_{n_i} is the nodal force of node n for crack front i

$u_{n_{i+1}}$ is the v displacement of node n due to its unpining

$i=1,2, \ldots$ indicates uncracked geometry.

This technique sometimes called "crack closure work" has been successfully used by Broekhoven and Spaas (75) in some three dimensional applications.

Bueckner (76) developed a similar technique to the "crack closure work" method. He has shown that the problem of evaluating the rate of change of strain energy with increasing crack length in a loaded body is the same as evaluating the rate of change of work done by tractions acting on the surface of the crack when the body is free from the initial loads.

The basis of Buekner's method as applied to the finite element technique is indeed very similar to the Paris and Sih replacement method which was briefly described in section 1.3.4.

The "J integral" method developed by Rice (77) has also been successfully applied to 2D cases by Chan et al.(70) and Neal (78). Its application to 3D problems seems to be rather complicated and no work using this technique was yet found in the literature.

Quite recently Parks (79) has developed a "stiffness derivative procedure" in which K values can be obtained directly by differentiating the potential energy of the finite element solution

$$P = \frac{1}{2} \{u\}^T [k] \{u\} - \{u\}^T \{f\} \tag{3.9}$$

with respect to crack length a of a 2D body under constant load conditions

$$\left.\frac{dP}{da}\right|_F = \frac{1}{2} \{u\}^T \frac{d[k]}{da} \{u\} \tag{3.10}$$

If the crack surfaces are load free then

$$-\left.\frac{dP}{da}\right|_F = \left.\frac{dU}{da}\right|_F = G = \frac{K^2(1-\nu^2)}{E} \tag{3.11}$$

where P is the potential energy

U is the strain energy

$\{u\}$ is the vector of nodal displacements

$[k]$ is the global stiffness matrix

$\{f\}$ is the vector of prescribed nodal forces.

This method has been recently used by Hellen (80) in 2D configurations. Broekhoven and Spaas (75) and Schmit et al. (4) applied this method to problems of cracked nozzles.

All computing efforts involved with the use of energy methods can be substantially reduced if the Front Method of solution is adopted in finite element programs.

These advanced numerical procedures for estimating G have been described by Hellen (80), Parks (79) and Broekhoven and Spaas (75).

Small extensions of the crack front can be modelled by changes of the few elements adjacent to the crack front.

In the case of the Parks method, for example, the only contributions to the d [k] term in expression (3.10) are provided by the elements containing the translated nodal points. Moreover if the nodes of the crack front and the elements containing them are suitably numbered, the values of d [k] to be used in expression (3.10) can be obtained by repeating (for an extended crack) only the very last stages of the forward elimination procedure.

If the displacements and stresses are not required for the entire structure, the components of the vectors $\{u\}$ and $\{u\}^T$ related to the non zero terms d [k] are then evaluated by carrying out only a few steps of the backwards substitution. In conclusion, it can be said that energy methods are bound to be more accurate as compared to the direct techniques. However, an efficient use of the former methods may involve a reasonably large effort in their implementation on a standard computer program as in the case of DIM3B.

On the other hand the inaccuracies involved with the application of the direct method with the use of "crack tip elements" are expected to be small enough at least for engineering purposes.

Finally, in Figure 3.3 the more relevant methods used to date to study 3D crack problems are summarized and the methods used in the present work are conveniently indicated.

3.3 - Theory of the Singularity Element

3.3.1 - Introduction

In this section it is intended to show how a singularity in stress and strain fields can be easily accommodated in the isoparametric (20 and 32 node) elements described in Chapter 2. This singularity can be made to occur within these elements at certain nodal points by carrying out some minor mathematical changes in the theory described in the previous Chapter.

3.3.2 - Theory

3.3.2.1 - One line elements

The modelling of near-tip fields by the second order 2D quadrilateral isoparametric elements, in which the mid-side nodes are displaced, has been illustrated by Henshell and Shaw (81) by reference to the corresponding line (1-dimensional) element. The same method is used here.

The equivalent one dimensional elements to the 3D (20,32 node) elements, in terms of the order of the shape functions, are the (3,4 node, respectively) elements, as they are shown in Figure 3.4.

In the second order line element (see Figure 3.4(a)) using a local natural non dimensional coordinate ξ, the coordinate r and displacement u in the global system are expressed in terms of the local coordinate ξ by

$$r = a_1 + a_2\xi + a_3\xi^2 \qquad (3.12)$$

$$u = b_1 + b_2\xi + b_3\xi^2 \qquad (3.13)$$

where the a_i and b_i are constants which are obtained from nodal values of r and u respectively and accordingly to expressions (2.3) and (2.8). In this case $[M]=[1\ \xi\ \xi^2]$ and $\{\alpha\}^T = [a_1\ a_2\ a_3]$.

Let us assume that the mid side node (node 2) can have a varying position identified with the value of p in the general system of coordinates r (see Figure 3.4(a)), thus equation (2.8) will be for this case

$$\begin{Bmatrix} 0 \\ p \\ 2 \end{Bmatrix} = \begin{bmatrix} 1 & -1 & 1 \\ 1 & 0 & 0 \\ 1 & 1 & 1 \end{bmatrix} \begin{Bmatrix} a_1 \\ a_2 \\ a_3 \end{Bmatrix} \tag{3.14}$$

hence

$$a_1 = p\ ;\quad a_2 = 1\ ;\quad a_3 = 1-p.$$

Substituting these values into equation (3.12),

$$r = p + \xi + (1-p)\ \xi^2 \tag{3.15}$$

When p=1 equation (3.15) becomes $r=1+\xi$ which is obviously the transformation of coordinates (0,1,2) to the scaled (-1,0,1).

Developing expression (2.9) for this case and when p=1

$$r= \frac{1}{2}\ (-\xi+\xi^2)r_1 + (1-\xi^2)r_2 + \frac{1}{2}(\xi+\xi^2)r_3 \tag{3.16}$$

To obtain strains, expression (2.18) will be simplified as follows

$$\frac{du}{d\xi} = \frac{dN_1}{d\xi} u_1 + \frac{dN_2}{d\xi} u_2 + \frac{dN_3}{d\xi} u_3 \qquad (3.17)$$

$$= \frac{1}{2} (2\xi-1)u_1 - 2\xi u_2 + \frac{1}{2}(1+2\xi)u_3$$

A plot of the shape functions N_i and its derivatives $f_i = dN_i/d\xi$ is shown in Figure 3.5.

The chain rule (2.21) to obtain the engineering strain ε_r is simplified as follows

$$\frac{du}{d\xi} = \frac{du}{dr} \frac{dr}{d\xi} \qquad (3.18)$$

$$= \frac{du}{dr} [J]$$

Hence

$$\varepsilon_r = \frac{du}{dr} = \frac{du}{d\xi} [J]^{-1} \qquad (3.19)$$

where $[J]^{-1} = (dr/d\xi)^{-1}$ is the inverse of the jacobian of the transformation of coordinates r to ξ .

Combining equations (3.18) and (3.15)

$$\varepsilon_r = \frac{du}{d\xi} \left\{ 1 + 2(1-p)\xi \right\}^{-1} \qquad (3.20)$$

The strain will be singular where

$$1 + 2 (1-p)\xi = 0 \qquad (3.21a)$$

If the singularity is to occur at r=0. i.e. at $\xi = -1$, p must satisfy the equation

$$1 - 2 (1-p) = 0 \qquad (3.21b)$$

$$\text{i.e. } p = \frac{1}{2}$$

Thus the mid-side node must be displaced to a point one quarter of the element length from the node at which the singularity occurs.

We now investigate the order of the singularity substituting $p = \frac{1}{2}$ into equation (3.15)

$$r = \frac{1}{2} + \xi + \frac{1}{2}\xi^2 \qquad (3.22)$$

solving equation (3.22) in terms of r, we have

$$\xi = -1 + (2r)^{\frac{1}{2}} \qquad (3.23)$$

Applying equation (3.13) to each of the nodal points and solving for b_i

$$b_1 = u_2 \; ; \; b_2 = \frac{1}{2}(u_3-u_1) \; ; \; b_3 = \frac{1}{2}(u_3 + u_1 - 2u_2)$$

Substituting these values into equation (3.13) and using expression (3.23) the displacements within the element

will be described as follows

$$u = \frac{2-3\sqrt{2r}+2r}{2}u_1 + (-2r+2\sqrt{2r})u_2 + \frac{2r-\sqrt{2r}}{2}u_3 \quad (3.24)$$

hence

$$\varepsilon_r = \left\{1-\frac{3}{2}(2r)^{-\frac{1}{2}}\right\}u_1 + \left\{-2+2(2r)^{-\frac{1}{2}}\right\}u_2 + \left\{1-\frac{1}{2}(2r)^{-\frac{1}{2}}\right\}u_3 \quad (3.25)$$

which exhibits the $r^{-\frac{1}{2}}$ singularity which occurs at the crack front.

Expressions (3.24) and (3.25) have the same form as expressions (2.12) and (2.29) respectively.

A plot of these new shape functions N_i and its derivatives $f_i = dN_i/dr$ is shown in Figure 3.6.

In the case of the third order line element (see Figure 3.4(b)), following the same steps as in (3.12) and (3.13), the transformation of coordinates will be

$$r = a_1 + a_2\xi + a_3\xi^2 + a_4\xi^3 \quad (3.26)$$

$$u = b_1 + b_2\xi + b_3\xi^2 + b_4\xi^3 \quad (3.27)$$

In the same manner, the intermediate nodes (2 and 3) are assumed to have varying positions identified with the values p_1 and p_2. Similarly to expression (3.14) the values of a_i, i=1,2,3,4 can then be evaluated.

$$a_1 = \frac{1}{8} + \frac{9}{16}(p_1 + p_2)$$

$$a_2 = -\frac{1}{8} + \frac{27}{16}(p_2 - p_1)$$

$$a_3 = \frac{9}{8} - \frac{9}{16}(p_1 + p_2) \qquad (3.28)$$

$$a_4 = \frac{9}{8} - \frac{27}{16}(p_2 - p_1)$$

Following for this case the steps (3.18) to (3.20)

$$\frac{dr}{d\xi} = a_2 + 2a_3\xi + 3a_4\xi^2 \qquad (3.29)$$

and the singularity will be made to occur at r=0 or $\xi = -1$ when

$$\frac{dr}{d\xi} = 0 \quad \text{for} \quad \xi = -1 \qquad (3.30)$$

or

$$a_2 - 2a_3 + 3a_4 = 0 \qquad (3.31)$$

Substituting the values a_i (3.28) into equation (3.31) yields to the following equation

$$p_2 = \frac{4}{9} + 2p_1 \qquad (3.32)$$

which corresponds to equation (3.22). The required positions of the intermediate nodes (2 and 3) are not uniquely defined for the third order line element, but related by equation (3.32).

However, if the normal position for node 3 is maintained $p_2 = \frac{4}{3}$, the position of node 2 is then given by (3.3) as $p_1 = 4/9$. For these particular values of p_1 and p_2 the shape functions N_i and its derivatives are represented in Figure 3.7.

It is impossible to solve analyticaly equation (3.26) for ξ in terms of r. However the function $\xi = \xi(r)$ equivalent to expression (3.23) should also contain an $r^{\frac{1}{2}}$ term and subsequently the equivalent to expression (3.25) should also exhibit the $r^{-\frac{1}{2}}$ singularity.

3.3.2.2 - Extension of the singularity in 2D

Let us consider now the 8 node isoparametric element as it is shown in Figure 3.8. In this case expression (3.15) leads to

$$x = p_1 + \xi + (1-p_1)\xi^2 \tag{3.33a}$$

$$y = p_2 + \eta + (1-p_2)\eta^2 \tag{3.33b}$$

The chain rule (2.21) will be as follows

$$\frac{\partial u}{\partial \xi} = \frac{\partial u}{\partial x}\frac{\partial x}{\partial \xi} + \frac{\partial u}{\partial y}\frac{\partial y}{\partial \xi} \tag{3.34}$$

and from (2.23)

$$\begin{Bmatrix} \frac{\partial u}{\partial \xi} \\ \\ \frac{\partial u}{\partial \eta} \end{Bmatrix} = \begin{bmatrix} \frac{\partial x}{\partial \xi} & \frac{\partial y}{\partial \xi} \\ \\ \frac{\partial x}{\partial \eta} & \frac{\partial y}{\partial \eta} \end{bmatrix} \begin{Bmatrix} \frac{\partial u}{\partial x} \\ \\ \frac{\partial u}{\partial y} \end{Bmatrix} \tag{3.35}$$

From equations (3.33) the inverse of the Jacobian can be evaluated as

$$[J]^{-1} = \begin{bmatrix} \frac{1}{1-2(1-p_1)} & 0 \\ 0 & \frac{1}{1-2(1-p_2)} \end{bmatrix} \tag{3.36}$$

If the singularity would be valid for all strains then the following conditions must be imposed

$$p_1 = p_2 = \frac{1}{2} \tag{3.37}$$

Two typical shape functions $N_i = N_i(\xi, \eta)$ are represented in figure 3.10, and the derivatives of these functions at node 1 have infinity values.

Following the same procedures as for the one line element the strain ε_x, for example will be

$$\varepsilon_x = \frac{\partial u}{\partial x} = \left[1 - \frac{3}{2}(2x)^{-\frac{1}{2}}\right] u_1 + \left[-2 + 2(2x)^{-\frac{1}{2}}\right] u_2 + \left[1 - \frac{1}{2}(2x)^{-\frac{1}{2}}\right] u_3 \tag{3.38}$$

the strains for any direction r (see Figure 3.8)

$$x = r \cos \theta \tag{3.39a}$$

$$y = r \sin \theta \tag{3.39b}$$

thus, from expression (3.38)

$$\frac{du}{dx} = f(r^{-\frac{1}{2}}, \cos^{-\frac{1}{2}}\theta, \sin^{-\frac{1}{2}}\theta, u_1, u_2, u_3) \tag{3.40}$$

which means that the singularity holds true for any direction r.

3.3.2.3 - Singularity in 3D elements

Let us consider now a 3D (20 node) isoparametric element as it is shown in Figure 3.9.

By inspection of the Jacobian in expression (2.20) it can be seen that by shifting the nodes 8, 9, 4 and 10 as it is indicated the same type of singularity can occur along the line AB, in planes perpendicular to that line.

Developing new expressions similar to expressions (3.33)

$$x = p_1 + \xi + (1-p_1)\xi^2 \qquad (3.41a)$$

$$y = p_2 + \eta + (1-p_2)\eta^2 \qquad (3.41b)$$

$$z = p_3 + \zeta + (1-p_3)\zeta^2 \qquad (3.41c)$$

if $p_1 = p_2 = .5$ and $p_3 = 1$

$$x = \frac{1}{2} + \xi + \frac{1}{2}\xi^2 \qquad (3.42a)$$

$$y = \frac{1}{2} + \eta + \frac{1}{2}\eta^2 \qquad (3.42b)$$

$$z = 1 + \zeta \qquad (3.42c)$$

therefore the derivatives in the third row of the Jacobian will only contain terms 1 or 0 which will not affect the

bidimensional singularity described in expression (3.40).

Conditions must be met to ensure the square root behaviour in node 2 (see Fig. 3.9) and will be described as follows.

Considering now a local system of coordinates x, y and z defined by nodes 6, 2 and 14. The shape functions of the nodes in the base of the element and for $\xi = 0$ and $\zeta = -1$ are (see exp. 2.13, Chp. 2)

$$N_1 = N_3 = N_5 = N_7 = -\frac{1}{4}(1 - \eta^2)$$
$$N_2 = N_6 = \frac{1}{2}(1 - \eta)$$
$$N_4 = N_8 = \frac{1}{2}(1 - \eta^2)$$

The relationship between y and η can be derived by using exp. 2.11, thus

$$y = \frac{1}{4}(1 - \eta^2)(2y_4 + 2y_8 - y_1 - y_3 - y_5 - y_7)$$
$$+ \frac{1}{2}(1 - \eta^2)y_6 \qquad (3.43)$$

Differentiating y with respect to η it can be shown that the singularity occurs when

$$y_6 = \frac{1}{2}(y_7 + y_5) - \frac{1}{2}(y_1 + y_3) \qquad (3.44a)$$

A similar condition can be derived for node 14 as follows:

$$z_{14} = \frac{1}{2}(z_{13} + z_{15}) - \frac{1}{2}(z_1 + z_3) \qquad (3.44b)$$

2.3.2.4 - Conclusions

A brief summary of the present theory is laid out in order to help to understand the manner in which singularities can occur in isoparametric elements.

Derivatives of displacements with respect to global coordinates x,y,z can be obtained by differentiating expressions (2.14) with respect to local coordinates multiplied by the Jacobian of the tranformation

$$\frac{\partial}{\partial x}, \frac{\partial}{\partial y}, \frac{\partial}{\partial z}, (\delta) = \frac{\partial}{\partial \xi}, \frac{\partial}{\partial \eta}, \frac{\partial}{\partial \zeta}, (\sum N_i \delta_i) \cdot J^{-1} \qquad (3.45a)$$

If the positions of the intermediate nodes i,j,m . . are described by varying parameters p_i, p_j, p_m . . , the Jacobian J will be a function of these parameters and the local coordinates ξ, η, ζ.

$$J = J(p_i, p_j, p_m \ldots, \xi, \eta, \zeta) \qquad (3.45b)$$

Singularities in stress and strain fields can be made to occur at particular nodes, i.e., at particular values of ξ, η, ζ, let us call them ξ_s, η_s, ζ_s, and the particular positions where these intermediate nodes have to be shifted can be found using the condition.

$$J(p_i, p_j, p_m \ldots, \xi_s, \eta_s, \zeta_s) = 0 \qquad (3.45c)$$

this condition will determine a function $g(p_i, p_j, p_m \ldots)$ which is the desired solution. The singularities are of several orders and depend only on the type of the element.

These elements are incompatible with their related conventional versions. However, if nodes i,j,k,l, (see Figure 3.9.) are kept on their original positions the singularity still occurs at the line AB.

If p_1 and p_2 (see figure 3.8) are assumed to vary linearly accross the element in order to satisfy the new positions of nodes 4 and 6 then

$$p_1 = \frac{3}{4} + \frac{1}{4}\xi \tag{3.46a}$$

$$p_2 = \frac{3}{4} + \frac{1}{4}\eta \tag{3.46b}$$

and new expressions (3.33) are derived as

$$x = \frac{1}{4}(3 + 3\xi + \xi^2 - \xi^3) \tag{3.47a}$$

$$y = \frac{1}{4}(3 + 3\eta + \eta^2 - \eta^3) \tag{3.47b}$$

Now, following the same procedures as from (3.34) to (3.38) it can be shown that the new strains ε_x still contain the $x^{-\frac{1}{2}}$ terms.

3.4 - Test Cases

3.4.1 - Introduction

Several series of test cases have been performed to

assess these crack tip elements. Various techniques have been used to generate the finite element meshes for the test case configurations.

A schematic flow chart of the strategy involved in the generation of the finite element data is shown in Figure 3.11.

Basically, a mesh generation program was developed for each configuration. These programs read in the relevant geometric parameters of the problem as well as data describing the loading conditions.

These programs produce three separate sets of data which are written on three separate output tapes. Firstly, the relevant data for execution of program DIMDIM is written on tape DDMDAT. A second tape, DIMDAT, will contain all the data necessary for the execution of DIM3B code.

Finally, data describing the geometry as well as the topology of the mesh is written on a tape called DRDAT. This tape contains the necessary data needed for a plot procedure (program DRAW) using some of the off-line graphic facilities available at the Imperial College Computer Centre.

Some of the data which are needed for the DIMDIM, DIM3B and DRAW codes but which are not relevant ot the mesh generation program, pass through it, unchanged, in the form of card images. These data are for instance, control parameters IIN, IOUT for DIM3B, sequential numbers for DIMDIM code, etc.

Initially, a relatively small job consisting of the execution of the mesh generation program and the subsequent

plotting procedure (execution of program DRAW) is carried out at I.C.C.C. using an "Instanturnround" batch service. The finite element mesh is then checked visually in a TEKTRONIX terminal, using a "QUICK-LOOK" facility available at I.C.C.C., (82) and the rest of the input data can be easily examined by printing out the files DDMDAT and DIMDAT.

The plot file generated by the program DRAW is then processed to generate the necessary magnetic tape format to drive a microfilem plotter (see Reference (83)).

Once the necessary checks have been made a complete run using now the DIM3B and DIMDIM codes is then executed by resubmitting the mesh generation program at U.L.C.C.

The plot procedure, Program DRAW

A general plot program, DRAW, was developed to produce an isometric perspective of the 3D finite element mesh which is obtained by transforming the original coordinates x,y,z into new x',y',z' coordinates.

This transformation, being the result of two rotations, as shown in figure 3.12, one around the z axis by an amount θ_x and the other around the y axis by an amount θ_z will be described by a matrix TF as follows

$$[TF] = \begin{bmatrix} \cos\theta_x\cos\theta_z & \sin\theta_x\cos\theta_z & \sin\theta_z \\ -\sin\theta_x & \cos\theta_x & 0 \\ -\sin\theta_x\cos\theta_z & -\sin\theta_z\sin\theta_x & \cos\theta_z \end{bmatrix} \quad (3.48)$$

Then the new coordinates x',y',z' are obtained by the relation

$$\begin{Bmatrix} x' \\ y' \\ z' \end{Bmatrix} = [TF] \begin{Bmatrix} x \\ y \\ z \end{Bmatrix} \qquad (3.49)$$

By specifying the view angle defined by θ_x and θ_z a prespective can be obtained by plotting the y',z' values as the logical plot coordinates for each nodal point.

The plot is then carried out one element at a time where the order of execution of the logical functions "pen up" and "pen down" are described in Figure 3.13.

Although this procedure involves the repetition of edges pertaining to more than one element it provides an easy check of systematic errors which may occur either in the topological description of the mesh or in the specification of the nodal coordinates.

A listing of the program DRAW is described in Appendix 4.

3.4.2 - Compact Tension Specimens

A mesh was generated, representing one quadrant of a Compact Tension Specimen (CTS) of length 2H, width W and thickness T, having a single edge crack of length 2a in the mid-plane. The specimen and mesh are shown in Figure 3.14.

A primary two-dimensional mesh was developed for the plane x = T/2 and was specified in the form of input data cards. The mesh generation program for this case, based on this two-dimensional type of information, generates all nodal coordinates for the rest of the mesh and subsequently

generates the topological description of the mesh.

Two layers of the 20-node elements were used through the thickness of a quadrant (i.e. four elements through the thickness of the specimen). The number of elements in the quadrant was 88 and the number of nodes 585. A uniform tensile stress was applied at the free end of the quadrant, in the direction normal to the plane of the crack. Appropriate boundary conditions were applied at nodes of faces representing planes of symmetry of the specimen excepting those in the free surface of the crack which were allowed to move freely.

Figures 3.15 and 3.16 show the variations of σ_z stresses ahead of the crack front. In one case, Figure 3.15, the standard 20 node elements were used throughout, in the other case, Figure 3.16, the elements adjacent to the crack front were distorted by displacing the mid-side nodes to the quarter points nearest to the crack front as described in Section 3.3 of this chapter and illustrated in Figure 3.10. Although the results may be somewhat inaccurate, the ability of the distorted elements to model a singularity in stresses is well illustrated in Figure 3.16.

The stress components in the thickness direction, σ_x, in the mid-plane of the specimen (x=0) are also shown in Figure 3.16.

Figure 3.17 shows the mid-element stresses as a function of the distance, x, from the middle surface of the specimen for the elements adjacent to the crack tip. These nodal points are at a distance 0.08T form the crack front.

Although the number of nodal points is very small to draw any quantitative conclusions it may be suggested from the results in Figure 3.17 that the in-plane stresses σ_y and σ_z are nearly constant throughout the thickness except for a rapid fall near the free surface.

The expression for the strain in the thickness direction is given by

$$\varepsilon_x = \frac{1}{E} [\, \sigma_x - \nu(\sigma_y + \sigma_z) \,] \tag{3.50}$$

Levey et al. (84) suggested that the condition of plane strain and plane stress can be described by a parameter, P_s, defined by the ratio

$$P_s = \frac{\sigma_x}{\nu(\sigma_y + \sigma_z)} \tag{3.51}$$

derived from expression (3.50), being unity when ε_x is either zero or bounded (generalised plane strain), and zero under plane stress conditions, $\sigma_x = 0$.

From the results in Figure 3.17 the variation of the parameter P_s has been plotted on the same figure, and it shows an immediate decrease from a maximum value of .72 even in the more central portions of the specimen. However, from the behaviour of the σ_x stresses in Figure 3.16, it is expected that a curve of values P_s in regions very close to the crack tip will be fairly constant reaching values of unity and presenting a drastic drop to values near zero only in a small region near the free surface.

Based on the reasoning referred to above, values of K which are not in the free surface have been obtained directly from the computed displacements by ploting the following function against r/a and extrapolating to r=0.

For plane strain conditions and from expression (3.2) with $\mu = E/2(1+\nu)$

$$K = \lim_{r\to 0} K^* = \frac{E}{4(1+\nu)(1-\nu)}\sqrt{\frac{2\pi}{r}}\, w \qquad (3.51)$$

and values of K at free surfaces have been obtained by using the corresponding plane stress function

$$K = \lim_{r\to 0} K^* = \frac{E}{4}\sqrt{\frac{2\pi}{r}}\, w \qquad (3.52)$$

where w is the displacement component normal to the crack face.

The extrapolation procedures using expressions (3.51) and (3.52) are shown in figures 3.19 and 3.20. In one case, Figure 3.19, the standard 20 node elements have been used whereas in the other case, Figure 3.20, the elements adjacent to the crack front were distorted as was described earlier in this Section. The results have been normalized to the stress intensity factor in an infinite plate ($K_o=\sigma\sqrt{\pi a}$).

By comparing Figures 3.19 and 3.20, the improvement in the value of K, which is obtained by the use of the distorted elements may be seen. The value obtained on the mid-plane using these elements differs by only 2.6% from the value obtained by Brown and Srawley (85) using a two dimensional

plane strain collocation method.

This slight increase in the extrapolated value of K in the mid-plane as compared to the two-dimensional plain strain analysis is in close qualitative agreement with the results shown in Figure 3.18 which were obtained by Yamamoto and Sumi (86) in their 3D finite element analysis of a standard single edge notch specimen (ASTM standard E-399-72).

A table is presented below in which the present results (i) for CTS are compared with those obtained by Leevers (72) (ii) using a 2D plane stress and plain strain analysis (see Section 3.2.2.2) assuming the same configuration with $a/W = 0.25$.

		Values of $K/\sigma \sqrt{\pi a}$
(i)	3D Finite Element Analysis	
	Mid-plane of the specimen	1.54
	Free surface	1.43
(ii)	Williams Series Solutions	
	Plane strain conditions	1.51
	Plane stress conditions	1.51

The discrepancies of the K* curves obtained by the two methods of analysis for this Compact Tension Specimen (see Figures 3.1 and 3.20) could be due to the following reason: if variations in K values have been found with the 3D finite element analysis it is also expected that the coefficients of the higher order terms in expression (3.6) would also vary across the thickness. In fact, by inspection of the

slopes of the K* curves obtained with the finite element method it can be seen that the variation, across the thickness, of the coefficient A_3 in expression (3.6) presents a similar trend to the variation of K values shown in Figure 3.20 .

Figure 3.21(b) shows the results obtained by use of the 32-node elements, distorted as shown in Figure 3.21(a). On the mid-plane close agreement is obtained with the plane strain results of Brown and Srawley.

3.4.3 - Compact Tension Specimens with Curved Crack Fronts

The results obtained for the compact tension specimen, with straight crack front, show a higher value of K in the interior planes, indicating a tendency for the crack to advance with a curved front. There is experimental evidence to support this conclusion (see for example Neale (87), and Johnson and Radon (88)).

In a second series of tests, the mesh was distorted by a simple skewing technique to model curved crack fronts, having the form of circular arcs, in which the ratio of crack front radius R to the specimen thickness T varied between 0.57 and 1.13.

The curved fronts and one of these meshes are shown in Figure 3.22. As in the first series of tests, values of K along the curved crack fronts were obtained by the extrapolation method from the computed displacements.

For these curved crack fronts the extrapolated values of K are expected to be somewhat inaccurate.

This is due to the fact that by using the mesh shown in Figure 3.22(b) the directions of the extrapolation procedures being parallel to the plane yz (see Figure 3.14) make an angle ϕ with the direction perpendicular to the crack front as it is shown in Figure 3.22(a).

This angle, ϕ, varies from zero in the mid-plane of the specimen (x=0) to a maximum in the outer planes and depending on the radius of curvature of the crack front.

If changes of displacements near the crack border possess a certain degree of constancy relative to the direction parallel to the crack front(*) the value of r in expression (3.51) should be replaced, in a first approximation, by the term r cos ϕ,(**). This correction is based on the assumption that for small values of r the differences in the opening displacements at the points A and B, as shown in figure 3.22(a) should be negligible.

It can be seen that the application of this correction factor for large values of r is no longer valid for two reasons: Firstly, the new points A' and B' (see Figure 3.22(a)) would be too far from each other, thus the assumption of displacement constancy between these two points no longer holds true. Secondly, the displacement fields in areas away from the crack tip, and in planes of x=constant, will be

---

(*) As suggested by Irwin in Reference (38)

(**) This type of correction has been already introduced by Sih and Cha (58) by describing the crack border stresses referred to the bi-normal and osculating planes of the crack front curve of an elliptical crack. In their work, another factor, λ is also introduced depending also on the crack front shape. For circular cracks $\lambda = \cos \phi$

mainly governed by the higher order terms of expression (3.4) which are expected to vary across the thickness (see previous Section) and at the same time to be less sensitive to the particulars of the crack front than the variations of the stress intensity factor.

Therefore the K* curve obtained from the extrapolation method should still present its linear behaviour for large values of r and provide a reasonable extrapolated K value. If the finite element mesh were highly refined in the vicinity of the crack front a drop of the K* curve would eventually occur for small values of r which could be corrected then by the introduction of the correction factor suggested earlier on, however, this particular behaviour was not noticeable with the coarse meshes used in the present work.

A comparison of the extrapolation procedures using the computed displacements in the free surface of the crack ($\theta=\pi$) and in planes perpendicular to the crack surface ($\theta = \pi/2$) is shown in Figure 3.23(b) (*) for the more critical curved front case when the ratio R/T is 0.57.

This relatively constant increase in K values obtained from the direction $\theta = \pi/2$ has already been justified earlier in this chapter and supports the assumptions referred to above.

Also, for each radius of curvature, a single value of K was obtained using the energy method based on equation (3.7). In this case the energy available for an increment of crack area dA is provided (see expression (3.7)) by the

(*) Figure 3.23(a) indicates the corresponding results for the straight crack front. The same results are also ploted in Figure 3.1.

work done by the nodal point forces P_i equivalent to the remote stress applied in the top faces of the specimen and required the computation

$$G = 2 \ (\Sigma \ P_i \ dw_i)/dA \ (*) \qquad (3.53)$$

where dw_i are the variations of the displacements, w, in the z direction of the nodal points where the forces P_i are applied. Again the results of K have been normalized to the value of K in an infinite plate. Figure 3.24 shows the results where the single value obtained by the energy method is indicated by a horizontal line. For each of these crack front radii, the value of K obtained for the mid-plane of the specimen was lower than the value obtained for the surface. Figure 3.25 shows a graph of the normalized K, obtained by the energy method, ploted against a parameter which represents the crack front curvature. The figure clearly shows the reduction of K with increasing tunnelling supporting observations of Neale (87).

It should be pointed out that these values of K obtained from the global energy method are associated with the values of K which are obtained experimentally using for example, a compliance test, provided the assumed extension of the crack front is similar to those verified in post mortem observations of a test specimen.

(*) The factor 2 arises from the fact that only one quarter of the specimen is considered.

A factor depending on a tunnelling geometric parameter should be introduced to correct the planar K calibration of a CTS specimen. This factor, based on results similar to those presented in Figure 3.25 would take into account in an adequate manner a possible non conservative interpretation of test data.

3.4.4 - Corner Crack

The mesh for this case, shown in Figure 3.26 was developed from a similar mesh of 20 node elements used in the earlier tests, by a cylindrical skewing technique about the z axis. The number of elements was 88 and the number of nodes was 553. This technique has resulted in an axial groove, see Figure 3.26, which has been made small so that its effect on the results is negligible. This groove could eventually be eliminated by the use of an additional type of element.

A uniform stress was applied in the direction z and the yz and zx faces were assumed to be free.

Values of K, obtained by the extrapolation method from computed displacements of the crack face, are shown in Figure 3.27. The figure also shows results obtained by Tracey (89) for a cylindrical specimen using a different type of singularity element. The discrepancy is verified to increase towards the mid point of the crack front having a maximum of 5%. at $\alpha = 45^{o}$.

In fact, for this direction, the uncracked ligament of the present specimen, being the diagonal of the square base,

is greater than in Tracey's geometry, which may be the reason of the decrease in values of K in the more central portions of the crack front of the present specimen.

3.4.5 - Part-through Semi-Ciruclar Crack

By using the mesh shown in Figure 3.26 , changing the boundary conditions to represent symmetry about the zx face, a specimen with a part-through semi-circular crack was modelled.

Values of K, obtained by the extrapolation method for computed displacements are shown in Figure 3.28. The figure also shows results obtained by Smith and Alavi (90). The maximum discrepancy is 2.0%.

3.4.6 - Thick-walled Cylinders with Radial Part-Through Semi-Circular Cracks.

Two different configurations of this type of structures have been studied and the results are presented in this Section.

A part-through semi-circular crack emanating from the inner surface of the cylinders were assumed to exist in a radial plane containing the axis of the cylinder, as shown in Figure 3.29.

The models investigated have the following geometries:

GEOMETRIC PARAMETERS	CASE CYL 1	CASE CYL2
R_1	71.9 mm	71.9 mm
R_2	135.9 mm	115.8 mm
$W=R_2/R_1$	1.88	1.61
$a/(R_2-R_1)$	.2	.29

In both cases the length of the cylinders is ten times the crack length. The cylinders were subjected to internal pressure fully penetrating the crack, which is the most critical case. These geometries were selected because their geometric parameters defined above are similar to those of the "T-Junction" structure to be described later, in Chapter 4.

3.4.6.1 - Mesh Generation

A mesh was generated representing 1/8th of the structure as it is shown in Figure 3.29.

This mesh was obtained from the previous corner crack finite element idealization by a three step skewing technique schematized in Figure 3.29.

Due to symmetry tangential boundary conditions were applied in the y and x directions to nodes in the planes xz and yz respectively. Of course nodes in the crack face were allowed to move freely.

In fact this representation assumes the existance of two equal cracks situated in the same radial plane and

diammetrically opposed.

Shannon (91) using the finite element method has calculated the SIF for a single radial crack in a thick-walled cylinder and presented also values of SIFs for two diametrically opposed cracks in cylinders of several diameter ratios. The results obtained by Shannon being derived from a two dimensional analysis are not applicable to curved crack fronts.

For the equivalent straight-front cracks having the same geometric parameters, W and $a/(R_2-R_1)$ of the cases CYL1 and CYL2, he predicts a decrease of about 9 and 6% respectively for the situation when two diametrically opposed cracks are present.

It is expected that these differences should be somewhat reduced in the part-through crack cases due to the constraint supplied by the uncracked material beyond the diameter of the crack in the z direction. The lack of such constraint with two infinite length cracks is bound to cause a higher interaction of the crack tip stress fields.

3.4.6.2 - Overall behaviour

A check on the equilibrium of forces in both x and y directions was made. The summation of reactions at nodes where boundary conditions were applied differs by less than 0.3% (in both cases, CYL1 and CYL2) from the total force applied due to internal pressure.

In figure 3.30 nodal values of hoop and radial stresses in the plane xz are compared with the Lamé solution for the

case CYL1, and a maximum error was found to be 3%. This discrepancy is quite acceptable in stress and is partially due to small deviations of the mid-side nodes from their correct positions, which is a result of the rather complicated skewing techniques applied to the mesh.

In Figure 3.31 the ratio of hoop stresses ahead of the crack tip divided by the respective Lame hoop stresses is plotted versus the distance from the crack tip. This plot illustrates the incapability of the finite element analysis to model the singular stress field described by expressions (1.5)(*). However, it can be seen that the raising effect caused by the presence of the crack die away quite rapidly (approximately one crack length) and reaches values slightly below the Lame's solution as it was expected due to the offset of the load in that plane. This behaviour as well as the results presented in Figure 3.30 clearly supports the assumptions made earlier, and representing only 1/8th of the structure.

The same behaviour and inaccuracies were verified for the case CYL2, therefore the results are not presented here.

3.4.6.3 - Stress Intensity Factors

Values of K along the crack front have been obtained by the extrapolation method using the computed displacements of the nodes in the free surface of the cracks.

(*) From expression (1.5) $\sigma = \alpha K r^{-\frac{1}{2}}$ thus

$\log\sigma = \text{Cte} - \frac{1}{2} \log r$ or $\log\sigma = \text{Cte} - \text{arc tg}(26.5) . \log r$

Plain strain conditions were assumed for all the extrapolation procedures but for those on lines in the inner surfaces of the cylinders where plane stress expressions were used.

The variations of the SIFs along the crack fronts for the CYL1 and CYL2 cases are shown in Figure 3.32. These values have been non-dimensionalized by dividing them by the quantity $p\sqrt{a}$ where p is the internal pressure and a the crack length.

Qualitatively these results present a rather reasonable behaviour as compared to those of the part-through crack configuration studied in Section 3.4.5 (see Figure 3.28). The ratio between the SIFs at the free surface ($\alpha = 90^{o}$) and at the point of deepest penetration of the crack ($\alpha = 0^{o}$) is 1.12 for CYL1 and 1.16 for CYL2. These ratios are greater than the same ratio in the part-through crack case, 1.1. This can be explained by the fact that the opening stresses in the uncracked cylinders are no longer constant but decrease across the thickness according to Lamé's expressions. By inspection of the Lamé solution for both cases the same reasoning can be used to explain the higher ratio for the CYL2 case.

On the other hand, the average increase of about 14 % of the SIFs from CYL1 to CYL2 can be associated with the ratio 1.17 between the maximum hoop stresses in CYL1 and CYL2 cases.

Values of SIFs for these particular configurations were not found in the literature and a combination of existing

analyses, as suggested by Underwood (92), will be carried out to obtain some estimates of K values and assess the validity of the present results.

This analysis is based on the assumption that crack shape effects in a pressurized cylinder can be similar, under certain conditions, to shape effects in a plate under tension. These analyses which will be combined are briefly described as follows:

i) Cylinders with straight front cracks

A long tube of internal radius R_1 and external radius R_2 contains a radial crack of length a from the inner surface. A uniform internal pressure acts on the cylinder and on the crack faces. Bowie and Freese (93) using a collocation method obtained the opening mode stress intensity factor K, over a wide range of radii and crack depth to thickness ratios. A plot of these results is shown in Figure 3.33.

ii) Cylinders with curved-front cracks

Cracks with curved fronts are more often found in structures and their shape can be idealized by a semi-ellipse with major axis, 2c, and minor axis, a. The present cases CYL1 and CYL2 having semi-circular cracks are particular cases of those ellipses.

Rice and Levy (94) obtained opening mode SIFs for a finite thickness plate under uniform tension with a semi-elliptical crack at the point of deepest penetration of the crack.

The proposed combination of these analysis can be expressed by the following relationship:

$$(K_1)_e = \alpha\ (K_1)_s \qquad (3.54)$$

where

$(K_1)_e$ = K_1 for a pressurised cylinder with a semi-elliptical crack

$(K_1)_s$ = K_1 for a pressurized cylinder with a straight front crack

$$\alpha = \frac{K_1 \text{ for a plate with a semi-elliptical crack}}{K_1 \text{ for a plate with a straight edge notch}}$$

The validity of expression (3.54) is limited either to thin walled cylinders or to thick-walled cylinders but with small crack depth to thickness ratio, as pointed out by Underwood.

The values of α depend on the ratio $a/(R_2-R_1)$ and on the aspect ratio, a/2c, of the ellipses representing the crack shape. A table of α values is presented in Reference (92).

The K values of the equivalent straight crack fronts to cases CYL1 and CYL2 are indicated by two circles in Figure 3.33, and these points are thought to lie within the range of validity of the expression (3.54).

It should be pointed out that this method is only applicable to non pressurized cracks. Now, using the principle of superposition, the effect of the pressure (P) acting on the crack surfaces can be dealth with by modifying expression (3.54) in the following manner.

$$(K_1)_{e_T} = (K_1)_e + (K_1)_{e_p} = \alpha(K_1)_s + \alpha_p(K_1)_{s_p} \qquad (3.55)$$

where $(K_1)_{e_p} = 2p\sqrt{\frac{a}{\pi}}$; $(K_1)_{s_p} = p\sqrt{\pi a}$

The following table shows more clearly the numerical results obtained by this combination method.

The discrepancies shown below are within the 10% accuracy suggested by Underwood, and the higher 6.6% discrepancy may be associated with the larger $a/(R_2-R_1)=.29$ ratio for the CYL2 case.

NUMERICAL RESULTS FOR THE COMBINATION ANALYSIS

Description	Cases	
	CYL1	CYL2
From Fig. 3.33 $K_o=2p\frac{R_2^2}{R_2^2-R_1^2}\sqrt{\pi a}$ (*)	.555 $MNm^{-3/2}$	.655 $MNm^{-3/2}$
From Fig. 3.33 K_1/K_o (see circles)	1.07	1.20
Thus $p\sqrt{\pi a} + (K_1)_s$	.594 $MNm^{-3/2}$	.786 $MNm^{-3/2}$
Non dimensionalized		
$p\sqrt{\pi a}/p\sqrt{a} + (K_1)_s/p\sqrt{a}$	1.77+3.52	1.77+5.16
$\alpha_p = 2p\sqrt{\frac{a}{\pi}}/(p\sqrt{\pi a})$	.64	.64
Values of from Ref.(92)	.44	.39
From expression 3.55 $(K_1)_{e_T}$	1.13+1.55 =2.58	1.13+2.01 =3.14
K_1 obtained from figure 3.32	2.62	2.94
% discrepancy 2. $\frac{K_1-(K_1)_{e_T}}{K_1+(K_1)_{e_T}}$	2.3	6.6

However, if in the combination analysis two diametrically opposed cracks were considered, in agreement with the present finite element idealization, the values K_{1s} would be reduced by about 10% according to Shannon's predictions(91) for these cases.

On the other hand, this 10% reduction of K_{1s} values for cylinders with straight-crack fronts are expected to be somewhat reduced for the case of cylinders with part-through cracks (see Section 3.4.6.2) thus the discrepancies shown in the table above should be somewhat changed; in the case CYL1 an increase and in the case CYL2 a decrease.

(*) Assuming $p = 1MNm^{-2}$

C H A P T E R 4

SURFACE CRACKS IN A T-JUNCTION OF THICK WALLED CYLINDERS

4.1 - General Considerations

Excessive deformation, leakage or fracture are the most common ways by which a containment system may fail (see Ref. (95)). It has been shown in the past that the first two modes of failure referred to above can be effectively prevented by the use of the more conventional methods of design.

However, peak tension stresses do occur in some regions of such containment systems and, particularly in thick-walled components, brittle failures can initiate either from defects in those areas, or cracks which may have grown to critical sizes by fatigue and/or corrosion.

As a result Linear Elastic Fracture Mechanics (LEFM) can be used to assess the structural integrity of these components as it is suggested in Appendix G of the ASME Code, Section III, (Ref.(96)).

The utilization of LEFM to prove the structural integrity of a containment system requires the inter-relationship of various aspects as follows:

i) Defect characterization

Flaws or cracks may be assumed to exist in the more critical areas (stress concentrations) of the vessel and with the most detrimental orientation.

ii) Dominant stresses during operation.

The design pressure and operating temperatures may be considered, as well as the effect of proof loading and a detailed estimate of the transient conditions must be made.

iii) The material fracture toughness (K_{1C}) may be measured by fracture tests and the variation of these values for heat affected zones and weld metals may have to be taken into consideration. In Nuclear Reactor Technology toughness degradation due to radiation may also have to be considered.

As can be seen from the foregoing, any safety analysis of a wide range of structures relating all these aspects in a rational basis may involve a major research program which is outside the scope of this work.

A more detailed description of the ways in which LEFM and general yielding fracture mechanics can be used in pressure vessels was presented by Burdekin and Dawes Ref.(97).

Mager and Riccardella Ref. (98) presented also a clear example of Fracture Mechanics Technology in analysing the integrity during the site life time of a heavy section nuclear reactor pressure vessel. An excellent compilation of papers on this subject can be found in Ref.(99).

It was already pointed out in Chapter 1 that LEFM is mainly valid for situations where fracture occurs prior to large scale yielding, and its use is mainly confined to the plain strain regime, Ref. (97).

Although the application of LEFM in cases where there is a considerable plastic region may be doubtful, it can still be used as a lower bound (e.g. Refs.(2) and (97)).

Moreover the evaluation of the stress intensity factors for assumed cracks in the containment systems under hydraulic test conditions is a necessary part of some methods of failure analysis(*) (e.g. Refs.(2) and (98)).

4.2 Definition of the Problem

A main steam vent pipe T-junction of a CEGB power plant was considered as the basis for the work reported in this Chapter. A sketch of this component is shown in Figure 4.1 and the data of the problem as supplied are:

Inside radius of the branch pipe	r_o = 73.1 mm
Thickness of the branch pipe (near the junction area)	t_o = 63.5 mm
Inside radius of the run pipe	R_o = 120.6 mm
Thickness of the run pipe	T_o = 43.9 mm
Young's Modulus	$E = 2.07 \times 10^5$ N/mm²
Poisson's ratio (assumed)	ν = 0.3
Internal pressure	P = 17.24 N/mm²

It is expected that high local stresses will occur at the nozzle discontinuities and these areas should be considered as key points for a detailed stress analysis bearing in mind the subsequent LEFM studies of possible crack configurations situated in such regions.

(*) As a result of a hydraulic test performed on a pressure vessel it may be reasonably assumed that no flaw greater than a certain size, say a, was initially present in the vessel. Thus, subsequent studies involving transient conditions may assume an initial crack of size a.

Based on reports of similar studies carried out by other workers, Refs. (1) - (5), and in view of past experience with the various finite element analyses described in the previous Chapter(*), it was anticipated that an adequate mesh idealization of the crack configurations could only be possible with the use of a substructuring technique. The number of degrees of freedom involved in an adequate mesh representation of the T-junction and, simultaneously, a considerable mesh density around the cracked regions would be incompatible with the capabilities of the computer facilities available at ULCC(**).

Therefore, following a similar procedure as that described by Hellen and Dowling, Ref.(2), the T-junction was idealized by a finite element mesh (main structure) and an initial stress analysis was performed using the DIM3B code. Subsequently, a subregion of the T-junction (substructure) was represented by a reasonably refined mesh where various crack configurations were idealized.

Boundary conditions were prescribed in this substructure based on the nodal displacements obtained from the previous analysis. These boundary conditions were applied in nodes pertaining to the interface between the main structure and the substructure.

(*) An account of the computer requirements and costs of the various finite element analyses described in this thesis, will be made in Chapter 5.

(**) CDC 6600

Unfortunately, experimental results were not available for comparison with the present finite element solutions. Therefore, the achievement of some confidence in the present analysis could only be obtained, with some intuition, by a thorough check on the stress analysis results and on the overall behaviour of the structure. Also some qualitative comparisons of the trends shown by the present results with others found in the literature for similar components but with rather different geometric parameters are presented. Thus, this stress analysis is described in Sections 4.3 - 4.5 and the crack studies return to Section 4.6.

4.3 Finite Element Mesh Idealizations

4.3.1 - General

For the situation when the T-junction is only subjected to internal pressure, as in the present case, the structure has two planes of symmetry. Taking advantage of this fact only one quarter of the structure has to be analysed as it is shown schematically in Figure 4.2. Appropriate boundary conditions were prescribed in nodes in these planes of symmetry.

The top ends of the branch pipe and the run pipe were subjected to axial loads representing the effects of end caps.

4.3.2 - 32 Node Element Mesh. CASE TJUN1

In the early stages of this work, a simplified model of the T-junction was idealized by a mesh of 32 node elements

as it is shown in Figure 4.3. Only one layer of these elements was used across the thickness and throughout the structure. This was justified by the fact that stresses are modelled within these elements by second order polynomials (see Section 2.2.3(*)), thus being able to model the Lame's solutions in regions of the cylinders away from the junction area.

It was also expected that this type of mesh would represent with reasonable accuracy the stresses in the nozzle regions. The number of elements was 49 and the number of nodes 728,

A mesh generation program was developed to generate the necessary data for the DIM3B code.

Due, mainly, to the lack of experience with such problems a rather complicated and unreliable mesh generation technique was developed. It was found that the bandwidth of this mesh was too high (208), resulting in large computing costs(**), despite the use of a simplified idealization of the structure which did not model adequately the weld details. As a consequence, only one run was performed and this mesh was abandoned. Some of the results of this analysis will be presented in the following sections of this chapter.

(*) Stresses are obtained by differentiating displacements, hence from expressions (2.13 f) and (2.13 g) it can be shown that stresses are modelled by second order polynomials.

(**) The computing costs involved in this analysis will be described later in Chapter 5.
The bandwidth is understood to be the maximum number of unknown variables at one time (NUNKVA).

4.3.3 - 20 Node Element Mesh. CASE TJUN2

4.3.3.1 - Mesh Generation

Based on the previous experience, an entirely different mesh generation technique was adopted. This technique is similar to that described in Section 3.4.2 for the idealization of the CTS configurations.

For the sake of the explanation let us assume the existence of radial planes containing the axis of the branch pipe and defined by an angle as illustrated in Figure 4.2. These planes will be subsequently referred to by the values of β.

This new mesh generation technique is based on the assumption that the entire structure can be defined by the specification of the cross section of the structure at $\beta = 0^{\circ}$ and the inner radii of the run pipe and branch pipe. Thus, for values of β between 0° and 90° the idealized details of the weld region may not be the same as those found in practice. However, it is assumed that this idealization is still acceptable for the present purposes.

A primary two dimensional mesh was developed for the cross section of the structure at $\beta = 0^{\circ}$ as it is shown in Figure 4.4.

The nodal coordinates input data were obtained from a scaled drawing of this section using a CADMAC digitiser This machine enables x,y coordinates of a drawing to be picked up by an electronic probe and automatically recorded on punched cards. The topological description of this 2D mesh was specified manually also in the form of punched cards.

The mesh generation program for this case, based on this 2D type of information generates all nodal coordinates for the 3D structure as well as the topological description of the 3D mesh.

Various skewing techniques have been used in order to obtain the final mesh and they can be divided into three stages.

Stage I: Construction of a slab with a cross section identical to that illustrated in Figure 4.4.

Stage II: Basically a cylindrical skewing technique around the z axis is used, generating a nozzle-on-a flat plate configuration.

These first two stages are illustrated in Figure 4.5. These drawings have been generated by the program DRAW using intermediate nodal coordinate data obtained immediately after each one of these stages.

Stage III: Another cylindrical skewing technique now around the y-axis, is applied to the plate and to a small portion of the branch pipe, generating then the run pipe. In this stage some difficulties arise in the specification of nodal coordinates in nodes near the junction area of the cylinders and for values of β near 90^{o}. Some particular procedures had to be used to correct in a proper manner these nodal coordinates. The mesh as finally used is shown in Figure 4.6.

As can be seen from the foregoing, this technique allows the generation of a 3D mesh of a T-junction based on a rather simple set of specifications which is normally

available in any design drawing of such components. It is also clear that changes in the original design details are very easily accommodated in the input data for the mesh generation program.

As illustrated in Figure 4.6 the structure was divided into four sections separated by radial planes of different value of β. In each section 2 layers of 20 node elements have been used throughout as it was specified intially in the drawing shown in Figure 4.4. The total number of elements was 104 and the total number of nodes 713. Due to the topological regularity of this mesh and of the fact that 20 node elements have been used, the bandwidth dropped sharply to the value NUNKVA=157, which is 25% less than the previous case. On the other hand a better mesh density was obtained, especially in the nozzle regions.

In this first case it was decided to assume that the face ABCD (see Figure 4.6) would be sufficiently away from the junction areas in order to neglect any disturbances, in stresses and displacements, caused by the presence of the nozzle. Therefore the nodal points in that face were only allowed to move in a radial plane in relation ot the y-axis which is the axis of the run pipe. Due to symmetry appropriate boundary conditions were prescribed in nodes in the planes $\beta = 0^{o}$ and $\beta = 90^{o}$.

4.3.3.2 - Results of Finite Element Analysis for Case TJUN2

Overall Behaviour.

The overall behaviour of this structure has been investigated in terms of stresses and displacements in various

sections of the structure.

A check on the equilibrium forces in the x,y and z directions was made. For each of these directions the summation of the calculated reactions at nodes where boundary conditions were applied differs by less than 0.1% form the total force applied due to internal pressure.

In Figure 4.7 the thicker lines represent the original sections of the structure for the planes $\beta = 90^{o}$ and $\beta = 0^{o}$. The thinner lines represent the displacement solution for these sections. A perspective view of the displaced structure is illustrated in Figure 4.8. From these results it was found that the computed radial displacement for the point P (see Figure 4.7) was 2.71 times greater than the value predicted by the following Lamc expression for displacements

$$u_r = \frac{1}{E} \frac{R_1^2 p_i}{R_2^2 - R_1^2} \left[(1-2\nu) r + (1+\nu) \frac{R_2^2}{r} \right] \qquad (4.1)$$

where E = Young's Modulus

ν = Poisson's ratio

p_i = internal pressure

R_1 = internal radius

R_2 = external radius

r = radial coordinate from the axis of the cylinder.

This fact clearly shows that the assumed boundary conditions in the face ABCD (see figure 4.6) are not valid for this structure. Moreover, if the radial displacements for the points situated in the face ABCD are affected by the presence of the nozzle discontinuity, as it appears to be, the rather large ratio, 2.71, referred to above is also associated

with the fact that two nozzles diametrically opposed have been assumed in the present mesh idealization.

From these results it is clear that a proper idealization of the structure has to include the lower part of the run pipe, thus representing a full quarter of the structure. The finite element analysis of this new mesh will be described in the next Section.

4.3.4 - 20 Node Element Mesh. Case TJUN3

4.3.4.1 - Mesh generation

As illustrated in Figure 4.9 the finite element mesh for this case was obtained from the previous mesh by simply adding eight more elements representing the rest of the run pipe. In the new face ABCD appropriate new boundary conditions were prescribed and one of the nodes in the line AB was totally fixed to avoid rigid body motion in the z direction.

The total number of elements and nodes was respectively 112 and 773. By using a suitable numbering scheme for the extra elements (see Figure 4.10) the bandwidth was kept the same as in the previous case.

4.3.4.2 - Results of the Finite Element Analysis for Case TJUN3. Overall behaviour.

Again, a check on the equilibrium forces in the x,y and z direction was made, and similarly to the previous case the same agreement was found (less than 0.1%).

Equivalent results to those shown in Figures 4.7 and

4.8 are illustrated for this case in Figures 4.11 and 4.12. From these results, basically two conclusions can be drawn.

Firstly, for the same point P as in the previous case, the ratio between the computed radial displacement and that predicted by expression (4.1) has been now reduced to the value 1.84. Moreover, it is clearly shown in Figure 4.11 that the line PQ loses its radial direction in the displaced section. These two results clearly show the invalidity of the idealization described in Section 4.3.3 for the case TJUN2.

Secondly, it can be seen from figures 4.11 and 4.12 that the computed displacements near the ends of both cylinders instead of converging to the predicted Lame solutions were developing an oval shape.

A better illustration of this behaviour in the ends of the branch pipe and the run pipe is shown in Figures 4.13 and 4.14 respectively. In these figures the displacements and stresses obtained with the present analysis are compared to the predicted Lame solutions.

By inspection of these results (see Figures 4.13(b) and 4.14(b)) it is interesting to note that the deviations of the computed stresses from the Lame solutions do indicate the presence of bending moments which have been superimposed on the internal pressure.

Although no report describing this phenomenon was found in the literature it is quite acceptable physically and it is due to the distribution of self equilibrating forces

in the junction area of the cylinders.(*)

By comparison of the displacement results described in Figures 4.7 and 4.11 it is clear that this phenomenon is less noticeable in the present case than in the previous TJUN2 configuration where two diametrically opposed nozzles were actually assumed.

For the cases TJUN2 and TJUN3, Figs. 4.15 and 4.16 show various contours maps of hoop stresses obtained in the nozzle regions with the present finite element analysis. For each case two cross sections were considered, $\beta=0^{o}$ and $\beta=90^{o}$ in Figures 4.15 and 4.16 respectively.

It can be seen that the stress patterns are very similar for both cases TJUN2 and TJUN3, however, a slight decrease in the overall stress levels was noticed for the case TJUN3. These relative differences in the stress levels and mainly for the plane $\beta=0^{o}$ (see Figure 4.15) are much smaller than the relative differences obtained for the displacements (compare Figures 4.7 and 4.11). This fact led to the conclusion that the prescription of radial displacements according to expression (4.1) in the ends of the cylinders, in order to avoid the ovalization effect, would have a negligible influence on the stress patterns indicated in Figures 4.15 and 4.16. Therefore, possible alterations to the prescribed conditions in the mesh TJUN3 were considered and discarded.

Figure 4.17 shows a contour map of hoop stresses in the nozzle region of a PWR pressure vessel similar to that shown in Figure 1.1. These results were obtained by Hellen and

---

(*) This type of behaviour can be easily visualized when subjecting one end of a cylinder to two types of loads: Either (i) a set of self-equilibrating axial loads or (ii) two diametrically radial loads.

Dowling, Ref.(2), using also a Finite Element Method.

In Figure 4.18 values of hoop stresses along the inner surface in the crotch corner region obtained by Broekhoven, Ref.(75), also for a PWR vessel,(*) are compared with the results obtained by the present analysis for the case TJUN3.

In both cases quantitiative comparisons of results are not possible due to major differences in the geometric parameters of this configurations and in the geometric nozzle details (see Figure 4.19) as compared with the present geometry. However, in the first case the similarity of the stress patterns with those of Figure 4.15 are encouraging.

In the second case, Figure 4.18, the present results are indicated by the full dots, the circles will be referred to later on, and the squares indicate the results from the case TJUN1. The results obtained by Broekhoven are indicated by the thinner lines.

In the ascending part of these curves reasonable agreement is verified and it is due to the fact that in both configurations the average ratios, thickness to internal radius, for the branch pipes, are very similar, (.94 in the present case and 1.04 in Ref. (75)). The larger discrepancies in the descending part of these curves are mainly due to the fact that in Ref.(75), the vessel is modelled by a flat plate, thus not allowing for an increase of hoop stresses in the inner surface as predicted theoretically if a cylinder was considered instead. The rather high peak value obtained

---

(*) modelled by a nozzle on a flat plate.

in the present results is associated with the sharp corner modelled in the TJUN3 finite element mesh. The proper idealization of this geometric detail as specified in Figure 4.1 will be made later on.

In view of the foregoing, the subsequent studies described in the following Sections of this Chapter will be referred to as the stress analysis results obtained in the TJUN3 case.

4.4 Validity of the Substructuring Technique

Part-through crack configurations in the section $\beta=0^{o}$ can be considered, from the stress analysis point of view, as the most critical situation regarding the fracture safety analysis of the present T-junction. This is due to the rather high stress concentration factor, 3.8, which was obtained in the crotch corner region of that section, (see Figure 4.18).

Because the assumed crack configurations are situated in a plane of symmetry of the T-junction, only one half of the region surrounding the crack has to be idealized in any substructuring technique.

Before entering the actual analysis of such crack configurations, using a detailed idealization of that part of the structure, a simple test was carried out to assess the validity of such procedure.

Using the previous finite element mesh, the node which represents the crotch corner in the plane $\beta = 0^{o}$ was released from its prescribed zero displacement in the x direction. As

it is illustrated in Figure 4.20 this procedure implies the existence of a corner crack having an approximate circular shape with an average radius of 23 mm. In addition, a force was applied on this node in the x-direction representing the pressure acting on the crack surfaces.

Some of the nodal points which will be part of the interface between the main structure and the substructure, have been chosen to monitor the computed displacements obtained in the present test. A comparison of these results with those obtained in the main structure analysis is shown in Figure 4.21. In this figure, the circles, which are referred to the right hand axis, indicate for each nodal point the ratio between the computed displacement components, u in the x direction for the uncracked and cracked situations. Similar results were obtained for the v and w components and the maximum discrepancy was found to be less than 0.05%.

As long as the boundaries of the idealized subregion are as remote from the crack regions as the nodal points referred to above, the results shown in Figure 4.21 clearly support the validity of the substructuring technique which will be described in the following sections of this chapter.

4.5 Substructure Analysis

4.5.1 - The Choice of Crack Configurations

Basically, in Appendix G of the ASME code, Section III, it is indicated that the plane strain fracture toughness values of the material should exceed by a given safety factor the K-values of a postulated defect. This defect has

a depth of one quarter of the section thickness and a length of six times that depth. It is also suggested that for the nozzle regions the postulated defect size may be a fraction of that postulated for the vessel.

If these defects are small they can be treated as cracks under constant stress fields magnified by a stress concentration factor. However, the use of simplified and approximate procedures for estimating K-values of larger crack configurations in the nozzle regions may yield rather inaccurate results. Therefore assessments of the severity of such cracks, based on this type of approach are bound to be too conservative.

Four circular crack configurations of successively increasing depth were thus studied. A sketch of these crack configurations is shown in Figure 4.22.

The particular choice of these geometries is due to three reasons. Firstly, post mortem observation of cracked nozzles (see Refs. (6) and (3)), indicate the existence of initial defects of circular or nearly circular shape.

Secondly, this shape is very convenient, bearing in mind some limitations associated with the evaluation of K-values, using the extrapolation method. This will be explained later on.

Finally, for engineering purposes, the values of SIFs along an elliptical crack front, may be estimated within 10% accuracy by assuming quarter circular corner cracks instead.(*) This assumption was based on the results presented by Cha[100]

(*) For ellipses with aspect ratios down to 0.4 (see Ref.(100))

and is also substantiated by Kobayashi and Enetanya[101] in their studies of elliptical corner crack configurations, even for the situation when linear varying stress distributions are considered.

4.5.2 Mesh Generation

A sketch of the subregion which was considered for the present substructure analysis is shown in Figure 4.23.

It is clear from this figure that all the nodes in the interfaces between the main structure and the substructure are situated at similar distances, from the crack region, as those of the nodes considered in Section 4.4 of this Chapter.

The technique used to generate the substructure was basically derived from that used in the idealization of the cracked cylinders described in Chapter 3 (see Section 3.4.6.1). Suitable geometric alterations to the external boundaries were initially specified in order to account for the weld details of the present geometry. The final mesh as illustrated in Figure 4.24 was then obtained by subsequently applying a cylindrical skewing technique similar to that referred to as stage III which was described in Section 4.3.3.1.

Some relevant features associated with this mesh are described as follows:

i) The total number of elements and nodes is 88 and 583 respectively.

ii) Using always the same topology, the various crack configurations were idealized by the application of simple linear skewing techniques. In these skewing procedures only

the interior nodes suffered changes in their geometric positions, whereas the nodes in the interfaces were kept unchanged. Hence, the boundary conditions based on the nodal displacements, such as those indicated in Figure 4.21, remained the same for the various crack configurations.

iii) At the time the TJUN3 mesh was developed it was possible to forsee for the substructure the spatial positions of the nodes in the interfaces. Therefore, identical spatial nodal positions were ensured, in the main structure, by an adequate specification of the values of β for the various radial planes in which the nodal points are located. Further complications and inaccuracies associated with the specification of boundary conditions are avoided with this procedure.

iv) With the present mesh, a proper representation of the crotch corner, as specified in Figure 4.1, replaced the sharp corner idealization of the main structure (TJUN3).

v) Internal pressure was specified in the inner surfaces and was assumed to fully penetrate the crack, thus acting on its surfaces.

vi) As it is shown in Figure 4.24, the nodes in the free surface of the crack are distributed in five radial directions emanating from the crotch corner. By assuming circular-shaped cracks, these directions remain perpendicular to the crack fronts. Thus the evaluation of SIFs along the crack front by using the extrapolation method in these radial directions is a straight forward procedure.(*)

(*) The use of the extrapolation methods in directions which are not perpendicular to the crack front have been discussed in Section 3.4.3.

4.5.3 - Analysis of the Uncracked Substructure

Overall Behaviour.

In order to obtain greater confidence in the substructuring procedure a defect-free substructure was considered before the idealization of any crack configurations. The overall behaviour of the substructure was investigated in terms of the stresses in the nozzle region.

A comparison of the hoop stress patterns obtained in both the main structure and the substructure is shown in Figure 4.26.

In Figure 4.18 the circles represent the values of the hoop stresses which were obtained in the inner surface with the present analysis. It is interesting to see that the peak stress value obtained in the main structure analysis, where a sharp corner was assumed, has been smoothed out with the proper idealization of the crotch corner geometry.

In both cases, Figures 4.18 and 4.26, the similarity of the stress patterns is again encouraging.

However, as illustrated in Figure 4.26, some minor differences are noticeable in the vicinity of the crotch corner and in the area close to the run pipe. In the former region the results obtained in the substructure analysis are believed to be more accurate whereas in the latter, the TJUN3 analysis should provide better results.

This is due to the fact that in the substructure idealization, a better mesh density was obtained in the crotch corner at the cost of a coarser mesh in the areas away from that region as illustrated in Figure 4.25.

4.6 Analysis of the Cracked Structure

4.6.1 - Idealization of the Cracks

The various cracks have been idealized by releasing the nodes in the free surface of the crack from their prescribed zero displacements in the x direction. Again, the mid-side nodes adjacent to the crack front were displaced to the quarter point positions nearest to the nodes in the crack front.

4.6.2 - Overall behaviour

The influence of the presence of various cracks on the overall behaviour of the substructure was investigated by monitoring the changes of the boundary reactions as the crack size increases.

The maximum changes for each crack configuration and in various radial planes β, are shown in the table below. The deviations are indicated in percentage values of the initial reactions which were obtained in the uncracked substructure analysis.

CHANGES IN THE NODAL REACTIONS

CRACK	SIZE mm	Max. Deviation %		
		$\beta = 0^{o}$	$\beta = 34^{o}$	$\beta = 90^{o}$
1	12.7	1.1	.8	.9
2	19.1	2.8	2.0	2.2
3	25.4	6.7	4.2	4.5
4	31.8	11.4	7.6	7.7

As can be seen from this table the deviations increase considerably with the crack depth and the application of the present substructuring technique may eventually underestimate the values of the SIFs for cracks deeper than the crack 3. The results obtained for crack 4 yet will be presented.

4.6.3 - Stresses Ahead of the Crack Fronts

The σ_x stress distributions for the sections $\alpha=0$, $\alpha = 45^o$, $\alpha = 90^o$ ahead of the crack fronts are shown in Figure 4.27.

It is interesting to note the values of these stresses in areas away form the crack regions are just slightly affected by the presence of cracks of increasing size. This may be due to the "fixed grip" conditions to which this substructure was subjected. Small variations of the stress levels in these areas would be expected to occur if a full structure were analysed instead.

Due to reasons which have already been described in Chapter 3, the stress data in the neighbourhood of the cracks can only support, in a qualitative manner, the distribution of the SIFs along the various crack fronts. In fact the stress values at the quarter point nodes are in close qualitative agreement with the variation of the SIFs along the various crack fronts (see Figure 4.28).

4.6.4 - Evaluation of K-Factors, Discussion of Results

As in the previous test cases, which were described in Chapter 3, the extrapolation method was applied using the

displacement components in the x directions of the nodes in the free surface of the cracks, thus $\theta=\pi$. Plain strain conditions were assumed for all the directions , with the exception of $\alpha= 0^{o}$ and $\alpha= 90^{o}$ where plane stress expressions were used instead. This first group of results is shown in Figure 4.28.

In order to obtain more confidence in these results the SIFs were also obtained using the extrapolation method in the directions perpendicular to the crack plane, thus for $\theta = \pi/2$. This second set of results is also shown in Figure 4.28.

It is interesting to note that the K-values obtained with this second procedure (for $\theta= \pi/2$) are consistently greater, by about 9%, than the results obtained with the extrapolation procedures in the free surface of the crack.

These differences, as pointed out in Chapter 3 (Section 3.2.2) are associated with the inaccuracies involved in the extrapolation procedures and mainly in the direction $\theta = \pi/2$. Due to this, the second set of results may be regarded as an upper bound to the true solution. Subsequently, based on these two sets of results, areas of uncertainty of the SIFs distributions, for each crack configuration, may be defined as illustrated in Figure 4.28.

Another procedure was used, based on the Global Energy Method and is described as follows.

As it is shown in Figure 4.29, when the crack is extended by skewing the mesh, the energy balance equation for the system can be expressed as

$$- \Delta U_{i \to i+1} = G\Delta A = \frac{1}{2} R_m^* \Delta u_m'^* \qquad (4.2)$$

provided no pressure is acting on the free surfaces of the crack.

Now using the principle of superposition, the work done by the nodal equivalent point forces to the internal pressure can be added to the right hand side of equation (4.2) thus

$$-\Delta U_{i \to i+1} + \sum_{n=1}^{m} \frac{P_{n_{i+1}} + P_{n_i}}{2} \Delta u_n = G\Delta A = \frac{1}{2} R_m \Delta u_m'$$

where $\Delta U_{i\ i+1}$ - Change of strain energy from crack i to crack i+1

R_m, R_m^* - Reaction on the node m

$\Delta u_m', \Delta u_m'^*$ - Crack opening displacement in the point A indicated in Figure 4.29.

$$\Delta U_n = U_{n_{i+1}} - U_{n_i}$$

$P_{n_{i+1}}, P_{n_i}$ - Nodal equivalent point forces to the the internal pressure.

The work done by the internal pressure is evaluated by assuming the displacement of forces which are an average of the forces obtained for crack i and crack i+1 and can be obtained from the output of DIM3B code.

The subsequent strain energy release rates obtained with this method are best associated with an intermediate crack by assuming the mean of the depths of cracks i and i+1.

From this method the values of strain energy release rates have been translated into K-values and were found to be

about 40% lower than those predicted by the extrapolation method. Very little importance should be attached to these discrepancies due to the following reasons:

i) Large inaccuracies involved in the evaluation of the u'_n value.

ii) Problems associated with the evaluation of the work done by the internal pressure on the crack surfaces.

iii) Rather coarse crack extensions have been assumed by using the results from the analysis of cracks 1 to 4.

iv) The present procedure, as well as the crack closure work method (see Section 3.2.3), are more accurately used when the crack extensions are idealized by supressing the prescribed conditions in nodes ahead of the crack front, instead using skewing techniques as in the present case.

It has already been confirmed by other workers in their LEFM studies of cracks in nozzles (see Refs. (2), (3), and (59)) that, for these types of configurations the use of simplified analytical or semi-analytical procedures to evaluate K-values, may result in a considerable inaccurate estimates of the true solutions. Therefore this type of analysis, which is bound to be inconclusive was not considered in the present work.

Alternatively, a comparative study of the present results with those described in Refs. (2) and (75) was carried out and is based on the following assumptions. It has been shown (see Figures 4.15, 4.17 and 4.18) that hoop stress patterns in the nozzle regions, for the section $\beta = 0^{o}$, are very similar for a relatively wide range of geometries.

In fact:

i) Maximum stress concentration factor is always found at the crotch corner, whereas very low stress levels are obtained in the opposite surfaces.

ii) The membrane stresses away from the nozzle regions are normally higher in the vessel or run pipe than in the branch pipe.

iii) However, for small distances away from the crotch corner the stresses in the inner surfaces die away more rapidly in the side of the vessel or run pipe.

iv) The hoop stress distributions for angles of α near 45^{o} are lower than the same distributions for $\alpha = 0^{o}$ and $\alpha = 90^{o}$.

v) The variations of SIFs along the crack fronts show similar trends to the stress distributions with the exception for crack depths smaller than the crotch corner radius.

vi) The values of the stress concentration factor in the crotch corner regions seem to increase when the crotch corner radius decrease.

From these conclusions, an average of SIFs for each crack configuration in the various nozzle geometries can be related by normalizing them to the SIF of a penny-shaped crack, K_o, (see exp. 1.13, Chapter 1), subjected to a remote stress equal to the membrane stress of the vessel, thus K_o can be expressed as

$$K_o = 2\ p\ \frac{R}{T}\sqrt{\frac{a}{\pi}} \qquad (4.4)$$

where p is the internal pressure

R is the internal radius of the vessel

T is the thickness of the vessel

a is the crack length

Moreover, the true geometric size of each crack can also be suitably normalized in relation to some geometric parameter which is obtained, on an empirical basis, from the design details of each nozzle. With this procedure cracks which may have rather large different sizes are then compared on the basis of the same depth to thickness ratio.

According to this procedure the results which were obtained are shown in Figure 4.30. The circles indicate the present results whereas the squares and the hexagonals are referred to the results obtained by Hellen and Dowling (2) and Broekhoven (59) respectively.

The thinner curve which is referred to the right hand axis indicate for the present case, only, the true K_o variations for a range of a/T up to .5.

The following conclusions can be drawn from these results.

i) The normalised K-values for the present crack configurations are considerably higher than the values corresponding to the other cracked nozzles 2 and 3.

ii) These differences can be associated with the higher hoop stresses which where obtained in the present case (see Figure 4.18) for the uncracked structure.

iii) On one hand, the present results are expected to underestimate the true solutions, due to the "fixed-grip"

conditions which were used in the present substructuring technique. This is somewhat confirmed by a faster decrease in the normalized K values as the ratio a/T increases.

iv) On the other hand, the hoop stresses in the present case (see Figure 4.18) die away, from the crotch corner, more rapidly as compared to the hoop stresses obtained by Broekhoven in nozzle 2.

v) However, due to the doubly-connected nature of these structures, regarding both the run pipe and the branch pipe, the present technique may not yield too large an error in the evaluation of K-values. This is more so in the present case, where the ratio of thickness to internal radius is much larger than in the other geometries 2 and 3.

This type of behaviour has been somewhat confirmed in the analysis of cracked cylinders described in Chapter 3.

In these cracked cylinders it was found that the disturbances caused by the presence of the crack are restricted to a small region in the plane of the crack and negligible in radial sections perpendicular to the crack plane. (See Figs. 3.30 and 3.31).

vi) The variations of reactions with increasing crack depth, which are described in Section 4.6.2, indicate that the substructure idealization could have been restricted to a smaller sector of the nozzle region between the planes $\beta = 0$ and, say, $\beta = 45^{o}$ thus allowing for a better mesh density in the cracked region.

vii) The cracked cylinder CYL1, described in Chapter 3, and the present branch pipe are very similar in their geometric

parameters, having the same thickness and differing by only 2% on the internal radius.

For the same crack depth to thickness ratio, a/T=.2 the normalized SIF at the free surface of the branch pipe is about 3.12 (see Figures 4.29 and 4.30) and the stress concentration factor SCF, at that point (see Figure 4.18) is 3.3 in the uncracked structure. Using the same K_o value as before (for comparison purposes) the SIF at the point where the crack meets the inner surface of the cylinder CYL1 was found to be .97. Multiplying this value by the SCF indicated above, yields to a correspondent SIF for the branch pipe of 3.03 which is only 3% lower than the 3.12 value obtained form Figures 4.29 and 4.30.

viii) In Figure 4.30, the full circle indicates the average normalized K value obtained in the corner crack configuration described in Chapter 3 (see Section 3.4.4). In that specimen the ratio thickness to crack depth is also .2. This averaged SIFs is 2.73 times smaller than the correspondent value in the present cracked nozzle, which can also be associated with the previous SCF, 3.3, referred to above. This larger difference is explained by the doubly-connected nature of the present geometry where bending is restricted thus reducing the SIFs as compared to the corner crack in the square specimen.

ix) From the scarce results indicated in Figure 4.30, similar trends can be observed to occur in the various geometries and for values a/T greater than .16. However, in these normalized SIFs strong differences, of up to about

50% are observed which are associated with differences in the geometric details and the stress distributions of the various nozzles. These differences and the complexity of these crack configurations seem to rule out any prospect of obtaining an exact analytical solution.

Finally, bearing in mind possible safety implications of the present crack configurations, some conclusions can be drawn based upon the following considerations.

i) The hoop stresses in the uncracked structure as well as the SIFs are higher in the branch pipe than in the run pipe, hence cracks tend to grow faster in the branch pipe.

ii) For materials such as the A533-B steel, which is a low alloy pressure vessel steel commonly used in the Americal reactor technology, typical K_{1C} values can be as low as 50 $MNm^{-\frac{3}{2}}$. This value is for very low temperatures or for higher temperatures under dynamic or impact testing conditions.

iii) From Figure 4.29 the maximum K_1 values for cracks 1,2,3 and 4 can be obtained. Based on the above K_{1C} value, it can be said that under extreme conditions (low temperatures or impact conditions) the following safety factors against instability or brittle fracture are indicated:

SAFETY FACTORS FOR CRACKS 1,2,3,4

FOR K_{1C} = 50 MN $m^{-3/2}$

CRACK	CRACK LENGTH	MAX K_1	SAFETY FACTOR
1	12.7	21	2.38
2	19.1	24.5	2.04
3	25.4	27	1.85
4	31.8	30	1.67

iv) In ultrasonic testing, the detectable defect size for the range of thickness values specified in the present geometry is found from Ref. (102) to be less than 2 mm. Thus the present crack configurations can be found and measured safely.

C H A P T E R 5

CONCLUSIONS AND RECOMMENDATIONS FOR FUTURE WORK

5.1 Achievements

i) A three dimensional general purpose linear elastic finite element program was brought into use. In this program (DIM3B) the input data format is quite general and applicable to any geometric and/or loading conditions, yet its generation may become a rather tedious and complicated job.

In order to ease some of these problems, facilities exist in the program which allow the user, if so desired, to chose various optional sets of coordinates to which the various input data may be referred.

ii) The DIM3B code can be submitted in a so-called "Dynamic mode of operation". For each analysis this procedure attempts to optimize, in a semi-automatic manner the computing costs (in CM and CPU(*) time) involved in running the program.

iii) Various mesh generation techniques have been developed for the three-dimensional analysis. In general, these programs generate the necessary data for the DIM3B code based on a rather simple 2D type of information. In all these mesh generation programs various stages can be identified.

1 - Full description of the topology of the 3D mesh

2 - Generation of a simple 3D geometry

3 - Application of various skewing techniques separated in distinct stages which yield to the desired geometric shape.

(*) CM - Central memory CPU - Central processor unit

These procedures ensure

1 - Validity of the mesh generation programs for a relatively wide range of the geometric parameters of the type of structure under study.

2 - Topolgical regularity in the 3D meshes, thus keeping the size of the bandwidth to a low level.

3 - Normally, changes in the geometric details of the structure can be easily accommodated by performing minor alterations in the 2D type of input data.

iv) Using some off-line graphics facilities available at I.C.C.C. a plotting program, DRAW, was developed whereby the various 3D meshes can be visualized and efficiently checked in terms of the topology, nodal coordinates and prescribed displacement boundary conditions. In this program an isometric view of the mesh is generated from a direction which can be suitably specified by the user.

v) An axi-symmetric general purpose linear elastic finite element program was developed. This program, FRONT, uses a simplified version of the FMS in which the symmetric property of the body stiffness matrix [k] is not taken into account. However, profiting from this fact, the introduction of slope boundary conditions was easily accommodated in the solution technique (see Appendix 1, Section A1.4.2.4) by performing relatively simple alterations in the coefficients of the matrix [k].

v) The theory outlined by Henshell and Shaw (Ref. (81)) for the "2D crack tip elements" was extended for the equivalent 3D element, i.e., for the 20 node isoparametric element (Section 3.3).

vi) It was also shown that this theory could be generalized so that "crack tip elements" can be derived from any isoparametric finite elements (Section 3.3) provided they have one or more than one intermediate nodes in the edges. This means that any field variable within the conventional elements must be described by quadratic or higher order shape functions.

vii) To substantiate this theory various test cases of CTS configurations were carried out in which the crack tip regions were idealized by using standard 20 node elements or their derived "singularity elements" (Section 3.4.2).

The validity of the theory was confirmed by the improvements which were observed in the K-values when the "crack tip elements" were used (see Figures 3.18 and 3.19).

viii) The generalization of the theory referred to in vi) was also substantiated by the results which were obtained when the same CTS geometries were idealized by 32 node element meshes (see Figures 3.21 b).

ix) Some other typical 3D crack configurations were then studied (Sections 3.4.4 to 3.4.6). The results which were obtained from these analyses compare favourably with suitable bounding approximate solutions and other results already given by other authors.

x) By applying an adequate substructuring scheme it was possible to study various crack configurations of increasing size in the crotch corner region of a thick-walled T-junction of cylinders. (Chapter 4).

5.2 Computing Costs

In Chapter 3, Section 3.4.1, the strategy which was adopted for running a typical case with the DIM3B code was described. This strategy, illustrated in Figure 3.11, can be divided into two main stages.

1 - Execution of the mesh generation program followed by the plotting procedure (execution of program DRAW)

2 - Resubmission of the mesh generation program followed by the execution of DIMDIM and DIM3B codes.

It was found that the costs involved in the stage 1 computations are, on average, about 2% of the total computing requirements of a complete analysis.

A table is presented here where the computer requirements for the execution of the DIM3B code are described in detail for the various finite element analysis reported in this thesis.

The usage of the CDC system at U.L.C.C. is combined via a complex formula and translated into a measure called unit as follows

$$\text{Units} = \frac{1}{128}\,CP\left(\frac{10+3CM}{30}\right) + \frac{TR \times DR}{1.44\times10^{6}}\,(1 + .3CM) + \frac{1}{128}\,(CR+LP)$$

where CP is the total central processor time

CM is the number of core memory words occupied

TR is the number of words transmitted to or from magnetic tapes

DR is the number of words transmitted to or from disk

COMPUTER REQUIREMENTS FOR THE EXECUTION OF DIM3B CODE (FTN compiler)

CASE	NN ELM	NELEM	NODTOT	NPRDEF	NKNVA	NUNKVA	NT(**)	COMPUTER REQUIREMENTS				COST £
								CM(*)	• CPU(*)	• PP(*)	UNITS	
1	20	22	202	109	24	101	606	29488	147.196	35.718	4.934	9.87
2	20	44	319	123	26	162	957	39990	290.682	84.486	8.338	16.68
3	32	22	340	175	36	164	1020	45230	331.517	88.935	18.476	36.95
4	20	88	553	68	14	291	1659	74730	817.823	110.962	65.388	130.78
5	20	88	553	151	30	278	1659	75853	795.010	105.084	58.339	116.68
6	20	88	553	215	39	269	1659	76011	782.157	105.285	54.328	108.66
7	32	49	728	213	29	208	2184	59444	899.766	163.412	53.761	107.52
8	20	104	713	239	23	157	2319	48221	656.421	91.038	30.969	61.94
9	20	112	773	256	19	157	2319	48414	686.750	113.153	32.534	65.07
10	20	88	553	325	56	282	1659	85916	864.77	99.7	64.686	129.37

(*) - CM - Control Memory; CPU - Central Processor Unit Time; PP - Peripheral Processor Time

• - Seconds

(**) - NT - Total number of degrees of freedom, NT = NODTOT x 3

Case 1 - Compact Tension Specimen
Case 2 - Compact Tension Specimen, Fig.3.14
Case 3 - Compact Tension Specimen, Fig.3.21(a)
Case 4 - Corner Crack Specimen, Fig.3.26
Case 5 - Part-through Crack Specimen, Fig.3.26
Case 6 - Cracked Cylinder, Fig.3.29
Case 7 - TJUN1, Fig.4.3
Case 8 - TJUN2, Fig.4.6
Case 9 - TJUN3, Fig.4.9
Case 10- Substructure, Fig.4.24.

CR is the number of cards read

LP is the number of lines printed

The estimation of the costs for the various computations is based on a rate of £2.00 per unit of the computer resources usage.

5.3 Final Conclusions

5.3.1 - The FEM and its LEFM applications.

i) The FEM is a very powerful technique to solve general stress analysis problems. However its application to three dimensional cases is hampered both by the present generation computer capabilities and the rather high costs involved in such computations. As a consequence, such analyses are still limited to relatively coarse mesh idealizations of the geometries in study.

ii) The utilization of "crack tip elements' in three dimensional LEFM studies seems to be compulsory if K factors are to be evaluated without unacceptable loss of accuracy. For the present meshes, discrepancies of about 20% are found if no "singulairy elements" are used.

iii) K-values obtained by the extrapolation method and using the displacement distribution in the free surface of the crack ($\theta=\pi$) show in general an agreement within 5% with other results already given by other authors.

iv) Less accurate estimates of the K-factors are obtained when the displacement method is applied in directions perpendicular to the crack plane ($\theta=\pi/2$). This is due to the strong square root behaviour of the K* curves (see Figure 3.1) as it was described in Chapter 3, Section 3.2.2.2.

v) However by using these two directions of extrapolation ($\theta = \pi$ and $\theta = \pi/2$) valuable information can be obtained about the coefficients of the higher order terms of the Williams series solution (exp. 3.4). These coefficients which are derived from the K* curves can eventually be physically interpreted by following the lines suggested by Cotterell (106).

vi) Such coarse meshes present some limitations on the validity of the computed stresses in the vicinity of the crack. Therefore finer meshes would be recommended if a detailed analysis of the near tip stress fields is required, or if K factors are to be calculated by the "stress method".

vii) Strain energy release rates, G, obtained from boundary load displacements can only be used by making two complete runs for adjacent crack configurations.

The averaged K-factors associated with the values of G (exp. 1.7) compare favourably with those obtained by the extrapolation method using the direction $\theta = \pi$ (see section 3.4.3).

viii) The variations of K-values which were obtained along the crack fronts of all the configurations studied, show the incapability of the FEM to detect any surface effects in regions where the cracks meet the free surfaces. However it is believed that in such areas the present results are still acceptable for engineering purposes.

ix) The computation costs associated with 32 node element meshes are considerably higher than those involved

in 20 node element mesh indealizations. Moreover it was found that better mesh densities are obtained with the use of 20 node elements.

5.3.2 - The LEFM Studies of Cracks in the Main Steam Vent Pipe "T-Piece".

i) Confidence in the validity of the results obtained from the finite element analysis of the defect-free "T-piece" geometry is based on the following observations:

- Agreement of the results which were obtained with two different mesh idealizations (see Figure 4.18). One using 32 node elements (Figure 4.3), another using 20 node elements (Figure 4.9).
- Apart from an ovalization effect which was observed in the ends of the cylinders, and shown to be physically explicable, the stresses and displacements in such areas agree well with the predicted Lame solutions.
- The hoop stress distributions in the crotch corner regions of the present geometry and two other nozzle configurations (see Figures 4.15 and 4.18) show rather similar trends.

ii) By comparing these stress distributions (in the present case and in the other two nozzle configurations) the following conclusions may be drawn.

- The smaller the crotch corner radius the higher the SCF in these areas.
- This suggests that better stress distributions may eventually be obtained if the crotch corner is smoothed

out by removing material and so increasing the crotch corner radius. Comparison with other workers indicates that this will lower the K values of possible cracks in such regions.

iii) When two diametrically opposite branch pipes are considered (case TJUN2) the overall stress levels in the crotch corner regions increase by about 10% in relation to the stress levels which were obtained for the single T-junction geometry (case TJUN3).

iv) For the present case the maximum hoop stress in the crotch corner regions was found to be 174 MNm^{-2} which is below the yield strength of a mild steel. This result demonstrates that, for this configuration, there will be no gross yielding and ensures the validity of the LEFM studies.

v) Whereas a relatively coarse mesh idealization was sufficient to obtain the stress and displacement distributions in the uncracked "T-piece" geometry, a much denser mesh was necessary to idealize in a proper manner the various crack configurations.

vi) Due to the limitations of the present computers, it is necessary to use a substructuring technique in order to achieve the desired mesh density in the regions of concern.

vii) Substructuring schemes are expected to under-estimate somewhat the true K-values, however, due to the doubly-connected nature of the present configuration, such errors may not be too large.

viii) For crack depths up to about one half of the thickness of the run pipe the present substructure idealization could be restricted to a smaller sector of the junction area of the cylinders.

5.4 Recommendations for Further Work

The results presented in this thesis clearly demonstrate the possibility of evaluation of K-values utilizing a standard 3D finite element stress analysis computer program.

However the rather high costs involved in such computations immediately suggest the development and implementation of new features into the DIM3B code.

i) Implementation of the 15 node wedge-shaped element. This element is fully compatible with the presently available 20 node hexahedron elements, and the main advantages associated with this element are:

- More versatility in the mesh idealizations
- In general, these elements yield smaller sizes of the bandwidth,
- "Crack tip elements" are still easily derived from this wedge-shaped element (the "quarter point distances" rule is still applicable).

As far as the programming aspects of the DIM3B code are concerned the implementations of these elements requires the following major procedures.

- Addition of an extra library subroutine containing the shape functions and its partial derivatives for these elements.
- Suitable alterations in subroutines LOAD, FEM and FEM2.

ii) Organization of book-keeping procedures for the stiffness coefficients so that possible substructuring schemes can be used in a more accurate manner and at lower costs.

This feature is not only suitable for general stress analysis problems but it is also rather useful bearing in mind the possible application of the Parks. "stiffness derivative procedure" for evaluating strain energy release rates.

iii) The implementation of initial stresses and/or initial strains due to temperature rises would obviously allow the solution of a wider range of problems of pratical interest as for instance, residual stresses and stress distributions due to thermal gradients.

Three dimensional LEFM studies are still very scarce. A wide range of practical problems is yet to be studied and a completely general approach to the solution of these problems has been provided.

As an immediate extension of the present work the following studies may be of interest.

iv) In Chapter 3, Section 3.4.3, it was suggested that a single averaged K factor obtained by the Global Energy Method can replace the 2D calibration factors for the specimens used in fracture toughness testing procedures.

For the CTS with curved crack fronts the results clearly show a reduction in K with increasing tunneling effect. A much more accurate analysis with a finer mesh would be required if proper correction factors are to be evaluated.

v) The present substructuring technique could eventually yield improved results by carrying out this scheme in a step wise manner. In other words, the imposed displacement boundary conditions which are obtained from the analysis of the entire structure can be updated for each crack length by grossly

idealizing equivalent cracks in the main structure mesh. The improvements of this modified scheme can be monitored by inspection of the reactions.

vi) Some LEFM studies are suggested which may be carried out using the FRONT code:

- Simulation of nozzle geometries by an axisymmetric nozzle on a flat plate.
- Long and narrow banana-like cracks occur in stuctures, as for instance, in off-shore oil rig "T-piece" components. These cracks can eventually be studied by an approximate axisymmetric idealization of their configurations.

vii) Finally, carefully controlled experiments are required so that the present results, which were obtained by a numerical method, could be properly substantiated.

A P P E N D I X 1

PROGRAM FRONT . DESCRIPTION . USER'S GUIDE

A1.1 - Introduction

The program FRONT is a finite element computer program using triangular axisymmetric finite elements. This program has been developed from the FLAP5 code for which a full User's Guide is given in Ref. (103). The elements used are the axisymmetric version of the well known "Constant Strain triangular elements" which are described in Ref. (46).

The FLAP5 program uses the Gaussian iteration method to solve the system of equations

$$[k]\{\Delta\} = \{F\} \qquad \text{(A1.1)}$$

where $[k]$ is the general body stiffness matrix

$\{\Delta\}$ is the unknown displacement vector

$\{F\}$ is the applied nodal forces vector

The iteration method is speeded up by using an over-relaxation factor reducing the number of cycles necessary to reach a given tolerance.

The rate of convergence of this method is highly dependant on: the over-relaxation factor, the shape of the structure, the boundary conditions and the initial geometry of the elements (see Refs. (48) and (104)).

Experience has shown that, in general, good results (apart from mesh density considerations) are obtained if a

tolerance(*) of the order 10^{-5} is reached. Nevertheless it has been found that in some cases this level of tolerance is very difficult, if not impossible, to reach, even using techniques for optimization of the over-relaxation factor (see Ref. (105)).

For these cases the Gaussian iteration method is no longer reliable and another method of solution of the equation (A1.1) is required, such as the Gaussian elimination technique. A description of this method has been given in Chapter 2, therefore will not be repeated here. Only its computer implementation will be described in some detail for the present case.

The mathematical theory involved in the prescription of displacement boundary conditions, for the present case, is described in the following section.

The programming aspects of the FRONT code will be outlined in Section A1.3 and a User's Guide as well as a listing of the program will be included in the final sections of this Appendix.

A1.2 - Displacement boundary conditions

In the DIM3B code full advantage is taken from the symmetry of the overall stiffness matrix $[k]$ whereas in the present program the completed equations are fully stored. As a result the partitioning of the matrices, as indicated by expression (2.48) in Chapter 2, is no longer necessary.

(*) In the present case, tolerance is expressed as

$$Tol = \frac{\varepsilon \Delta u_i}{\varepsilon u_i} \quad \text{where } \Delta u_i = |u_{i+1} - u_i|$$

u_i = nodal displacements at iteration i

A description of the method whereby initial prescribed displacements are accommodated in the present solution technique will follow.

A1.2.1 - Prescribed Displacements in the Radial or Axial Directions.

Suppose the set of equations (A1.1) can be expressed as

$$\begin{bmatrix} S_{1,1}\,\delta_1 + S_{1,2}\,\delta_2 + \ldots + S_{1,2n} \\ S_{2,1}\,\delta_1 + S_{2,2}\,\delta_2 + \ldots + S_{2,2n} \\ \ldots \\ S_{2n,1}\,\delta_1 + S_{2n,2}\,\delta_2 + \ldots + S_{2n,2n} \end{bmatrix} \begin{Bmatrix} \delta_{2n} \\ \delta_{2n} \\ \cdot \\ \delta_{2n} \end{Bmatrix} = \begin{Bmatrix} F_1 \\ F_2 \\ \cdot \\ F_{2n} \end{Bmatrix} \qquad \text{(A1.2)}$$

where in this two dimensional case $\delta_{2k-1} = u_k$ and $\delta_{2k} = u_k$ for each node k.

If δ_s is a prescribed displacement at node k, a suitable alteration of equations (A1.2) can be performed as follows: The quantities $S_{is}\,\delta_s$ (for i=1, 2 .. 2_n) will be transferred to the right hand side of all equations i as known quantities. F_s is the sum of the external applied forces R_s, the internal forces due to initial strains and body forces for the node s.

$$F_s = R_s + R_{bs} + R_{\epsilon s} \qquad \text{(A1.3)}$$

where R_s = external forces

R_{bs} = Forces which are statically equivalent to body forces

$R_{\varepsilon s}$ = Forces to suppress initial strains (thermal strains in the present case.)

If δ_s is known, R_s becomes an unknown reaction as well as F_s. This unknown quantity is replaced in the solution vector, Δ, and can be evaluated if reactions are to be calculated. In view of the foregoing all equations will be changed as follows

$$S_{i,1}\delta_1 + S_{i,2}\delta_2 + \ldots + 0.\delta_s + \ldots + S_{i,2n}\delta_{2n} = F_i - S_{i,s}\delta_s \tag{A1.4}$$

and the equation s which contains δ_s in the leading diagonal will be changed to

$$S_{s,1}\delta_1 + S_{s,2}\delta_2 + \ldots - F_s + \ldots + S_{s,2n}\delta_{2n} = -S_{s,s}\delta_s \tag{A1.5}$$

thus equation (A1.2) can now be expressed in matrix form as

$$\begin{bmatrix} S_{1,1} & S_{1,2} \ldots 0 \ldots S_{1,2n} \\ S_{2,1} & S_{2,2} \ldots 0 \ldots S_{2,2n} \\ \ldots\ldots\ldots\ldots\ldots\ldots \\ S_{s,1} & S_{s,2} \ldots -1 \ldots S_{s,2n} \\ \ldots\ldots\ldots\ldots\ldots\ldots \\ S_{2n,1} & S_{2n,2} \ldots 0 \ldots S_{2n,2n} \end{bmatrix} \begin{Bmatrix} \delta_1 \\ \delta_2 \\ \vdots \\ F_s \\ \vdots \\ \delta_{2n} \end{Bmatrix} = \begin{Bmatrix} F_1 - S_{1,s}\delta_s \\ F_2 - S_{2,s}\delta_s \\ \vdots \\ -S_{ss}\delta_s \\ \vdots \\ F_{2n} - S_{2n,s}\delta_s \end{Bmatrix} \tag{A1.6}$$

It is obvious that this procedure can only be performed in equations which have already been completed, or, in finite element terminology, when all the elements adjacent to the node $k = (s+1)/2$ have been processed.

A1.2.2 - Slope Boundary Conditions

If a node k is only allowed to move on a particular direction, as it is illustrated in Figure A1.1, the displacements u_k and v_k for that node remain unknown and a relationship

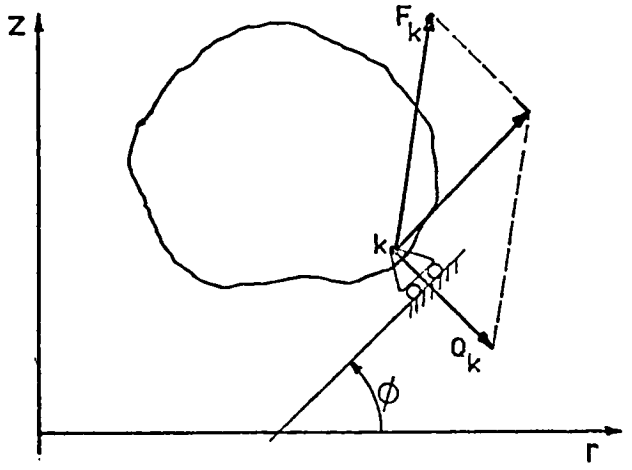

Figure A1.1 - Slope boundary condition in node k

between these two values can be established as

$$u_k = q \cdot v_k \qquad \text{(A1.7)}$$

where $q = 1/\tan \phi$

Resulting from this boundary condition, a reaction Q_k perpendicular to the prescribed direction has to be added to the force F_k, so that the resulting total force applied in node k will follow the prescribed direction as it is indicated in Figure A1.1.

It is obvious that the quantities in the right hand side of equations 2k-1 and 2k are no longer known quantities. However, bearing in mind that the reaction Q_k must remain perpendicular to the prescribed direction, its components Q_{k_r} and Q_{k_z} will be related by the following expression

$$Q_{k_z} = -q \cdot Q_{k_r} \qquad \text{(A1.8)}$$

The set of equations (A1.2) becomes then

$$\begin{cases} S_{1,1}u_1 + S_{1,2}v_1 + \ldots S_{1,2n}v_n = F_1 \\ \ldots\ldots\ldots\ldots\ldots\ldots \\ S_{2k-1,1}u_1 + S_{2k-1,2}v_1 + \ldots + S_{2k-1,2n}v_n = F_{2k-1} + Q_{k_r} & \text{(a)} \\ S_{2k,1}u_1 + S_{2k,2}v_1 + \ldots\ldots S_{2k,2n}v_n = F_{2k} + Q_{k_z} & \text{(b)} \\ u_k - qv_k = C & \text{(c)} \\ Q_{k_z} + qQ_{k_r} = 0 & \text{(d)} \\ \ldots\ldots\ldots\ldots\ldots\ldots \end{cases} \qquad \text{(A1.9)}$$

From this set of equations it can be seen that the number of unknowns has increased by two so the number of equations, and this fact will drastically increase some programming aspects of the computer code. In order to overcome this problem and bearing in mind that the evaluation of reactions is not the aim of the problem, Q_{k_r} and Q_{k_z} can be eliminated by substituting equations (a) and (b) into equation (d) in (A1.9) as follows:

$$
\begin{cases}
\cdots\cdots\cdots\cdots \\
(S_{2k,1} + q.S_{2k-1,1})u_1 + (S_{2k,2} + q.S_{2k-1,2})v_1 + \cdots \\
\cdots + (S_{2k,2n} + q.S_{2k-1,2n})v_n = F_{2k} + q.F_{2k-1} & \text{(a)} \\
u_k - q.v_k = 0 & \text{(b)} \\
\cdots\cdots\cdots\cdots & \text{(A1.10)}
\end{cases}
$$

As it is shown in the set of equations (A1.10) the introduction of a slope boundary condition for a particular node k is made by means of replacing the pair of equations 2k-1 and 2k in (A1.2) by the equations (a) and (b) in expression (A1.10).

A1.3 - Program Breakdown

This section described the layout of the program and gives a survey of each subroutine included in the FRONT code.

Similarly to the DIM3B code the computer program FRONT consists of four main parts

A - Initializations

B - Determination of forces. Evaluation of the stiffness coefficients for each element and assembly of the stiffness matrix.

C - Forward Elmination

D - Evaluation of displacements and stresses.

The primary flow chart referred to DIM3B code is also applicable to the program FRONT (see Figure. 2.2 of Chapter 2). A detailed flow chart of the present program is described in Section A1.3.4 of this Appendix.

A1.3.1 - Initializations

In this part, the program reads the initial input data such as the title of the analysis, TITLE, and the basic parameters, LBW(size of the bandwith). NEL (total number of elements), NNP (total number of nodes), NBR (Number of prescribed conditions) and NMAT (Number of materials).

Material properties, the topological description and the geometry of the structure are fed into the program, and finally the loads are defined.

Subroutine INIAL is then called where the last appearances are calculated and identified with a minus sign. Boundary conditions are fed in, defining the array PRENIC and the prescribed displacements are immediately stored in the displacement solution array UV.

Some working variables, ANP, NAP, are prepared for the main DO LOOP and the stiffness matrix STIF is reset to zero.

A1.3.2 - Total Nodal Forces, Stiffness Coefficients. Forward Elimination.

From now on the program proceeds within a general DO LOOP until all finite elements have been processed.

Firstly, subroutine LOAD is called and evaluates the total nodal point forces, REX, adding to the external applied forces the internal body forces as well as nodal equivalent point forces due to thermal strains.

Subroutine ELSTIF follows subroutine LOAD and evaluates the stiffness coefficients, KEL, by performing a single point integration over the volume of the element of the matrix product

$$KEL = [B]^T [D] [B]$$

where [B] is the shape function matrix

[D] is the elasticity matrix for each element

The subroutine STTR is called immediately after ELSTIF and distributes KEL coefficients which were previously calculated, into the main stiffness matrix STIF.

If a certain number of equations is complete and ready for elimination, this subroutine, in a second stage, performs the necessary alterations to the equations in order to deal with the boundary conditions and according to the theory described in Sections A1.2 of this Appendix.

Three variables, KROWI, KROWF and KROWFA are set up to monitor the advance of the front through the structure (one node at a time). KROWI indicates the initial node of the front and starts with the value 1 and increases by 1 each time a forward elimination (for the pair of equations corresponding to node KROWI) is performed. KROWF describes the largest node related with KROWI. Thus the front is described each time by the nodes between KROWI and KROWF. After each forward elimination KROWF is increased according to new KROWI and the previous KROWF value is assigned to the KROWFA variable.

For the sake of a better understanding of this subroutine, a simple example is put forward describing the basic operations mentioned above.

Let us assume a finite element mesh composed of triangular axi-symmetric finite elements as it is indicated in Figure A1.2.

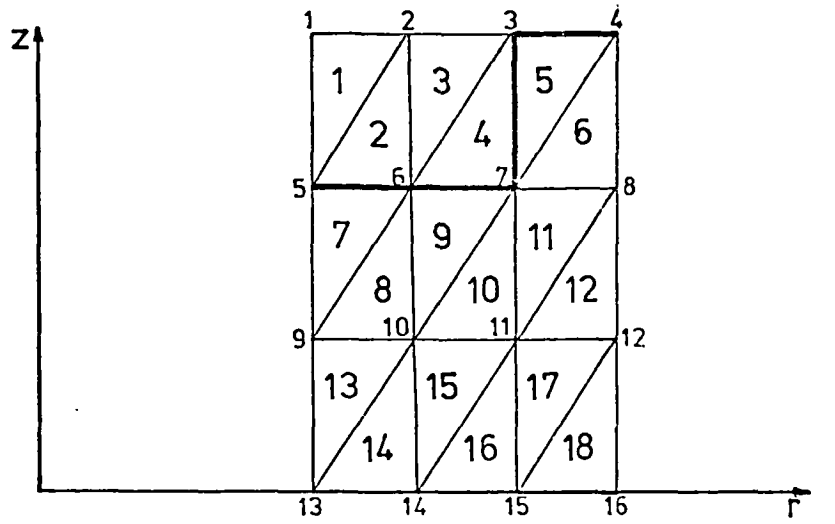

Figure A1.2 - Mesh Idealization For a Thick Walled Cylinder

A table is presented below in which the evolution throughout the structure of the process referred to above is described.

FMS. MONITORING THE FORWARD ELMINATION

ELEM NO	NPI (*)	NPJ (*)	NPM (*)	KROWI	KROWF	KRUWFA	SUB. FORWARD	Pair of Eq. Elim
1	1	5	2	1	5	1	-	-
2	2	5	6	1	5	1	-	-
3	-2	6	3	1	5	1	-	-
4	3	6	7	1	5	2	-	-
5	-3	7	4	1	5	2	-	-
6	-4	7	8	1	5	3	-	-
7	-5	9	6	1	5	4	called	1
8	6	9	10	2	6	5	-	
9	-6	10	7	2	6	5	called	2
10	7	10	11	3	7	6	-	
11	-7	11	8	3	7	6	called	3
12	-8	11	12	4	8	7	called	4
13	-9	13	10	5	9	8	called	5
14	10	-13	14	6	10	9	-	
15	-10	14	11	6	10	9	called	6
16	11	-14	15	7	11	10	called	7
17	-11	15	12	8	12	11	called	8
18	-12	-15	-16	9	16	12	called	9-16

(*) NPI, NPJ, NPM describe the topology of each element in the mesh. The minus sign indicates the last appearance.

The overall stiffness matrix is represented in Figure A1.3 when KROWI assumes the value 3 and immediately before calling the subroutine FORWAD. The front of active nodes is indicated by

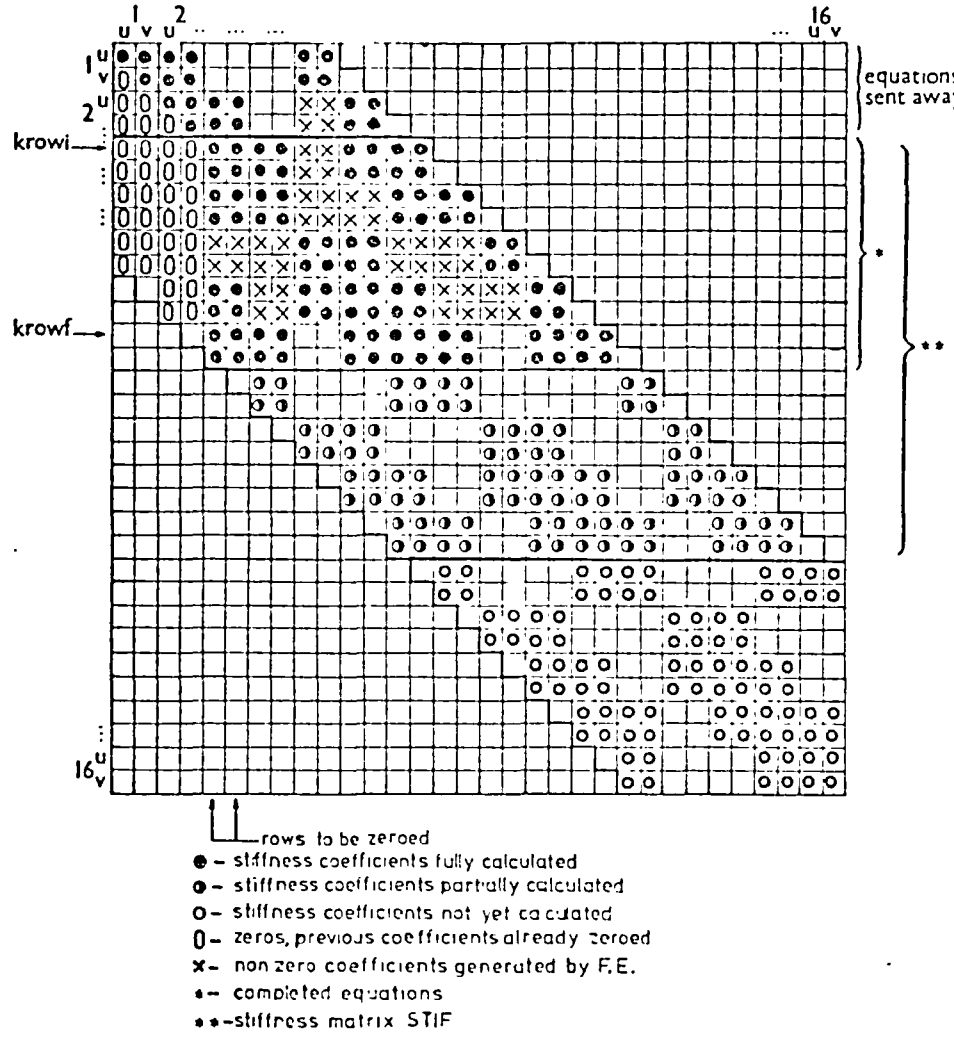

Figure A1.3 Overall Stiffness Matrix

the thicker line in Figure A1.2.

Subroutine FORWARD, when called, performs the elimination of the pair of equations related to the node KROWI. After the elmination process, the equations referred to above are stored in an array COMP. The first two rows in the STIF matrix are freed and the rest of the equations are shifted 2 rows upwards.

It should be pointed out that the coefficients in the STIF matrix are kept in the computer in a rectangular matrix of LBW + 1 columns and LBW rows. This book keeping procedure is aimed to reduce to a minimum the amount of computer memory necessary for the storage in fast core of the non-zero coefficients.

In order to reduce the tape operations, the transfer to a disk file of all the elminated nodes takes place in blocks. This is done using a non standard subroutine, WRITMS, which is called from subroutine FORWAD where all the equations already placed in a buffer area, COMP, are to be transferred to a random access file.

The larger the buffer area, the faster is the execution of the program, for less transfer operations take place. However it will be less efficient in terms of the central memory needed.

The size of this buffer area is such that it can share the same core spaces which will be needed later on for the arrays describing the element stresses. This is done by use of EQUIVALENCE statements in both the main program and the subroutine FORWAD.

A1.3.3 - Evaluation of Displacements and Stresses

After all the elements have been processed and the Gaussian elimination has been performed for all the equations, the system (A1.1) is now ready for the backward substitution. The main program calls subroutine BACKWD to perform this operation.

In this subroutine, the equations are retrieved from the random access file in reverse order and the displacement solution for the entire structure is evaluated as it is described in Chapter 2.

When in the presence of a previously prescribed displacement the backward substitution operations are skipped to preserve the initial displacement values which have been stored in UV when the boundary conditions have been fed into the program in subroutine INIAL. Otherwise these particular locations UV would contain the equivalent reaction forces as it was described in A1.2.1.

After this procedure is completed the main program evaluates the element and/or nodal stresses if required, in the same manner as it is done in the program FLAP5.

A1.3.4 - Flow chart of the Program FRONT

A detailed flow chart of the present code is illustrated in Figure A1.4 on the next page.

A1.4 - User's Guide

A1.4.1. Introduction

The FRONT code is a computer program written in FORTRAN IV.

In order to adapt its capacity to different cases , this code is provided with an additional program, EDT, which makes FRONT to operate in a "dynamic version".

EDIT is a facility available in the CDC system at ICCC which enables the contents of a particular file to be changed by using a set of control editing commands.

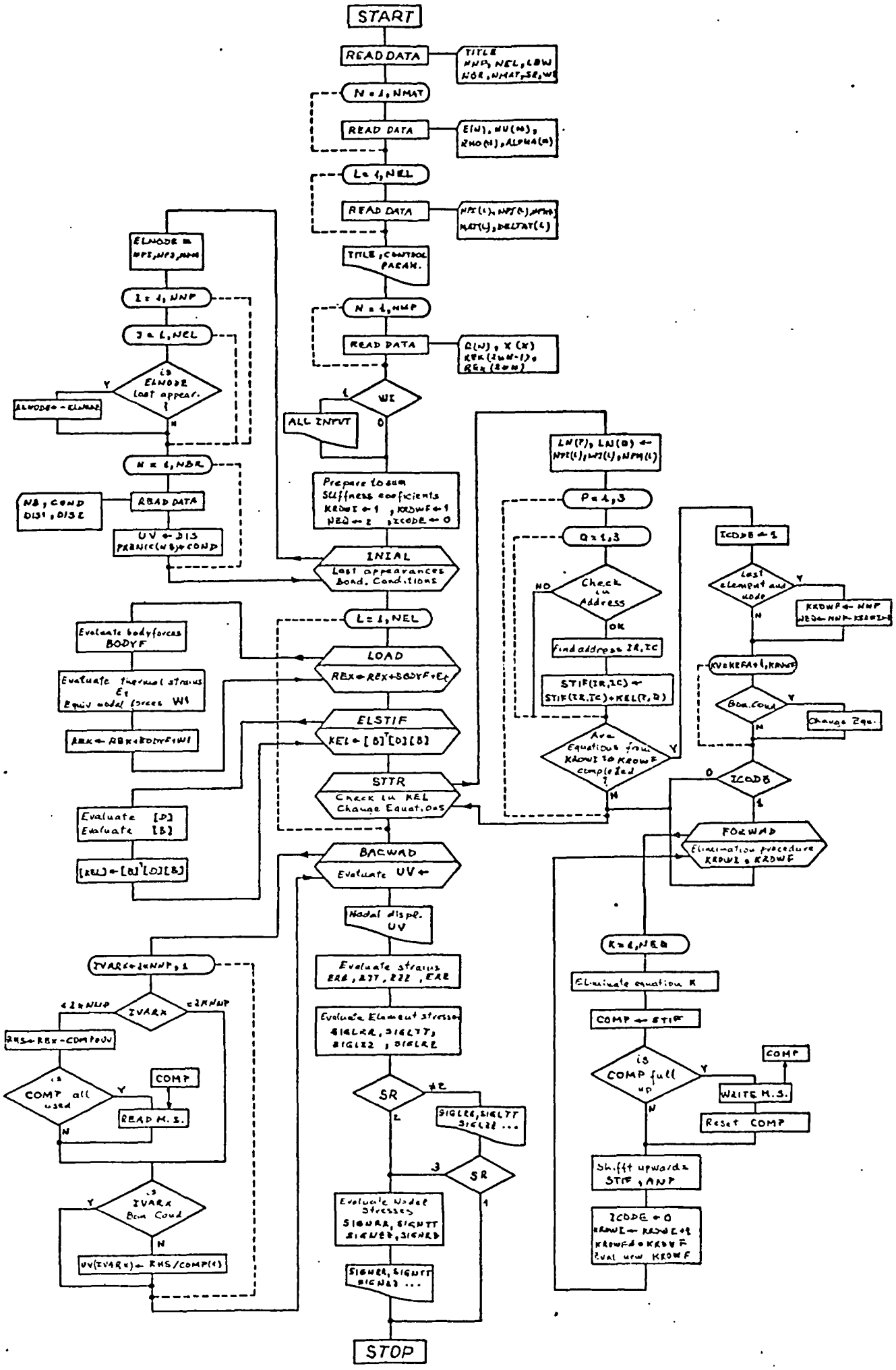

Figure A1.4 - Flow Chart of the FRONT Code.

The program EDT defines the exact amount of storage needed and calculates each array size in the COMMON block of the FRONT code. Moreover the EDT program writes into a file, TEXT, the necessary control directives by which a file containing the FRONT code will be suitably modified using the EDIT facility. The modified version of FRONT is then prepared to be compiled and executed.

Some environmental aspects of the programs FRONT and EDT will be described later on.

A1.4.2 - Preparation of the Problem

A1.4.2.1 - Material properties

Values of the Young's Modulus, the Poisson's ratio, the material density and the thermal expansion coefficients must be provided. The program allows for the use of five different materials. One will be specificed for each element.

A1.4.2.2 - Mesh Generation

The elements available are described by their cross-section made by a plane containing the axis of symmetry as illustrated in Figure A1.2.

For describing the topology of the mesh, it is necessary to define for each element three values NPI, NPJ, NPM containing three different nodal numbers in the mesh, following the topological order (anticlockwise) of that particular element.

Temperature rises are defined for each element and assumed to be constant within it.

It is also necessary to define the coordinates for all the nodes of the mesh in terms of the set of r,z coordinates.

A1.4.2.3 - Loading.

The program will only accept point forces applied to the nodes of the structure.

The sign of the load components is positive if it follows the positive direction of the r or z axis.

The forces will be interpreted as the total forces applied to a circle described by a particular loaded node rotating about the axis of symmetry.

A1.4.2.4 - Displacement Boundary Conditions

It is possible to prescribe any initial displacement in any node of the mesh by the components in the two directions r,z.

Slope boundary conditions can be prescribed as well, i.e., a node can be forced to displace within a particular direction making an angle ø with the r axis. This information is given to the program as follows

Prescribed Displacements

NB	ICOND	DIS 1	DIS 2	COMMENTS
Node	1	Displ. u	-	Restricted in the r direct.
Node	2	Displ. v	-	" " " z direct.
Node	3	Displ. u	Displ. v	" " both, r and z.

Slope Boundary Conditions

NB	ICOND	DIS 1	DIS 2	COMMENTS
Node	4	Q	-	u = Qv

A1.4.3 - List of Input Variables

The variable data are categorized by the designations

is integer

ia integer array

rs real single

ra real array

hs hollerith single

ha hollerith array

The unit can be any consistent set with angles in degrees.

ALPHA	ia	thermal expansion coefficient
DELTAT	ra	temperature rise in the element
DIS 1, DIS 2	rs	prescribed displacements, or DIS 1=Q in slope b. conditions
E	ra	Young's Modulus
ICOND	is	Prescribed displacements code
I	is	member of the element
LBW	is	size of the bandwidth
MAT	ia	Material identification number in the elem.
MATN	is	Material identification number
NBR	is	Total number of diaplacement boundary conditions
NEL	is	Total number of elements
NMAT	is	Total number of different materials.

NNP	is	Total number of nodes
NPI,NPJ, NPM	ia	Topological description of the elements
NU	ra	Poisson's ratio
R	ra	Nodal radial coordinate
REX	ra	Nodal point forces
RHO	ra	Material density
SR	is	Control parameter for output
		SR=1 Output displacement solution and element stresses
		SR=2 Output displacement solution and nodal stresses
		SR=3 Output displacement solution and nodal and element stresses
WI	is	Control parameter for input print out
		WI=0 Title, control parameters
		WI=1 Title, control parameters and the rest of input data
TITLE	ha	Title of the analysis

A1.4.4 - Input Data Format

The following table describes the order of input of the data defining the analysis.

CARD ORDER GROUPS OF CARDS	PROGRAM NAMES	FORMAT
1	TITLE	13A6
2	LBW, NEL, NNP, NBR, NMAT, SR, WI	5I5, 2I3
3	MAIN, E(MATN), NU(MATN), RHO(MATN),ALPHA(MATN), MATN=1,NMAT	I5,4E13.5

4	L,NPI(L),NPJ(L),NPM(L), MAT(L),DELTAT(L),L=1,NEL	I5,4E13.5
	. (NEL cards)	
5	N,R(N),Z(N),REX(2*N-1), REX(2*N),N=1,NNP	I5,4E12.5
	. (NNP cards)	
6	NB,ICOND,DIS1,DIS2	2I5,2E10.0
	. (NBR cards)	

A1.4.5 - Operating FRONT Using Program EDT

The listings of the programs FRONT and EDT are described in Sections A1.5 and A1.6 repectively.

This section indicates the control cards which are necessary for running the FRONT code at ICCC under the KRONOS 2.1 system.

No specific data is needed for running the program EDT, for it reads the necessary information from the basic parameters LBW, NNP and NEL which are specified in the second card of the FRONT code data deck.

The control cards are as follows

```
JOB(       )
PASSWORD(        )
MNF(B=BINEDT)
COPYBR(INPUT,FLDAT)
COPYBR(INPUT,FRONT)
BINEDT(FLDAT)
REWIND(FLDAT)
RENAME(INPUT=TEXT)
EDIT(FRONT)
MNF(I=FRONT,B=BFRONT)
BFRONT(FLDAT)
EOR
    Program EDT
EOR
EOR Data for program FRONT
    Program FRONT
EOF
```

If an editing facility is not available, the necessary alterations to the FRONT code can be obtained by printing out the TEXT file which may be generated by a seperate run of the program EDT.

In this file TEXT, for instance, commands such as

rs:/(NNNN)/,/(273)/;*

indicate that the string of characters (NNNN) should be repleced by the new string (273). These changes should be carried out for all the occurrences of (NNNN) in the FRONT code, if the ;* sings are included in the end of the command.

A1.4.6 - Environmental aspects

Experience has shown that for a large number of cases the number of elements in a 2D mesh of triangular elements is related to the number of nodes by a factor of about 1.8.

$$NEL \simeq 1.8\ NNP$$

Based on this ratio the necessary central memory which is needed to run the FRONT code, for different cases, can be calculated with a reasonable accuracy taking into account only the number of nodes and the size of the bandwidth.

A table is presented on the following page showing the number of central memory words (*) which are needed to run the FRONT code for a typical range of the parameters NNP and LBW.

(*) For the CDC 6400 machine available at ICCC

CENTRAL MEMORY WORDS NECESSARY FOR

RUNNING THE FRONT CODE

Bandwidth LBW	Number of Nodes in the Mesh				
	200	500	1000	1500	2000
21	12971	17810	25910	34010	42110
41	14260	19120	27820	35370	43420
61	16370	21230	29330	37430	45530
81	19270	24140	32240	40340	48440
101	22990	27855	35955	44050	52150
121	27500	32360	40469	48560	56660

25 K 30K 40K 50K

K = 1000 CM words

Al. 5 - Listing of the FRONT code

A listing of the FRONT code is presented in the following pages.

```
      PROGRAM FRONT(INPUT=10000,OUTPUT=10000,TAPE5=INPUT,TAPE6=OUTPUT,
     1           TAPE7=TPLEN)
C
C     0 SPECIFICATION AND DATA INITIALIZATION STATEMENTS.
      INTEGER  TITLE,    SR,       QA,       O,
     1         CASCTL,   XI,       ANP,      P,
     2                   COND,               Q
      REAL     NU,       KEL
      COMMON      TITLE(13),  NPI(LLLL),      NPJ(LLLL),      NPM(LLLL),
     1            E(5),XI,    R(NPNP),        PRENIC(NNNN),   NAME(REC),
     2            NU(5),      Z(NPNP),        REX(NPNP2),     LN(3),W(4,6),
     3            RHO(5),     MAT(LLLL),      UV(NPNP2),      B(4,6),
     4            ALPHA(5),   DELTAT(LLLL),   ANP(QQ,9),      D(4,4),
     5                        STIF(891,888),  NAP(NNNN),      KEL(6,6),
     6            SIGRR(LLLL),SIGTT(LLLL),SIGZZ(LLLL),SIGRZ(LLLL)
      COMMON /PARAM/ NEL,NPP,NBR,NMAT,LBW,L
      COMMON /FLIGHT/ KROJI,KROXF,ICODE,NEQ,KROWFA,K1,ICO,LREC
      DATA  CASCTL / 6HENDCASE /
C
C
C     10 INPUT THE CASE TITLE BUT STOP IF THERE IS NO FURTHER CASE.
   11 READ (5, 12)  TITLE
   12 FORMAT (13A6)
      IF (TITLE (1) .EQ. CASCTL)  STOP
C
C
C     20 INPUT THE CONTROL PARAMETERS AND PREPARE TO INPUT THE ARRAY DATA.
      READ(5,21) LBW,NEL,NPP,NBR,NMAT,SR,WI
   21 FORMAT(5I5,2I3)
      DO 22  NM = 1, NMAT
   22 E (NM) = -1.
      DO 23  L = 1, NEL
   23 NPI (L) = -1
      DO 24  N = 1, NPP
   24 R (N) = -0.12345678E35
C
C
C     30 INPUT AND CHECK THE ARRAY DATA.
      READ (5, 31)  (MATN, E (MATN), NU (MATN),
     1               RHO (MATN), ALPHA (MATN),  NM = 1, NMAT)
   31 FORMAT (I5, 4E13.5)
      DO 33  NM = 1, NMAT
      IF (E (NM) .NE. -1.)  GO TO 33
      WRITE (6, 32)  TITLE
   32 FORMAT (1H1 ////// 5H IN 3, 13A6, 1H0 /
     1        35H THERE IS A MISSING INPUT DATA CARD.,
     2        24H   THE JOB IS ABANDONED.)
      STOP
   33 CONTINUE
      READ (5, 34)  (LE, NPI (LE), NPJ (LE), NPM (LE),
     1               MAT (LE), DELTAT (LE),  L = 1, NEL)
   34 FORMAT (5I5, F10.3)
```



```
      DO 35  L = 1, NEL
      IF (NPI (L) .NE. -1)  GO TO 35
      WRITE (6, 32)  TITLE
      STOP
   35 CONTINUE
      READ(5,36) (N,R(NP),Z(NP),REX(2*NP-1),REX(2*NP),NP=1,NNP)
   36 FORMAT(I5,4E12.5)
      DO 37  N = 1, NNP
      IF (R (N) .NE. -0.12345678E35)  GO TO 37
      WRITE (6, 32)  TITLE
      STOP
   37 CONTINUE
C
C
C     40 OUTPUT THE TITLE AND THE CONTROL PARAMETERS.
      WRITE (6, 41)
   41 FORMAT (1H1 //////
     1        45X, 41HTHE CASE TITLE AND THE CONTROL PARAMETERS /
     2        45X, 41H---------------------------------------- /////)
      WRITE (6, 42)  TITLE
   42 FORMAT (1H , 13A6)
      WRITE(6,43) NEL,NPP,NBR,NMAT,LBW
   43 FORMAT (26HOTHE NUMBER OF ELEMENTS IS, I5, 1H. /
     1        30HOTHE NUMBER OF NODAL POINTS IS, I5, 1H. /
     2        43HOTHE NUMBER OF RESTRAINED BOUNDARY NODES IS, I5, 1H. /
     3        37HOTHE NUMBER OF DIFFERENT MATERIALS IS, I5, 1H. /
     5        16HOTHE BANDWITH IS,I5,1H./
     8        23HOSTRESSES ARE FOUND FOR)
      IF (SR .EQ. 0)  WRITE (6, 44)
   44 FORMAT (1H+, 23X, 42HNEITHER THE ELEMENTS NOR THE NODAL POINTS.)
      IF (SR .EQ. 1)  WRITE (6, 45)
   45 FORMAT (1H+, 23X, 10HTHE ELEMENTS ONLY.)
      IF (SR .EQ. 2)  WRITE (6, 46)
   46 FORMAT (1H+, 23X, 22HTHE NODAL POINTS ONLY.)
      IF (SR .EQ. 3)  WRITE (6, 47)
   47 FORMAT (1H+, 23X, 39HBOTH THE ELEMENTS AND THE NODAL POINTS.)
      IF (XI .EQ. 0)  WRITE (6, 48)
   48 FORMAT (37HOTHE INPUT ARRAY DATA ARE NOT OUTPUT.)
      IF (XI .EQ. 1)  WRITE (6, 49)
   49 FORMAT (33HOTHE INPUT ARRAY DATA ARE OUTPUT.)
C
C
C     50 OUTPUT THE ARRAY DATA.
      IF (XI .EQ. 0)  GO TO 61
      WRITE (6, 51)  (NM, E (NM), NU (NM), RHO (NM),
     1                ALPHA (NM),  NM = 1, NMAT)
   51 FORMAT (1H1 //////
     1        56X, 19HINPUT MATERIAL DATA /
     2        56X, 19H------------------ /////
     3        28X, 42HMATERIAL  ELASTIC MODULUS  POISSONS RATIO,
     4             34H      DENSITY      THML EXPN COEFF //
```

```
     5        (I33, X, 4E17.5))
      WRITE (6, 52)
   52 FORMAT (1H1 //////
     1        57X, 18HINPUT ELEMENT DATA /
     2        57X, 18H------------------ /////
     3         3X, 48HELMT NPI  NPJ  NPM  MTRL  DELTA T
     4             48HELMT NPI  NPJ  NPM  MTRL  DELTA T
     5             33HELMT NPI  NPJ  NPM  MTRL  DELTA T /)
      L1 = (NEL + 2) / 3
      DO 53  L2 = 1, L1
      L3 = MIN0 (L2 + 2 * L1, NEL)
   53 WRITE (6, 54)  (L, NPI (L), NPJ (L), NPM (L),
     1                MAT (L), DELTAT (L),  L = L2, L3, L1)
   54 FORMAT (1H , 5I5, F10.3, 13X, 5I5, F10.3, 13X, 5I5, F10.3)
      WRITE(6,55)
   55 FORMAT(1H1 //////
     1        58X,15HINPUT NODE DATA /
     2        58X,15H---------------/////
     3        2(6X,2HNODE      R           Z     ,
     4             2HN      RR          RZ    )///)
      N1=(NNP+1)/2
      DO 57 N2=1,N1
      N3=MIN0(N2+N1,NNP)
   57 WRITE(6,58) (N,R(N),Z(N),REX(2*N-1),REX(2*N),N=N2,N3,N1)
   58 FORMAT(2(5X,I5,4E12.5))
      WRITE(6,56)
   56 FORMAT (1H1 //////
     1        48X, 35HINPUT RESTRAINED BOUNDARY NODE DATA /
     2        48X, 35H----------------------------------- /////
     3        33X, 2HRESTND BODY NODE
     4             37HRESTNT CONDITION                DISPLA //)
C
C
C
C     PREPARE TO SUM THE STIFFENESS COEFICIENTS
C
   61 DO 81 NR=1,LBW-1
      DO 81 NC=1,LBW
   81 STIF(NR,NC)=0.0
      DO 82 NR=1,LBW/2
      DO 82 NC=1,9
      NAP(NR,NC)=0
   82 NAP(NR,1)=NR
      DO 83 NR=1,NNP
   83 NAP(NR)=1
      KRSET=1
      ICODE=0
      KROWA=1
      KROWF=1
      DET=2
      LHALF=(2*NNP-1)/RCO+1
```



```
      LREC=RCO*(LBW/2+1)
      CALL OPENMS(7,NAME,LNAME,0)
C
C     LAST NODAL APPEARANCES AND INPUT BOUNDARY CONDITIONS
C
      CALL INIAL
C
C     DO LOOP FOR ALL THE ELEMENTS
C
      DO 72 L=1,NEL
C
C     CALCULATE TOTAL EXTERNAL NODAL FORCES REX(I)
C
      CALL LOAD
C
C     CALCULATE ELEMENT STIFNESS MATRIX KEL(I,J)
C
      CALL ELSTIF
C
C     CHECK IN ELEMENT STIFFNESS COEFICIENTS INTO MATRIX M AND
C     THEN INTO RECTANGULAR MATRIX STIF(I,J) AND IMPOSE BOUNDARY CONDITI
C
      CALL STIR
   72 CONTINUE
C
C     BACK SUBSTITUTION CALCULATING NODAL DISPLACEMENTS
C
      CALL BACKWD
C
C
C 150 OUTPUT THE NODE DISPLACEMENTS IN THE PLANE SECTION REVOLVED.
  151 WRITE (6, 152)
  152 FORMAT (1H1 //////
     1        49X, 33HTHE CALCULATED NODE DISPLACEMENTS /
     2        49X, 33H--------------------------------- /////
     3         3X, 47HNODE          U                  V
     4             47HNODE          U                  V
     5             30HNODE          U                  V /)
      N1 = (NNP + 2) / 3
      DO 153  N2 = 1, N1
      N3 = MIN0 (N2 + 2 * N1, NNP)
  153 WRITE(6,154) (N,UV(2*N-1),UV(2*N),N=N2,N3,N1)
  154 FORMAT (1H , I5, 2E16.5, I15, 2E16.5, I15, 2E16.5)
C
C
C 160 CALCULATE THE ELEMENT STRESS COMPONENTS.
      IF (SR .EQ. 0)  GO TO 221
      DO 184  L = 1, NEL
      I=IABS(NPI(L))
      J=IABS(NPJ(L))
      M=IABS(NPM(L))
```

```
      BI=Z(J)-Z(M)    &    BJ=Z(M)-Z(I)    &    BM=Z(I)-Z(J)
      CI=-R(J)+R(M)   &    CJ=-R(M)+R(I)   &    CM=-R(I)+R(J)
      AREA=(BJ*CM-BM*CJ)/2.
      RBAR = (R (I) + R (J) + R (M)) / 3.
      WA=12.*AREA)/13.*RBAR)
      EERR=(BI*UV(2*I-1)+BJ*UV(2*J-1)+BM*UV(2*M-1))/(2.*AREA)
      EETT=(UV(2*I-1)+UV(2*J-1)+UV(2*M-1))/(3.*RBAR)
      EEZZ=(CI*UV(2*I)+CJ*UV(2*J)+CM*UV(2*M))/(2.*AREA)
      EERZ=(CI*UV(2*I-1)+BI*UV(2*I)+CJ*UV(2*J-1)+BJ*UV(2*J)+
     1       CM*UV(2*M-1)+BM*UV(2*M))/(2.*AREA)
      MATN = MAT (L)
      W1 = NU (MATN)
      W2 = 1. - W1
      W3 = 1. + W1
      W4 = 1. - 2. * W1
      W5 = E (MATN) / (W3 * W4)
      ETH = ALPHA (MATN) * DELTAT (L)
      ERR = EERR - ETH
      ETT = EETT - ETH
      EZZ = EEZZ - ETH
      ERZ = EERZ
      SIGLRR (L) = W5 * (W2 * ERR + W1 * ETT + W1 * EZZ)
      SIGLTT (L) = W5 * (W1 * ERR + W2 * ETT + W1 * EZZ)
      SIGLZZ (L) = W5 * (W1 * ERR + W1 * ETT + W2 * EZZ)
      SIGLRZ (L) = W5 * W4 * ERZ / 2.
C
C
C 170 CALCULATE THE ELEMENT PRINCIPAL AND MEAN STRESSES IN THE PLANE
C     SECTION REVOLVED.
      IF (SR .EQ. 2)  GO TO 184
      W1 = (SIGLRR (L) + SIGLZZ (L)) / 2.
      W2 = (SIGLRR (L) - SIGLZZ (L)) / 2.
      W3 = SIGLRZ (L)
      W4 = SQRT (W2 ** 2 + W3 ** 2)
      SIGL1 = W1 + W4
      SIGL2 = W1 - W4
      IF (ABS (W2) .GT. 1.E-35 .OR. ABS (W3) .GT. 1.E-35)  GO TO 171
      ANGLEL = 0.
      GO TO 172
  171 ANGLEL = 28.647889756 * ATAN2 (W3, W2)
  172 SIGL3 = SIGLTT (L)
      SIGLM = SQRT ((SIGL1 + SIGL2 + SIGL3) ** 2
     1            - 3. * (SIGL2 * SIGL3 + SIGL3 * SIGL1 + SIGL1 * SIGL2))
C
C
C 180 OUTPUT THE ELEMENT STRESSES.
      IF (L .NE. 1)  GO TO 182
      WRITE (6, 181)
  181 FORMAT (1H1 //////
     1         4X, 44HTHE CALCULATED ELEMENT STRESS COMPONENTS AND,
     2             43H MEAN STRESS IN THE SPACE AND THE PRINCIPAL,
```



```
     3             39H STRESSES IN THE PLANE SECTION REVOLVED /
     4         4X, 44H--------------------------------------------,
     5             43H-------------------------------------------,
     6             39H--------------------------------------- /////
     7         1X, 45HELEMENT      SIGMRR          SIGMTT          ,
     8             45HSIGMZZ           SIGMRZ          ANGLE1      ,
     9             37HSIGM1            SIGM2             SIGMM /)
  182 WRITE (6, 183)  L, SIGLRR (L), SIGLTT (L), SIGLZZ (L),
     1                SIGLRZ (L), ANGLEL, SIGL1, SIGL2, SIGLM
  183 FORMAT (1H , I5, 4E16.5, F12.2, X, 3E16.5)
  184 CONTINUE
      IF (SR .EQ. 1)  GO TO 221
C
C
C 190 FIND THE NODE STRESS COMPONENTS.
      DO 212  N = 1, NUP
      SIGNRR = 0.
      SIGNTT = 0.
      SIGNZZ = 0.
      SIGNRZ = 0.
      QA = 1
      DO 191  L = 1, NEL
      IF(IABS(NPI(L)).NE.N.AND.IABS(NPJ(L)).NE.N.AND.IABS(NPM(L)).NE.N)
     1                                                          GO TO 191
      SIGNRR = SIGNRR + SIGLRR (L)
      SIGNTT = SIGNTT + SIGLTT (L)
      SIGNZZ = SIGNZZ + SIGLZZ (L)
      SIGNRZ = SIGNRZ + SIGLRZ (L)
      QA = QA + 1
      IF(QA.EQ.IABS(NAP(N))) GO TO 192
  191 CONTINUE
  192 W1 = FLOAT (QA - 1)
      SIGMRR = SIGNRR / W1
      SIGMTT = SIGNTT / W1
      SIGMZZ = SIGNZZ / W1
      SIGMRZ = SIGNRZ / W1
C
C
C 200 CALCULATE THE NODE PRINCIPAL AND MEAN STRESSES IN THE PLANE
C     SECTION REVOLVED.
  201 W1 = (SIGMRR + SIGMZZ) / 2.
      W2 = (SIGMRR - SIGMZZ) / 2.
      W3 = SIGMRZ
      W4 = SQRT (W2 ** 2 + W3 ** 2)
      SIGN1 = W1 + W4
      SIGN2 = W1 - W4
      IF (ABS (W2) .GT. 1.E-35 .OR. ABS (W3) .GT. 1.E-35)  GO TO 202
      ANGLEN = 0.
      GO TO 203
  202 ANGLEN = 28.647889756 * ATAN2 (W3, W2)
  203 SIGN3 = SIGMTT
```

```
      SIGNM = SQRT ((SIGN1 + SIGN2 + SIGN3) ** 2
     1           - 3. * (SIGN2 * SIGN3 + SIGN3 * SIGN1 + SIGN1 * SIGN2))
C
C
C 210 OUTPUT THE NODE STRESSES.
      IF (N .NE. 1)  GO TO 212
      WRITE (6, 211)
  211 FORMAT (1H1 //////
     1          6X, 41HTHE CALCULATED NODE STRESS COMPONENTS AND,
     2              43H MEAN STRESS IN THE SPACE AND THE PRINCIPAL,
     3              39H STRESSES IN THE PLANE SECTION REVOLVED /
     4          6X, 41H----------------------------------------,
     5              43H----------------------------------------,
     6              39H---------------------------------------- /////
     7          3X, 43HNODE        SIGMRR          SIGMTT          ,
     8              45HSIGMZZ          SIGMRZ          ANGLE1        ,
     9              37HSIGM1           SIGM2             SIGMM /)
  212 WRITE (6, 213)  N, SIGMRR, SIGMTT, SIGMZZ, SIGMRZ,
     1                ANGLEN, SIGM1, SIGM2, SIGMM
  213 FORMAT (1H , I5, 4E16.5, F12.2, X, 3E16.5)
C
C
C 220 RETURN TO THE BEGINNING OF THE PROGRAM FOR THE NEXT CASE.
  221 STOP
      END



      SUBROUTINE INIAL
C     THIS SUBROUTINE FINDS THE LAST NODE APPEARANCES FOR EACH ELEMENT
C     AND READS IN BOUNDARY CONDITIONS
C
      INTEGER PRENIC,TITLE,QA,WI,ANP,P,Q,ELNODE
      REAL NU,KEL
      COMMON      TITLE(13),  NPI(LLLL),      NPJ(LLLL),      NPM(LLLL),
     1            E(5),XI,    R(NNNP),        PRENIC(NNNP),   NAME(REC),
     2            NU(5),      Z(NNNP),        REX(NNN2),      LM(3),W(4,6),
     3            RHO(5),     MAT(LLLL),      UV(NNN2),       B(4,6),
     4            ALPHA(5),   DELTAT(LLLL),   ANP(QQ,9),      D(4,4),
     5                        STIF(NB1,NPB),  BAP(NNNN),      KEL(6,6),
     6            SIGLRR(LLLL),SIGLTT(LLLL),SIGLZZ(LLLL),SIGLRZ(LLLL)
      COMMON /PARAM/NEL,NNP,NNR,NMAT,LRA,L
      COMMON /ELIMIN/ KROW1,KROWF,ICODE,NEQ,KROWFA,K1,ICO,LREC
      DIMENSION ELNODE(LLLL,3)
      EQUIVALENCE (ELNODE(1,1),NPI(1))
C
C     FIND LAST APPEARANCES MARKING WITH A - SIGN FOR EACH ELEMENT
C
      DO 5 N=1,NNP
      DO 3 I=1,NEL
      I1=NEL-I+1
```



```
      DO 3 J=1,3
      J1=3-J+1
      IF(ELNODE(I1,J1).EQ.N) GO TO 4
    3 CONTINUE
    4 ELNODE(I1,J1)=-ELNODE(I1,J1)
    5 CONTINUE
C
C     BOUNDARY CONDITIONS
C
      DO 100 I=1,NNP
  100 PRENIC(I)=0
      DO 30 K=1,NBR
      READ(5,16) NB, ICOND,DIS1,DIS2
   16 FORMAT(2I5,2E10.0)
      PRENIC(NB)=ICOND
      DIS=DIS1
      IF(ICOND.EQ.4) GO TO 40
      III=1
      IF(PRENIC(NB)-2) 60,70,60
   60 IND=2*NB-1
      GO TO 80
   70 IND=2*NB
   80 UV(IND)=DIS1
      III=III-1
      IF(PRENIC(NB).EQ.3.AND.III.EQ.0) GO TO 50
      GO TO 10
   50 DIS1=DIS2
      GO TO 70
   40 UV(2*NB)=DIS
   10 IF(NI.EQ.0) GO TO 30
      WRITE(6,20) NB,PRENIC(NB),DIS,DIS2
   20 FORMAT(1H2,I24,2E20.5)
   30 CONTINUE
      RETURN
      END



      SUBROUTINE LOAD
C     THIS SUBROUTINE CALCULATES THE EXTERNAL NODAL FORCES DUE TO
C     APPLIED FORCES,BODY FORCES AND INITIAL STRAIN CONDITIONS
C
      INTEGER PRENIC,ANP,WI
      REAL NU,KEL
      COMMON      TITLE(13),  NPI(LLLL),      NPJ(LLLL),      NPM(LLLL),
     1            E(5),XI,    R(NNNP),        PRENIC(NNNP),   NAME(REC),
     2            NU(5),      Z(NNNP),        REX(NNN2),      LM(3),W(4,6),
     3            RHO(5),     MAT(LLLL),      UV(NNN2),       B(4,6),
     4            ALPHA(5),   DELTAT(LLLL),   ANP(QQ,9),      D(4,4),
     5                        STIF(NB1,NPB),  BAP(NNNN),      KEL(6,6),
     6            SIGLRR(LLLL),SIGLTT(LLLL),SIGLZZ(LLLL),SIGLRZ(LLLL)
```

```
      COMMON/MATB/BI,BJ,BM,CI,CJ,CM,AREA
      COMMON /PARAM/ NEL,NNP,NBR,NMAT,LBW,L
C  60 DO GEOMETRIC CALCULATIONS ON THE ELEMENTS.
      I=IABS(NPI(L))
      J=IABS(NPJ(L))
      M=IABS(NPM(L))
      BI=Z(J)-Z(M)    £   BJ=Z(M)-Z(I)    £   BM=Z(I)-Z(J)
      CI=-R(J)+R(M)   £   CJ=-R(M)+R(I)   £   CM=-R(I)+R(J)
      AREA=(BJ*CM-BM*CJ)/2.
      IF (AREA .GT. 1.E-35)  GO TO 71
      WRITE (6, 62)  L
   62 FORMAT (1H1 ////// 8H ELEMENT, I5, 25H HAS A NON-POSITIVE AREA. /
     1        23H THE CASE IS ABANDONED.)
      STOP
C
C  70 SUM THE TOTAL NODAL POINT FORCES.
C
   71 MATN = MAT (L)
      RBAR = (R (I) + R (J) + R (M)) / 3.
      W1 = 3.1415926536 * RBAR * E (MATN) * ALPHA (MATN) * DELTAT (L)
     1                                    / (1. - 2. * NU (MATN))
      W2 = (2. * AREA) / (3. * RBAR)
      BODYF = 2. * 3.1415926536 * RBAR * AREA * RHO (MATN) / 3.
      REX(2*I-1)=REX(2*I-1)+W1*(BI+W2)   £  REX(2*I)=REX(2*I)+W1*CI-BODYF
      REX(2*J-1)=REX(2*J-1)+W1*(BJ+W2)   £  REX(2*J)=REX(2*J)+W1*CJ-BODYF
      REX(2*M-1)=REX(2*M-1)+W1*(BM+W2)   £  REX(2*M)=REX(2*M)+W1*CM-BODYF
      RETURN
      END
```

```
      SUBROUTINE ELSTIF
C     THIS SUBROUTINE EVALUATES THE STIFNESS MATRIX KEL(I,J) FOR EACH EL
C
      REAL NU,KEL
      INTEGER A,P,Q,WI
      COMMON      TITLE(13),   NPI(LLLL),      NPJ(LLLL),      NPM(LLLL),
     1            E(5),WI,     R(NNNN),        PRENIC(NNNN),   NAME(REC),
     2            NU(5),       Z(NNNN),        REX(NNN2),      LM(3),W(4,6),
     3            RHO(5),      MAT(LLLL),      UV(NNN2),       B(4,6),
     4            ALPHA(5),    DELTAT(LLLL),   ANP(NN,9),      D(4,4),
     5                         STIF(NB1,NBR),  NAP(NNNN),      KEL(6,6),
     6            SIGLRR(LLLL),SIGLTT(LLLL),SIGLZZ(LLLL),SIGLRZ(LLLL)
      COMMON/MATB/BI,BJ,BM,CI,CJ,CM,AREA
      COMMON /PARAM/ NEL,NNP,NBR,NMAT,LBW,L
C
      DO 92  P = 1, 4
      DO 91  Q = 1, 6
   91 B (P, Q) = 0.
      DO 92  Q = 1, 4
   92 D (P, Q) = 0.
```



```
      B(1,1)=BI    £   B(1,3)=BJ    £   B(1,5)=BM
      I=IABS(NPI(L))
      J=IABS(NPJ(L))
      M=IABS(NPM(L))
      RBAR = (R (I) + R (J) + R (M)) / 3.
      W1 = (2. * AREA) / (3. * RBAR)
      B(2,1)=W1    £   B(2,3)=W1    £   B(2,5)=W1
      B(3,2)=CI    £   B(3,4)=CJ    £   B(3,6)=CM
      B(4,1)=CI    £   B(4,2)=BI    £   B(4,3)=CJ
      B(4,4)=BJ    £   B(4,5)=CM    £   B(4,6)=BM
      MATN = MAT (L)
      W1 = NU (MATN)
      W2 = 1. - W1
      W3 = 1. + W1
      W4 = 1. - 2. * W1
      W5 = 3.1415926536 * RBAR * E (MATN) / (2. * AREA * W3 * W4)
      D (1, 1) = W5 * W2
      D (1, 2) = W5 * W1
      D (1, 3) = W5 * W1
      D (2, 1) = W5 * W1
      D (2, 2) = W5 * W2
      D (2, 3) = W5 * W1
      D (3, 1) = W5 * W1
      D (3, 2) = W5 * W1
      D (3, 3) = W5 * W2
      D (4, 4) = W5 * W4 / 2.
      DO 94  P = 1, 4
      DO 93  Q = 1, 6
      W (P, Q) = 0.
      DO 93  A = 1, 4
   93 W (P, Q) = W (P, Q) + D (P, A) * B (A, Q)
      DO 94  P = 1, 6
      DO 94  Q = 1, 6
      KEL(P,Q)=0.
      DO 94  A = 1, 4
   94 KEL(P,Q)=KEL(P,Q) + B(A,P) * W(A,Q)
      RETURN
      END
```

```
      SUBROUTINE STIR
C     THIS SUBROUTINE CHECKS IN STIFNESS COEFFICIENTS KEL
C     INTO THE RECTANGULAR MATRIX STIF(I,J)
C
      INTEGER P,Q, ANP,PRENIC,QA
      REAL KEL
      COMMON      TITLE(13),   NPI(LLLL),      NPJ(LLLL),      NPM(LLLL),
     1            E(5),WI,     R(NNNN),        PRENIC(NNNN),   NAME(REC),
     2            NU(5),       Z(NNNN),        REX(NNN2),      LM(3),W(4,6),
     3            RHO(5),      MAT(LLLL),      UV(NNN2),       B(4,6),
```

```
     4            ALPHA(5),   DELTAT(LLLL),  ANP(QQ,9),     D(4,4),
     5                        STIF(BB1,BBB), NAP(NNNN),     KEL(6,6),
     6            SIGLRR(LLLL),SIGLTT(LLLL),SIGLZZ(LLLL),SIGLRZ(LLLL)
      COMMON /PARAM/ NEL,NNP,NBR,NMAT,LBW,L
      COMMON /ELIMIN/ KROWI,KROWF,ICODE,NEQ,KROWFA,K1,IC0,LREC
      LN(1)=NPT(L)    &   LN(2)=NPJ(L)    &   LN(3)=NPK(L)
      DO 106 P=1,3
      IKROWF=KROWF
      NP=IABS(LN(P))
      LNP=NP-KROWI+1
      DO 105 Q=1,3
      QA=0
  101 QA=QA+1
      IF(QA.LE.9) GO TO 103
      WRITE(6,102) NP
  102 FORMAT (1H1 ////// 5H NODE, I5,
     1        36H HAS MORE THAN EIGHT ADJACENT NODES. /
     2        23H THE CASE IS ABANDONED.)
      STOP
  103 IF(ANP(LNP,QA).EQ.IABS(LN(Q))) GO TO 104
      IF(ANP(LNP,QA).NE.0) GO TO 101
      ANP(LNP,QA)=IABS(LN(Q))
      NAP(NP)=QA
  104 IR=2*(NP-KROWI)+1
      IC=2*ANP(LNP,QA)-1+LBW/2-(2*NP-1)+1
      STIF(IR  ,IC  )=STIF(IR  ,IC  ) + KEL(2*P-1,2*Q-1)
      STIF(IR  ,IC+1)=STIF(IR  ,IC+1) + KEL(2*P-1,2*Q  )
      STIF(IR+1,IC-1)=STIF(IR+1,IC-1) + KEL(2*P  ,2*Q-1)
  105 STIF(IR+1,IC  )=STIF(IR+1,IC  ) + KEL(2*P  ,2*Q  )
      IF(LN(P).GT.0) GO TO 111
      NAP(NP)=-NAP(NP)
      IF(NP.GT.KROWF) GO TO 111
      IF(NP.NE.1) GO TO 107
      KROWF=ANP(1,1)
      DO 108 I=2,9
  108 KROWF=MAX0(ANP(1,I),KROWF)
  107 IF(.NOT.(P.EQ.3.AND.L.EQ.NEL)) GO TO 109
      NEQ=2*(NNP-KROWI)+1
      KROWF=NNP
      GO TO 1
  109 DO 110 I=KROWFA+1,KROWF
      IF(NAP(I).GT.0) GO TO 111
  110 CONTINUE
      IF(NEQ.NE.2) KROWF=IKROWF
      ICODE=1
      GO TO 1
  111 ICODE=0
      IF(ICODE.EQ.0) GO TO 106
C     BOUNDARY CONDITIONS
C
    1 DO 51 KV=KROWFA+1,KROWF
```



```
      KRII=ANP(KV-KROWI+1,1)
      KREF=KRII
      LNAP=IABS(NAP(KV))
      DO 12 I=2,LNAP
      KREF=MAX0(KREF,ANP(KV-KROWI+1,I))
   12 KRII=MIN0(ANP(KV-KROWI+1,I),KRII)
      DO 50 KH=KRII,KREF
      IF(PRENIC(KH).EQ.0.OR.PRENIC(KH).EQ.4) GO TO 50
      III=1
      IF(PRENIC(KH)-2) 60,70,60
   60 NB=2*(KH-KROWI)+1
      GO TO 200
   70 NB=2*(KH-KROWI)+2
  200 IT=2*KV-1
      IV1=IT-(2*KROWI-1)+1
      IV2=IV1+1
      IC1=NB+LBW/2-IV1+1
      IC2=IC1-1
      IF(IC1.EQ.LBW/2+1) REX(IT)=0.0
      IF(IC2.EQ.LBW/2+1) REX(IT+1)=0.0
      IF(PRENIC(KH).EQ.2) III=0
      REX(IT)=REX(IT)-STIF(IV1,IC1)*UV(2*KH-III)
      REX(IT+1)=REX(IT+1)-STIF(IV2,IC2)*UV(2*KH-III)
      STIF(IV1,IC1)=0.0
      STIF(IV2,IC2)=0.0
      IF(IC1.EQ.LBW/2+1) STIF(IV1,IC1)=-1.
      IF(IC2.EQ.LBW/2+1) STIF(IV2,IC2)=-1.
      III=III-1
      IF(PRENIC(KH).EQ.3.AND.III.EQ.0) GO TO 70
   50 CONTINUE
      IF(PRENIC(KV).NE.4) GO TO 51
      DO 55 I=1,LNAP
      NO=ANP(KV-KROWI+1,I)-KROWI+1
      IV1=2*(KV-KROWI)+1
      IV2=IV1+1
      IC1=2*NO+LBW/2-IV1
      IC2=IC1-1
      STIF(IV1,IC1)=STIF(IV2,IC2)+UV(2*KV)*STIF(IV1,IC1)
   55 STIF(IV1,IC1+1)=STIF(IV2,IC2+1)+UV(2*KV)*STIF(IV1,IC1+1)
      REX(2*KV-1)=REX(2*KV)+UV(2*KV)*REX(2*KV-1)
      DO 56 J=1,LBW
   56 STIF(IV2,J)=0.0
      STIF(IV2,LBW/2)=1.0
      STIF(IV2,LBW/2+1)=-UV(2*KV)
      REX(2*KV)=0.0
   51 CONTINUE
      IKROWF=KROWF
C
C     FORWARD ELIMINATION
C     IF EQUATIONS FROM KROWI TO KROWF ARE COMPLETED PROCEED TO
C
```

```
      CALL FORWAD
      ICODF=0
  106 CONTINUE
      RETURN
      END



      SUBROUTINE FORWAD
C     THIS SUBROUTINE USES FOWARD ELIMINATION TO A SET OF NEQ COLUMNS
C     STORES IN A PERIPHERAL DEVICE THE COMPLETED EQUATIONS AND SHIFTS
C     UPWARDS NEQ TIMES THE MATRIX STIF(I,J) AND (NEQ+1)/2 TIMES
C     THE MATRIX ANP(NP,9A)
C
      INTEGER TITLE,SR,NA,O,PRENIC,WI,ANP,P
      REAL NU,KEL
      DIMENSION  COMP(RCO,BBR)
      COMMON     TITLE(13),   NPI(LLLL),     NPJ(LLLL),     NPM(LLLL),
     1           E(5),WI,     R(NNNN),       PRENIC(NNNN),  NAME(REC),
     2           NU(5),       Z(NNNN),       REX(NNN2),     LN(3),W(4,6),
     3           RHO(5),      MA1(LLLL),     UV(NNN2),      B(4,6),
     4           ALPHA(5),    DELTAT(LLLL),  ANP(3C,9),     D(4,4),
     5                        STIF(BB1,BBR), NAP(NBBN),     KEL(6,6),
     6           SIGLRR(LLLL),SIGLTT(LLLL),SIGLZZ(LLLL),SIGLRZ(LLLL)
      COMMON /PARAM/ NEL,NNP,NBR,NMAT,LBW,L
      COMMON /ELIMIN/ KROWI,KROWF,ICODE,NEQ,KROWFA,K1,ICO,LREC
      EQUIVALENCE(COMP(1,1),SIGLRR(1))
    1 KRI=KROWI
      IF(KRI.EQ.1) ICO=0
      DO 134 ICOEL=1,NEQ
      ICO=ICO+1
      LIDE=2*(KROWF-KRI+1)
      LIRC=LIDE
      DO 136 IDE=ICOEL+1,LIDE
      I=IDE
      J=ICOEL+LBW/2-I+1
      IF(ABS(STIF(I,J)).LT..1E-35) GO TO 136
      K=ICOEL
      M=LBW/2+1
      Q=STIF(I,J)/STIF(K,M)
      DO 135 IRC=ICOEL,LIRC
      I=IDE
      J=IRC+LBW/2-I+1
      K=ICOEL
      M=IRC+LBW/2-K+1
      STIF(I,J)=STIF(I,J)-Q*STIF(K,M)
  135 CONTINUE
      REX(I+KRI*2-1-1)=REX(I+KRI*2-1-1)-Q*REX(ICOEL+KRI*2-1-1)
  136 CONTINUE
      K1=(2*(KRI-1)+ICOEL)/RCO
      DO 40 I=1,LBW/2+1
```



```
   40 COMP(ICO,I)=STIF(ICOEL,LBW/2+I)
      IF(ICO.NE.RCO) GO TO 30
      CALL WRITMS(7,COMP(1,1),LREC,K1)
      DO 41 ICOM=1,RCO
      DO 41 JCOM=1,LBW/2+1
   41 COMP(ICOM,JCOM)=0.0
      ICO=0
   30 IF(MOD(ICOEL,2).NE.0) GO TO 134
      KROWI=KROWI+1
      KROWFA=KROWF
      KROWF=ANP(KROWI-KRI+1,1)
      DO 71 I=2,9
   71 KROWF=MAX0(ANP(KROWI-KRI+1,I),KROWF)
      IF(KROWF.LT.KROWFA) KROWF=KROWFA
  134 CONTINUE
      IF(NEQ.EQ.2) GO TO 60
      DO 43 I=1,LBW/2+1
   43 COMP(ICO+1,I)=STIF(NEQ+1,I+LBW/2)
      ICO=ICO+1
      GO TO 50
C
C      SHIFTING MATRIX STIF(I,J) UPWARDS
C
   60 DO 10 IR=1,LBW-1
      DO 10 IC=1,LBW
      IF(IR.GT.LBW-1-NEQ) GO TO 12
      STIF(IR,IC)=STIF(IR+NE),IC)
      GO TO 10
   12 STIF(IR,IC)=0.0
   10 CONTINUE
      DO 20 IR=1,LBW/2
      DO 20 IC=1,9
      IF(IR.EQ.LBW/2) GO TO 22
      ANP(IR,IC)=ANP(IR+1,IC)
      GO TO 20
   22 ANP(IR,IC)=0
      ANP(IR,1)=KRI+IR
   20 CONTINUE
      IF(KROWF.EQ.KROWFA) GO TO 1
   50 CONTINUE
      RETURN
      END
      SUBROUTINE BACKWD
C     BACK SUBSTITUTION CALCULATING NODAL DISPLACEMENTS
C
      INTEGER TITLE,SR,NA,O,P,O,PRENIC,WI,ANP
      REAL NU,KEL
      DIMENSION COMP(RCO,BBR)
      COMMON     TITLE(13),   NPI(LLLL),     NPJ(LLLL),     NPM(LLLL),
     1           E(5),WI,     R(NNNN),       PRENIC(NNNN),  NAME(REC),
     2           NU(5),       Z(NNNN),       REX(NNN2),     LN(3),W(4,6),
```

```
     3            RHO(5),      MAT(LLLL),      UV(NNN2),       B(4,6),
     4            ALPHA(5),    DELTAT(LLLL),   AMP(QQ,9),      D(4,4),
     5                         STIF(BB1,BBB),  NAP(NMMN),      KEL(6,6),
     6            SIGLRR(LLLL),SIGLTT(LLLL),SIGLZZ(LLLL),SIGLRZ(LLLL)
      COMMON /PARAM/ NEL,NNP,NBR,NMAT,LBW,L
      COMMON /ELIMIN/ KRONI,KROWF,ICODE,NEQ,KROWFA,K1,ICO,LREC
      EQUIVALENCE(COMP(1,1),SIGLRR(1))
      IVARX=2*NNP
      DO 140 IBR=1,K1+1
      NREC=K1-IBR+2
      IF(IBR.GE.1) CALL READMS(7,COMP(1,1),LREC,NREC)
      DO 150 ISWEEP=1,ICO
      I=ICO-ISWEEP+1
      RHS=REX(IVARX)
      IF(ISWEEP.EQ.1.AND.IBR.EQ.1) GO TO 145
      KV=MIN0(IVARX+LBW/2,2*NNP)
      DO 142 IKV=IVARX+1,KV
      J=IKV-IVARX+1
  142 RHS=RHS-COMP(I,J)*UV(IKV)
  145 J=1
      IND=(IVARX+1)/2
      IF(PRESBC(IND).EQ.3) GO TO 50
      IF(PRESBC(IND)+2*(IND-1).EQ.IVARX) GO TO 50
      UV(IVARX)=RHS/COMP(I,J)
   50 IVARX=IVARX-1
      DO 150 II=1,LBW/2+1
      COMP(I,II)=0.0
  150 CONTINUE
      ICO=NCO
  140 CONTINUE
      RETURN
      END
```

A1.6 - Listing of the program EDT

```
      PROGRAM EDT(INPUT,OUTPUT,TEXT,TAPE5=INPUT,TAPE6=OUTPUT,TAPE7=TEXT)
      INTEGER RCD,TPLEN,TITLE
      READ(5,98) TITLE
   98 FORMAT(A10)
      REWIND 7
      READ(5,10)LBW,NEL,NNP
   10 FORMAT(3I5)
C
C     EVALUATION OF NUMBER OF RECORDS (LREC)
C     EVALUATION OF NUMBER OF EQUATIONS CONTAINED IN EACH RECORD(RCD)
C     CALCULATE THE SIZE OF THE BUFFER AREA COMP (TPLEN)
C
      RCD=4*NEL/(LBW/2+1)
      TPLEN=RCD*(LBW/2+1)
      IF(TPLEN.GT.1000) TPLEN=1000
      LREC=(2*NNP-1)/RCD+1
      NNP2=2*NNP
      LANP=LBW/2
      LBW1=LBW-1
      LBW21=LANP+1
C
C     WRITE ALL DIRECTIVES INTO TAPE TEXT
C
      WRITE(7,99)NNP,TPLEN,NEL,NNP2,LBW1,LBW,RCD,LBW21,LREC,RCD,LANP,NEL
   99 FORMAT(14HPS:/(NNNN)/,/(,I4,4H)/;*/
     D        12HPS:/TPLEN/,/,I5,1H//
     1        14HPS:/(LLLL)/,/(,I4,4H)/;*/
     2        14HPS:/(NNN2)/,/(,I4,4H)/;*/
     3        17HPS:/(BB1,BBB)/,/(,I3,1H,,I3,4H)/;*/
     4        17HPS:/(RCD,BBB)/,/(,I3,1H,,I3,4H)/;*/
     5        13HPS:/(REC)/,/(,I3,4H)/;*/
     D        10HPS:/RCD/,/,I3,3H/;*/
     6        14HPS:/(00,9)/,/(,I2,6H,9)/;*/
     7        16HPS:/(LLLL,3)/,/(,I4,6H,3)/;*/
     9        10HS:/COMMON//
     A         3HL;7/
     B         3HEND)
      END FILE 7
      REWIND7
      STOP
      END
```

A P P E N D I X 2

DIM3B CODE USER'S GUIDE

A2.1 - Introduction

The DIM3B code is a computer program written in FORTRAN IV. The size of the problems it can handle is very small compared with a typical problem, so it is provided with an additional program which makes DIM3B operate in a so called "Dynamic version" in order to adapt its capacity to a larger case.

This additional program (DIMDIM) is not fully described, only the necessary details for its use are given.

A2.2 - Preparation of the problem

A2.2.1 - Material properties

Values for Poisson's Ratio and Young's Modulus must be provided. These values will be taken to apply to all the elements of the structure.

A2.2.2 - Mesh generation

As it is a three dimensional problem, the generation of a mesh of 3D finite elements becomes a tedious and complicated process for all but straightforward cases. A particularly complex example is a T-junction of thick pipes. The most common way to tackle this problem is to have a mesh generation program to supply all or part of the input data.

The elements available have hexahedron shape with 20 or 32 nodes as it is shown in Fig. A.2.1.

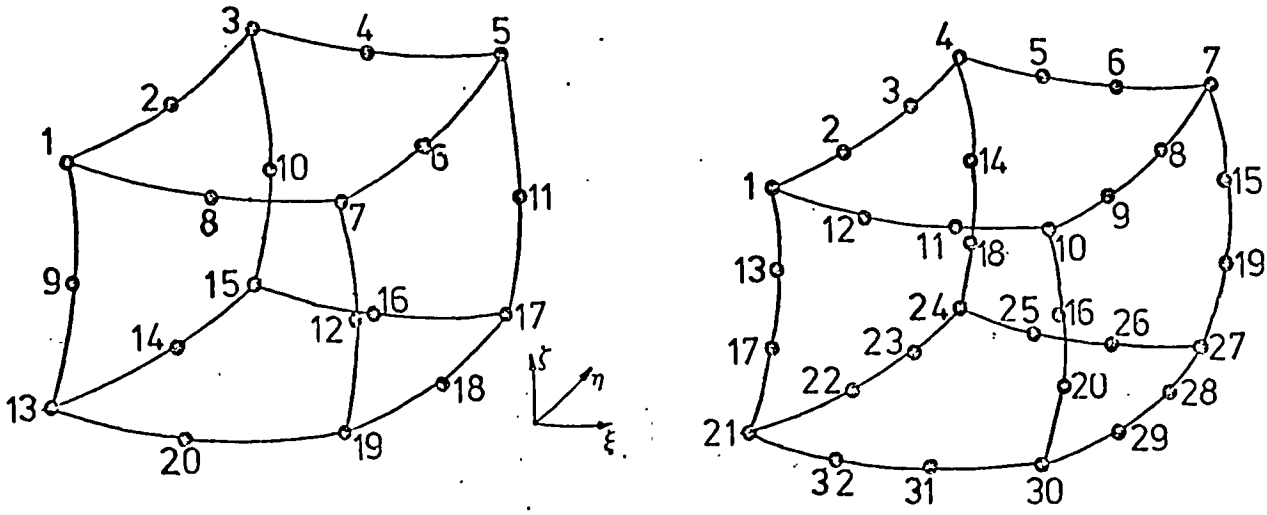

20 node element 32 node element

Figure A2.1 - Isoparametric elements available in DIM3B code

It is not possible to use the two types of elements in the same mesh.

The topology of the element is also shown in figure A2.1 which indicates the order of the nodes in the element in relation to the local set of coordinates.

The nodes must be also numbered throughout the mesh.

Therefore, for describing the topology of the mesh, it is necessary to define for each element an array ELNODE containing 20 or 32 (depending on the element chosen) different values of nodal numbers in the mesh following the topological order of that particular element.

The elements are also numbered along the mesh.

It is necessary for a full description of the mesh to define the coordinates of all nodes.

A2.3 - Sets of Coordinates

All the theory related to the program is developed on the basis of a general system of cartesian coordinates.

It is first necessary to define the terms: Basic Global System, Basic Problem System, Global System for Input, Main Problem System, A Main Problem System and Local Curvilinear System.

Basic Global System (x,y,z) is a cartesian system of coordinates. This system will be orientated in relation to the structure according to the geometrically preferential directions of the structure if there are any.

Basic Problem System (x',y',z') is a cartesian system of coordinates. The orientation of this system can be different from the Basic Global System and will be chosen according to the loading conditions of the structure.

In order to define the position of this system in relation to the global system it is necessary to define the direction of the new x' and y' axis.

These new directions are specified by two angles defining each direction and these angles are similar to those used in spherical coordinates as it is shown in Figure A2.2. The z' direction is defined implicitly and the program works out internally that direction.

Both systems have the same origin.

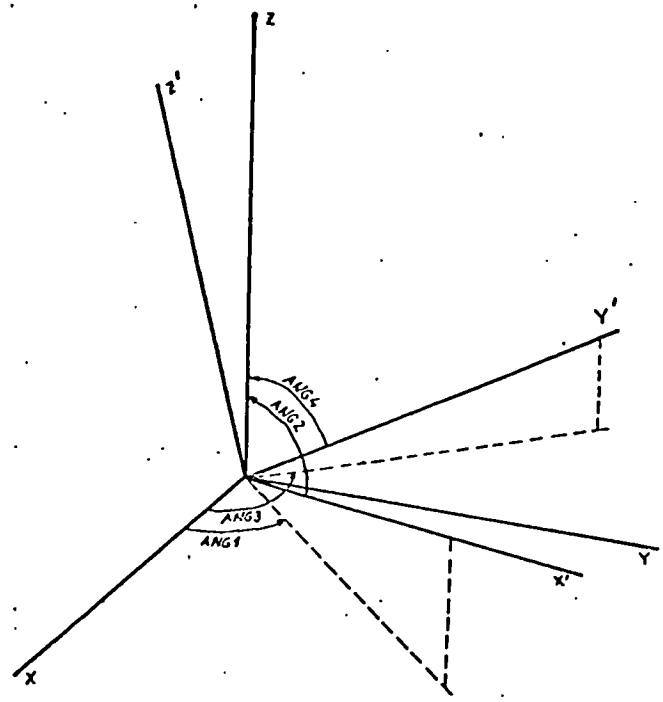

Figure A2.2 - Basic Problem System and Basic Global System

The concept and definition of the following systems are defined from the two basic systems.

Global System for Input: This system can be a cartesian, cylindrical or spherical system of coordinates. The choice of this system is up to the user. It is a matter of convenience depending only on the main geometrical shape of the structure to be studied. The basic frame and orientation of this system will be coincident with the basic global system. The nodal coordinates are referred to this system.

Main Problem System: Can be also cartesian, cylindrical or spherical, but the basic frame and orientation of this system will be coincident with the basic problem system.

The prescribed displacements (boundary conditions), the applied forces, the reactions, the nodal displacements

and stresses, all the components of these quantities are referred to this main problem system.

A Main Problem System: Is a system that can be different from the Main Problem System and it is used to define in a more efficient way part or all the stresses applied to the faces of elements which are loaded.

A table and an example are presented to help the explanation of these concepts and relations between these systems.

BASIC SYSTEMS	DERIVED SYSTEMS	TYPE
Basic Gobal System (Cartesian)	Global System for Input	cartesian, cylindrical, spherical
Basic Problem System (Cartesian) *	Main Problem System	cartesian, cylindrical, spherical
	A Main Problem System	cartesian, cylindrical, spherical

(*) - these two systems have the same origin and are related by 4 angles to be specified by the user.

Example

Let us think of a multinozzle-on-sphere structure as it is shown in Figure A2.3 and subjected to internal pressure P.

It is most suitable to define the Basic Global system as it is represented in Figure A2.3 with its origin on

the geometric centre of the sphere. It is most suitable to define the coordinates referred to a cylindrical system, so the Global System for Input will be cylindrical.

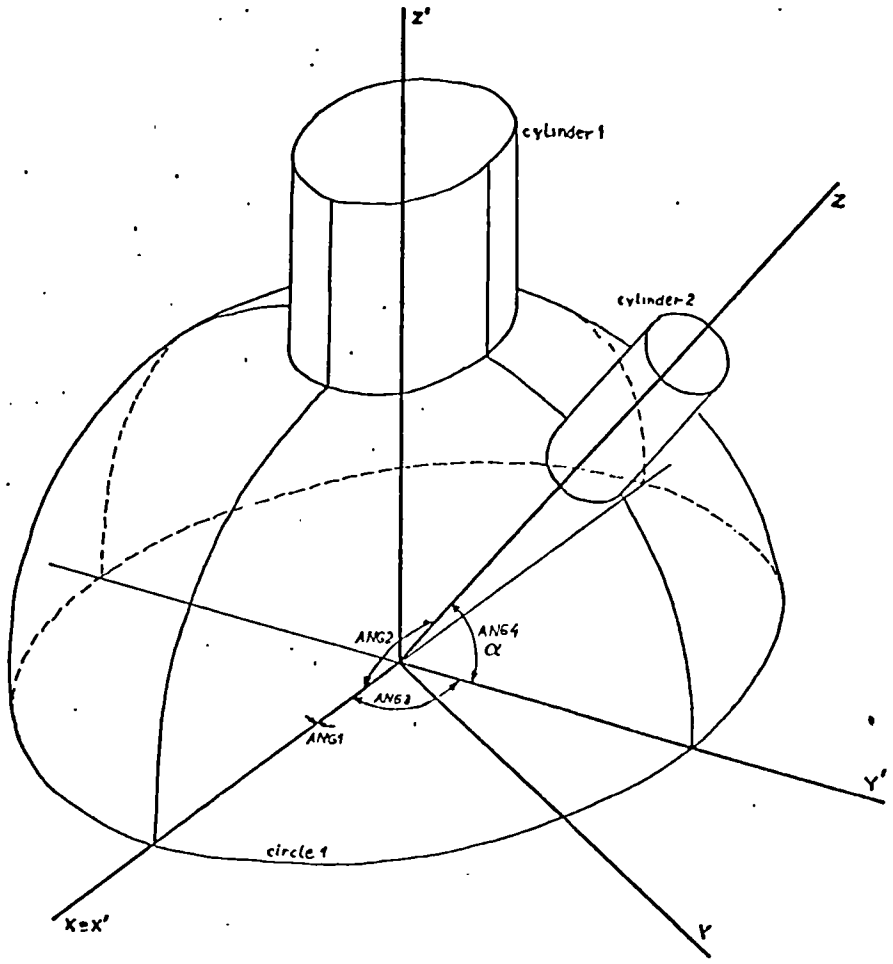

Figure A2.3 - Multinozzle-on-sphere structure

The specification of the nodal coordinates on the cylinder (2) is a straight forward problem. The nodal coordinates on the cylinder (1) and on the spherical part will be easily specified bearing in mind a clockwise rotation of these parts of the structure by an angle α as it is shown.

The four anlges specifying the relative positions of these two basic systems are also shown in Figure A2.3 where

$ANG_1 = 0.0$, $ANG_2 = 90^{o}.0$, $ANG_3 = 90^{o}.0$, and $ANG_4 = \alpha$.

The main problem system can also be cylindrical, therefore all the quantities mentioned in Section A2.3 refer to a cylindrical system of coordinates, for instance, due to physical reasons of equilibrium, all nodes situated on circle (1) will have zero displacements on the z' direction.

The pressure acting on the cylindrical part (1) of the structure is referred to the Main Problem System and obviously the only non zero component of applied stresses will be the radial component with a value of P throughout this part of the structure.

The same will happen to the cylindrical part (2) provided the applied stresses in this area are referred to the Global System for Input.

Finally for the spherical part it is possible to define the applied stresses in spherical coordinates (A Main Problem System) so again with only a radial component P, provided, it is specified the type of system to which P is referred.

Local Curvilinear System of Coordinates: For these hexahedron elements, dimensionless coordinates ξ,η,ζ are chosen each varying between -1, +1 so that in the (ξ,η,ζ) space the hexahedron become cubes with side lengths of 2 units.

Note: With respect ot all the coordinate systems, the order of coordinates and components is understood to be

ORDER	1st	2nd	3rd
Cartesian	X	Y	Z
Cylindrical	R	θ	Z
Spherical	R	θ	ø

A2.4 Loading

There are two main types of loading:

i) Nodal Point Forces

ii) Constant Stresses on faces of the elements.

The components of the Nodal Point Forces are referred to the Basic Problem System.

The stresses are defined on the same Basic Problem System, or if it is convenient, on A Main Problem System.

The face of the element where the stresses are applied, is identified in relation to the local curvilinear system.

Let us define the axis ξ as direction 1, η as direction 2 and ζ as direction 3. The face is referred to as the direction to which it is perpendicular and with a+,- sign indicating if it is on the positive or negative side of that direction.

For example:

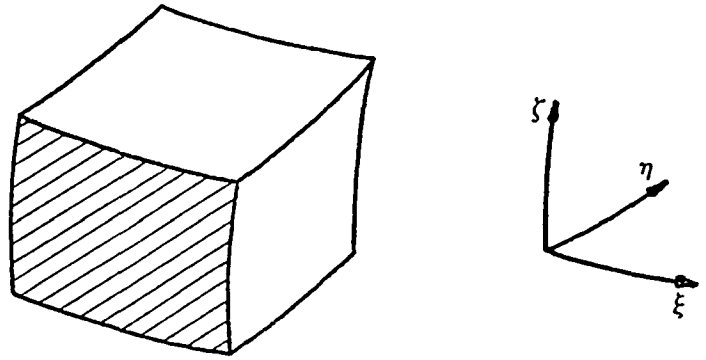

Figure A2.4

In Figure A2.4 the cross-hatched face is specified by the code - 2.

Note: The sign of the loads is positive if it follows the positive sense of the axis of the system to which the loads are referred.

A2.5 - Boundary Conditions and Prescribed Deflections:

It is possible to prescribe any initial displacements in any node of the mesh by the components in the three directions.

This information is given to the program in two input variables for each component: a number called nickname (PRENIC) containing the information of the number of the node in the mesh plus the direction on which the displacement is prescribed. This is done by multiplying the number of the node by 100 and then adding the identification number of the direction (1,2,3). The other variable (PREDEF) will specify the amount of deflection.

Let us suppose the node 72 restrained with an initial displacement of .001 (any length unit) in the y direction, considering the basic problem system to be a cartesian one.

The nickname will be 7202 and the corresponding deflection .001.

A2.6 - Computation Data

Into this category falls the data which govern the variable aspects of the numerical analysis and which addresses the program by specifying optional features.

In the course of execution of the program it is necessary to perform some numerical integrations using the Gaussian-Quadrature formula. Therefore it is required to give the Gauss points, XG, and the respective weight coefficients, CG. The number of Gauss points, IGAUS, can be up to four.

A table with these values is presented below

IGAUS	XG	CG
2	$XG_1=-XG_o=$ .57735027	$CG_1=CG_o=$ 1.000000
3	$XG_1=0.000000$ $XG_2=-XG_o=$ .77459667	$CG_1=.8888889$ $CG_2=CG_o=$ .5555556
4	$XG_2=-XG_1=$ .33998104 $XG_3=-XG_o=$ .86113631	$CG_2=CG_1=$ .65214515 $CG_3=CG_o$ .34785485

A2.7 - Special Modes of Operation

Facilities exist which allow the user, if so desired, to choose a certain number of optional types of output. The option codes are values 1,2,3 for the variable IIN which specifies the amount of input data to be printed out. Values 1,2,3,4 for the variable IOUT describe the amount of data processed and stress analysis.

If IIN =	Will be printed out
1	Title, IIN, IOUT
2	Coordinate systems, Gaussian Points. Number of elements and nodes, Number of nodes per element, Prescribed conditions, Young's Modulus, Poisson's Ration
3	The rest of input data, except for topological description of the mesh, ELNODE.

If IOUT =	Will be calculated and printed out
1	Number of elements where data are processed, Diagnostic advice, Elasticity Matrix, Number of known and unknown variables, integer results, Displacements.
2	Nodal Stresses
3	Calculated reactions, Nodal loading per each element
4	Topological description of the mesh, with last appearances.

Note: The higher levels of INN and IOUT include also everything described on the lower levels.

A2.8 - List of input variables

The variable data are categorized by the designations

is integer single

ia integer array

rs real single

ra real array

hs hollerith single

ha hollerith array

The unit can be any consistent set with angles in degrees.

ANG	ra	angles for defining the position of Basic Problem System
CCORD	ra	nodal coordinates
CG	ra	coefficients for Gaussian-Quadrature formula
E	rs	Young's Modulus
ELNODE	ia	topological description of each element
I	is	element number
GL	ra	stress components
HED	ha	title for the analysis
ICODE	is	identification of the loaded face in the element
IGAUS	is	number of Gauss points
IGS	is	type of Global System for Input 1 = Cartesian 2 = Cylindrical 3 = Spherical
IIN	is	control of the input data print out
IOUT	is	control of the amount of output
IPS	is	type of Main Problem System 1 = Cartesian 2 = Cylindrical 3 = Spherical

ISGL	is	type of A Main Problem System 1 = Global system for Input 2 = Basic Global System 3 = Basic Problem System 4 = Main Problem System (def. by IPS) 5 = A Main Problem System (cylindrical) 6 = A Main Problem System (spherical)
NELEM	is	number of elements in the mesh
NFACE	is	number of loaded faces in the element
NFREE	is	number of degrees of freedom (always =3)
NNELM	is	number of nodes per element (20 or 32)
NODTOT	is	total number of nodes in the mesh
NOSTR	is	number stress cases (always =1)
NPLOC	ia	loaded element numbers (in ascending order)
NPLOC1	is	index of loaded element
NPRDEF	is	number of components of prescribed deflections
NPRSEL	is	number of elements loaded
PRENIC	ia	nicknames for specification of prescribed defl.
PREDEF	ra	prescribed deflections
RHSI	ra	components of nodal point forces
UN	rs	Poisson's ratio
XG	is	Coordinates of Gauss points

A2.9 - Data Format

A2.9.1 - Data order

The following table describes the order of input of data defining the analysis. It should be read in conjunction with the previous section.

The program variable names of various data items are given as they are used to describe the input of the data following them.

GROUP OF CARDS	CARD ORDER	PROGRAM NAMES	FORMAT
1st	1	HED	8A10
	2	IIN,IOUT	2I5
	3	IGS,IPS,(ANG(I), I=1,4)	2I5,4F10.0
	4	IGAUS	I5
	5	(XG(I),CG(I),I=1, IGAUS)	8F10.0
	6	NELEM,NFREE,NNELM NPRDEF,NOSTR,NODTOT	6I5
2nd	1	I,19 of the nodal indices of element I	2014
	2	I, the rest of nodal indices of element I	14I4
	.	.I=1,2 . . NELEM	
3rd	1	(PRENIC(1,I),PREDEF (1,I), I=1,NPRDEF)	4(I10,E10.0)
	.	(as many cards as	
	.	are needed)	
4th	1	E,UN	2E15.2
5th	1	J((CCORD(I,Y),I=1,3), RHSI(I,Y),I=1,3)	I10,6E10.0
	.	J=1,2, . . .,NODTOT	

6th	1	NPRSEL (when NPRSEL>0, then include)	I5
	2	NPLOC(I),I=1,NPRSEL (in ascending order) for each NPLOC specify	16I5
	3	NPLOC1,NFACE	2I5
	4	NPLOC1,ICODE,ISGL, (GL(I),I=1,3)	3I5,3E10.0
	.	The last group of cards 3,4 is repeated NPRSEL times	
	.		

A2.9.2 - Data Deck

Each data deck as defined above will consist of

[9+2*NELEM+NODTOT+NPRDEF/4+I+2xNPRSEL] cards

I=0 if NPRDEF is multiple of 4

I=1 if NPRDEF is not multiple of 4

A2.10 - Error Messages

1. WRITING CONTROL PARAMETER IS INCORRECTLY SPECIFIED

   This message occurs if IIN is different from 1,2,3 or/and if IOUT is different from 1,2,3,4. The program stops.

2. THE COORDINATE SYSTEM DATA ARE INCORRECT

   If IGS ans IPS are different from the values 1,2,3 This message also occurs if the second and fourth angles defining the Basic Problem System are out of the range 0^{o}-180^{o}.

3. PROGRAM STOPPED DUE TO THE CASE BEING TOO BIG FOR THE DIMENSIONS SPECIFIED

   If the number of known variables (NKNVA) and the number of unknown variables (NUNKVA) exceed respectively 24 and 60, the program stops. This happens only on the basic version of DIM3B. However this message will occur if the dynamic version is not working properly.

4. J

   SEQUENCE ERROR IN COORDINATE DATA

   J, is the number of the node where the error was found.

5. SEQUENCE ERROR IN NPLOC DATA

   If the numbers of stressed elements are not defined in ascending order this message will appear. The program stops.

6. PARAMETER READ BY INIAL IS INCORRECTLY SPECIFIED

   The parameters are in basic version

   NELEM=3

   NPRDEF $\leq$ 24

   NODTOT $\leq$ 44

   NNELM=20

7. I,J

   SEQUENCE ERROR IN ELNODE INPUT DATA

   I, indicates where there is a sequential error in the topological description of the mesh, J is the wrong number

8. THE DATUM I IN THE ELEMENT OR PRESCRIBED DEFLECTION J IS OUT OF RANGE

   This occurs if the part of the nickname describing the node number is greater than NODTOT, and if the direction indicated is out of the range 1 to 3.

9. STRESS DATUM IS SPECIFIED INCORRECTLY

   This message occurs when the number of loaded faces in a stressed element is out of the range 1 to 6.

10. DETJ=0 PROGRAM HALTED

    The value of the determinant of the Jacobian matrix concerning the transformation of coordinates from the problem system to the local curvilinear coordinates is zero.

    It is advised to check again the coordinates of the mesh and the topological description.

A2.11 - DIMDIM code

A2.11.1 - Problem Size

The restrictions of the problem size assuming the basic verison of DIM3B are indicated below. (The restrictions on the program variables are stated in parenthesis where applicable.)

i) Total number of nodes must not be greater than 44, (NODTOT $\leq$ 44)

ii) Total number of elements must not be greater than 3, (NELEM $\leq$ 3)

iii) The number of nodes per element must be 20 (NNELM=20)

iv) The number of prescribed deflections must not exceed 24 (NPRDEF ≤ 24)

v) The problem must contain only one stress case (NOSTR=1). The same will apply for the dynamic version.

vi) The number of prestressed elements must not exceed 2 (NPRSEL ≤ 2)

vii) The number of known variables at one time must not be greater than 24 (NKNVA ≤ 24)

viii) The number of unknown variables at one time must not exceed 60 (NUNKVA ≤ 60).

A2.11.2 - General Description

Any excess in computer central memory storage with a three dimensional Finite Element Analysis usually causes tremendous overheads unnecessarily.

The DIMDIM program attempts to minimize the demands the DIM3B code makes on computer facilities (storage, CPU time, etc) by using special features of the CDC systems.

UPDATE is a facility available in the CDC system at I.C.C.C. and U.L.C.C., which enables the storage on disk of card images of programs in a compact form.

This facility is useful for batch jobs and has various features with which a program can be modified either temporarily or permanetly by a set of control directives.

According to the particular problem to be studied, DIMDIM defines the exact amount of storage needed by calculating each array size.

Following the execution of DIMDIM the basic UPDATE library (in this case DIM3B code) is modified by a set of control directives and new FORTRAN statements generated by DIMDIM.

This modified version of DIM3B, now with the suitable declaration and executable statements is then prepared to be compiled and executed.

A2.11.3 - List of Input Variables

Following the same categorization used in A2.8, the list of input variables for DIMDIM is indicated below.

VARIABLE	TYPE	DESCRIPTION
TITLE	ih	Hed for the input data
NELEM	is	the same as for DIM3B
NNELM	is	the same as for DIM3B
NFREE	is	the same as for DIM3B
NPRDEF	is	the same as for DIM3B
NOSTR	is	the same as for DIM3B
NODTOT	is	the same as for DIM3B
NPRSEL	is	the same as for DIM3B
NKNVA	is	number of known variables at one time in the overall stiffness matrix
NUNKVA	is	number of unknown variables at one time in the overall stiffness matrix
CON	ra	constants of a function P with values $CON(1)=-.105615\times10^{-3}$ $CON(2)=.135723\times10^{-3}$ $CON(3)=.166273\times10^{-4}$

CON(4)=.913812x10^{-1}

CON(5)=-.217439x10^{-1}

CON(6)=5000

NWB	is	size of the basic storage required without the variable arrays which are to be changed NWB=17943
MCL	is	Core memory declared in job control card, is a limit information
MCE(*)	is	Anticipated core field length required for the execution of DIM3B
PP(**)	ir	Anticipated peripheral processor time required for the execution of DIM3B
MCI(**)	is	The same as MCL
SEQ	ia	Series of sequential numbers indicating the order of the lines in the basic version of DIM3B where statements are to be replaced.

A2.11.4 - Data Format for DIMDIM

The following table describes the order of input of data for DIMDIM program.

The program variable names of various data items are given as they are used to describe the input of data following them.

(**) - PP and MCI are obtained from experience and can be found from the Dayfile in the printed output

(*) This value is the calculated MCL from DIMDIM less the size required for the loader ($\simeq$ 4500).

CARD ORDER	PROGRAM NAMES	FORMAT
1	TITLE	8A10
2	NELEM, NFREE, NNELM, NPRDEF,NOSTR,NODTOT, NPRSEL,NKNVA,NUNKVA	9I5
3	CON(I),I=1,6	6E10.0
4	NWB,MCL,MCE,PP,MCI	3I10.0,F10.0,I10
5	SEQ(K),K=1,58 (*) . (4 cards)	16(1X,A4)
6	SEQ(K),K=1,24(**) . (2 cards)	16(1X,A4)
7	SEQ(K),K=1,26 (***) . (2 cards)	16(1X,A4)

* - Referred to COMMON statements

** - Referred to DIMENSION statements

*** - Referred to executable statements

The last eight cards referred to the sequential numbers are indicated below.

0007	0011	0013	0016	0018	0021	0398	0402	0489	0493	0541	0546		
0573		0576	0579		0754	0756		0759		0871	0874	0921	0926
0929	0930	1095	1098	1099	1130	1135	1138	1139	1264	1287	1291	1294	1295
1360		1363	1364	1443	1554		1707	1709					
0025	0026	0405	0581	0582	0761		0877		0931	1100		1141	
1267		1297	1299	1366	1712								
0161	0162	0188	0385		0413		0418	0419	0520	0565		0567	
1107		1119	1122		1167		1307						

A2.11.5 - Job File

In order to submit both programs together under the running system KRONOS 2.1 at the present in ICCC the card deck has the following structure.

```
   JOB ( ...)
UPDATE, N=PL3, L=1.
FUN (G).
UPDATE, P=PL3,L=1.
RETURN,PL3, CORRET.
REWIND, LG0.
FTN, I=COMPILE, OPT=1, L=Ø.
LGO.
EOR
*DECK DIM3B
```

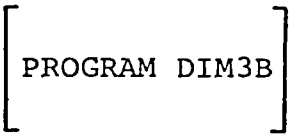


```
EOR
```

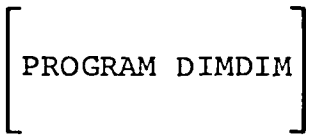


```
EOR
* IDENT NEWDIM, K=DIM3B
* READ CORRET
EOR
```

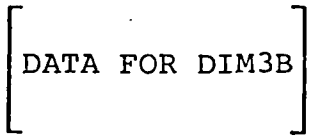


```
EOF
```

A similar structure is used for running these programs under the system SCOPE 3.4 at ULCC.

A2.12 - Sample Problems

In order to help the user two sample problems are presented and for each case the necessary input data are described.

A2.12.1 - Cantilever Beam Loaded at the End

Consider a cantilever beam having a square cross section with a force F applied at the end.

As it is illustrated in Figure A2.5 the beam was idealized by three 20 node elements.

All the nodes in the built-in end were totally fixed in the three directions and the force F was modelled by a constant shear stress applied in the free end of the beam.

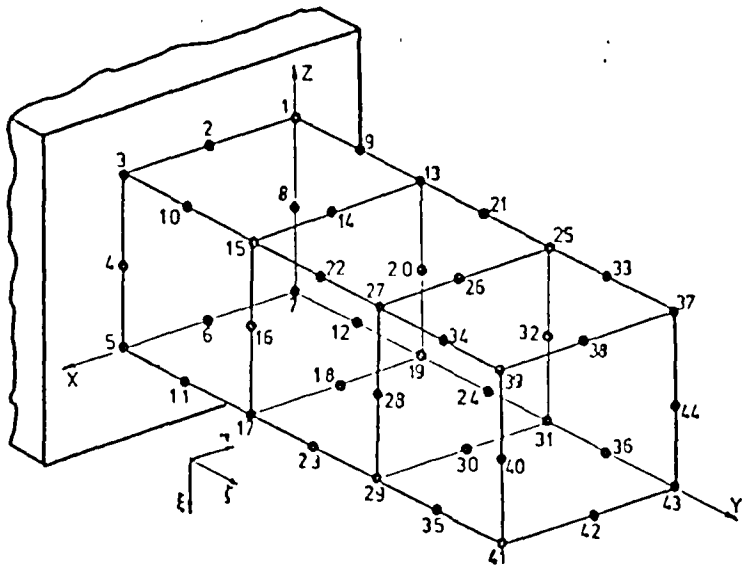

Figure A2.5 - Cantilever Beam

The input data is described as follows.

```
TEST CASE 2
    3    4
    1    1          0.          90.          90.          90.
    3
-0.7745967 0.5555556 0.          0.8888889 0.7745967 0.5555557
    3    3   20   24    1   44
    1  15  14  13  20  19  18  17  16  10   9  12  11   3   2   1   8   7   6   5
    1   4
    2  27  26  25  32  31  30  29  28  22  21  24  23  15  14  13  20  19  18  17
    2  16
    3  27  28  29  30  31  32  25  26  34  35  36  33  39  40  41  42  43  44  37
    3  38
       101          0.         102          0.         103          0.         201          0.
       202          0.         203          0.         301          0.         302          0.
       303          0.         401          0.         402          0.         403          0.
       501          0.         502          0.         503          0.         601          0.
       602          0.         603          0.         701          0.         702          0.
       703          0.         801          0.         802          0.         803          0.
          10.E6                0.2
       10.          10.
         1          0.          0.          8.
         2          4.          0.          8.
         3          8.          0.          8.
         4          8.          0.          4.
         5          8.          0.          0.
         6          4.          0.          0.
         7          0.          0.          0.
         8          0.          0.          4.
         9          0.          4.          8.
        10          8.          4.          8.
        11          8.          4.          0.
        12          0.          4.          0.
        13          0.          8.          8.
        14          4.          8.          8.
        15          8.          8.          8.
        16          8.          8.          4.
        17          8.          8.          0.
        18          4.          8.          0.
        19          0.          8.          0.
        20          0.          8.          4.
        21          0.         12.          8.
        22          8.         12.          8.
        23          8.         12.          0.
        24          0.         12.          0.
        25          0.         16.          8.
        26          4.         16.          8.
        27          8.         16.          0.
        28          8.         16.          4.
        29          8.         16.          0.
        30          4.         16.          0.
        31          0.         16.          0.
        32          0.         16.          4.
        33          0.         20.          8.
        34          8.         20.          8.
        35          8.         20.          0.
        37          0.         24.          0.
        38          4.         24.          8.
        39          8.         24.          8.
        40          0.         24.          4.
        41          8.         24.          0.
        42          4.         24.          0.
        43          0.         24.          0.
        44          0.         24.          4.
    1
    3
    3    1
    3    3    1          0.          0.          100.
```

A2.12.2 - Thick-Walled Cylinder Subjected to Internal Pressure.

In this case 32 node elements have been used in the finite element mesh idealization as it is shown in Figure A2.6

The internal pressure was specified in the inner faces of the elements by radial components using a cylindrical system of coordinates.

This problem exceeds the capacity of the basic DIM3B version, thus the DIMDIM program has to be used.

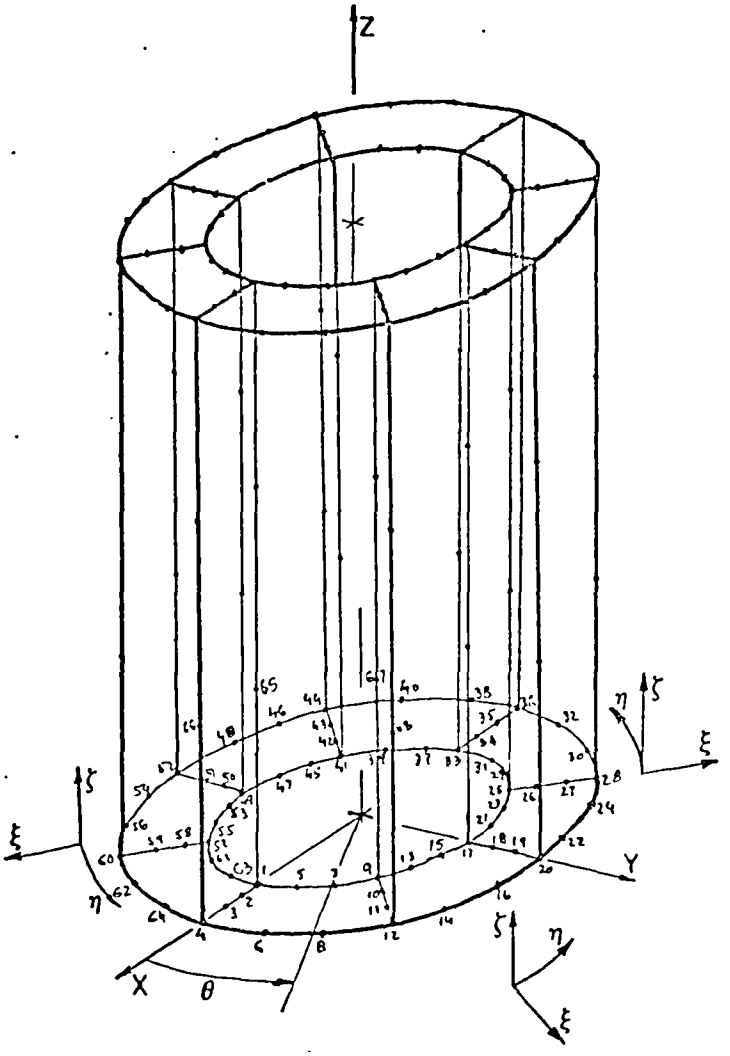

Figure A2.6 - Thick-Walled Cylinder

The necessary data for this analysis is described as follows.

```
INTERNALLY PRESSURIZED THICK CYLINDER,
    8     3    32    67     1   160     8   140    35
-.10561E-3.13372E-3.156273E-4.918312E-1-.217445-1 5000E00
     17943        90000        35000        100.        90000
0007 0011 0013          0016 0018 0021           0399 0402 0489 0493 0541           0546
0573      0576          0579      0754           0756      0759           0871 0874 0921 0926
0929 0930 1095          1098 1099 1130 1135 1138 1139 1264           1287 1291 1294 1295
1362      1363 1364 1443           1534           1707 1709
0025 0026 0405          0581 0582 0761           0877           0931           1100      1141
1267      1297 1299 1366           1712
0161 0162 0188          0385      0413           0418 0419 0520           0565      0567
1107      1119          1122      1167           1307
```

data for DIMDIM

data for DIM3B

```
TEST CASE 4A   INTERNALLY PRESSURIZED THICK CYLINDER
   3    4
   2    2         0.          90.          90.          90.
   3
-.77459667 .55555556 .0          .88888889 .77459667 .55555556
    8     3    32    67     1     4
  1  97 101 103 105 106 107 108 104 102 100  99  98  81  83  84  82  65  67  68
  1  66   1   5   7   9  10  11  12   8   6   4   3   2
  2 105 109 111 113 114 115 116 112 110 108 107 106  83  85  86  84  67  69  70
  2  68   9  13  15  17  18  19  20  16  14  12  11  10
  3 113 117 119 121 122 123 124 120 118 116 115 114  85  87  88  86  69  71  72
  3  70  17  21  23  25  26  27  28  24  22  20  19  18
  4 121 125 127 129 130 131 132 128 126 124 123 122  87  89  90  88  71  73  74
  4  72  25  29  31  33  34  35  36  32  30  28  27  26
  5 129 133 135 137 138 139 140 136 134 132 131 130  89  91  92  90  73  75  76
  5  74  33  37  39  41  42  43  44  40  38  36  35  34
  6 137 141 143 145 146 147 148 144 142 140 139 138  91  93  94  92  75  77  78
  6  76  41  45  47  49  50  51  52  48  46  44  43  42
  7 145 149 151 153 154 155 156 152 150 148 147 146  93  95  96  94  77  79  80
  7  78  49  53  55  57  58  59  60  56  54  52  51  50
  8 153 157 159  97  98  99 100 160 158 156 155 154  95  81  82  96  79  65  66
  8  80  57  61  63   1   2   3   4  64  62  60  59  58
   207.00E+09          0.30E+00
        1          3.          0.          0.
        2          4.          0.          0.
        3          5.          0.          0.
        4          6.          0.          0.
        5          3.         15.          0.
        6          6.         15.          0.
        7          3.         30.          0.
        8          6.         30.          0.
        9          3.         45.          0.
       10          4.         45.          0.
       11          5.         45.          0.
       12          6.         45.          0.
       13          3.         60.          0.
       14          6.         60.          0.
       15          3.         75.          0.
       16          6.         75.          0.
       17          3.         90.          0.
       18          4.         90.          0.
       19          5.         90.          0.
       20          6.         90.          0.
       21          3.        105.          0.
       22          6.        105.          0.
       23          3.        120.          0.
       24          6.        120.          0.
       25          3.        135.          0.
       26          4.        135.          0.
       27          5.        135.          0.
       28          6.        135.          0.
       29          3.        150.          0.
       30          6.        150.          0.
       31          3.        165.          0.
       32          6.        165.          0.
       33          3.        180.          0.
       34          4.        180.          0.
       35          5.        180.          0.
       36          6.        180.          0.
       37          3.        195.          0.
       38          6.        195.          0.
       39          3.        210.          0.
       40          6.        210.          0.
       41          3.        225.          0.
       42          4.        225.          0.
       43          5.        225.          0.
       44          6.        225.          0.
       45          3.        240.          0.
       46          6.        240.          0.
       47          3.        255.          0.
       48          6.        255.          0.
       49          3.        270.          0.
       50          4.        270.          0.
       51          5.        270.          0.
       52          6.        270.          0.
       53          3.        285.          0.
       54          6.        285.          0.
       55          3.        300.          0.
       56          6.        300.          0.
       57          3.        315.          0.
       58          4.        315.          0.
       59          5.        315.          0.
       60          6.        315.          0.
       61          3.        330.          0.
       62          6.        330.          0.
       63          3.        345.          0.
       64          6.        345.          0.
       65          3.          0.          4.
       66          6.          0.          4.
       67          3.         45.          4.
       68          6.         45.          4.
       69          3.         90.          4.
       70          6.         90.          4.
       71          3.        135.          4.
       72          6.        135.          4.
       73          3.        180.          4.
       74          6.        180.          4.
       75          3.        225.          4.
       76          6.        225.          4.
       77          3.        270.          4.
       78          6.        270.          4.
       79          3.        315.          4.
       80          6.        315.          4.
```

```
  80        6.       315.         4.
  81        3.         0.         8.
  82        6.         0.         8.
  83        3.        45.         8.
  84        6.        45.         8.
  85        3.        90.         8.
  86        6.        90.         8.
  87        3.       135.         8.
  88        6.       135.         8.
  89        3.       180.         8.
  90        6.       180.         8.
  91        3.       225.         8.
  92        6.       225.         8.
  93        3.       270.         8.
  94        6.       270.         8.
  95        3.       315.         8.
  96        6.       315.         8.
  97        3.         0.        12.
  98        4.         0.        12.
  99        5.         0.        12.
 100        6.         0.        12.
 101        3.        15.        12.
 102        6.        15.        12.
 103        3.        30.        12.
 104        6.        30.        12.
 105        3.        45.        12.
 106        4.        45.        12.
 107        5.        45.        12.
 108        6.        45.        12.
 109        3.        60.        12.
 110        6.        60.        12.
 111        3.        75.        12.
 112        6.        75.        12.
 113        3.        90.        12.
 114        4.        90.        12.
 115        5.        90.        12.
 116        6.        90.        12.
 117        3.       105.        12.
 118        6.       105.        12.
 119        3.       120.        12.
 120        6.       120.        12.
 121        3.       135.        12.
 122        4.       135.        12.
 123        5.       135.        12.
 124        6.       135.        12.
 125        3.       150.        12.
 126        6.       150.        12.
 127        3.       165.        12.
 128        6.       165.        12.
 129        3.       180.        12.
 130        4.       180.        12.
 131        5.       180.        12.
 132        6.       180.        12.
 133        3.       195.        12.
 134        6.       195.        12.
 135        3.       210.        12.
 136        6.       210.        12.
 137        3.       225.        12.
 138        4.       225.        12.
 139        5.       225.        12.
 140        6.       225.        12.
 141        3.       240.        12.
 142        6.       240.        12.
 143        3.       255.        12.
 144        6.       255.        12.
 145        3.       270.        12.
 146        4.       270.        12.
 147        5.       270.        12.
 148        6.       270.        12.
 149        3.       285.        12.
 150        6.       285.        12.
 151        3.       300.        12.
 152        6.       300.        12.
 153        3.       315.        12.
 154        4.       315.        12.
 155        5.       315.        12.
 156        6.       315.        12.
 157        3.       330.        12.
 158        6.       330.        12.
 159        3.       345.        12.
 160        6.       345.        12.
8
1    2    3    4    5    6    7    8
1    1
1   -1    4  621.E+06
2    1
2   -1    4  621.E+06
3    1
3   -1    4  621.E+06
4    1
4   -1    4  621.E+06
5    1
5   -1    4  621.E+06
6    1
6   -1    4  621.E+06
7    1
7   -1    4  621.E+06
8    1
8   -1    4  621.E+06
```

A2.13 - DIMDIM code.

Finally, a listing of the DIMDIM code is presented in the following pages.

```
      PROGRAM DIMDIM(INPUT,OUTPUT,TAPE5=INPUT,TAPE6=OUTPUT,
     1CORRET,TAPE1=CORRET)
      INTEGER SEQ,TITLE
      DIMENSION TITLE(8),SEQ(58),CON(6)

    0 DEFINE THE DIMENSION CONSTANTS.
      REWIND 1
      READ(5,1)TITLE
    1 FORMAT(8A10)
      WRITE(6,2)TITLE
    2 FORMAT(1H1////1H0,8A10)
      READ(5,3)NELEM,NFREE,NNELM,NPROEF,NOSTR,NODTOT,NPRSEL,NKNVA,NUNKVA
    3 FORMAT(9I5)
      WRITE (6,7)
    7 FORMAT (116H0THE DIMENSIONS OF THE ARRAYS IN THE PROGRAM DIM3B ARE
     1 DETERMINED BY THE FOLLOWING MAXIMUM PROBLEM PARAMETER VALUES.)
      WRITE(6,6)NELEM,NFREE,NNELM,NPROEF,NOSTR,NODTOT,NPRSEL,NKNVA,NUNKV
     1A
    6 FORMAT (8H0NELEM =,I3/8H NFREE =,I2/8H NNELM =,I3/9H NPROEF =,I4/
     19H NOSTR =,I2/9H NODTOT =,I4/9H NPRSEL =,I3/8H NKNVA =,I4/
     29H NUNKVA =,I4)
      READ (5, 84)  (CON (I),  I = 1, 6)
   84 FORMAT (6E10.0)
      WRITE (6, 85)  (CON (I),  I = 1, 6)
   85 FORMAT (35H0THE P FUNCTION CONSTANTS INPUT ARE / 1H , 6E14.6)
      READ(5,4) MCL,MCE,PP,MCI
    4 FORMAT(3I10,F10.0,I10)
      WRITE (6,9)
    9 FORMAT (51H0THE EXECUTION OF DIM3B IS ASSUMED TO REQUIRE THE FOLLO
     1WING JOB PARAMETER VALUES.)
      WRITE (6,8) MCE,PP,MCI
    8 FORMAT (24H0THE CORE FIELD LENGTH =,I6,7H WORDS./32H THE PERIPHERA
     1L PROCESSOR TIME =,F6.1,9H SECONDS./48H THE MAXIMUM CORE FIELD LEN
     2GTH OF THE COMPUTER =,I7,7H WORDS.)
      NKNVA1=(NKNVA*(NKNVA+1))/2
      NUNKV1=(NUNKVA*(NUNKVA+1))/2
      NCELN1=NFREE*NNELM
      NCELN0=NCELN1+1
      NTOTAL=NKNVA*NUNKVA
      NT=NFREE*NODTOT
      NAB=6*MAX0(NKNVA,NUNKVA)
      NBUF=MIN(NTOTAL,NT,IFLOAT(MCE),PP,0.,CON)
      READ(5,81)(SEQ(K),K=1,58)
   81 FORMAT(16(1X,A4))
    5 NREC=NT/NBUF
      IF(FLOAT(NT)/FLOAT(NBUF).GT.FLOAT(NREC))NREC=NREC+1
      WRITE (6,82)
   82 FORMAT (50H0THE DERIVED DIMENSIONAL CONSTANTS ARE AS FOLLOWS.)
      WRITE (6,83) NKNVA1,NUNKV1,NCELN1,NCELN0, NTOTAL, NT, NAB, NBUF,
     1NREC
   83 FORMAT (9H0NKNVA1 =,I5/9H NUNKV1 =,I5/9H NCELN1 =,I3/9H NCELN0 =,
```



```
     1I3/9H NTOTAL =,I4/5H NT =,I4/6H NAB =,I5/7H NBUF =,I3/7H NREC =,I3
     2)
C
C   10 CORRECT THE COMMON STATEMENTS.
      K=1
      NW=NWB
      CALL DELETE(SEQ(K),SEQ(K+1),K)
      CALL S1(NPROEF,N)
      NW=NW+N
      CALL S2(NPROEF,NUNKVA,NKNVA,NCELN1,NKNVA1,NUNKV1,NODTOT,NAB,N)
      NW=NW+N
      CALL S6(NELEM,NCELN0,NCELN1,NODTOT,N)
      NW=NW+N
      CALL DELETE(SEQ(K),SEQ(K+1),K)
      CALL S10(NNELM,NCELN1,NTOTAL,N)
      NW=NW+N
      CALL DELETE(SEQ(K),SEQ(K+1),K)
      CALL F2(NBUF,NTOTAL+1,NREC+1,N)
      NW=NW+N
      CALL C3(NNELM,N)
      NW=NW+N
      CALL DELETE(SEQ(K),SEQ(K+1),K)
      CALL COR(NNELM,NODTOT,NELEM+1,N)
      NW=NW+N+NPRSEL
      WRITE(6,12)NWB,NW,MCL
   12 FORMAT (117H0THE SPECIFIED CORE FIELD LENGTH NEEDED FOR LOADING TH
     1E PROGRAM LESS THAT FOR BASIC ARRAYS WITH VARIABLE DIMENSIONS =,I6
     2,7H WORDS./54H THE CALCULATED CORE FIELD LENGTH NEEDED FOR LOADING
     3 =,I6,7H WORDS./42H THE SPECIFIED MAXIMUM CORE FIELD LENGTH =,I6,7
     4H WORDS.)
      IF(NW.LE.MCL)GO TO 14
      WRITE(6,13)
   13 FORMAT(64H THE BIGGEST CORE MEMORY SPACE NECESSARY IS MORE THAN SP
     1ECIFIED.)
      IF (MCL.GT. MCI )  GO TO 15
      NBA = NBUF*(5+NTOTAL) + NREC + 2 - (NW - MCL)
      IF (NBA.LE.0)  GO TO 15
      NBUF1 = NBUF
      NBUF = MG (NTOTAL, NT, FLOAT (MCE), PP, FLOAT (NBA), CON)
      WRITE (6,17)  NBUF1, NBUF
   17 FORMAT (72H0HOWEVER IN ORDER THAT AN EXPECTED LARGE CASE MAY BE AC
     1COMODATED NBUF IS/ 13H REDUCED FROM, I4, 3H TO, I4, 51H WHICH WILL
     2 INCREASE THE PERIPHERAL PROCESSOR TIME.)
      REWIND 1
      GO TO 5
   15 BACKSPACE 99
   14 CALL DELETE(SEQ(K),SEQ(K+1),K)
      CALL S1(NPROEF,N)
      CALL S2(NPROEF,NUNKVA,NKNVA,NCELN1,NKNVA1,NUNKV1,NODTOT,NAB,N)
      CALL S6(NELEM,NCELN0,NCELN1,NODTOT,N)
      CALL DELETE(SEQ(K),SEQ(K+1),K)
```

```
      CALL S1(NPRDEF,N)
      CALL S2(NPRDEF,NUMKVA,NKNVA,NCELN1,NKNVA1,NUMKV1,NODTOT,NAB,N)
      CALL S6(NELEM,NCELNO,NCELN1,NODTOT,N)
      CALL DELETE(SEQ(K),SEQ(K+1),K)
      CALL DELETE(SEQ(K),SEQ(K+1),K)
      CALL S6(NELEM,NCELNO,NCELN1,NODTOT,N)
      CALL COR(NNELM,NODTOT,NELEM+1,N)
      CALL DELETE(SEQ(K),SEQ(K+1),K)
      CALL S10(NNELM,NCELN1,NTOTAL,N)
      CALL DELETE(SEQ(K),SEQ(K+1),K)
      CALL C3(NNELM,N)
      CALL DELETE(SEQ(K),SEQ(K+1),K)
      CALL COR(NNELM,NODTOT,NELEM+1,N)
      CALL DELETE(SEQ(K),SEQ(K+1),K)
      CALL S6(NELEM,NCELNO,NCELN1,NODTOT,N)
      CALL DELETE(SEQ(K),SEQ(K+1),K)
      CALL S10(NNELM,NCELN1,NTOTAL,N)
      CALL DELETE(SEQ(K),SEQ(K+1),K)
      CALL COR(NNELM,NODTOT,NELEM+1,N)
      CALL DELETE(SEQ(K),SEQ(K+1),K)
      CALL S2(NPRDEF,NUMKVA,NKNVA,NCELN1,NKNVA1,NUMKV1,NODTOT,NAB,N)
      CALL S6(NELEM,NCELNO,NCELN1,NODTOT,N)
      CALL DELETE(SEQ(K),SEQ(K+1),K)
      CALL S1(NPRDEF,N)
      CALL S2(NPRDEF,NUMKVA,NKNVA,NCELN1,NKNVA1,NUMKV1,NODTOT,NAB,N)
      CALL S6(NELEM,NCELNO,NCELN1,NODTOT,N)
      CALL S10(NNELM,NCELN1,NTOTAL,N)
      CALL DELETE(SEQ(K),SEQ(K+1),K)
      CALL C2(NBUF,NTOTAL+1,NREC+1,N)
      CALL DELETE(SEQ(K),SEQ(K+1),K)
      CALL S10(NNELM,NCELN1,NTOTAL,N)
      CALL DELETE(SEQ(K),SEQ(K+1),K)
      CALL C2(NBUF,NTOTAL+1,NREC+1,N)
      CALL DELETE(SEQ(K),SEQ(K+1),K)
      CALL S1(NPRDEF,N)
      CALL S2(NPRDEF,NUMKVA,NKNVA,NCELN1,NKNVA1,NUMKV1,NODTOT,NAB,N)
      CALL S6(NELEM,NCELNO,NCELN1,NODTOT,N)
      CALL S10(NNELM,NCELN1,NTOTAL,N)
      CALL DELETE(SEQ(K),SEQ(K+1),K)
      CALL C2(NBUF,NTOTAL+1,NREC+1,N)
      CALL DELETE(SEQ(K),SEQ(K+1),K)
      CALL S6(NELEM,NCELNO,NCELN1,NODTOT,N)
      CALL DELETE(SEQ(K),SEQ(K+1),K)
      CALL S2(NPRDEF,NUMKVA,NKNVA,NCELN1,NKNVA1,NUMKV1,NODTOT,NAB,N)
      CALL S6(NELEM,NCELNO,NCELN1,NODTOT,N)
      CALL S10(NNELM,NCELN1,NTOTAL,N)
      CALL DELETE(SEQ(K),SEQ(K+1),K)
      CALL C3(NNELM,N)
      CALL COR(NNELM,NODTOT,NELEM+1,N)
      CALL DELETE(SEQ(K),SEQ(K+1),K)
      CALL S10(NNELM,NCELN1,NTOTAL,N)
```



```
      CALL DELETE(SEQ(K),SEQ(K+1),K)
      CALL C3(NNELM,N)
      CALL COR(NNELM,NODTOT,NELEM+1,N)
      CALL DELETE(SEQ(K),SEQ(K+1),K)
      CALL S10(NNELM,NCELN1,NTOTAL,N)
      CALL DELETE(SEQ(K),SEQ(K+1),K)
      CALL S10(NNELM,NCELN1,NTOTAL,N)
      CALL DELETE(SEQ(K),SEQ(K+1),K)
      CALL S2(NPRDEF,NUMKVA,NKNVA,NCELN1,NKNVA1,NUMKV1,NODTOT,NAB,N)
C
C  20 CORRECT THE DIMENSION STATEMENTS.
      READ(5,81)(SEQ(K),K=1,24)
      K=1
      CALL DELETE(SEQ(K),SEQ(K+1),K)
      WRITE(1,21)NPRSEL,NCELN1,NUELM,NNELM,NNELM
   21 FORMAT(6X,32HDIMENSION EI(6,6),HT(6,9),NPLOC(,I4,8H),TRHSL(,I4,1H)
     1/6X,13HDIMENSION V1(,I4,5H),V2(,I4,5H),V3(,I4,1H))
      CALL DELETE(SEQ(K),SEQ(K+1),K)
      WRITE(1,22)NAB,NAB
   22 FORMAT(6X,12HDIMENSION A(,I5,4H),B(,I5,1H))
      CALL DELETE(SEQ(K),SEQ(K+1),K)
      WRITE(1,23)NCELN1,NNELM,NCELN1
   23 FORMAT(6X,15HDIMENSION RHSL(,I4,32H),DETM(6),TRH(3),GL(3),JAC(3,3)
     1,/5X,6H1DE(4,,I4,4H),TRHSL(,I4,17H),TP(3,3),TRGL(3))
      CALL DELETE(SEQ(K),SEQ(K+1),K)
      M=(NCELN1*(NCELN1+1))/2
      WRITE(1,24)M,NUELM
   24 FORMAT(6X,20HDIMENSION A(3,3),SK(,I5,26H),JAC(3,3),IJAC(3,3),DE(4,
     1,I4,1H))
      CALL DELETE(SEQ(K),SEQ(K+1),K)
      WRITE(1,25)M
   25 FORMAT(6X,13HDIMENSION SK(,I5,1H))
      CALL DELETE(SEQ(K),SEQ(K+1),K)
      WRITE(1,26)NTOTAL
   26 FORMAT(6X,'5HDIMENSION COMP(,I4,1H))
      CALL DELETE(SEQ(K),SEQ(K+1),K)
      WRITE(1,26)NTOTAL
      CALL DELETE(SEQ(K),SEQ(K+1),K)
      M=3*NODTOT
      WRITE(1,27)M,NTOTAL
   27 FORMAT(6X,13HDIMENSION U2(,I4,7H),COMP(,I4,1H))
      CALL DELETE(SEQ(K),SEQ(K+1),K)
      WRITE(1,28)M
   28 FORMAT(6X,13HDIMENSION U2(,I4,1H))
      CALL DELETE(SEQ(K),SEQ(K+1),K)
      WRITE(1,29)NCELN1,NODTOT,",NODTOT,NCELN1
   29 FORMAT(6X,12HDIMENSION C(,I4,35H),STR(6),STG(3,3),STGT(3,3),SL(3,3
     1)/6X,15HDIMENSION DELV(,I4,5H),U2(,I4,1H)/6X,15HDIMENSION STSS(,I4
     2,1HR,6),GRT(6,,I4,1H))
      CALL DELETE(SEQ(K),SEQ(K+1),K)
      WRITE(1,30)NCELN1,NCELN1,NUELM
```

```
   30 FORMAT(6X,16HDIMENSION DBT(6,,I4,7H),DB(6,,I4,18H),A(6,3),JAC(3,3)
     1,/5X,16HIIJAC(3,3),CC(4,,I4,1H))
      CALL DELETE(SEQ(K),SEQ(K+1),K)
      WRITE(1,31)NODTOT
   31 FORMAT(6X,15HDIMENSION STSS(,I4,3H,6))
C
C  40 CORRECT THE EXECUTABLE STATEMENTS.
      READ (5, 81)  (SEQ (K),  K = 1, 26)
      K=1
      CALL DELETE(SEQ(K),SEQ(K+1),K)
      WRITE(1,41)NKUVA,NUNKVA
   41 FORMAT(3X,15HIF(NKUVA.GT.,I4,12H) GO TO 3001/6X,13HIF(NUNKVA.GT
     1.,I4,12H) GO TO 3001)
      CALL DELETE(SEQ(K),SEQ(K+1),K)
      WRITE(1,42)NPRSEL
   42 FORMAT(3X,16HIF(NPRSEL.GT.,I4,12H) GO TO 3001)
      CALL DELETE(SEQ(K),SEQ(K+1),K)
      M=NELEM*NCELNO
      WRITE(1,43)
   43 FORMAT(6X,27HCALL READMS (3,ELNODE(1,1),,I5,3H,1))
      CALL DELETE(SEQ(K),SEQ(K+1),K)
      WRITE(1,44)MA
   44 FORMAT(6X,4HMA=,I5)
      CALL DELETE(SEQ(K),SEQ(K+1),K)
      WRITE(1,45)NELEM,NPRDEF,NODTOT,NMELM
   45 FORMAT (6X,12HIF(NELEM.LE.,I4,15H.AND.NPRDEF.LE.,I4,15H.AND.NODTOT
     1.LE.,I4 /5X,15H1.AND.NMELM.LE.,I2,10H) GO TO 60)
      CALL DELETE(SEQ(K),SEQ(K+1),K)
      WRITE(1,46)
   46 FORMAT(6X,27HCALL WRITMS (3,ELNODE(1,1),,I5,3H,1))
      CALL DELETE(SEQ(K),SEQ(K+1),K)
      M1=NELEM+1
      M2=12*NMELM
      WRITE (1, 47)  M1
   47 FORMAT (6X, 31HIF (N.EQ.1) CALL OPENMS (2,JRA,,I4,3H,0))
      CALL DELETE (SEQ (K), SEQ (K + 1), K)
      WRITE (1, 53)  M2
   53 FORMAT (6X, 25HCALL WRITMS (2,CORD(1,1),,I4,3H,N))
      CALL DELETE(SEQ(K),SEQ(K+1),K)
      M=NREC+1
      WRITE(1,48)M
   48 FORMAT(6X,19HCALL OPENMS (1,IRA,,I4,3H,0))
      CALL DELETE(SEQ(K),SEQ(K+1),K)
      WRITE(1,49)NBUF
   49 FORMAT(6X,10HIF(NLG.EQ.,I4,10H) GO TO 10)
      CALL DELETE(SEQ(K),SEQ(K+1),K)
      M=NDOF*(5+NTOTAL)+1
      WRITE(1,50)
   50 FORMAT(6X,19HCALL WRITMS (1,NLG,,I5,6H,NREC))
      CALL DELETE(SEQ(K),SEQ(K+1),K)
      WRITE(1,51)
```



```
   51 FORMAT(6X,19HCALL READMS (1,NLG,,I5,6H,NREC))
      CALL DELETE(SEQ(K),SEQ(K+1),K)
      WRITE(1,52)M2
   52 FORMAT(6X,25HCALL READMS (2,CORD(1,1),,I4,4H,LL))
      ENDFILE 1
      REWIND 1
      STOP
      END


      FUNCTION NB(NTOTAL,NT,CM,PP,DMMAX,CON)
      DIMENSION CON (6)
      UP=(1.+CM/16000.)/300.
      UM=PP/4.8E6
      R=FLOAT(5+NTOTAL)
      B = 1.
      NB = 0
      X = 1.E35
    1 Q = B * R + 1.
      P = CON (1) + CON (2) * EXP (CON (3) * Q)
     1            + CON (4) * EXP (CON (5) * Q)
      NREC = NT/IFIX(B)
      IF (FLOAT(NT)/B.GT.FLOAT(NREC))  NREC = NREC + 1
      REC = FLOAT(NREC)
      DELTAP = P*2.*REC* Q
      DELTAM = 1. + REC + Q
      IF (DMMAX.GT.0. .AND. DELTAM.GT.DMMAX)  GO TO 2
      DELTAU = UP*DELTAP + UM*DELTAM
      IF (DELTAU.GE.X)  GO TO 2
      X = DELTAU
      NB = IFIX(B)
    2 B = B + 1.
      IF (1.+R*B.LE.CON(6)) GO TO 1
      IF (NB.GE.1)  GO TO 3
      WRITE (6,4)
    4 FORMAT (93HEVEN THOUGH RUNNING A LARGE CASE MAY BE INTENDED NBUF
     1CAN NOT BE REDUCED ENOUGH TO ALLOW IT.)
      BACKSPACE 99
    3 RETURN
      END


      SUBROUTINE DELETE(G,H,K)
      INTEGER D,E,F,G,H
      DIMENSION E(5),F(4)
      DATA D/4H    /
      DATA E(1)/10H(14H*DELET/,E(2)/10HE DIM3B,,A/,E(3)/2H4)/,E(4)/10H4,
     17H,DIM3B/,E(5)/5H,,A4)/
      K=K+2
      DO 1 I=1,3
    1 F(I)=E(I)
```

```
      IF(M.EQ.0)GO TO 2
      E(3)=E(4)
      E(4)=E(5)
      WRITE(1,F)G,H
      GO TO 3
    2 WRITE(1,F)G
    3 RETURN
      END


      SUBROUTINE S1(L,M)
      N=L
      WRITE(1,1)L
    1 FORMAT(6X,19HCOMMON/S1/PREDEF(1,,I4,1H))
      RETURN
      END


      SUBROUTINE S2(L1,L2,L3,L4,L5,L6,L7,L8,N)
      M1=MAX0(L6,6*L7,L8)
      M2=L8/L2
      IF(FLOAT(L8)/FLOAT(L2).GT.FLOAT(M2))M2=M2+1
      M2=MAX0(L3,M2)
      N=L1+2*L2+4*L3+2*L4+L5*M1+L2*M2
      WRITE(1,1)L1,L2,L3,L3,L2,L4,L5,M1,L2,M2
    1 FORMAT(6X,19HCOMMON     PRENIC(1,,I4,11H),UNKNIC(1,,I4,11H),KNONIC(
     12,,I4,2H),/5X,9H1ORHS(1,,I4,11H),KNORHS(1,,I4,11H),ELPOSN(2,,I4,2
     20),/5X,10H2KNOMAT(1,,I5,11H),UNKMAT(1,,I5,8H),UNCLE(,I4,1H,,I4,1H)
     3)
      RETURN
      END


      SUBROUTINE S6(L1,L2,L3,L4,N)
      M1=(L3*(L3+1))/2
      M2=M1/L1
      IF(FLOAT(M1)/FLOAT(L1).GT.FLOAT(M2))M2=M2+1
      M1=MAX0(L2,M2)
      N=L1*M1+L3+3*L4
      WRITE(1,1)L1,M1,L3,L4
    1 FORMAT(6X,17HCOMMON/S6/FLNODE(,I4,1H,,I5,11H),RHSRED(1,,I4,9H),RHS
     11(3,,I4,8H),KRA(2))
      RETURN
      END


      SUBROUTINE S10(L1,L2,L3,N)
      M=L3/9
      IF(FLOAT(L3)/9..GT.FLOAT(M))M=M+1
      M=MAX0(L2,M)
      N=3*L1+9*M
```



```
      WRITE(1,1)L1,M
    1 FORMAT(6X,19HCOMMON/S10/DEXYZ(3,,I4,20H),DH(6,9),P(9,9),OP(,I4,3H,
     19))
      RETURN
      END


      SUBROUTINE C2(L1,L2,L3,N)
      N=L1*(L2+4)+L3
      WRITE(1,1)L1,L2,L1,L3
    1 FORMAT(6X,18HCOMMON/C2/NLG,BUF(,I4,1H,,I4,7H),IBUF(,I4,15H,4),NREC
     1,NTREC,/5X,27H1RHS,NIC,LP1,LP2,NPOSN,IRA(,I4,1H))
      RETURN
      END


      SUBROUTINE C3(L,N)
      N=3*L
      WRITE(1,1)L
    1 FORMAT(6X,12HCOMMON/C3/V(,I4,3H,3))
      RETURN
      END


      SUBROUTINE COR(L1,L2,L3,N)
      N=12*L1+3*L2+L3
      WRITE(1,1)L,L1,L2,L3
    1 FORMAT(6X,18HCOMMON/COR/CORD(3,,I4,5H),TR(,I4,14H,3,3),CCORD(3,,I4
     1,6H),JRA(,I4,1H))
      RETURN
      END
```

APPENDIX 3

DIM3B CODE LISTING

```
      PROGRAM DIM3B(INPUT=502,OUTPUT=1002,TAPE5=INPUT,TAPE6=OUTPUT,
     1       TAPE1=1002,TAPE2=1002,TAPE3=1002)
      REAL KNOMAT,KNORHS
      INTEGER ELPOSN,ELNODE,PRENIC,UNKNIC
      INTEGER  AA
      COMMON/S1/ PREDEF(1, 24)
      COMMON     PRENIC(1, 24),UNKNIC(1, 60),KNONIC(2,24),UNKRHS(1,24),
     1KNORHS(1, 60),ELPOSN(2,60),KNOMAT(1, 300),UNKMAT(1,1830),
     2UNCLEF( 60,24)
      COMMON/S6/ELNODE(3,610),RUSRED(1,60),RUSI(3, 44),KRA(2)
      COMMON/S8/XG(4),CG(4),IGAUS
      COMMON/S10/ELXT/(3,20),DH(6,9),P(9,9),QP(60,9)
      COMMON/C1/ NUNKVA,NKNVA,NOSTR,NCELOO,NCELO1,NTOTAL,NPRDEF,NT,
     1NELEM,NFREE,NNELN,NODTOT,D
      COMMON/C2/NLG,NUF(9,85),IBUF(9,4),NREC,NTREC,NUS,NIC,LP1,LP2,
     1NPOSN,IRA(16)
      COMMON/C3/V(20,3)
      COMMON/C4/IGS,IPS,TB(3,3)
      COMMON/C5/IIN,IOUT
      COMMON/COR/COOR(3,20),TR(20,3,3),CCOR(3, 40),JRA(4)
      COMMON/SP/G,H,E,SS
      DIMENSION HED(4)
      DIMENSION ANG(4), C(4), S(4)
      DIMENSION EI(6,6),HT(6,9),MPLOC(2),TRUSL(60)
      DIMENSION V1 (20), V2 (20), V3 (20)
      EQUIVALENCE (V (1, 1), V1 (1)), (V (1, 2), V2 (1)),(V(1,3),V3(1)),
     1(TRUSL(1),QP(200)),(EI(1),QP(1)),(HT(1),QP(100))
C***********************************************************************
C
C
C***********************************************************************
      READ(5,5000) HED
 5000 FORMAT(8A10)
      WRITE(6,5001) HED
 5001 FORMAT(1H1 ///////    10X, 8A10)
      READ (5, 5002) IIN, IOUT
      WRITE (6, 5005) IIN, IOUT
 5005 FORMAT (/// 61H0THE INPUT PARAMETER CONTROLLING THE WRITING OF INP
     1UT DATA IS, I2 / 66H THE INPUT PARAMETER CONTROLLING THE WRITING O
     2F PROGRAM RESULTS IS, I2)
      IF (IIN.GE.0 .AND. IIN.LE.3 .AND. IOUT.GE.0 .AND. IOUT.LE.4)
     1                                                    GO TO 75
      WRITE (6, 74)
   74 FORMAT (54H0A WRITING CONTROL PARAMETER IS INCORRECTLY SPECIFIED.)
      STOP
   75 READ (5, 5002)  IGS, IPS, (ANG (I), I= 1, 4)
 5002 FORMAT (2I5, 4F10.1)
      IF (IIN.EQ.1)  GO TO 48
      WRITE (6, 5004)  IGS, IPS, (ANG (I), I=1, 4)
 5004 FORMAT (// 52H0THE SPECIFIED GLOBAL COORDINATE SYSTEM FOR INPUT IS
     1, I2 / 46H THE SPECIFIED MAIN PROBLEM COORDINATE SYSTEM IS, I2 /
```



```
     256H THE SPECIFIED ANGLES RELATING THE TWO BASIC SYSTEMS ARE,
     3                    4F8.2, 9H DEGREES.)
   48 IF (.NOT.(IGS.LT.0 .OR. IGS.GT.3 .OR. IPS.LT.0 .OR. IPS.GT.3
     1         .OR. ANG(2).LT.0. .OR. ANG(2).GT.180.
     2         .OR. ANG(4).LT.0. .OR. ANG(4).GT.180.))  GO TO 43
      WRITE (6, 44)
   44 FORMAT (42H0THE COORDINATE SYSTEM DATA ARE INCORRECT.)
      STOP
   43 DO 40  I = 1, 4
      A        = 0.017453292520 * ANG (I)
      C (I) = COS (A          )
   40 S (I) = SIN (A          )
      TB (1, 1) = S (2) * C (1)
      TB (2, 1) = S (2) * S (1)
      TB (3, 1) = C (2)
      IF (ANG(2).NE.0. .AND. ANG(2).NE.180.)  GO TO 46
      A = 1.5707963268
      GO TO 45
   46 IF (ANG(2).NE.90.)  GO TO 47
      A = 0.017453292520 * ANG(4)
      GO TO 45
   47 A = ATAN (-C (2) / (S (2) * (C(1)*C(3)+S(1)*S(3))))
      IF (A .LT. 0.)  A = A + 3.1415926536
   45 C (4) = COS (A)
      S (4) = SIN (A)
      TB (1, 2) = S (4) * C (3)
      TB (2, 2) = S (4) * S (3)
      TB (3, 2) = C (4)
      TB (1, 3) = TB (2, 1) * TB (3, 2) - TB (2, 2) * TB (3, 1)
      TB (2, 3) = TB (3, 1) * TB (1, 2) - TB (3, 2) * TB (1, 1)
      TB (3, 3) = TB (1, 1) * TB (2, 2) - TB (1, 2) * TB (2, 1)
      READ(5,9) IGAUS
    9 FORMAT(I5)
      IF(IGAUS.GT.4) GO TO 3001
      READ(5,8)(XG(I),CG(I),I=1,IGAUS)
    8 FORMAT(8F10.0)
      CALL INIAL
      IF (IIN.EQ.1)  GO TO 49
      WRITE(6,103)
  103 FORMAT (/// * SPECIFIED GAUSS ABSCISSAE AND COEFFICIENTS FOR ELEME
     1NTAL INTEGRATION IN THE LOCAL COORDINATE SYSTEM*)
      WRITE(6,104) ((XG(I),CG(I)),I=1,IGAUS)
  104 FORMAT (1H , 2E16.8)
   49 IF (IIN.LT.3)  GO TO 60
      WRITE(6,41)
   41 FORMAT (1H1 ////    31X, * SPECIFIED PRESCRIBED NICKNAMES AND DEFLE
     1CTIONS IN THE MAIN PROBLEM SYSTEM* /)
      WRITE(6,42) ((PRENIC(I,J),PREDEF(I,J),J=1,NPRDEF),I=1,NOSTR)
   42 FORMAT (52H0 , 5(I10, E15.5) /(,
     1(1H1 /////    52(1H , I10, E15.3, I10, E15.3, I10, E15.3,
     2I10, E15.3, I10, E15.3/)))
```

```
   60 READ(5,5003) E,UN
 5003 FORMAT (2E15.2)
      DO 39 I=1,6
      DO 39 J=1,6
   39 EI(I,J)=0.0
      PATH=E/((1.+UN)*(1.-2.*UN))
      EI(1,1)=PATH*(1.-UN)
      EI(1,2)=PATH*UN
      EI(1,3)=EI(1,2)
      EI(2,1)=EI(1,2)
      EI(2,2)=EI(1,1)
      EI(2,3)=EI(2,1)
      EI(3,1)=EI(1,3)
      EI(3,2)=EI(2,3)
      EI(3,3)=EI(2,2)
      EI(4,4)=PATH*(0.5-UN)
      EI(5,5)=EI(4,4)
      EI(6,6)=EI(4,4)
      WRITE(6,4001)
 4001 FORMAT (1H1 //////   1H , *RESULTING GENERAL ELASTICITY MATRIX* /)
      WRITE(6,4002) ((EI(I,J),J=1,6),I=1,6)
 4002 FORMAT (1H , 6E16.8)
C        ******          INITIALISATION          *******
      NCELN1=NCELD0-1
      NT=NDREE*NODTOT
      NTOTAL=NKNVA+NUNKVA
      NUNKV1=(NUNKVA*(NUNKVA+1)/2)
      NKNVA1=(NKNVA*(NKNVA+1)/2)
      NREC = NTOTAL + 1
      NREC = 0
      NLG = 0
      NLOAD=1
      IF (IIN.EQ.1)  GO TO 61
      WRITE (6, 62)  NELEM, NDREE, NNELM, NPROEF, NOSTR, NODTOT, IGAUS
   62 FORMAT (/// 23H0SPECIFIED INTEGER DATA, //
     1          1X,*NUMBER OF ELEMENTS(NELEM)=*I5/
     11X,*NUMBER OF DEGREE OF FREEDOM(NDREE)=*I5/
     21X,*NUMBER OF NODES PER ELEMENT(NNELM)=*I5/
     41X,*NUMBER OF PRESCRIBED DEFLECTION (NPROEF)=*I5/
     51X,*NUMBER OF STRESSING CASE(NOSTR)=*I5/
     81X,*TOTAL NUMBER OF NODES IN THE STRUCTURE(NODTOT)=*I5/
     91X,*NUMBER OF GAUSS POINTS IN EACH DIRECTION (IGAUS) =*I5)
   61 WRITE (6, 63)  NUNKVA, NKNVA, NCELD0, NCELN1, NT, NTOTAL, NUNKV1,
     1                                                             NKNVA1
   63 FORMAT (/// 23H0RESULTING INTEGER DATA, //
     61X,*NUMBER OF UNKNOWN VARIABLE AT ONE TIME(NUNKVA)=*I5/
     71X,*NUMBER OF KNOWN VARIABLE AT ONE TIME(NKNVA)=*I5/
     21X,*NUMBER OF COLUMNS IN ELNODE MATRIX(NCELD0)=*I5/
     31X,*NUMBER OF COLUMNS IN ELNODE MATRIX MINUS ONE(NCELN1)=*I5/
     41X,*TOTAL NUMBER OF DEGREES OF FREEDOM OF THE STRUCTURE(NT)=*I5/
     51X,*TOTAL SIZE OF MATRIX REQUIRED FOR SOLUTION(NTOTAL)=*I5/
```



```
     61X,*SIZE OF UNKNOWN MATRIX(NUNKV1)=*I7/
     71X,*SIZE OF KNOWN MATRIX(NKNVA1)=*I7)
      IF (IIN.EQ.1)  GO TO 64
      WRITE (6, 3004)  E, UN
 3004 FORMAT 1//// 32H SPECIFIED ELASTIC MODULUS (E) =, E13.5 /
     1               32H SPECIFIED POISSONS RATIO (UN) =, E13.5)
   64 IF(NKNVA.GT.24) GO TO 3001
      IF(NUNKVA.GT.60) GO TO 3001
      GO TO 3002
 3001 WRITE(6,3003)
 3003 FORMAT(76H0PROGRAM STOPPED DUE TO THE CASE BEING TOO BIG FOR THE D
     1IMENSIONS SPECIFIED.)
      STOP
 3002 CONTINUE
      RHSISM = 0.
      DO 200 J=1,NODTOT
      READ(5,201)NON,(CCORD(I,J),I=1,3),(RHSI(I,J),I=1,3)
  201 FORMAT(I10,3E10.0,3E13.0)
      IF(NON.NE.J) GO TO 202
      DO 200  I = 1, 3
      RHSISM = RHSISM + ABS (RHSI (I, J))
 200  CONTINUE
      GO TO 203
 202  WRITE(6,204) J
 204  FORMAT(1H0,*SEQUENCE ERROR IN COORDINATE DATA AT*I5)
      STOP
 203  CONTINUE
      READ (5, 10)  NPRSEL
 10   FORMAT(16I5)
      IF (IIN.EQ.1)  GO TO 68
      WRITE (6, 69)  NPRSEL
   69 FORMAT (/// 59H0SPECIFIED NUMBER OF ELEMENTS TO WHICH STRESS IS AP
     1PLIED IS, I4)
   68 IF(NPRSEL.GT.2) GO TO 3001
      IF (IIN .LT.3)  GO TO 65
      WRITE(6,205) (J,(CCORD(I,J),I=1,3),(RHST(I,J),I=1,3),J=1,NODTOT)
  205 FORMAT(1H1///*J        SPECIFIED NODAL COORDINATE AND APPLIED FORCE D
     1ATA IN THE GLOBAL SYSTEM FOR INPUT AND THE MAIN PROBLEM SYSTEM RES
     2PECTIVELY* // 7X, *NODE*, 11X, *COORD X*, 13X, *COORD Y*, 13X, *CO
     3ORD Z*, 13X, *RX*, 18X, *RY*, 18X, *RZ*  // 50(1H , I9, 6E20.3 /),
     41H1 //////    50(1H , I9, 6E20.3 /))
   65 IF (IGS.EQ.1)  GO TO 18
      DO 17  J = 1, NODTOT
   17 CALL GTRANS (IGS, CCORD (1, J), CCORD (2, J), CCORD (3, J))
   18 IF(NPRSEL .EQ.0) GO TO 14
      READ (5, 10) (NPLOC(I), I=1,NPRSEL)
      IF (NPRSEL .EQ. 1)  GO TO 14
      DO 11 I=2,NPRSEL
      IF(NPLOC(I).LE.NPLOC(I-1)) GO TO 12
 11   CONTINUE
      IF(NPLOC(NPRSEL).LE.NELEM) GO TO 14
```

```
      WRITE(6,15)
   15 FORMAT(25HDUPLOC DATA OUT OF RANGE.)
      GO TO 16
   12 WRITE(6,13)  DUPLOC(I-1),DUPLOC(I)
   13 FORMAT (32HDUPLOC ERROR IN DUPLOC DATA AT , 2I5)
   16 STOP
   14 CONTINUE
C
C        INITIALIZATION
C
      DO 320 J=1,NDOFKV1
  320 DOFKMAT(1,J)=0.0
      DO 330 J=1,NDOFKVA
  330 DFIXDC(1,J)=0
      DO 340 I=1,NDOFKVA
      DO 340 J=1,NSTKVA
  340 DOUBLE(I,J)=0.0
      DO 350 J=1,NSTKVA1
  350 KDOUBL(1,J)=0.0
      DO 360 I=1,2
      DO 360 J=1,NSTKVA
  360 KDOUBC(I,J)=0
      DO 370 I=1,NDOSTR
      DO 370 J=1,NDOFKVA
  370 KDOUBS(I,J)=0.0
      DO 38 K=1,NSTKVA
   38 DOUBS(1,K)=0.0
      DO 1 I=1,6
      DO 1 J=1,9
    1 DT(I,J)=0.0
      DT(1,1)=DT(2,5)=DT(3,9)=DT  (4,6)=DT(4,8)=DT(5,3)=DT(5,7)=DT(6,2)=
     1DT(6,4)=1.0
      DO 2 I=1,6
      DO 2 J=1,9
      DD(I,J)=0.0
      DO 2 K=1,6
      DD(I,J)=DD(I,J)+E1(I,K)*DT(K,J)
    2 CONTINUE
      DO 3 I=1,9
      DO 3 J=1,9
      P(I,J)=0.0
      DO 3 K=1,6
      P(I,J)=P(I,J)+DT(K,I)*DD(K,J)
    3 CONTINUE
      IF(NELEM.GT.20) GO TO 5
      DO 4 I=1,12
      V3(I) = 1.
      IPP = I+20
    4 V3(IPP) = -1.
      V3(13)=V3(14)=V3(15)=V3(16) = 1./3.
      V3(17)=V3(18)=V3(19)=V3(20)= -V3(16)
```



```
      V1(1) =V1(2) =V1(3) =V1(4) =V1(13) =V1(14)=V1(17)=V1(18)=V1(21)=
     1V1(22)=V1(23)=V1(24) = -1.
      V1(7)=V1(8) =V1(9) =V1(10)=V1(15)=V1(16)=V1(19)=V1(20)=V1(27)=
     2V1(28)=V1(29)=V1(30) = 1.
      V1(5) =V1(12)=V1(25)=V1(32) = -1./3.
      V1(6)=V1(11)=V1(26)=V1(31) = 1./3.
      V2(1) =V2(10)=V2(11)=V2(12)=V2(13)=V2(14)=V2(17)=V2(20)=V2(21)=
     3V2(30)=V2(31)=V2(32) = -1.
      V2(2) =V2(9) =V2(22)=V2(29) = -1./3.
      V2(3) =V2(8) =V2(23)=V2(28) =  1./3.
      V2(4) =V2(5) =V2(6) =V2(7) =V2(14)=V2(15)=V2(18)=V2(19)=V2(24)=
     4V2(25)=V2(26)=V2(27) = 1.
      GO TO 7
    5 DO 6 I=1,9
      V3(1)=1.
      IPP = 1+ 12
    6 V3(IPP) = -1.
      V3(9) =V3(10)=V3(11)=V3(12) = 0.
      V1(1) =V1(12) =V1(3) =V1(9) =V1(10)=V1(13)=V1(14)=V1(15) = -1.
      V1(5) =V1(6) =V1(7) =V1(11)=V1(12)=V1(17)=V1(18)=V1(19) = 1.
      V1(4) =V1(8) =V1(16)=V1(20) = 0.
      V2(1) =V2(7) =V2(8) =V2(9) =V2(12)=V2(13)=V2(19)=V2(20) =-1.
      V2(3) =V2(4) =V2(5) =V2(10)=V2(11)=V2(15)=V2(16)=V2(17) = 1.
      V2(2) =V2(6) =V2(18)=V2(18) = 0.
    7 CONTINUE
C
C        FORWARD  ELIMINATION
C        LOOP ----  1001 ---  IS FOR EACH ELEMENT
C
      IF (NDOF.LT.4)  GO TO 66
      WRITE(6,2000)
 2000 FORMAT (1H1 /// 10X, 96X, 93HPROCESSED ELMODE TO THE MAIN PROBLEM
     1SYSTEM / 1H , 13X,10HTHE FIRST COLUMN (ELEMENT INDICES) AND THEN
     2THE FIRST OF EVERY THREE COLUMNS (FIRST NODAL DEGREE OF FREEDOM))
      DO 2001 I=1,NELEM
      WRITE (6, 2002)  ELMODE(I,1), (ELMODE(I,J), J=2,NCELNO,3)
 2002 FORMAT (1HO, I5/ (1H , 16I8))
      IF (ISUB(I,15).NE.0 .OR. I.EQ.NELEM)  GO TO 2001
      WRITE (6, 73)
   73 FORMAT (1H1 ///)
 2001 CONTINUE
      NSET = 0
   66 DO 1001 N=1,NELEM
      IF (N .EQ. 1)  GO TO 79
      IF (III .EQ. 3 .OR. IOUT .GE. 3)  GO TO 76
   77 NSET = NSET + 1
      IF (ISUB (NSET, 27) .EQ. 0)  GO TO 79
      GO TO 78
   76 IF (NLOAD .EQ. 1)  GO TO 80
      IF (NPRSET .EQ. 0)  GO TO 81
      IF (N-1.GE.NPLOC(NLOAD+1) .AND. N-1.NE.NPLOC(NLOAD))  GO TO 80
```

```
      NSET = 0
      GO TO 79
   80 IF (NPRSEL .EQ. 0)  GO TO 81
      IF (N .EQ. NPLOC (NLOAD))  GO TO 79
   81 IF (IRUSISM .EQ. 0..OR. 100) .LT. 3)  GO TO 77
   79 WRITE (6, 67)
   67 FORMAT (1H1 //)
   78 WRITE(6,3010) N
 3010 FORMAT (1H0, *ELEMENT NUMBER *, I3, *  IS ABOUT TO ENTER THE STIF
     1FNESS EQUATION.*)
      CALL COMMN
      IF (N .NE. NPLOC (NLOAD))  GO TO 28
      CALL LOAD
      DO 20  I = 1, NCELN
   20 RHSRED (1, I) = RHSRED (1, I) + TRUSL (I)
   28 IF (IPUT.LT.5 .OR. RHSISM.EQ.0. .AND. N.NE.NPLOC(NLOAD))  GO TO 70
      WRITE(6,3020)
 3020 FORMAT (/// 7X, *CALCULATED LOAD VECTOR FOR THIS ELEMENT IN THE MA
     1IN PROBLEM SYSTEM*)
      WRITE(6,3021)
 3021 FORMAT (1H0, 9X, *FORCE ALONG X*, 11X, *FORCE ALONG Y*, 11X,
     1                    *FORCE ALONG Z*/)
      WRITE(6,3030) (RHSRED(1,I),I=1,NCELN)
 3030 FORMAT(5(8X,E16.8))
   70 IF (N .EQ. NPLOC (NLOAD) .AND. NLOAD .LT. NPRSEL)  NLOAD = NLOAD+1
      DO 510 J=2,NCELNO
      JM1=J-1
      AA=IABS(ELNODE(N,J))
C
C        TO CHECK IN UNKNOWN NICK NAME
C
      DO 520 K=1,NUNKVA
      IF(UNKNIC(1,K).EQ.AA) GO TO 530
  520 CONTINUE
C
C        TO CHECK IN KNOWN NICK NAME
C
      DO 540 L=1,NKNVA
      IF(KNONIC(1,L).EQ.AA) GO TO 550
  540 CONTINUE
C
C        TO CHECK IN PRESCRIBED DEFLECTION
C
      DO 560 M=1,NPRDEF
      IF(PREDIC(1,M).EQ.AA) GO TO 570
  560 CONTINUE
C
C        IF NOT INSERT IN UNKNOWN NICK NAME
C
      DO 580 NN=1,NUNKVA
      IF(UNKNIC(1,NN).EQ.0) GO TO 590
```



```
  580 CONTINUE
  590 UNKNIC(1,NN)=ELNODE(N,J)
      KNOWUS(1,NN)=RHSRED(1,JM1)
      ELPOSN(1,JM1)=NN
      ELPOSN(2,JM1)=0
      GO TO 510
  530 UNKNIC(1,K)=ELNODE(N,J)
      KNOWUS(1,K)=KNOWUS(1,K)+RHSRED(1,JM1)
      ELPOSN(1,JM1)=K
      ELPOSN(2,JM1)=0
      GO TO 510
  550 KNONIC(1,L)=ELNODE(N,J)
      ELPOSN(1,JM1)=L
      ELPOSN(2,JM1)=1
      GO TO 510
  570 DO 610 MM=1,NKNVA
      IF(KNONIC(1,MM).EQ.0) GO TO 620
  610 CONTINUE
  620 KNONIC(1,MM)=ELNODE(N,J)
      KNONIC(2,MM)=M
      ELPOSN(1,JM1)=MM
      ELPOSN(2,JM1)=1
  510 CONTINUE
      CALL LFM
      CALL STFTR
      CALL READMS (3, ELNODE(1,1), 183, 1)
      CALL FORWAD
 1001 CONTINUE
      CALL BACKWD
      CALL DEFOUT
      IF (IOUT.EQ.1)  GO TO 72
      CALL STRESS
      CALL STROUT
   72 STOP
      END


      SUBROUTINE INIAL
      INTEGER ELNODE,PREDIC
      INTEGER AA,A,B
      COMMON/SIZ/ PREDEF(1, 24)
      COMMON    PREDIC(1, 24),UNKNIC(1, 60),KNONIC(2,24),UNKUS(1,24),
     1KNOWUS(1, 60),ELPOSN(2,60),KNOMAT(1, 300),UNKMAT(1,1830),
     2UNCLE( 60,24)
      COMMON/S6/ELNODE(3,610),RHSRED(1,60),RHSI(3, 99),KPA(2)
      COMMON/LIZ/NUNKVA,NKNVA,NOSTR,NCELNO,NCELN1,NTOTAL,NPRDEF,NT,
     1NELEM,NCELL,NELEM,ZNUNTOT,N
      DIMENSION A(300),B(300)
      EQUIVALENCE (A(1),UNKMAT(1)),(B(1),UNCLE(1))
C
```

```
C
C       CHECKING FOR KNOWN VARIABLE AND UNKNOWN VARIABLE
C       APPEARING AT ONE TIME
C
      NAB=300
      READ(5,3000) NELEM,NCELL,NDELM,NPRDEF,NOSTR,NOUTOT
 3000 FORMAT (5I5)
      IF(NCELL.NE.3.OR.NOSTR.NE.1)
     1GO TO 61
      IF (NDELM.LE.3.AND.NPRDEF.LE.24.AND.NOUTOT.LE.99.AND.NNELM.LE.20)
     1GO TO 60
   61 WRITE(6,62)
   62 FORMAT(32H0A PARAMETER READ BY INIAL IS INCORRECTLY SPECIFIED.)
      STOP
   60 NCELLD=NCELL*NDELM+1
      CALL GOOF
      DO 70 I = 1, NAB
      A(I)=0
   70 B(I)=0
      NUNKVA=0
      NKNVA=0
      DO 80 I=1,NELEM
      DO 200 J=2,NCELLD
      AA=IABS(ELNODE(I,J))
C
C       TO CHECK WHETHER NICKNAME IS IN  A  OR  B  ALREDY
C
      DO 90 K = 1, NAB
      IF(A(K).EQ.AA) GO TO 100
      IF(B(K).EQ.AA) GO TO 110
   90 CONTINUE
      GO TO 120
  100 A(K)=ELNODE(I,J)
      GO TO 210
  110 B(K)=ELNODE(I,J)
      GO TO 210
C
C       TO CHECK WHETHER NICKNAME IS IN  PREDIC  IF SO STORE IN  B
C
  120 DO 130 K=1,NOSTR
      DO 130 L=1,NPRDEF
      IF(AA.EQ.PRED(K,L)) GO TO 140
  130 CONTINUE
      GO TO 170
  140 DO 150 M = 1, NAB
      IF(B(M).EQ.0) GO TO 160
  150 CONTINUE
  160 B(M)=ELNODE(I,J)
      GO TO 210
C
```



```
C       IF IT IS NOT IN  A  OR  B OR PREDIC STORE IT IN  A
C
  170 DO 180 N = 1, NAB
      IF(A(N).EQ.0) GO TO 190
  180 CONTINUE
  190 A(N)=ELNODE(I,J)
  210 IF(J.EQ. NCELLD) GO TO 220
  200 CONTINUE
  220 DO 230 II = 1, NAB
      III = NAB + 1 - II
      IF(A(III).NE.0) GO TO 240
  230 CONTINUE
  240 IF(III.GT.NUNKVA) NUNKVA=III
      DO 250 JJ = 1, NAB
      IF(A(JJ).LT.0) A(JJ)=0
  250 CONTINUE
      DO 260 KK = 1, NAB
      KK1 = NAB + 1 - KK
      IF(B(KK1).NE.0) GO TO 270
  260 CONTINUE
  270 IF(KK1.GT.NKNVA) NKNVA=KK1
      DO 280 LL = 1, NAB
      IF(B(LL).LT.0) B(LL)=0
  280 CONTINUE
   80 CONTINUE
      RETURN
      END



      SUBROUTINE GOOF
      INTEGER ELNODE,PREDIC
      INTEGER A
      COMMON/S1/ PREDLE(1, 24)
      COMMON    PREDIC(1, 24),UNKNIC(1, 60),KNOWIC(2,24),UNRHS(1,24),
     1KNOWRS(1, 60),ELPOSN(2,60),KNOMAT(1, 300),UNKMAT(1,1830),
     2NUCLE( 60,24)
      COMMON/S2/ELNODE(3,510),NOSRED(1,60),RHSI(3, 44),KKA(2)
      COMMON/C1/NUNKVA,NKNVA,NOSTR,NCELLD,NCELL1,NTOTAL,NPRDEF,NT,
     1NELEM,NDELM,NNELM,NOUTOT,N
      NCELL2 = NCELLD - 2
      DO 2 I=1,NELEM
      READ(5,1) ELNODE(I,1),(ELNODE(I,J),J=2,56,3),INDEX,(ELNODE(I,J),J=
     159,NCELL2,3)
    1 FORMAT(20I3)
      IF(ELNODE(I,1).NE.I .OR.ELNODE(I,1).NE.INDEX) GO TO 40
      DO 2 J=2,NCELLD,3
      A=ELNODE(I,J)
      IF(A.LT.1.OR.A.GT.NOUTOT) GO TO 70
      DO 2 K=1,3
      L=J+K-1
```

```
2     ELNODE(I,L)=100*A+K
      DO 5 N=1,NUMTOT
      DO 3 I=1,NELEM
      I1=NELEM-I+1
      DO 3 J=2,NELEMN,3
      J1=NELEMN-J
      IF(ELNODE(I1,J1).EQ.100*N+1) GO TO 4
3     CONTINUE
4     DO 5 K=1,3
      L=J1+K-1
      ELNODE(I1,L)=-ELNODE(I1,L)
5     CONTINUE
      CALL OPENMS (3, KRA, 2, 0)
      CALL WRITMS (3, ELNODE(1,1), 183, 1)
      GO TO 6
40    ARITF(6,50) ELNODE(I-1,1), ELNODE(I,1)
50    FORMAT(34H0SEQUENCE ERROR IN ELNODL INPUT DATA AT ,2I5)
   60 STOP
   70 WRITE(6,80)A,I
   80 FORMAT(10H0THE DATA ,I5,36H IN ELEMENT OR PRESCRIBED DEFLECTION,I5
     1,17H IS OUT OF RANGE.)
      GO TO 60
6     READ(5,7) (PREDIC(I,1),PREDEF(1,I),I=1,NPRDEF)
7     FORMAT(4(I10,E10.0))
      DO 10 I=1,NPRDEF
      A=PREDIC(I,1)/100
      IF(A.LT.1.OR.A.GT.NUMTOT) GO TO 70
      A=PREDIC(I,1)-100*A
      IF(A.LT.1.OR.A.GT.3) GO TO 70
   10 CONTINUE
      RETURN
      END



      SUBROUTINE COORD
      INTEGER ELNODE
      COMMON/S6/ELNODE(3,610),RUSRED(1,60),RUSI(3, 44),KRA(2)
      COMMON/C1/ NUNKVA,NKNVA,NOSTR,NELEMO,NELEM1,NTOTAL,NPRDEF,NT,
     1NELEM,NEREL,NNELM,NUMTOT,N
      COMMON/C4/IGS,IPS,IN(3,3)
      COMMON/C5/IIN,IOUT
      COMMON/COR/CORD(3,20),TR(20,3,3),CCORD(3, 44),JRA(4)
      DIMENSION TP(3,3)
      DO 1 J=1,NNELM
      K=IABS(ELNODE(N,3*J-1))/100
      DO 1 I=1,3
      L=3*J-3+I
      CORD(I,J)=CCORD(I,K)
      RUSRED (1, L) = 0.
      IF(ELNODE(N, L +1).GT.0) GOTO 1
```



```
      RUSRED(1,L)=RUSI(I,K)
1     CONTINUE
      DO 7  I = 1, NNELM
      CALL PTRANS(CORD(1,1),TP)
      DO 7 J=1,3
      DO 7  K = 1, 3
      TR (I, J, K) = 0.
      DO 7  L = 1, 3
      TR (I, J, K) = TR (I, J, K) + IN (J, L) * TP (L, K)
    7 CONTINUE
      IF (N .EQ. 1) CALL OPENMS (2, JRA, 4, 0)
      IF (IOUT .LE. 1)  GO TO 2
      CALL WRITMS (2, CORD (1, 1), 240, N)
    2 RETURN
      END



      SUBROUTINE LOAD
      REAL JAC
      COMMON/S8/XG(4),CG(4),IGAUS
      COMMON/S10/DLXYZ(3,20),DN(6,9),P(9,9),GP(60,9)
      COMMON/C1/ NUNKVA,NKNVA,NOSTR,NELEMO,NELEM1,NTOTAL,NPRDEF,NT,
     1NELEM,NEREL,NNELM,NUMTOT,N
      COMMON/C3/V(20,3)
      COMMON/C4/IGS,IPS,IN(3,3)
      COMMON/C5/IIN,IOUT
      COMMON/COR/CORD(3,20),TR(20,3,3),CCORD(3, 44),JRA(4)
      COMMON/SP/G,H,F,MS
      DIMENSION RUSL(60),DETN(6),TRN(3),GL(3),JAC(3,3),DE(4,20),TRUSL(60
     1),TP(3,3),TRGL(3)
      EQUIVALENCE (DE(1),GP(1)),(TRUSL(1),RUSL(1),GP(200))
      DO 6  I = 1, NCELNT
    6 TRUSL (I) = 0.
      IF (IIN.LT.3)  GO TO 1
      WRITE (6, 90)
   90 FORMAT (// 42H0STRESS LOADING INPUT DATA FOR THE ELEMENT/
     1         54H0FACE  CRD SYST  X COMPONENT  Y COMPONENT  Z COMPONENT/)
    1 READ(5,2)NPLOC1,NFACE
    2 FORMAT (2I5)
      IF (NPLOC1.NE.N)  GO TO 56
      IF(I.EQ.0.(NFACE.LT.1.OR.NFACE.GT.6)) GO TO 50
   56 WRITE(6,51)
   51 FORMAT (41H0A STRESS DATUM IS SPECIFIED INCORRECTLY.)
   52 STOP
   50 DO 4 LO=1,NFACE
      READ(5,3)NPLOC1,ICODE,ISGL,(GL(I),I=1,3)
    3 FORMAT(3I5,3F10.0)
      IF (IIN.LT.3)  GO TO 5
      WRITE(6,4))ICODE,ISGL,(GL(I),I=1,3)
   41 FORMAT (1H , I5, I7, 4X, 3E13.5)
```

```
    5 IF (NPLOC1.NE.N)  GO TO 56
      IF (ISGL.LT.1.OR.ISGL.GT.6)  GO TO 56
      IF(.NOT.(ISGL.EQ.1.AND.IGS.NE.1))  GO TO 42
      CALL GTRANS (IGS, GL (1), GL(2), GL(3))
   42 IACODE=IABS(ICODE)
      ISCODE=ICODE/IACODE
      IF (IACODE.LT.1.OR.IACODE.GT.3)  GO TO 56
   53 DO 1000 IGL=1,NNELM
      IF(IFIX(V(IGL,IACODE)).NE.ISCODE) GO TO 1000
      DO 1001  JGL = 1, 3
      KGL=3*(IGL-1)+JGL
      DO 1001  IG = 1, IGAUS
      DO 1001  JG = 1, IGAUS
      GO TO (11,12,13),IACODE
   11 G=ISCODE
      H=XG(IG)
      F=XG(JG)
      GO TO 14
   12 H=ISCODE
      G=XG(IG)
      F=XG(JG)
      GO TO 14
   13 F=ISCODE
      G=XG(IG)
      H=XG(JG)
   14 IF(NNELM.EQ.20) GO TO 15
      CALL SHAP32
      GO TO 16
   15 CALL SHAP20
   16 DO 17 I=1,3
      DO 17 K=1,3
      JAC(I,K)=0.
      IF (IACODE .NE. I)  GO TO 18
      JAC(I,K)=1.
      GO TO 17
   18 DO 23  J = 1, NNELM
   23 JAC(I,K)=JAC(I,K)+DE(I,J)*CORD(K,J)
   17 CONTINUE
      DETM(1)=JAC(1,1)*JAC(2,2)*JAC(3,3)
      DETM(2)=JAC(1,2)*JAC(2,3)*JAC(3,1)
      DETM(3)=JAC(1,3)*JAC(2,1)*JAC(3,2)
      DETM(4)=JAC(3,1)*JAC(2,2)*JAC(1,3)
      DETM(5)=JAC(3,2)*JAC(2,3)*JAC(1,1)
      DETM(6)=JAC(3,3)*JAC(2,1)*JAC(1,2)
      IF(IACODE-2) 19,20,21
   21 AX      =DETM(2)-DETM(4)
      AY      =DETM(3)-DETM(5)
      AZ      =DETM(1)-DETM(6)
      GO TO 22
   20 AX      =DETM(3)-DETM(6)
      AY      =DETM(2)-DETM(5)
```



```
      AZ      =DETM(1)-DETM(4)
      GO TO 22
   19 AX      =DETM(1)-DETM(5)
      AY      =DETM(2)-DETM(6)
      AZ      =DETM(3)-DETM(4)
   22 IF (ISGL.GE.3)  GO TO 25
      CMPT=GL(JGL)
      GO TO 24
   25 CMPT=0.
      IF (ISGL.EQ.3) GO TO 27
      DO 60 I=1,3
      TRGL(I)=0.
      DO 60 J=1,NNELM
   60 TRGL(I)=TRGL(I)+DE(4,J)*CORD(I,J)
      IPS1 = IPS
      IF (ISGL .GE. 5)  IPS = ISGL - 3
      CALL PTRANS (TRGL,TP)
      IPS = IPS1
      DO 61 K=1,3
      TRGL(K)=0.
      DO 61 J=1,3
   61 TRGL(K)=TRGL(K)+TB(JGL,J)*TP(J,K)
      DO 26  I=1,3
   26 CMPT=CMPT+TRGL(I)*GL(I)
      GO TO 24
   27 DO 28  I=1,3
   28 CMPT=CMPT+TB(JGL,I)*GL(I)
   24 RHSL (KGL) = RHSL (KGL) + CG (IG) * CG (JG) * DE (4, IGL)
     1                * CMPT     * SQRT (AX * AX + AY * AY + AZ * AZ)
 1001 CONTINUE
 1000 CONTINUE
    4 CONTINUE
      DO 31  I = 1, NNELM
      JJ=3*(I-1)
      DO 30 K=1,3
      TRH (K) = 0.
      DO 30 J=1,3
      JK=JJ+J
   30 TRH (K) = TRH (K) + TR (I, J, K) * RHSL (JK)
      DO 31  K = 1, 3
      KI=JJ+K
   31 TRHSL (KI) = TRH (K)
      RETURN
      END



      SUBROUTINE GTRANS (IGS, X, Y, Z)
      A = 0.017453292520 * Y
      C = COS (A)
      S = SIN (A)
```

```
      R = X
      X = R * C
      Y = R * S
      IF (IGS.EQ.2)  GO TO 1
      A = 0.017453292520 * Z
      C = COS (A)
      S = SIN (A)
      X = X * S
      Y = Y * S
      Z = R * C
    1 RETURN
      END



      SUBROUTINE PTRANS (U, TP)
      COMMON/C4/IGS,IPS,TR(3,3)
      DIMENSION TP(3,3),UD(3),U(3)
      DO 3  J = 1, 3
      DO 2  K = 1, 3
    2 TP (J, K) = 0.
    3 TP (J, J) = 1.
      IF (IPS.EQ.1)  GO TO 6
    4 DO 5  J = 1, 3
      UD (J) = 0.
      DO 5  K = 1, 3
    5 UD(J)=UD(J)+TR(K,J)*U(K)
      IF (ABS(UD(1)).GT.1.E-35 .OR. ABS(UD(2)).GT.1.E-35)  GO TO 8
      THED = 0.
      GO TO 9
    8 THED = ATAN2 (UD (2), UD (1))
    9 C = COS (THED)
      S = SIN (THED)
      TP (1, 1) = C
      TP (1, 2) = -S
      TP (2, 1) = S
      TP (2, 2) = C
      IF (IPS.EQ.2)  GO TO 6
      IF (ABS(UD(3)).GT.1.E-35)  GO TO 10
      PHID = 1.5707963268
      GO TO 11
   10 PHID = ATAN (SQR (UD (1) ** 2 + UD (2) ** 2) / UD (3))
      IF (PHID.LT.0.)  PHID = PHID + 3.1415926536
   11 C = COS (PHID)
      S = SIN (PHID)
      TP (1, 1) = TP (1, 1) * C
      TP (2, 1) = TP (2, 1) * C
      TP (3, 1) = -S
      TP (1, 3) = TP (2, 2) * S
      TP (2, 3) = -TP (1, 2) * S
      TP (3, 3) = C
    6 RETURN
      END
```



```
      SUBROUTINE FEM
      REAL JAC,IJAC,MVJAC
      COMMON/S6/ELNODE(3,610),RHSRED(1,60),RHSI(3, 44),KRA(2)
      COMMON/S8/XG(4),CG(4),IGAUS
      COMMON/S10/DEXYZ(3,20),DH(6,9),P(9,9),GP(60,9)
      COMMON/C1/ NUMKVA,MKNVA,NOSTR,NCELN0,NCELN1,NTOTAL,NPROEF,NT,
     1NELEM,NFREE,NNELM,NODTOT,N
      COMMON/COR/CORD(3,20),TR(20,3,3),CCORD(3, 44),JRA(4)
      COMMON/SP/G,H,F,MS
      DIMENSION A(3,3),SK(1830),JAC(3,3),IJAC(3,3),DE(4,20)
      EQUIVALENCE (SK(1),ELNODE(1)),(DE(1),GP(1))
      I = (NCELN1 * (NCELN1 + 1)) / 2
      DO 5 KS=1,I
    5 SK(KS)=0.
C
C        NUMERICAL INTEGRATION LOOP
C
      DO 1000 IG=1,IGAUS
      DO 1000 JG=1,IGAUS
      DO 1000 KG=1,IGAUS
      G=XG(IG)
      H=XG(JG)
      F=XG(KG)
      IF(NNELM.EQ.20) GO TO 30
      CALL SHAP32
      GO TO 31
   30 CALL SHAP20
   31 CONTINUE
C
C        FORMATION OF JACOBIAN MATRUX -- JAC
C
      DO 10 I=1,3
      DO 10 K=1,3
      JAC(I,K)=0.0
      DO 10 J=1,NNELM
   10 JAC(I,K)=JAC(I,K)+DE(I,J)*CORD(K,J)
C
C        VALUE OF DETERMINANT OF JAC  -- VJAC
C
      VJAC=JAC(1,1)*(JAC(2,2)*JAC(3,3)-JAC(2,3)*JAC(3,2))-
     1JAC(1,2)*(JAC(2,1)*JAC(3,3)-JAC(2,3)*JAC(3,1))+
     2JAC(1,3)*(JAC(2,1)*JAC(3,2)-JAC(2,2)*JAC(3,1))
      IF(VJAC) 12,11,12
   11 WRITE(6,13)
   13 FORMAT(1H0,21HDLTJ=0 PROGRAM HALTED)
      STOP
   12 CONTINUE
C
C        INVERSION OF JACOBIAN  -- IJAC
C
      IJAC(1,1)=(JAC(2,2)*JAC(3,3)-JAC(3,2)*JAC(2,3))/VJAC
```

```
      IJAC(1,2)=-(JAC(1,2)*JAC(3,3)-JAC(3,2)*JAC(1,3))/VJAC
      IJAC(1,3)=(JAC(1,2)*JAC(2,3)-JAC(2,2)*JAC(1,3))/VJAC
      IJAC(2,1)=-(JAC(2,1)*JAC(3,3)-JAC(3,1)*JAC(2,3))/VJAC
      IJAC(2,2)=(JAC(1,1)*JAC(3,3)-JAC(3,1)*JAC(1,3))/VJAC
      IJAC(2,3)=-(JAC(1,1)*JAC(2,3)-JAC(2,1)*JAC(1,3))/VJAC
      IJAC(3,1)=(JAC(2,1)*JAC(3,2)-JAC(2,2)*JAC(3,1))/VJAC
      IJAC(3,2)=-(JAC(1,1)*JAC(3,2)-JAC(1,2)*JAC(3,1))/VJAC
      IJAC(3,3)=(JAC(1,1)*JAC(2,2)-JAC(2,1)*JAC(1,2))/VJAC
      DO 20 J=1,3
      DO 20 L=1,NNELM
      DEXYZ(J,L)=0.0
      DO 20 K=1,3
   20 DEXYZ(J,L)=DEXYZ(J,L)+IJAC(J,K)*DE(K,L)
      MVJAC=VJAC*CG(IG)*CG(JG)*CG(KG)
      DO 19 I=1,NCELN1
      DO 19 J=1,9
   19 OP(I,J)=0.0
      DO 21 I=1,NNELM
      I1=3*I-2
      I2=3*I-1
      I3=3*I
      DO 21 K=1,9
      DO 21 J=1,3
      J1=J+3
      J2=J+6
      OP(I1,K)=OP(I1,K)+DEXYZ(J,I)*P(J,K)
      OP(I2,K)=OP(I2,K)+DEXYZ(J,I)*P(J1,K)
      OP(I3,K)=OP(I3,K)+DEXYZ(J,I)*P(J2,K)
   21 CONTINUE
      DO 22 K=1,NNELM
      DO 22 II=1,3
      K1=(K-1)*3+II
      J2=(II-1)*3
      DO 22 I=1,K1
      K2=I+((K1-1)*K1)/2
      DO 22 J=1,3
      J1=J2+J
   22 SK(K2)=SK(K2)+OP(I,J1)*DEXTZ(J,K)*MVJAC
 1000 CONTINUE
      DO 106 M = 1,NNELM
      M1= 3*(M-1)
      DO 106 L = 1,M
      L1 = 3*(L-1)
      DO 102 I = 1,3
      DO 102 J = 1,3
      A(I,J)=0.
      J1 = ((M1+J) * (M1+J-1))/2+L1
      DO 102 K=1,3
      IF(L.EQ.M .AND. K.GT.J) GO TO 101
      KS = J1+K
      GO TO 102
```



```
  101 KS=((L1+K)*(L1+K-1))/2+M1+J
  102 A(I,J)=A(I,J)+TR(L,K,I)*SK(KS)
      DO 103 J = 1,3
      J1 = ((M1+J)*(M1+J-1))/2+L1
      DO 103 I=1,3
      IF(L.EQ.M .AND. I.GT.J) GO TO 103
      KS = J1 + I
      SK(KS) = 0.
      DO 105 K=1,3
  105 SK(KS) = SK(KS) + A(I,K)*TR(M,K,J)
  103 CONTINUE
  106 CONTINUE
      RETURN
      END



      SUBROUTINE STFTR
      REAL KNOMAT
      INTEGER ELPOSN
      COMMON    PRENIC(1, 24),UNKNIC(1, 60),KNONIC(2,24),UNRHS(1,24),
     1KNORHS(1, 60),ELPOSN(2,60),KNOMAT(1, 300),UNKMAT(1,1830),
     2UNCLE( 60,24)
      COMMON/S6/ELNODE(3,610),RHSRED(1,60),RHSI(3, 44),KKA(2)
      COMMON/C1/ NUNKVA,NKNVA,NUSTR,NCELNO,NCELN1,NTOTAL,NPRDEF,NT,
     1NELEM,DFREE,NNELM,NODTOT,N
      DIMENSION SK(1830)
      EQUIVALENCE (SK(1),ELNODE(1))
C
C
C        ROUTINE TO DISTRIBUTE ELEMENT STIFFNESS MATRIX IN
C        UNKMAT,KNOWN AND UNCLE MATRICES ( MAIN MATRIX)
C
      DO 900 I=1,NCELN1
      I1=ELPOSN(1,I)
      I2=ELPOSN(2,I)
      DO 900 J=1,NCELN1
      IF(J.GE.I) GO TO 901
      IS=J+((I*(I-1))/2
      GO TO 902
  901 IS=I+((J*(J-1))/2
  902 CONTINUE
      J1=ELPOSN(1,J)
      J2=ELPOSN(2,J)
      IF(I2.EQ.0) GO TO 810
C
C        TO FILL KNOWN MATRIX  IF NICK NAME IS IN KNONIC
C
      IF(J2.EQ.0) GO TO 900
      IF(J1.GT.I1) GO TO 900
      IJ=(I1*(I1-1))/2+J1
```

```
      KNOMAT(1,IJ)=KNOMAT(1,IJ)+SK(IS)
      GO TO 900
C
C        TO FILL UNCLE AND UNKMAT WHEN NICKNAME IS AN UNKNOWN ONE
C
  810 IF(J2.EQ.1) GO TO 830
      GO TO 840
  830 UNCLE(I1,J1)=UNCLE(I1,J1)+SK(IS)
      GO TO 900
  840 IF(J1.GT.I1) GO TO 900
      IJ=(I1*(I1-1))/2+J1
      UNKMAT(1,IJ)=UNKMAT(1,IJ)+SK(IS)
  900 CONTINUE
      RETURN
      END



      SUBROUTINE FORWAD
      REAL KNOMAT,KNORHS
      INTEGER ELPOSN,UNKNIC,ELNODE
      INTEGER COPIOE
      COMMON/S1/ PRCOLF(1, 24)
      COMMON    PRCNIC(1, 24),UNKNIC(1, 60),KNOWIC(2,24),UNRHS(1,24),
     1KNOWHS(1, 60),ELPOSN(2,60),KNOMAT(1, 300),UNKMAT(1,1830),
     2UNCLE( 60,24)
      COMMON/S6/ELNODE(3,610),RHSREF(1,60),RHSI(3, 44),KKA(2)
      COMMON/S10/XEXYZ(3,20),DH(6,9),P(9,9),GP(60,9)
      COMMON/C1/ NUMKVA,NKNVA,NOSTR,NCELNO,NCELN1,NTOTAL,NPROEF,NT,
     1IELEM,NEREL,NUELM,NUMTOT,N
      COMMON/C2/NLG,BUF(9,85),IBUF(9,4),NREC,NTREC,RHS,NIC,LP1,LP2,
     1NPOSN,IRA(15)
      DIMENSION COMP(84)
      EQUIVALENCE(COMP(1),GP(1))
C
C        ROUTINE FOR MODIFYING ELEMENTS IN MAIN MATRIX FOR A COMPLETED
C        UNKNOWN NICKNAME
C
      DO 100 N=1,NCELN1
      IF(ELNODE(N,IM+1).LT.0) GO TO 101
      GO TO 100
  101 I=ELPOSN(1,IM)
      IF(ELPOSN(2,IM).EQ.1) GO TO 210
C
C        STORING COMPLETED ROW IN AN AUXILIARY ROW MATRIX -- COMP--
C
  110 I1=1+NKNVA
      III = (I * (I - 1)) / 2
      DO 120 J=1,NKNVA
  120 COMP(J)=UNCLE(I,J)
      DO 130 J1=1,I
      IJ1=III+J1
```



```
      MJ1=NKNVA+J1
  130 COMP(MJ1)=UNKMAT(1,IJ1)
      IP1=I+1
      IF(IP1.GT.NUMKVA) GO TO 141
      DO 140 I2=IP1,NUMKVA
      IJ2=(I2*(I2-1))/2+I
      MI2=NKNVA+I2
  140 COMP(MI2)=UNKMAT(1,IJ2)
  141 CONTINUE
C
C        MODIFY KNOMAT MATRIX
C
      DO 150 I4=1,NKNVA
      II2 = (I4 * (I4 - 1)) / 2
      CMP=COMP(I4)/COMP(I1)
      DO 150 J4=1,I4
      IJ4=II2+J4
  150 KNOMAT(1,IJ4)=KNOMAT(1,IJ4)-CMP*COMP(J4)
C
C        MODIFY UNCLE MATRIX
C
      DO 160 I5=1,NUMKVA

      MI5=I5+NKNVA
      CMP=COMP(MI5)/COMP(I1)
      DO 160 J5=1,NKNVA
  160 UNCLE(I5,J5)=UNCLE(I5,J5)-CMP*COMP(J5)
C
C        MODIFY UNKMAT MATRIX
C
      DO 170 I6=1,NUMKVA
      II3 = (I6 * (I6 - 1)) / 2
      MI6=I6+NKNVA
      CMP=COMP(MI6)/COMP(I1)
      DO 170 J6=1,I6
      MJ6=J6+NKNVA
      IJ6=II3+J6
  170 UNKMAT(1,IJ6)=UNKMAT(1,IJ6)-CMP*COMP(MJ6)
C
C        RELEASE THE STORED EQUATION SPACE
C
      DO 420 J=1,NKNVA
  420 UNCLE(I1,J)=0.0
      DO 440 J1=1,I
      IJ1=III+J1
  430 UNKMAT(1,IJ1)=0.0
      IF(IP1.GT.NUMKVA) GO TO 441
      DO 440 I2=IP1,NUMKVA
      IJ2=(I2*(I2-1))/2+I
  440 UNKMAT(1,IJ2)=0.0
  441 CONTINUE
```

```
C
C        STORING REQUIRED DATA IN A BUFFER AREA
C
      NIC=IABS(UNKNIC(1,I))
      RHS=KNORHS(1,I)
      LP1=ELPOSN(1,IM)
      LP2=ELPOSN(2,IM)
      NPOSN=0
      CALL BUFFER
C
C        MODIFY RIGHT HAND SIDE
C
      RHSK=KNORHS(1,I)
      RHK=RHSK/COMP(I1)
      DO 180 I7=1,NKNVA
  180 UNRHS(1,I7)=UNRHS(1,I7)-COMP(I7)*RHK
      DO 190 I8=1,NUNKVA
      MI8=I8+NKNVA
  190 KNORHS(1,I8)=KNORHS(1,I8)-COMP(MI8)*RHK
      KNORHS(1,I)=0.0
C
C        UNKNIC IS MADE ZERO
C
      UNKNIC(1,I)=0
      GO TO 100
C
C        ROUTINE FOR COMPLETED KNOWN NICKNAMES
C        STORING COMPLETED ROW TERMS OF KNOMAT IN AUXILARY MATRIX COMP
C
  210 II1=(I*(I-1))/2
      DO 220 J1=1,I
      IJ1=II1+J1
      COMP(J1)=KNOMAT(1,IJ1)
  220 KNOMAT(1,IJ1)=0.0
      IF(I.EQ.NKNVA) GO TO 240
C
C        STORING COMPLETED COLUM TERMS OF KNOMAT
C
      IP1=I+1
      DO 230 I2=IP1,NKNVA
      IJ2=(I2*(I2-1))/2+I
      COMP(I2)=KNOMAT(1,IJ2)
  230 KNOMAT(1,IJ2)=0.0
C
C        STORING COMPLETED COLUM TERMS OF UNCLE
C
  240 DO 250 I3=1,NUNKVA
      MI3=NKNVA+I3
      COMP(MI3)=UNCLE(I3,I)
  250 UNCLE(I3,I)=0.0
C
```



```
C        FINDING THE VALUE OF PRESCRIBED DEFLECTION(PREKNW)
C        CORRESPONDING TO THE COMPLETED NICKNAMES
C
      COPRDE=KNONIC(2,I)
      PREKNW=PREDEF(1,COPRDE)
C
C        MODIFY THE UNKNOWN RHS EXCEPT THE COMPLETED RHS
C
      DO 260 I4=I,NKNVA
      IF(I4.EQ.I) GO TO 260
      UNRHS(1,I4)=UNRHS(1,I4)-COMP(I4)*PREKNW
  260 CONTINUE
C
C      MODIFY THE KNOWN RHS
C
      DO 270 I5=1,NUNKVA
      MI5=NKNVA+I5
  270 KNORHS(1,I5)=KNORHS(1,I5)-COMP(MI5)*PREKNW
C
C        STORING REQUIRED DATA IN A BUFFER AREA
C
      NIC=IABS(KNONIC(1,I))
      RHS=UNRHS(1,I)
      LP1=ELPOSN(1,IM)
      LP2=ELPOSN(2,IM)
      NPOSN=KNONIC(2,I)
      CALL BUFFER
C
C        RESET FOR NEXT ELEMENT
C
      KNONIC(1,I)=0
      KNONIC(2,I)=0
      UNRHS(1,I)=0.0
  100 CONTINUE
      IF(N.EQ.NELEM) GO TO 1002
      GO TO 1003
 1002 IF(NLG.EQ.-) GO TO 1003
      NLG=-NLG
      CALL BUFFER
 1003 CONTINUE
      RETURN
      END



      SUBROUTINE BUFFER
      COMMON/S10/DEXYZ(3,20),DII(6,9),P(9,9),UP(60,9)
      COMMON/C1/ NUNKVA,NKNVA,NOSTR,NCELNO,NCELN1,NTOTAL,NPREDEF,NT,
     1NELEM,NFREE,NBLLM,NOUTOT,N
      COMMON/C2/NLG,BUF(9,85),IBUF(9,4),NREC,NTREC,RHS,NIC,LP1,LP2,
     1NPOSN,IRA(16)
```

```
      DIMENSION COMP(84)
      EQUIVALENCE(COMP(1),QP(1))
C
C        ROUTINE IN WHICH THE ROW CORROSPONDING TO THE COMPLETED
C        VARIABLE IS STORED IN A BUFFER AREA
C
      IF(NREC.NE.0.OR.NLG.NE.0) GO TO 3
      CALL OPENMS(1,IRA,16,0)
    3 IF(NLG.GE.0) GO TO 2
      NLG=-NLG
      GO TO 10
    2 NLG=NLG+1
      DO 1 I=1,NTOTAL
    1 BUF(NLG,I)=COMP(I)
      BUF(NLG,NTREC) = RHS
      IBUF(NLG,1)=LP1
      IBUF(NLG,2)=LP2
      IBUF(NLG,3)=NIC
      IBUF(NLG,4)=NPOSN
      IF(NLG.EQ.9 ) GO TO 10
      GO TO 20
   10 NREC=NREC+1
      CALL WRITMS(1,NLG,802,NREC)
      NLG=0
   20 CONTINUE
      RETURN
      END


      SUBROUTINE BACKWD
      REAL KNORHS
      INTEGER PRNIC,UNKNIC
      COMMON/S1/ PREDEF(1, 24)
      COMMON     PRNIC(1, 24),UNKNIC(1,60),KNONIC(2,24),UNKRHS(1,24),
     1KNORHS(1, 60),ELPOSN(2,60),KNOMAT(1, 300),UNKMAT(1,1830),
     2UNCLE( 60,24)
      COMMON/S6/ELMODE(3,610),RHSRED(1,60),RHSI(3, 44),KRA(2)
      COMMON/S10/ULXYZ(3,20),DH(6,9),P(9,9),QP(60,9)
      COMMON/C1/ NUNKVA,NKNVA,NOSTR,NCELN0,NCELN1,NTOTAL,NPREDEF,NT,
     1NELEM,NPREE,NUELM,NOOTOT,0
      COMMON/C2/NLG,BUF(9,85),IBUF(9,4),NREC,NTREC,RHS,NIC,LP1,LP2,
     1NPOSN,IRA(16)
      COMMON/C5/IIO,IOUT
      DIMENSION U2(132),COMP(84)
      EQUIVALENCE(U2(1),RHSI(1)),(COMP(1),QP(1))
C
C        INITIALISATION
C
      K = 0
      IF (IOUT.LT.3)  GO TO 3
```



```
      WRITE(6,2)
    2 FORMAT (1H1 ////   1H , *CALCULATED REACTIONS IN THE MAIN PROBLEM
     1SYSTEM*/)
    3 DO 202 I=1,NKNVA
      DO 202 J=1,2
  202 KNONIC(J,I)=0
      DO 203 I=1,NUNKVA
  203 UNKNIC(1,I)=0
      DO 1 M=1,NUNKVA
    1 KNORHS(1,M)=0.0
      DO 20 M1=1,NT
      U2(M1)=0.0
   20 CONTINUE
C
C        READ BACK THE STORED DATA IN BLOCKS IN A REVERSED ORDER
C
      NREC1=NREC
      DO 10 L=1,NREC1
      NREC=NREC1-L+1
      CALL READMS(1,NLG,802,NREC)
      LG=NLG
  300 DO 4 I=1,NTOTAL
    4 COMP(I)=BUF(LG,I)
      RHS=BUF(LG,NTREC)
      LP1=IBUF(LG,1)
      LP2=IBUF(LG,2)
      NIC=IBUF(LG,3)
      NPOSN=IBUF(LG,4)
      LG=LG-1
C
C        CHECK WHETHER  FNIC  IS IN  KNONIC
C
      IF(LP2.NE.1) GO TO 140
C
C        IF  FNIC  IS IN  KNONIC  MULTIPLY  KNOMAT WITH  PREDEF
C
      ANS1=0.0
      KNONIC(1,LP1)=NIC
      KNONIC(2,LP1)=NPOSN
      DO 120 I2=1,NKNVA
      NPOSN=KUONIC(2,I2)
      IF(NPOSN.EQ.0) GO TO 120
      ANS1=ANS1+COMP(I2)*PREDEF(1,NPOSN)
  120 CONTINUE
C
C        THEN MULTIPLY UNCLE WITH UNKDEF NOW STORED IN KNOWN RHS
C
      ANS2=0.0
      DO 130 I3=1,NUNKVA
      MI3=I3+UKNVA
  130 ANS2=ANS2+COMP(MI3)*KNORHS(1,I3)
```

```
C
C        FINDING THE CORRESPONDING UNKNOWN REACTION
C
      AUS=AUS1+AUS2-RHS
      IF (IDOF.LT.4)  GO TO 200
      IF (NODE(K,52).EQ.0 .AND. K.NE.0)  WRITE (6, 5)
    5 FORMAT (1H1 ////)
      K = K + 1
      WRITE(6,1000) NIC,AUS
 1000 FORMAT(19H REACTION AT NODE  ,I7 ,2X,5H IS  ,E16.8)
      GO TO 200
C
C        TO FIND THE UNKNOWN DEFL IF  FNIC  IS NOT IN  KNONIC
C        TO ALSO FIND THE ROW IT OCCUPIES DURING FORWARD ELIMINATION
  140 UNKNIC(1,LP1)=NIC
      IS=LP1
      IMS=IS-1
      IPS=IS+1
      IUS=IS+UNKNVA
C
C        DEFL IS MULTIPLIED WITH KNOWN DISPLACEMENTS
C
      AUS1=0.0
      DO 170 I=1,UNKNVA
      NPOSN=KNONIC(2,I)
      IF(NPOSN.EQ.0) GO TO 170
      AUS=AUS+COMP(I)*PREDEF(1,NPOSN)
  170 CONTINUE
C
C        KKMAT IS MULTIPLIED WITH UNKNOWN DISPL NOW KNOWN AND STORED
C        IN KNORHS --- EXCEPT THE DIAGONAL TERM
C
      AUS2=0.0
      IF(IMS.LE.0) GO TO 181
      DO 180 I7=1,IMS
      II7=UNKNVA+I7
  180 AUS2=AUS2+COMP(II7)*KNORHS(1,I7)
  181 AUS3=0.0
      IF (IPS.GT.UNKNVA) GO TO 191
      DO 190 I8=IPS,UNKNVA
      II8=UNKNVA+I8
  190 AUS3=AUS3+COMP(II8)*KNORHS(1,I8)
  191 CONTINUE
      KNORHS(1,IS)=(AUS-AUS1-AUS2-AUS3)/COMP(IDS)
C
C        WRITING THE UNKNOWN DISPLACEMENTS
C
      DEFEL=KNORHS(1,IS)
      JJ=NIC/100
      II=NIC-JJ * 100
      J = NFREE*(JJ-1)+II
      U2(J)=UNDEFL
  200 IF(LG.NE.0) GO TO 300
   10 CONTINUE
      DO 430 J=1,NPRDEF
      DEFL=PREDEF(1,J)
      NIC=PREDIC(1,J)
      JK = NIC/100
      II = NIC-JK * 100
      JJ = NFREE*(JK-1)+II
  441 U2(JJ)=DEFL
  430 CONTINUE
      RETURN
      END



      SUBROUTINE DEFOUT
      COMMON/S6/ELNODE(3,610),RHSRED(1,60),RHSI(3, 44),KRA(2)
      COMMON/C1/ NUMKVA,UKNVA,NOSTR,NCELN0,NCELN1,NTOTAL,NPRDEF,NT,
     1NELEM,NFREE,NNELM,NODTOT,N
      DIMENSION U2(132)
      EQUIVALENCE(U2(1),RHSI(1))
      WRITE(6,2)
    2 FORMAT (1H1 ///   1H0,  1X, 84HTHE NODAL DISPLACEMENT SOLUTION OF
     1THE STIFFNESS EQUATION IN THE MAIN PROBLEM SYSTEM/ 1H0, 11X, *NODE
     2*, 7X, *DISPL ALONG X*, 7X, *DISPL ALONG Y*, 7X, *DISPL ALONG Z*/)
      MPRINT= 50
      DO 1 JJ=1,NODTOT
      J=NFREE*(JJ-1)+1
      IF(MPRINT).GT.0) GO TO 4
      WRITE (6, 5)
    5 FORMAT (1H1 /////)
      MPRINT = 50
    4 MPRINT=MPRINT-1
    1 WRITE(6,3) JJ,U2(J),U2(J+1),U2(J+2)
    3 FORMAT(I16,3(4X,E16.8))
      RETURN
      END



      SUBROUTINE STRESS
      INTEGER ELNODE
      COMMON    PREDIC(1, 24),UNKNIC(1, 60),KNONIC(2,24),UNRHS(1,24),
     1KNORHS(1, 60),ELPOSN(2,60),KNOMAT(1, 300),UNKMAT(1,1830),
     2UNCLE( 60,24)
      COMMON/S6/ELNODE(3,610),RHSRED(1,60),RHSI(3, 44),KRA(2)
      COMMON/S10/DEXYZ(3,20),DJ(6,9),P(9,9),DP(60,9)
      COMMON/C1/ NUMKVA,UKNVA,NOSTR,NCELN0,NCELN1,NTOTAL,NPRDEF,NT,
     1NELEM,NFREE,NNELM,NODTOT,N
      COMMON/C3/V(20,3)
```

```
      COMMON/COR/CORD(3,20),TR(20,3,3),CCORD(3, 44),JRA(4)
      COMMON/SP/G,H,F,MS
      DIMENSION C(60),STR(6),  STG(3,3),STGT(3,3),SL(3,3)
      DIMENSION NDIV(44),U2(132)
      DIMENSION STSS(44,6), DBT (6,60)
      EQUIVALENCE(STSS(1),UNKMAT(1)),(DBT(1),QP(150)),(NDIV(1),CCORD(1))
     1,(U2(1),RHSI(1)),(C(1),RHSRED(1))
      DO 52 I=1,NODTOT
      NDIV(I)=0
      DO 52 J=1,6
52    STSS(I,J) = 0.
      DO 20 LL=1,NELEM
      CALL READMS (2, CORD(1,1), 240, LL)
      DO 30 K=2,NCELNO
      NIC=IABS(ELNODE(LL,K))
      JK=NIC/100
      II=NIC-JK * 100
      JJ=NFREE*(JK-1)+II
      KMI=K-1
      C(KMI)=U2(JJ)
30    CONTINUE
      DO 650 MS=1,NNELM
      CALL FEM2
      DO 630 I=1,6
      STR(I)=0.0
      DO 630 K=1,NCELN1
630   STR(I)=STR(I)+DBT(I,K)*C(K)
      STG(1,1)=STR(1)
      STG(1,2)=STR(6)
      STG(1,3)=STR(5)
      STG(2,1)=STR(6)
      STG(2,2)=STR(2)
      STG(2,3)=STR(4)
      STG(3,1)=STR(5)
      STG(3,2)=STR(4)
      STG(3,3)=STR(3)
      DO 201 I=1,3
      DO 201 J=1,3
      STGT(I,J)=0.0
      DO 201 K=1,3
201   STGT(I,J)=STGT(I,J)+STG(I,K)*TR(MS,K,J)
      DO 202 J=1,3
      DO 202 L=J,3
      SL(J,L)=0.0
      DO 202 K=1,3
202   SL(J,L)=SL(J,L)+TR(MS,K,J)*STGT(K,L)
      STR(1)=SL(1,1)
      STR(2)=SL(2,2)
      STR(3)=SL(3,3)
      STR(4)=SL(2,3)
      STR(5)=SL(1,3)
      STR(6)=SL(1,2)
      NODE=IABS(ELNODE(LL,3*MS-1))/100
```



```
      NDIV(NODE)=NDIV(NODE)+1
      DO 51 K=1,6
51    STSS(NODE,K) = STSS(NODE,K) + STR (K)
      IF(ELNODE(LL,3*MS-1).GE.0) GO TO 650
      DO 53 K=1,6
53    STSS(NODE,K)=STSS(NODE,K)/FLOAT(NDIV(NODE))
650   CONTINUE
20    CONTINUE
      RETURN
      END


      SUBROUTINE FEM2
      REAL JAC,IJAC
      COMMON/S10/DEXYZ(3,20),DH(6,9),P(9,9),QP(60,9)
      COMMON/C1/ NUNKVA,NKNVA,NOSTR,NCELNO,NCLLN1,NTOTAL,NPKDEF,NT,
     1NELEM,NFREE,NNELM,NODTOT,N
      COMMON/C3/V(20,3)
      COMMON/COR/CORD(3,20),TR(20,3,3),CCORD(3, 44),JRA(4)
      COMMON/SP/G,H,F,MS
      DIMENSION DBT(6,60),DB(6,60),A(6,3),JAC(3,3),IJAC(3,3),DE(4,20)
      EQUIVALENCE(DE(1),QP(1)),(DB(1),DBT(1),QP(150))
      G = V (MS, 1)
      H = V (MS, 2)
      F = V (MS, 3)
      IF (NNELM .EQ. 20)  GO TO 30
      CALL SHAP32
      GO TO 31
30    CALL SHAP20
31    CONTINUE
C
C        FORMATION OF JACOBIAN MATRUX -- JAC
C
      DO 10 I=1,3
      DO 10 K=1,3
      JAC(I,K)=0.0
      DO 10 J=1,NNELM
10    JAC(I,K)=JAC(I,K)+DE(I,J)*CORD(K,J)
C
C        VALUE OF DETERMINANT OF JAC  -- VJAC
C
      VJAC=JAC(1,1)*(JAC(2,2)*JAC(3,3)-JAC(2,3)*JAC(3,2))-
     1JAC(1,2)*(JAC(2,1)*JAC(3,3)-JAC(2,3)*JAC(3,1))+
     2JAC(1,3)*(JAC(2,1)*JAC(3,2)-JAC(2,2)*JAC(3,1))
      IF(VJAC) 12,11,12
11    WRITE(6,13)
13    FORMAT(1HO,21HDETJ=0 PROGRAM HALTED)
      VJAC=.1E-25
12    CONTINUE
C
```

```
C
C       INVERSION OF JACOBIAN  -- IJAC
C
      IJAC(1,1)=(JAC(2,2)*JAC(3,3)-JAC(3,2)*JAC(2,3))/VJAC
      IJAC(1,2)=-(JAC(1,2)*JAC(3,3)-JAC(3,2)*JAC(1,3))/VJAC
      IJAC(1,3)=(JAC(1,2)*JAC(2,3)-JAC(2,2)*JAC(1,3))/VJAC
      IJAC(2,1)=-(JAC(2,1)*JAC(3,3)-JAC(3,1)*JAC(2,3))/VJAC
      IJAC(2,2)=(JAC(1,1)*JAC(3,3)-JAC(3,1)*JAC(1,3))/VJAC
      IJAC(2,3)=-(JAC(1,1)*JAC(2,3)-JAC(2,1)*JAC(1,3))/VJAC
      IJAC(3,1)=(JAC(2,1)*JAC(3,2)-JAC(2,2)*JAC(3,1))/VJAC
      IJAC(3,2)=-(JAC(1,1)*JAC(3,2)-JAC(1,2)*JAC(3,1))/VJAC
      IJAC(3,3)=(JAC(1,1)*JAC(2,2)-JAC(2,1)*JAC(1,2))/VJAC
      DO 20 J=1,3
      DO 20 L=1,NNELM
      DEXYZ(J,L)=0.0
      DO 20 K=1,3
   20 DEXYZ(J,L)=DEXYZ(J,L)+IJAC(J,K)*DE(K,L)
      DO 21 I=1,6
      DO 21 J=1,NELLM1
   21 DB(I,J)=0.0
      DO 22 K=1,NNELM
      K1=3*K-2
      K2=3*K-1
      K3=3*K
      DO 22 I=1,6
      DO 22 J=1,3
      J1=J+3
      J2=J+6
      DB(I,K1)=DB(I,K1)+DH(I,J)*DEXYZ(J,K)
      DB(I,K2)=DB(I,K2)+DH(I,J1)*DEXYZ(J,K)
      DB(I,K3)=DB(I,K3)+DH(I,J2)*DEXYZ(J,K)
   22 CONTINUE
      DO 102  L = 1, NNELM
      J2 = 3 * L - 3
      DO 101  I = 1, 6
      DO 101  K = 1, 3
      A (I, K) = 0.
      DO 101 J = 1, 3
      J1 = J2 + J
  101 A (I, K) = A (I, K) + DB (I, J1) * BR (L, J, K)
      DO 102  I = 1, 6
      DO 102  J = 1, 3
      J1 = J2 + J
      DBT (I, J1) = A (I, J)
  102 CONTINUE
      RETURN
      END
```



```
      SUBROUTINE SHAP20
      COMMON/S10/DEXYZ(3,20),DH(6,9),P(9,9),DP(60,9)
      COMMON/SP/G,H,F,MS
      DIMENSION DE(4,20)
      EQUIVALENCE(DE(1),DP(1))
      GP1=1.+G
      GM1=1.-G
      HM1=1.-H
      HP1=1.+H
      FP1=1.+F
      FM1=1.-F
      G2PH=2.*G+H
      G2MH=2.*G-H
      H2PF=2.*H+F
      H2MF=2.*H-F
      F2PG=2.*F+G
      F2MG=2.*F-G
      H1=HM1*FP1
      H2=HP1*FP1
      H3=HM1*FM1
      H4=HP1*FM1
      G1=GM1*FP1
      G2=GP1*FP1
      G3=GM1*FM1
      G4=GP1*FM1
      G5=GM1*HM1
      G6=GM1*HP1
      G7=GP1*HP1
      G8=GP1*HM1
      DE(1,1)=0.125*H1*(G2PH+FM1)
      DE(1,2)=-0.25*HP1*H1
      DE(1,3)=0.125*H2*(G2MH+FM1)
      DE(1,4)=-0.5*G*H2
      DE(1,5)=0.125*(G2PH-FM1)*H2
      DE(1,6)=-DE(1,2)
      DE(1,7)=0.125*(G2MH-FM1)*H1
      DE(1,8)=-0.5*G*H1
      DE(1,9)=-0.25*FM1*H1
      DE(1,10)=-0.25*FM1*H2
      DE(1,11)=-DE(1,10)
      DE(1,12)=-DE(1,9)
      DE(1,13)=0.125*(G2PH+FP1)*H3
      DE(1,14)=-0.25*HP1*H3
      DE(1,15)=0.125*(G2MH+FP1)*H4
      DE(1,16)=-0.5*G*H4
      DE(1,17)=0.125*(G2PH-FP1)*H4
      DE(1,18)=-DE(1,14)
      DE(1,19)=0.125*(G2MH-FP1)*H3
      DE(1,20)=-0.5*G*H3
      DE(2,1)=0.125*(GP1+H2MF)*G1
      DE(2,2)=-0.5*H*G1
```

```
DE(2,3)=0.125*(H2MF-GP1)*G1
DE(2,4)=0.25*GP1*G1
DE(2,5)=0.125*(H2PF-GM1)*G2
DE(2,6)=-0.5*H*G2
DE(2,7)=0.125*(H2MF+GM1)*G2
DE(2,8)=-DE(2,4)
DE(2,9)=-0.25*FM1*G1
DE(2,10)=-DE(2,9)
DE(2,11)=0.25*FM1*G2
DE(2,12)=-DE(2,11)
DE(2,13)=0.125*(H2PF+GP1)*G3
DE(2,14)=-0.5*H*G3
DE(2,15)=0.125*(H2MF-GP1)*G3
DE(2,16)=0.25*GP1*G3
DE(2,17)=0.125*(H2MF-GM1)*G4
DE(2,18)=-0.5*H*G4
DE(2,19)=0.125*(H2PF+GM1)*G4
DE(2,20)=-DE(2,16)
DE(3,1)=0.125*(F2MG-HP1)*G5
DE(3,2)=0.25*HP1*G5
DE(3,3)=0.125*(F2MG-HM1)*G6
DE(3,4)=0.25*GP1*G6
DE(3,5)=0.125*(F2MG-HM1)*G7
DE(3,6)=0.25*HM1*G7
DE(3,7)=0.125*(F2MG-HP1)*G8
DE(3,8)=0.25*GP1*G5
DE(3,9)=-0.5*F*G5
DE(3,10)=-0.5*F*G6
DE(3,11)=-0.5*F*G7
DE(3,12)=-0.5*F*G8
DE(3,13)=0.125*(F2PG+HP1)*G5
DE(3,14)=-DE(3,2)
DE(3,15)=0.125*(F2PG+HM1)*G6
DE(3,16)=-DE(3,4)
DE(3,17)=0.125*(F2MG+HM1)*G7
DE(3,18)=-DE(3,6)
DE(3,19)=0.125*(F2MG+HP1)*G8
DE(3,20)=-DE(3,8)
DE(4,1)=0.125*FP1*(GM1+HM1+FP1-5.0)*G5
DE(4,2)=0.25*G5*H2
DE(4,3)=0.125*FP1*(GM1+HP1+FP1-5.0)*G6
DE(4,4)=0.25*G6*G2
DE(4,5)=0.125*FP1*(GP1+HP1+FP1-5.0)*G7
DE(4,6)=0.25*G8*H2
DE(4,7)=0.125*FP1*(GP1+HM1+FP1-5.0)*G8
DE(4,8)=0.25*G5*G2
DE(4,9)=0.25*G5*H1
DE(4,10)=0.25*G3*H2
DE(4,11)=0.25*G4*H2
DE(4,12)=0.25*G4*H1
DE(4,13)=0.125*FM1*(GM1+HM1+FM1-5.0)*G5
```



```
DE(4,14)=0.25*G5*H4
DE(4,15)=0.125*FM1*(GM1+HP1+FM1-5.0)*G6
DE(4,16)=0.25*G6*G4
DE(4,17)=0.125*FM1*(GP1+HP1+FM1-5.0)*G7
DE(4,18)=0.25*G7*H3
DE(4,19)=0.125*FM1*(GP1+HM1+FM1-5.0)*G8
DE(4,20)=0.25*G5*G4
RETURN
END


SUBROUTINE SHAP32
COMMON/S10/UEXYZ(3,20),DH(6,9),P(9,9),QP(60,9)
COMMON/SP/G,H,F,MS
DIMENSION DE(4,32)
EQUIVALENCE(DE(1),QP(1))
C1=1./64.
C2=9./64.
A=9.*(G*G+H*H+F*F)-19.
G1=1.+G
G2=1.-G
H1=1.+H
H2=1.-H
F1=1.+F
F2=1.-F
G3=G1*G2
G4=1.-3.*G
G5=1.+3.*G
H3=H1*H2
H4=1.-3.*H
H5=1.+3.*H
F3=F1*F2
F4=F.-3.*F
F5=1.+3.*F
DE(1,1)=C1*H2*F1*(-A+G2*18.*G)
DE(1,2)=-C2*H3*H4*F1
DE(1,3)=-C2*H3*H5*F1
DE(1,4)=C1*H1*F1*(-A+G2*18.*G)
DE(1,5)=C2*H1*F1*(-2.*G*G4-3.*G3)
DE(1,6)=C2*H1*F1*(-2.*G*G5+3.*G3)
DE(1,7)=C1*H1*F1*(A+G1*18.*G)
DE(1,8)=C2*H3*H5*F1
DE(1,9)=C2*H3*H4*F1
DE(1,10)=C1*H2*F1*(A+G1*18.*G)
DE(1,11)=C2*H2*F1*(-2.*G*G5+3.*G3)
DE(1,12)=C2*H2*F1*(-2.*G*G4-3.*G3)
DE(1,13)=-C2*F3*H5*H2
DE(1,14)=-C2*F3*H5*H1
DE(1,15)=C2*F3*F5*H1
DE(1,16)=C2*F3*F5*H2
```

```
DE(1,17)=-C2*F3*F4*H2
DE(1,18)=-C2*F3*F4*H1
DE(1,19)=C2*F3*F4*H3
DE(1,20)=C2*F3*F4*H2
DE(1,21)=C1*H2*F2*(-A+G2*18.*G)
DE(1,22)=-C2*H3*H4*F2
DE(1,23)=-C2*H3*H5*F2
DE(1,24)=C1*H1*F2*(-A+G2*18.*G)
DE(1,25)=C2*H1*F2*(-2.*G*G4-3.*G3)
DE(1,26)=C2*H1*F2*(-2.*G*G5+3.*G3)
DE(1,27)=C1*H1*F2*(A+G1*18.*G)
DE(1,28)=C2*H3*H5*F2
DE(1,29)=C2*H3*H4*F2
DE(1,30)=C1*H2*F2*(A+G1*18.*G)
DE(1,31)=C2*H2*F2*(-2.*G*G5+3.*G3)
DE(1,32)=C2*H2*F2*(-2.*G*G4-3.*G3)
DE(2,1)=C1*G2*F1*(-A+H2*18.*H)
DE(2,2)=C2*G2*F1*(-2.*H*H4-3.*H3)
DE(2,3)=C2*G2*F1*(-2.*H*H5+3.*H3)
DE(2,4)=C1*G2*F1*(A+H1*18.*H)
DE(2,5)=C2*G3*G4*F1
DE(2,6)=C2*G3*G5*F1
DE(2,7)=C1*G1*F1*(A+H1*18.*H)
DE(2,8)=C2*G1*F1*(-2.*H*H5+3.*H3)
DE(2,9)=C2*G1*F1*(-2.*H*H4-3.*H3)
DE(2,10)=C1*G1*F1*(-A+H2*18.*H)
DE(2,11)=-C2*G3*G5*F1
DF(2,12)=-C2*G3*G4*F1
DE(2,13)=-C2*F3*F5*G2
DE(2,14)=C2*F3*F5*G2
DE(2,15)=C2*F3*F5*G1
DE(2,16)=-C2*F3*F5*G1
DE(2,17)=-C2*F3*F4*G2
DE(2,18)=C2*F3*F4*G2
DE(2,19)=C2*F3*F4*G1
DE(2,20)=-C2*F3*F4*G1
DE(2,21)=C1*G2*F2*(-A+H2*18.*H)
DE(2,22)=C2*G2*F2*(-2.*H*H4-3.*H3)
DE(2,23)=C2*G2*F2*(-2.*H*H5+3.*H3)
DE(2,24)=C1*G2*F2*(A+H1*18.*H)
DE(2,25)=C2*G3*G4*F2
DE(2,26)=C2*G3*G5*F2
DE(2,27)=C1*G1*F2*(A+H1*18.*H)
DE(2,28)=C2*G1*F2*(-2.*H*H5+3.*H3)
DE(2,29)=C2*G1*F2*(-2.*H*H4-3.*H3)
DE(2,30)=C1*G1*F2*(-A+H2*18.*H)
DE(2,31)=-C2*G3*G5*F2
DE(2,32)=-C2*G3*G4*F2
DE(3,1)=C1*G2*H2*(A+F1*18.*F)
DE(3,2)=C2*H3*G2*H4
DE(3,3)=C2*H3*G2*H5
```



```
DE(3,4)=C1*G2*H1*(A+F1*18.*F)
DE(3,5)=C2*G3*G4*H1
DE(3,6)=C2*G3*G5*H1
DE(3,7)=C1*G1*H1*(A+F1*18.*F)
DE(3,8)=C2*H3*G1*H5
DE(3,9)=C2*H3*G1*H4
DE(3,10)=C1*G1*H2*(A+F1*18.*F)
DE(3,11)=C2*G3*G5*H2
DE(3,12)=C2*G3*G4*H2
DE(3,13)=C2*G2*H2*(-2.*F*F5+3.*F3)
DE(3,14)=C2*G2*H1*(-2.*F*F5+3.*F3)
DE(3,15)=C2*G1*H1*(-2.*F*F5+3.*F3)
DE(3,16)=C2*G1*H2*(-2.*F*F5+3.*F3)
DE(3,17)=C2*G2*H2*(-2.*F*F4-3.*F3)
DE(3,18)=C2*G2*H1*(-2.*F*F4-3.*F3)
DE(3,19)=C2*G1*H1*(-2.*F*F4-3.*F3)
DE(3,20)=C2*G1*H2*(-2.*F*F4-3.*F3)
DE(3,21)=C1*G2*H2*(-A+F2*18.*F)
DE(3,22)=-C2*H3*G2*H4
DE(3,23)=-C2*H3*G2*H5
DE(3,24)=C1*G2*H1*(-A+F2*18.*F)
DE(3,25)=-C2*G3*G4*H1
DE(3,26)=-C2*G3*G5*H1
DE(3,27)=C1*G1*H1*(-A+F2*18.*F)
DE(3,28)=-C2*H3*G1*H5
DE(3,29)=-C2*H3*G1*H4
DE(3,30)=C1*G1*H2*(-A+F2*18.*F)
DE(3,31)=-C2*G3*G5*H2
DE(3,32)=-C2*G3*G4*H2
DE(4,1)=C1*G2*H2*F1*A
DE(4,2)=C2*H3*G2*H4*F1
DE(4,3)=C2*H3*G2*H5*F1
DE(4,4)=C1*G2*H1*F1*A
DE(4,5)=C2*G3*G4*H1*F1
DE(4,6)=C2*G3*G5*H1*F1
DE(4,7)=C1*G1*H1*F1*A
DE(4,8)=C2*H3*G1*H5*F1
DE(4,9)=C2*H3*G1*H4*F1
DE(4,10)=C1*G1*H2*F1*A
DE(4,11)=C2*G3*G5*H2*F1
DE(4,12)=C2*G3*G4*H2*F1
DE(4,13)=C2*F3*F5*G2*H2
DE(4,14)=C2*F3*F5*G2*H1
DE(4,15)=C2*F3*F5*G1*H1
DE(4,16)=C2*F3*F5*G1*H2
DE(4,17)=C2*F3*F4*G2*H2
DE(4,18)=C2*F3*F4*G2*H1
DE(4,19)=C2*F3*F4*G1*H1
DE(4,20)=C2*F3*F4*G1*H2
DE(4,21)=C1*G2*H2*F2*A
DE(4,22)=C2*H3*G2*H4*F2
```

```
      DE(4,23)=C2*H3*G2*H5*F2
      DE(4,24)=C1*G2*H1*F2*A
      DE(4,25)=C2*G3*G4*H1*F2
      DE(4,26)=C2*G3*G5*H1*F2
      DE(4,27)=C1*G1*H1*F2*A
      DE(4,28)=C2*H3*G1*H5*F2
      DE(4,29)=C2*H3*G1*H4*F2
      DE(4,30)=C1*G1*H2*F2*A
      DE(4,31)=C2*G3*G5*H2*F2
      DE(4,32)=C2*G3*G4*H2*F2
      RETURN
      END


      SUBROUTINE STROUT
      COMMON    PRENIC(1, 24),UNKNIC(1, 60),KNONIC(2,24),UNKHS(1,24),
     1KNOKHS(1, 60),ELPOSN(2,60),KNOMAT(1, 300),UNKMAT(1,1830),
     2UNCLE( 60,24)
      COMMON/C1/ NUMKVA,NKNVA,NOSTR,NCELNO,NCELN1,NTOTAL,NPRDEF,NT,
     1NELEM,NFREE,NNELM,NODTOT,N
      DIMENSION STSS(44,6)
      EQUIVALENCE(STSS(1),UNKMAT(1))
      WRITE(6,3)
    3 FORMAT (1H1 ////   37X, *THE RESULTING NODAL STRESSES IN THE MAIN
     1PROBLEM SYSTEM*// 6X, *NODE*, 9X, *XX*, 18X, *YY*, 18X, *ZZ*, 18X,
     2*YZ*, 18X, *ZX*, 18X, *XY*/)
      DO 1 I=1,NODTOT
      IF (MOD(I-1,50).EQ.0 .AND. I.NE.1)  WRITE (6, 4)
    4 FORMAT (1H1 /////)
1     WRITE(6,2) I, (STSS(I,K), K=1,6)
```

APPENDIX 4

LISTING OF DRAW CODE

```
      PROGRAM DRAW (DRDAT,TAPE1=DRDAT,OUTPUT,TAPE2=OUTPUT,TAPE62)
C
      REAL LEN
      INTEGER TITLE, PRENIC
      COMMON L(105,20), X(715), Y(715), Z(715), XP(715), YP(715),
     1       TF(3,3), PRENIC(600), TITLE(8)
C
      READ(1,6) TITLE
    6 FORMAT(8A10)
      READ(1,1) NELEM, NODTOT, NPRDEF, NNELM
    1 FORMAT(4I5)
      IF (NNELM.EQ.32) GO TO 400
      DO 2 K=1,NELEM
    2 READ(1,3) I, (L(I,J), J=1,20)
      GO TO 410
  400 DO 420 K=1,NELEM
  420 READ(1,421) I, (L(I,J), J=1,32)
  421 FORMAT(33I4)
  410 READ(1,4) (N, X(I), Y(I), Z(I), I=1,NODTOT)
    3 FORMAT(2I4)
    4 FORMAT(I10,3F10.4)
      READ(1,5) TETAX, TETAZ, DISTOR
    5 FORMAT(3F12.4)
      READ(1,180) (PRENIC(I), I=1,NPRDEF)
  180 FORMAT(8I10)
      PI=2.0*ASIN(1.0)
      TETAX=TETAX*PI/180.0
      TETAZ=TETAZ*PI/180.0
      TF(1,1)=COS(TETAX)*COS(TETAZ)
      TF(1,2)=SIN(TETAX)*COS(TETAZ)
      TF(1,3)=SIN(TETAZ)
      TF(2,1)=-SIN(TETAX)
      TF(2,2)=COS(TETAX)
      TF(2,3)=0.0
      TF(3,1)=-SIN(TETAZ)*COS(TETAX)
      TF(3,2)=-SIN(TETAZ)*SIN(TETAX)
      TF(3,3)=COS(TETAZ)
      EMAX=0.0
      RMAX=0.0
      EMAY=0.0
      RMAY=0.0
      DO 10 I=1,NODTOT
      XP(I)=X(I)*TF(2,1)*DISTOR+Y(I)*TF(2,2)
      YP(I)=X(I)*TF(3,1)*DISTOR+Y(I)*TF(3,2)+Z(I)*TF(3,3)
      IF(XP(I).GT.RMAX) RMAX=XP(I)
      IF (XP(I).LT.EMAX) EMAX=XP(I)
      IF (YP(I).GT.RMAY) RMAY=YP(I)
      IF (YP(I).LT.EMAY) EMAY=YP(I)
   10 CONTINUE
      TOTALX=RMAX-EMAX
      TOTALY=RMAY-EMAY
```



```
      FACX=13.0/TOTALX
      FACY=13.0/TOTALY
      FAC=FACX
      IF (FACY.LT.FACX) FAC=FACY
      X0=3.0+FAC*ABS(EMAX)
      Y0=2.0+FAC*ABS(EMAY)
      CALL START(2)
      CALL SYMBOL (0.,0.,.7,TITLE,0.,80)
      CALL PLOT (16.,2.5,3)
C
C     DRAWING ELEMENT BY ELEMENT.
      CALL INTENSE(15)
      X1=16.0+TF(2,1)*DISTOR*FAC
      Y1=2.5+TF(3,1)*DISTOR*FAC
      CALL SYMBOL (X1, Y1, 0.35, 11, 0.0, -2)
      X1=X1+0.35*FAC
      Y1=Y1-0.35*FAC
      CALL SYMBOL (X1, Y1, 0.35, 51, 0.0, -1)
      CALL PLOT (16., 2.5, 3)
      X2=16.0+TF(2,2)*FAC
      Y2=2.5+TF(3,2)*FAC
      CALL SYMBOL (X2, Y2, 0.35, 11, 0.0, -2)
      Y2=Y2+0.35*FAC
      CALL SYMBOL (X2, Y2, 0.35, 52, 0.0, -1)
      CALL PLOT (16., 2.5, 3)
      X3=16.0
      Y3=2.5+TF(3,3)*FAC
      CALL SYMBOL (X3, Y3, 0.35, 11, 0.0, -2)
      X3=16.0+0.35
      CALL SYMBOL (X3, Y3, 0.35, 53, 0.0, -1)
      CALL PLOT (0., 0., 3)
      CALL PLOT (X0, Y0, -3)
      CALL FACTOR (FAC)
      LIMKB=9
      IF (NNELM.EQ.32) LIMKB=13
      DO 100 N=1,NELEM
      INIAL=L(N,1)
      CALL PLOT (XP(INIAL), YP(INIAL), 3)
      DO 101 KB=1,LIMKB-1
      IND=KB+1
      IF (KB.EQ.LIMKB-1) IND=1
      K=L(N,IND)
  101 CALL PLOT (XP(K), YP(K), 2)
      IND=NNELM-LIMKB+2
      INIAL=L(N,IND)
      CALL PLOT (XP(INIAL), YP(INIAL), 3)
      DO 102 KB=1,LIMKB-1
      IND=NNELM-LIMKB+KB+2
      IF (KB.EQ.LIMKB-1) IND=NNELM-LIMKB+2
      K=L(N,IND)
  102 CALL PLOT (XP(K), YP(K), 2)
```

```
      DO 103 KL=1,4
      K1=(KL-1)*(NNELM/32+2)+1
      K=L(N,K1)
      CALL PLOT (XP(K), YP(K), 3)
      K=L(N,KL+LINKN-1)
      CALL PLOT (XP(K), YP(K), 2)
      IF (NNELM.LE.20) GO TO 105
      K=L(N,KL+LINKN-1+4)
      CALL PLOT (XP(K), YP(K), 2)
  105 IND=NNELM-LINKN*K1+1
      K=L(N,IND)
  103 CALL PLOT (XP(K), YP(K), 2)
  100 CONTINUE
      CALL INTENSE (30)
      DO 110 I=1,NNDTOT
      CALL SYMBOL (XP(I), YP(I), 0.015, 1, 0.0, -1)
  110 CONTINUE
      ICODE=2
      T=1.5
      IF (ICODE.EQ.0) ICODE=1
      CALL INTENSE (15)
      Q=0.05*T*FLOAT(3-2*ICODE)
      DO 200 N=1,NPROBF
      NO=PRENIC(N)/100
      IDI=PRENIC(N)-100*NO
      CALL PLOT (XP(NO), YP(NO), 3)
      IF (IDI-2) 300, 310, 320
  300 XX=XP(NO)+Q*TF(2,1)*DISTOR
      YY=YP(NO)+Q*TF(3,1)*DISTOR
      GO TO 250
  310 XX=XP(NO)+Q*TF(2,2)
      YY=YP(NO)+Q*TF(3,2)
      GO TO 250
  320 XX=XP(NO)
      YY=YP(NO)-0.1*T*TF(3,3)
  250 CALL SYMBOL (XX, YY, 0.015, 1, 0.0, -2)
  200 CONTINUE
      CALL ENPLOT
      STOP
      END
```

APPENDIX 5

REFERENCES

1. Gilman, J.D. and Rashid, Y.R.; "Three Dimensional Analysis of Reactor Pressure Vessel Nozzles", Proc. 1st. Int. Conf. Struct. Mech. in React. Techn., Berlin, 1971, paper G2/6.

2. Hellen, T.K. and Dowling, A.R.; "Three Dimensional Crack Analysis Applied to an LWB Nozzle-Cylinder Intersection". CEGB rep. RD/B/N3042, July 1974.

3. Broekhoven, M.J.G.; "Theoretical and Experimental Analysis of Crack Extension at Nozzle Junctions". Cracks and Fracture, ASTM STP 601, ASME, 1976, p.535.

4. Schmit, W., Bartholome, G., Grostad, A. and Miksch, M.; "Calculation of Stress Intensity Factors of Cracks in Nozzles". Int. J. of Fracture, Vol.12, No.3, June 1976 p.381.

5. Reynen, J.; "Analysis of Cracked Pressure Vessel Nozzles by Finite Elements". Proc. 3rd Int. Conf. Struct. Mech. in React. Techn., 1975, paper G5/1.

6. Pressure Vessel and Piping Design, Collected Papers. 1927 - 1959, Vol.1, New York, ASME, 1960.

7. Lancaster, V.F.; "A Comparison of United States, European and British Commonwealth Codes for the Construction of Welded Boilers and Pressure Vessels." ASME paper 61-SA-40 presented at ASME Summer Meeting, Los Angeles, 1961.

8. Shank, M.E.; "A Critical Survey of Brittle Fracture in Carbon Plate Steel Structures other than Ships." Pub. Welding Research Council of the Engineering Foundations, New York, 1954.

9. Tiffany, C.F.; "Aerospace Pressure Vessels." Fracture Mechanics of Aircraft Structures, AGARDOgraph No. 176, Jan 1974, Paper VC-5, p.294.

10. Boyd, G.M.; "Brittle Fracture in Steel Structures". Pub. Butterworth, London 1970.

11. Pellini and Puzak, J. Eng. for Power ASME,Oct. 1964.

12. Pressure Vessel and Piping Design and Analysis. Vol. 1 - Analysis. ASME, New York 1972.

13. Proc. 2nd Int. Conf. on Pressure Vessel Technology, Part 1 - Design and Analysis, ASME, 1973.

14. Proc. 3rd Int. Conf. on Struct. Mech. in React. Techn. London 1 - 5 Sept. 1975.

15. Timoshenko, S.P. and Goodier, G.N.; "Theory of Elasticity". pub. McGraw-Hill, Kogakusha, Tokyo, 1970.

16. Inglis, C.E.; "Stresses in a Plate Due to the Prescence of Cracks and Sharp Corners". Trans. Inst. Naval Architects, Vol. 60, 1913, p.219.

17. Muskhelishvilli, N.I.; "Some Basic Problems of the Mathematical Theory of Elasticity." Noordhoff, Groningen, 1953.

18. Griffith, A.A.; "The Phenomena of Rupture and Flaw in Solids". Phil. Trans. Roy. Soc., 1921, A221, p.163.

19. Irwin, G.R.;"Relation of Stresses Near a Crack to the Crack Extension Force". 9th Int. Congr. Appl. Mech., Brussels, 1957.

20. Orowan, E.; "Fracture and Strength of Solids". Rep. Prog. Phys., 1949, Vol. 12, p.185.

21. Brown, W.F. Ed. "Review of Developments in Plain Strain Fracture Toughness Testing". ASTM STP 463, 1970.

22. Irwin, G.R.; "Analysis of Stresses and Strains near the End of a Crack Transversing a Plate". J. App. Mech., Vol. 24, 1957, p.361.

23. Irwin, G.R.; "Fracture". Hanbuck der Physik, Vol. VI, Springer, Berlin, 1958.

24. Westergaard, H.M.; "Bearing Pressures and Cracks". J. Appl. Mech., 1939, Vol. 61, p.A49.

25. Paris, P.C. and Sih, G.C.; "Stress Analysis of Cracks" in "Fracture Toughness Testing and its Applications" ASTM STP 381, 1965, p.31.

26. Knott, J.F.; "Fundamentals of Fracture Mechanics". Pub. Butterworths, London, 1973.

27. Cartwright, D.J. and Rooke, D.P.; "Evaluation of Stress Intensity Factors". J. Strain Analysis, 1975, Vol 10 (4), p.217.

28. Sih, G.C.; "Mechanics of Fracture; Methods of Analysis and Solution of Crack Problems". Noordhoff, Leyden, 1973.

29. Rooke, D.P. and Cartwright, D.J.; "A Method of Compounding Stress Intensity Factors for Complex Configurations". Technical Rep. 75063, RAE, April 1975.

30. Rooke, D.P. and Cartwright, D.J.; "Compendium of Stress Intensity Factors". Her Majesty's Stationery Officer, London, 1976.

31. Hartranft, R.J. and Sih, G.C.; "Alternating Method Applied to the Edge and Surface Crack Problems". paper in Ref.(28), p.179.

32. Smith, F.W., Kobayashi, A.S. and Emery, A.F.; "Stress Intensity Factors for Semi-Circular Cracks, Part 2 - Semi Infinite Solid". J. Appl. Mech., Vol. 34, 1976, p. 947.

33. Benthem, J.P.; "Three-Dimensional State of Stress at the Vertex of a Quarter-Infinite Crack in a Half-Space". Rep. No. 563, Laboratory of Eng. Mech.,Delft. Sept. 1975.

34. Smith, F.W. and Alavi, M.J.; "Stress Intensity Factors for a Part-Circular Surface Flaw". Proc. 1st Int. Conf. on Pressure Vessel Technology, Delft, 1968.

35. Swedlow, J.L. and Ritter, M.A.; "Toward Assessing the Effects of Crack Front Curvature (CFC)". ASTM STP 513, 1972, p.79.

36. Sneddon, I.N.; "The Distribution of Stress in the Neighbourhood of a Crack in an Elastic Solid". Proc. of the Royal Soc., London, Series A, 187, 1946, p.229.

37. Green, A.E. and Sneddon, I.N.; "The Stress Distribution in the Neighbourhood of a Flat Eliptical Crack in an Elastic Solid". Proc. of the Cambridge Phil. Soc., Vol. 46, 1956.

38. Irwin, G.R.; "The Crack Extension Force for a Part-Through Crack in a Plate". J. Appl. Mech.,Dec. 1962 p.651.

39. Kobayashi, A.S., Zii, M. and Hall, L.R.; "Approximate Stress Intensity Factor for an Embedded Eliptical Crack near to Parallel Free Surfaces". Int. J. Fracture Mech., Vol. 1, 1965, p.81.

40. Broech, D.; "Fail-Safe Design Procedures". Fracture Mechanics of Aircraft Structures, AGARDograph No. 176, Jan. 1974, p.121.

41. Kobayashi, A.S., Enetanya, A.N., Shah, R.C.; "Stress Intensity Factors for Eliptical Cracks". Prospects of Fracture Mechanics (Proceedings of an Int. Conf.) ed. G.C. Sih, H.C. van Elst and D. Broeck. Pub. by Noordhoff International Publishing, Leyden, 1974, p.525.

42. "Experimental Techniques in Fracture Mechanics" SESA Monograph No. 1, 1973.

43. Smith, F.W., Emery, A.F. and Kobayashi, A.S.; "Stress Intensity Factors for Semi-Circular Cracks". J. Appl. Mech., Vol. 34, 1967, p.953.

44. Thresher, R.W. and Smith, F.W.; "Stress Intensity Factors for a Surface Crack in a Finite Solid". J.Appl. Mech., Vol. 39, 1972, p.195.

45. Shah, R.C. and Kobayashi, A.S.; "Stress Intensity Factor for an Eliptical Crack Approaching the Surface of a Plate in Bending". ASTM STP 513, 1972, p.3.

46. Zienkiewicz, O.C.; "The Finite Element Method in Engineering Science". McGraw-Hill, London,2nd Ed. 1971.

47. Desai, C.S. and Abel, J.F.; "Introduction to the Finite Element Method". Van Nostrand Rheinhold Co., New York.

48. Fenner, R.T.; "Finite Element Methods for Engineers". Macmillan, London, 1975.

49. Natarajan, R.; "Finite Element Analysis of Pipe Bends Using Doubly Curved Shall Elements". Ph.D. thesis, Imperial College, University of London, April, 1971.

50. Alujevic, A.; "The Analysis of Stresses in Irradiated Nuclear Reactor Fuel Elements Using Three-Dimensional Isoparametric Finite Elements". Ph.D. thesis, Imperial College, University of London, March 1973.

51. Conte, S.D.; "Elementary Numerical Analysis, An Algorithm Approach". McGraw-Hill, New York, 1965.

52. Ford, H.; "Advanced Mechanics of Materials". Longmans, London, 1969.

53. Irons, B.M.; "Economical Computer Techniques for Numerically Integrated Finite Elements". Int. J. Num. Meth. in Eng., Vol.1, 1969.

54. Irons, B.M.; "A Frontal Solution Program for Finite Element Analysis". Int. J. Num. Meth. in Eng., Vol.2, 1970.

55. McCracken, D.D.; "A Guide to FORTRAN IV Programming". John Willey and Sons, Inc., New York, 1965.

56. Priest, A.H.; "Experimental Methods for Fracture Toughness Measurements". J. Strain Analysis, Vol.10 (4), 1975, p.225.

57. Sih, G.C. And Hartranft, R.J.; "Growth Characteristics of Surface Flaws in Pressure Vessels". Proc. 3rd Int. Conf. Struct. Mech. in Nucl. React. Techn., London Sept. 1975, paper G4/2.

58. Sih, G.C. and Cha, B.C.K.; "A Fracture Criterium for Three Dimensional Crack Problems". J. Eng. Fract. Mech., Vol. 6, 1974, p.698.

59. Broekhoven, K.J. and Ruijtenbeek, M.G.; " Fatigue Crack Extension in Nozzle Junctions: Comparison of Analytical Approximations with Experimental Data". 3rd Int. Conf. in Struct. Mech. in Nucl. React. Techn., London Sept, 1975. paper G4/7.

60. Sommer, E., Hodulak, L. and Kordish, H; "Growth Characteristcs in Part-Through Cracks in Plates and Tubes". Euromech-Colloquium No 77, Paris, Sept. 1976, paper submitted to Int. Joint Pressure Vessels and Piping and Petroleum Mech. Eng. Conf., ASME, Mexico City, Sept. 1976.

61. Moura Branco, C.A.; "A Fracture Mechanics Approach to Environmental and Elastic-Plastic Fatigue Crack Propagation". Ph.D. Thesis, Imperial College, University of London June 1976.

62. Wilson, W.K.; "Some Crack Tip Finite Elements for Plane Elasticity". ASTM STP 513, 1972, p.90.

63. Hilton, P.D. and Sih, G.C.; "Applications of the Finite Element Method to the Calcualtions of Stress Intensity Factors". Mechanics of Fracture 1, Methods of Analysis and Solutions of Crack Problems. Ed. (G. Sih), Vol.1, Noordhoff, Int. Pub., 1973.

64. Williams, M.L.; "On the Stress Distribution at the Base of a Stationary Crack". J. Appl. Mech., Vol. 24, 1957, p.109.

65. Rice, J.R. and Tracey, D.M.; "Computational Fracture Mechanics". Numerical and Computer Methods in Structural Mechanics, Academic Press, New York, 1973.

66. Jerram, K. and Hellen, T.K.; "Finite Element Techniques in Fracture Mechanics". Proc. Int. Conf. Welding Research related to Power Plant, Southampton, 1972, paper 14, p.165.

67. Atluri, S.N.,Kobayashi, A.S. and Nakagaki, M.; "Fracture Mechanics Application of an Assumed Displacement Hybrid Finite Element Procedure". AIAA Journal, Vol. 13, No. 6, 1975, p.734.

68. Blackburn, W.S.; "Calculation of Stress Intensity Factors at Crack Tips using special Finite Elements". Conf. Maths. of Finite Elements and Appls., Brunel University, April 1972.

69. Tracey, D.M.; "Finite Elements for Three Dimensional Elastic Crack Analysis". Nuclear Eng. and Design, Vol. 26, 1974, p.282.

70. Chan, S.K., Tuba, I.S. and Wilson, W.K.; "On the Finite Element Method in Fracture Mechanics". Engng, Fracture Mechanics, Vol. 2, 1970, p.1.

71. Ewing, P.D., Swedlow, J.L. and Williams, J.G.; "Further Results on the Angled Crack Problem". Int. J. Fracture, Vol. 12, No.1., 1976.

72. Leevers, P.; Unpublished results, Imperial College, 1976.

73. Dixon, J.R. and Strannigan, J.S.; "Determination of Strain Energy Release Rates and Stress Intensity Factors by the Finite Element Method". J. Strain Analysis, Vol. 7, No. 2, 1972.

74. Discussion of paper in Ref.(34), Part III, Discussion of Papers presented in the 1st Int. Conf. On Pressure Vessel Technology, ASME, 1970, New York.

75. Broekhoven, M.J.G. and Spaas, H.A.C.M.; "Application of the Finite Element Technique to a Complex 3D Elastic Problem (nozzle junction with cracks)". Rep. MMPP-101, Delf University of Technology, Delft, The Netherlands, August 1974.

76. Buekner, H.F., Trans, of ASME, Vol. 80, 1958, p.1225.

77. Rice, J.R.; "A Path Independent Integral and the Approximate Analysis of Strain Concentrations by Notches and Cracks". J. Appl. Mech., Vol. 35, 1968, p.379.

78. Neale, B.K.; "Finite Element Crack Analysis Using the J-Integral Method". CEGB report RD/B/N2785, Sept. 1973.

79. Parks, D.M.; "A Stiffness Derivative Finite Element Technique for Determination of Crack Tip Stress Intensity Factors". Int. J. of Fracture, Vol.10, 1974 p.487

80. Hellen, T.K.; "On the Method of Virtual Crack Extensions". Int. J. Num. Meth. in Engng., Vol.9, 1975, p.187.

81. Henshell R.D. and Shaw, K.G.;"Crack Tip Finite Elements Are Unnecessary". Int. J. Num. Meth. in Engng., Vol.9, 1975, p.495

82. ICCC Bulletin, ICST 6.3/7 November 1974, Imperial College.

83. ICCC Bulletin, ICST 4.6/1.6, June 1971, Imperial College.

84. Levy, N., Marcal, P.V. and Rice, J.R.; "Progress in Three Dimensional Elastic Plastic Stress Analysis for Fracture Mechanics". Nuclear Eng. and Design, Vol.17, 1971, p.64.

85. Brown, W.F. and Srawley, J.E.; "Plane Strain Crack Toughness Testing of High Strength Metallic Materials". AST STP 410, 1966.

86. Yamamoto, Y. and Sumi, Y.; "Stress Intensity Factors for Three Dimensional Cracks". To be presented at the 14th Int. Congress in Theoretical and Applied Mechanics, Delft, 1976.

87. Neal, B.K. "The Influence of Crack Shape on Fracture Toughness Testing". Int. J. of Fracture, Vol. 12, 1976, p.499.

88. Johnson, R.A. and Radon, J.C.; "Fracture Energy and Crack Tunnelling". J. of Testing and Evaluation, Vol. 4, No. 3, May 1976, p.209.

89. Tracey, D.M.; "3-D Elastic Singularity Element for Evaluation of K Along an Arbitrary Crack Front". Int. J. of Fracture, Vol.9, 1973, p.340.

90. Smith, F.W. and Alavi, M.J.; "Stress Intensity Factors for a Part Circular Surface Flaw". Proc. 1st Int. Conf. on Pressure Vessel Technology, Delft, 1968.

91. Shannon, R.W.E.; "Stress Intensity Factors for Thick Walled Cylinders". Int. J. Pressure Vessels and Piping Vol. 2, 1974.

92. Underwood, J.H., "Stress Intensity Factors for Internally Pressurized Thick Walled Cylinders". Proc. of the 1971 National Symposium on Fracture Mechanics, Part I, ASTM STP 513, 1972, p.59.

93. Bowie, O.L. and Freese, C.E.; "Elastic Analysis for a Radial Crack in a Circular Ring". Engng. Fracture Mechanics, Vol. 4, 1972, p.315.

94. Rice, U.R. and Levi, N.; "The Part-Through Surface Crack in an Elastic Plate". Tec. Rep. NASA NGL 40-002-080/3, 1970.

95. Nichols, R.W.; "Steel's Contribution to Nuclear Power: It's Problems and Promise". Metals and Materials, The J. of the Metals Society, April 1976, p.24.

96. "Protection Against Noductile Failure". Section III, Appendix G, ASME Code, 1974.

97. Burdekin, F.M. and Dawes, M.G.; "Practical Use of Linear Elastic and Yielding Fracture Mechanics with Particular Reference to Pressure Vessels". Paper C5/71 in Ref. (99), p.56.

98. Mager, T.R. and Riccardella, P.C.; "Use of LEFM in Safety Analysis of Heavy Section Nuclear Reactor Pressure Vessels". Paper C8/71 in Ref.(99), p.56.

99. "Practical Application of Fracture Mechanics to Pressure Vessel Technology". Pub. by I. Mech. Eng., 1971.

100. Cha, R.C.; "Stress Intensity Factors for Through and Part-Through Cracks Originating at Fastener Holes". Mechanics of Crack Growth, ASTM STP 590, 1976, p.429.

101. Kobayashi, A.S. and Enetanya, A.N.; Mechanics of Crack Growth, ASTM STP 590, 1976, p.477.

102. Bartholome, G. and Dorner, H.; "Safety Evaluation of Nuclear Reactor Pressure Vessels for Pressurized Water Reactors". Paper C51/71 in Ref.(99), p.175.

103. Slater, D.J.F.; "A User's Manual for FLAPS a Finite Elements Computer Program for an Elastic Body of Revolution". Internal publication, Imperial College, November 1971.

104. Pereira, M.S.; "Remarks on Iterative or Elimination Methods of Solution: The Frontal Method". Computation Methods in Fracture Mechanics. Welding Institute/ Imperial College Post Experience Course June 1976.

105. Carre, B.A.; "The Determination of the Optimum Accelerating Factor for Successive Over-Relaxation". Computer Journal, Vol.4, 1961, p.73.

106. Cotterell, B.; "Notes on the Paths and Stability of Cracks". Int. J. Fracture Mechanics, Vol.2, No. 3, 1966, p.526.

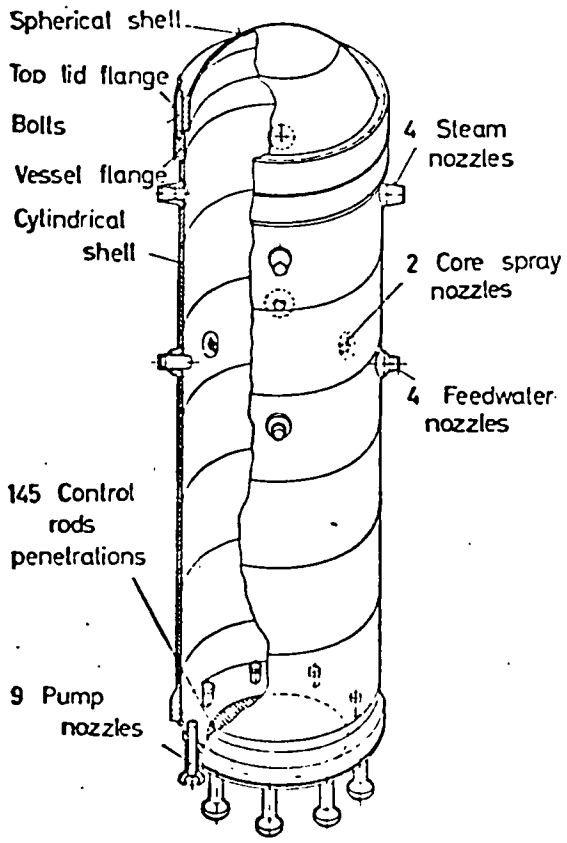

(a) Prespective view of Pressure Vessel

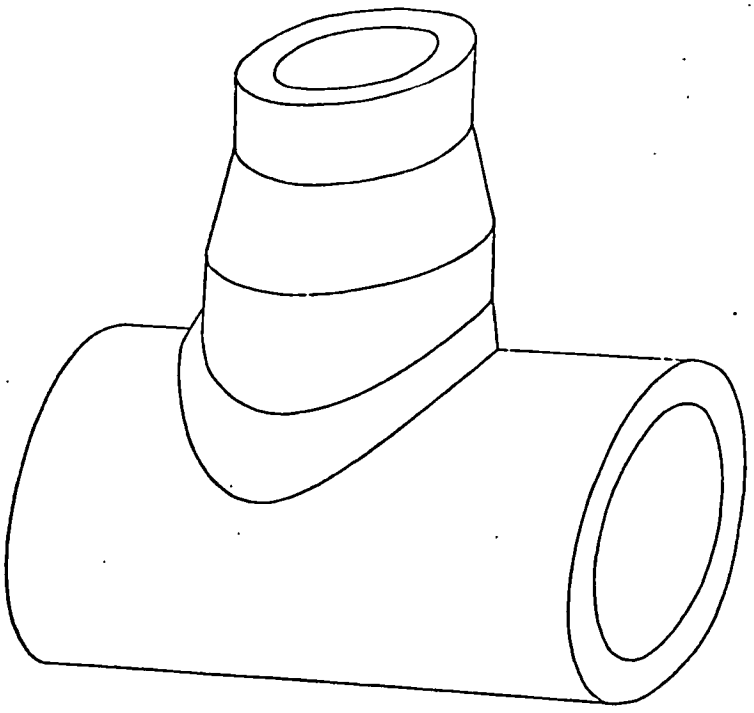

(b) Tee Junction of thick walled cylinders

Figure 1.1

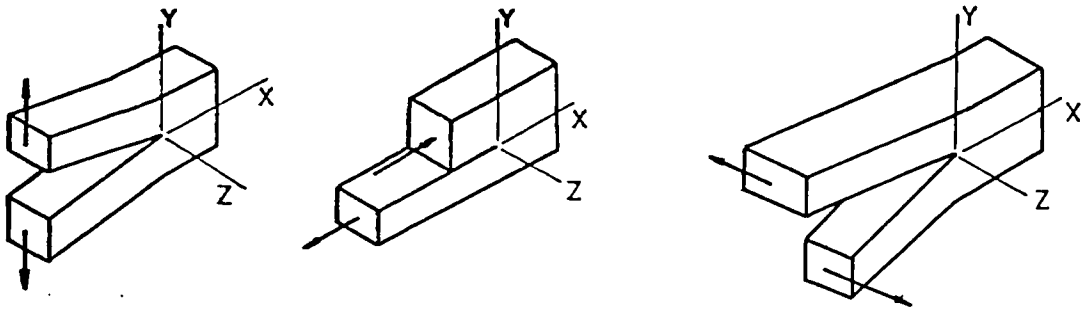

Fig. 1.2 Basic modes of crack surface displacements

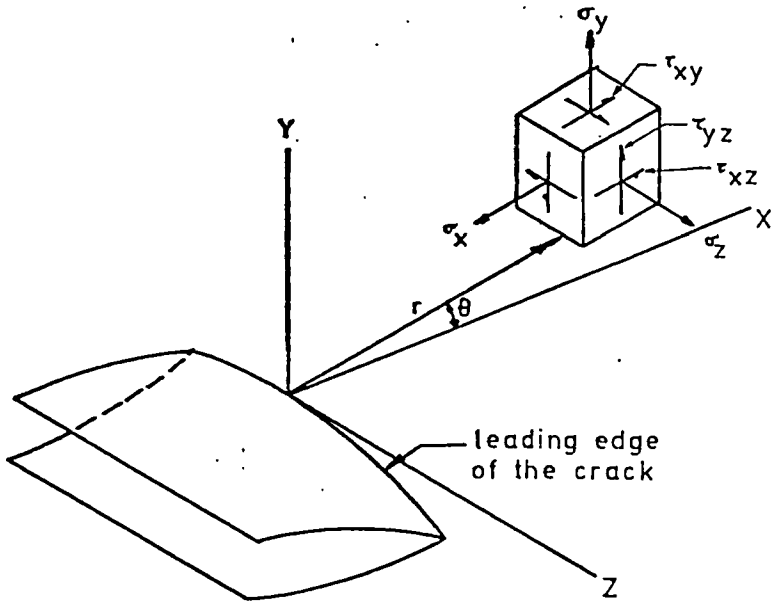

Fig. 1.3 Coordinates measured from the leading edge of a crack and the stress components in the crack tip stress field

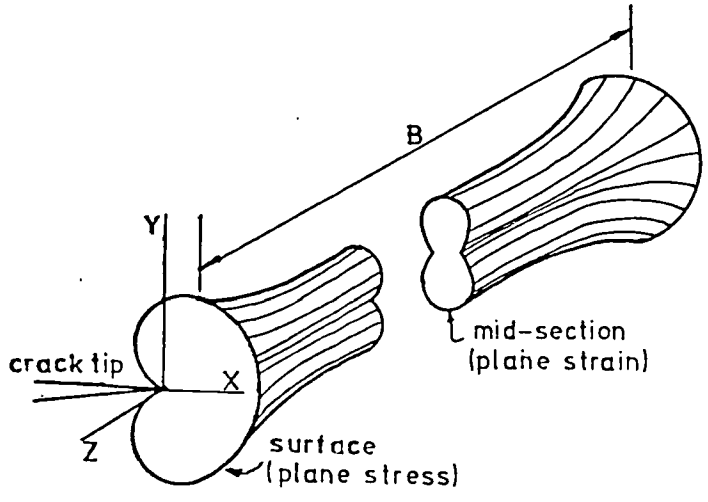

Fig. 1.4 Plastic zone ahead of a crack in a plate of thickness B

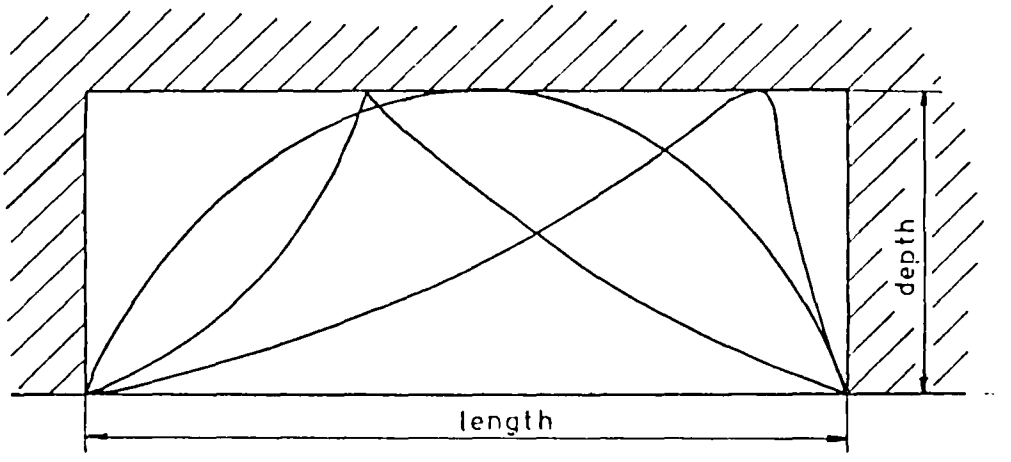

Fig. 1.5 Various crack configurations having the same length and depth

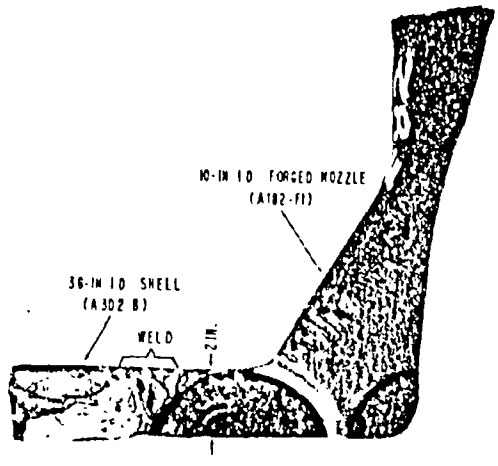

Fig. 1.6 Section of a nozzle showing two fatigue cracks

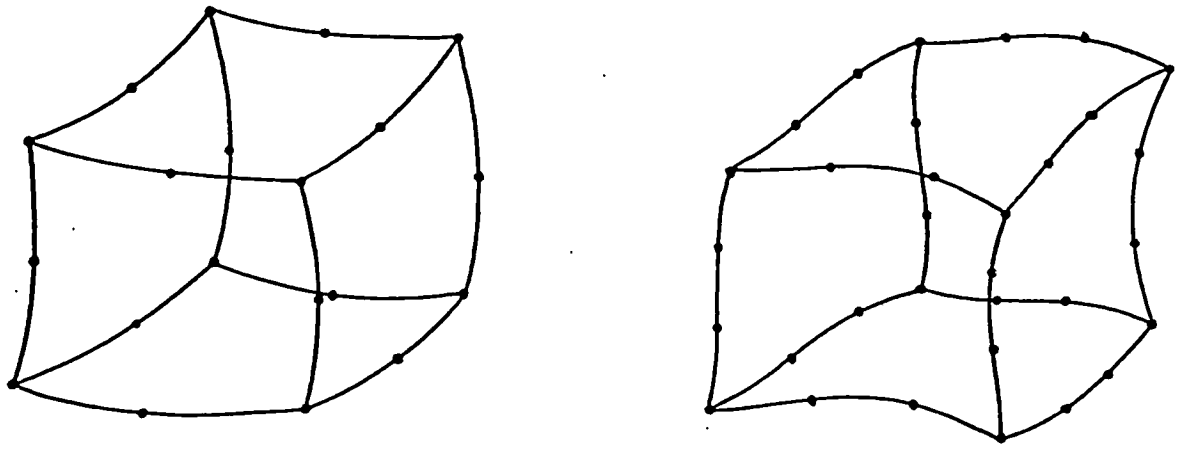

(a) second order (quadratic)
20 nodes

(b) third order (cubic)
32 nodes

Fig. 2.1 3D hexahedron finite elements

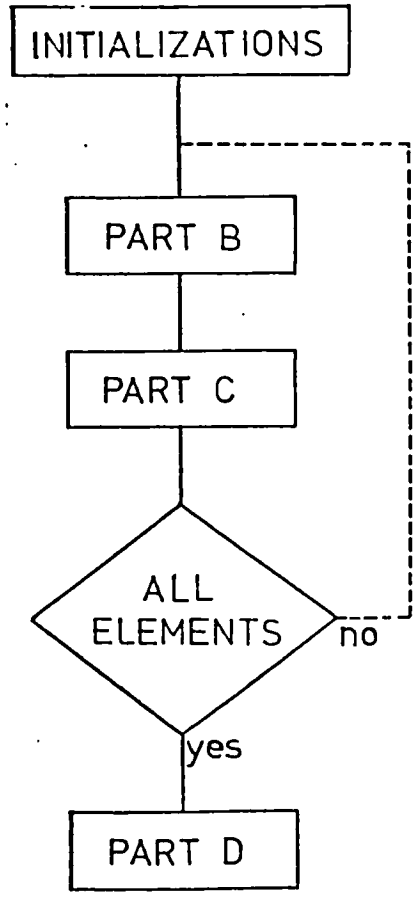

Fig. 2.2 Primary Flow-Chart of DIM3B code

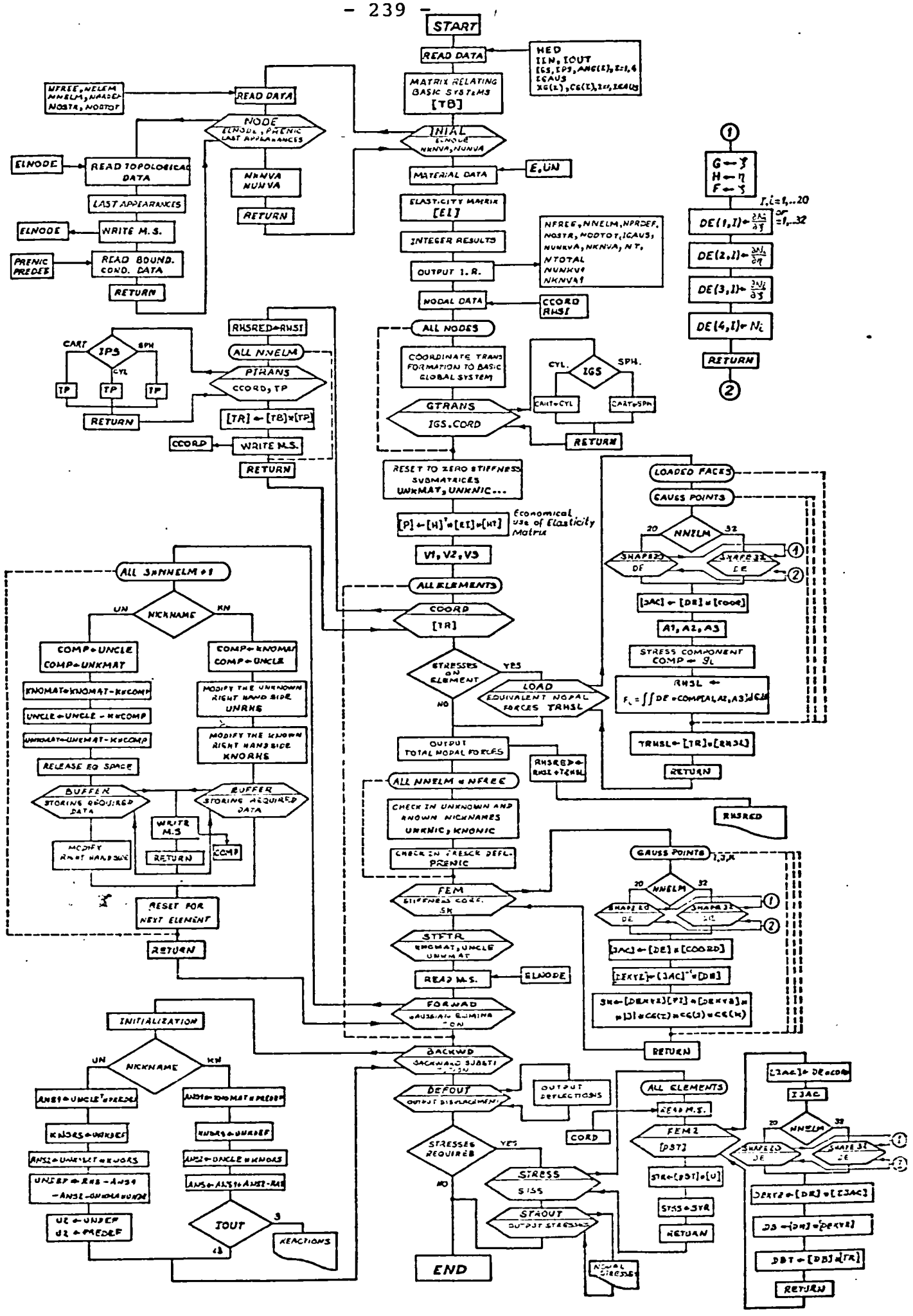

Fig. 2.3 Flow-Chart of DIM3B code

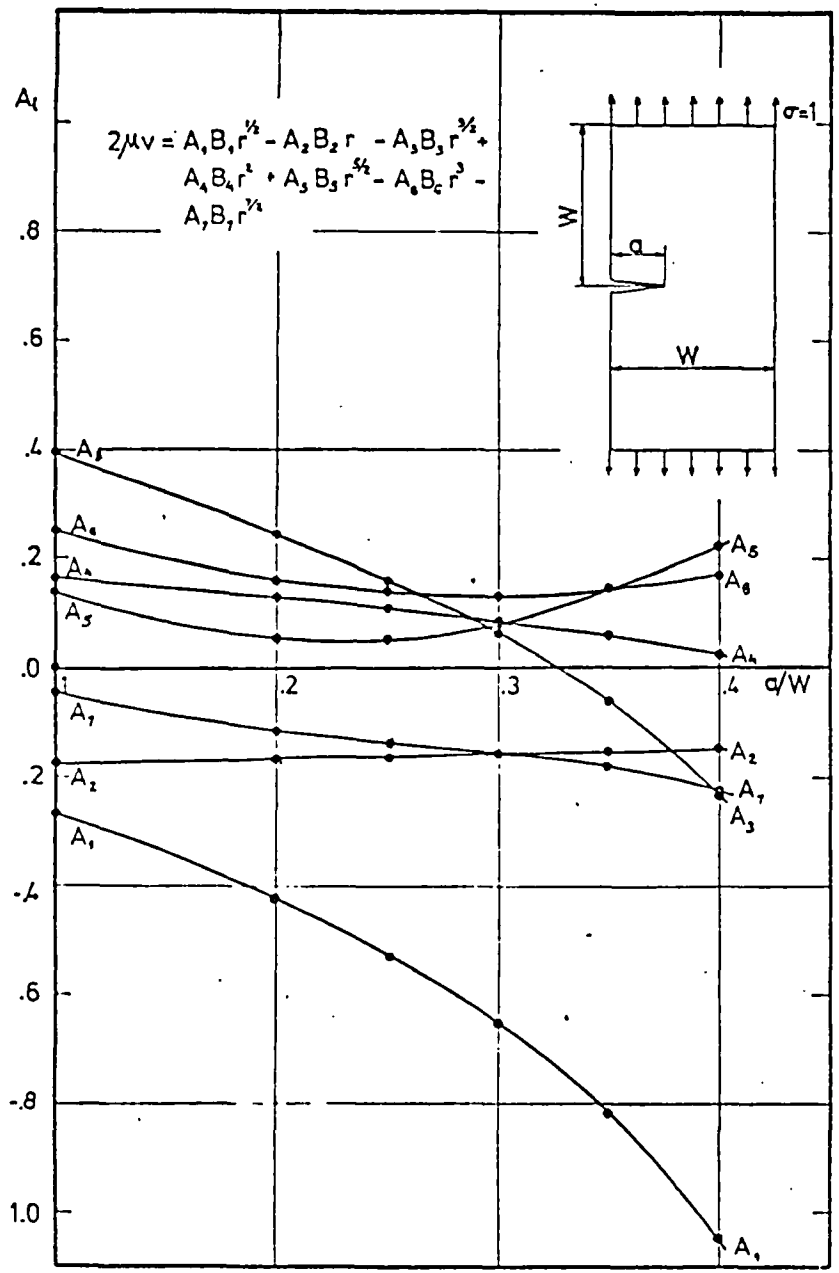

(a) Variation of the coefficients A_i of the Williams series solution

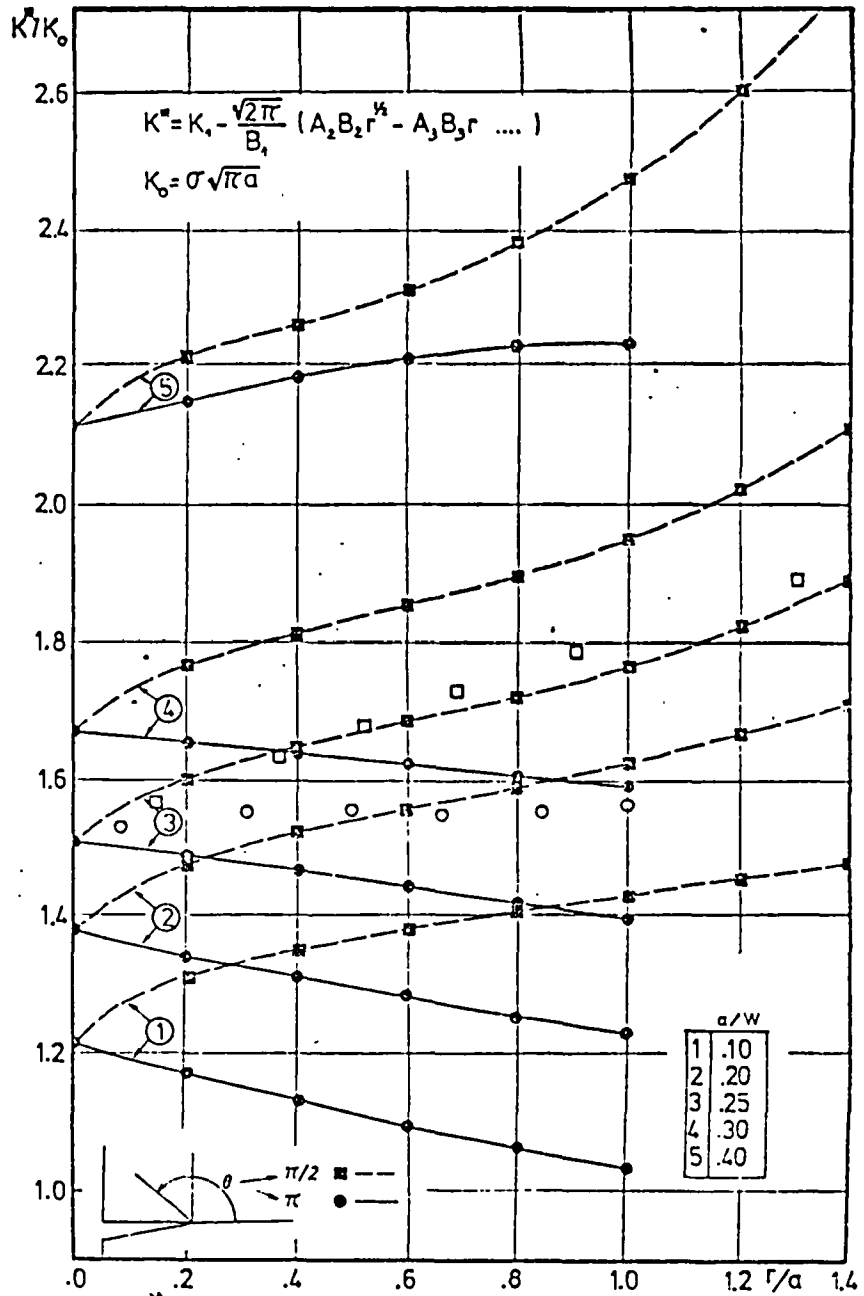

(b) K^* curves for various ratios a/W of a CTS

Fig. 3.1 Results from a 2D analysis as it applies to the Williams series solution to crack problems

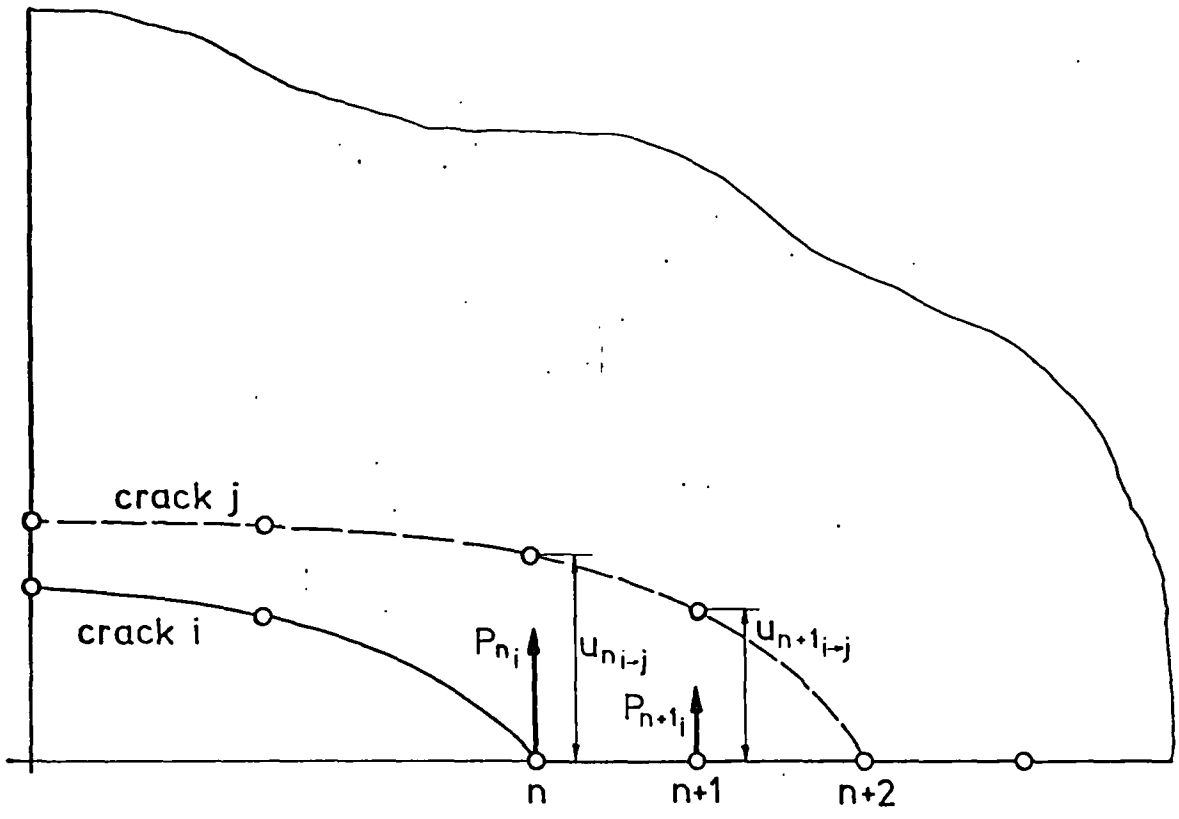

Fig. 3.2 Application of the Energy Method to the derivation of K factors from the crack plane nodal forces and displacements

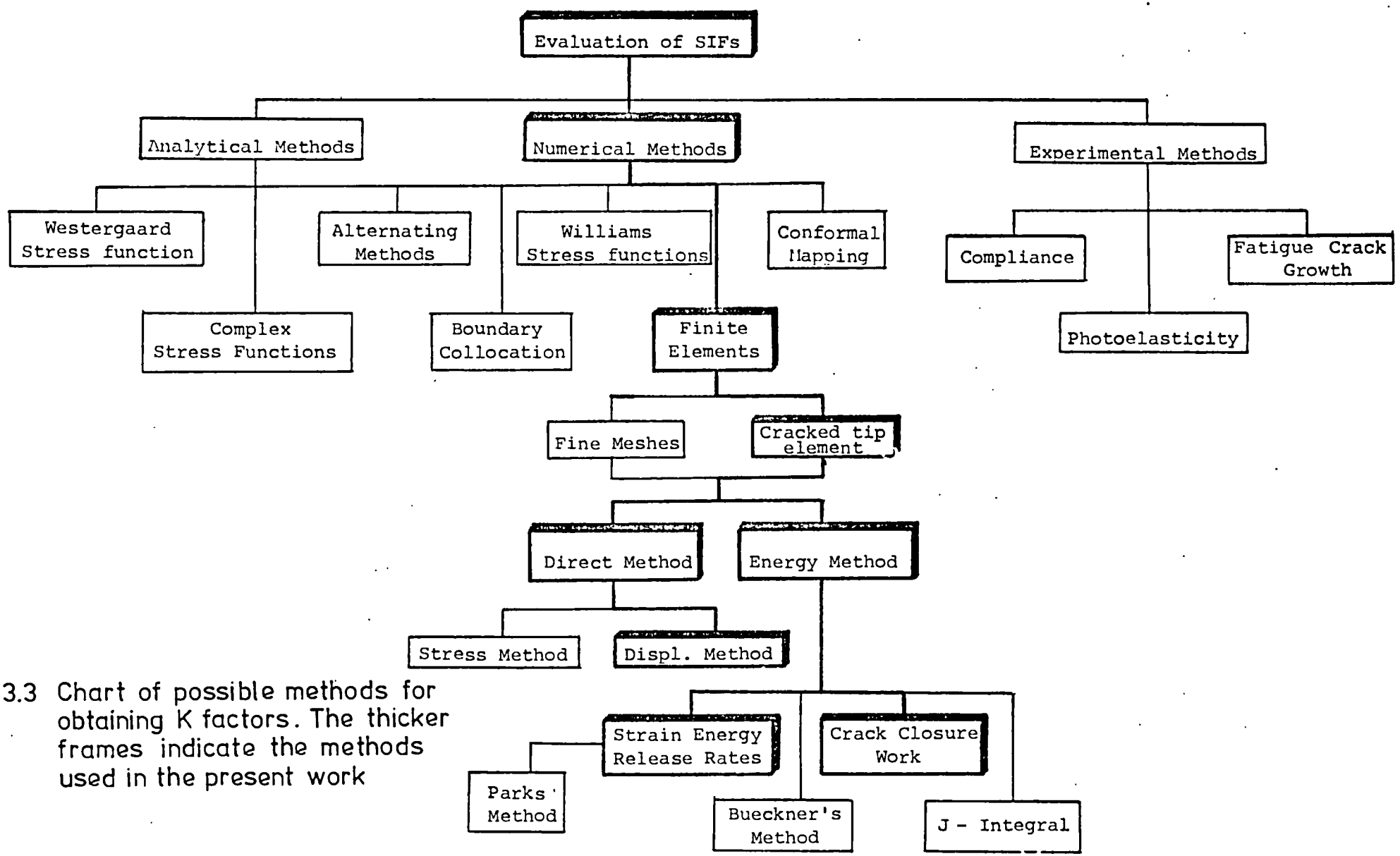

Fig. 3.3 Chart of possible methods for obtaining K factors. The thicker frames indicate the methods used in the present work

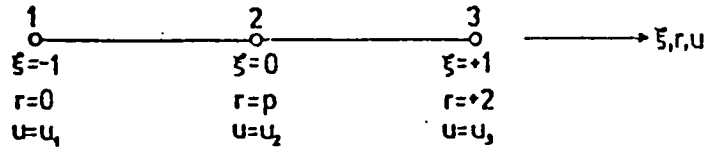

(a) Second Order (quadratic)

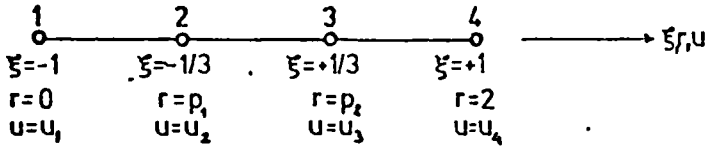

(b) Third Order (cubic)

ξ = local coordinate
r = global coordinate
p = coordinate of mid-side node in global system

Fig. 3.4 One dimensional line elements

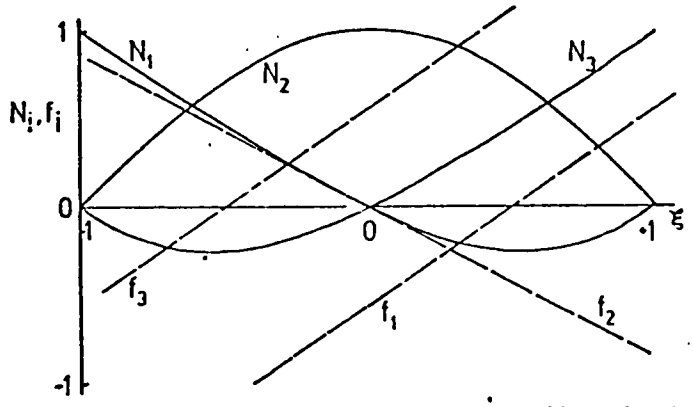

Fig. 3.5 Shape functions N_i and its derivatives f_i for the second order line element

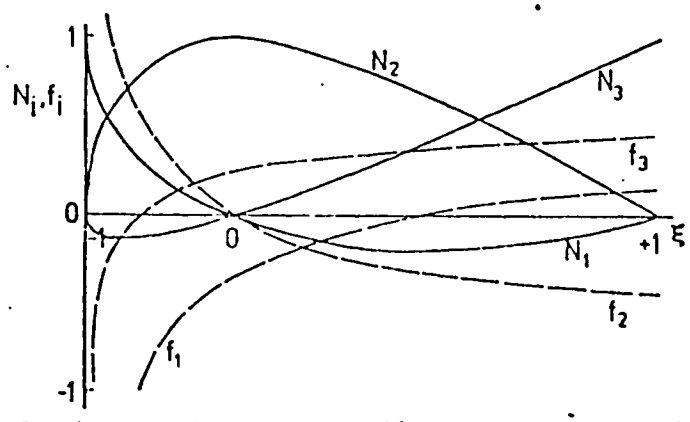

Fig. 3.6 New shape functions N_i and its derivatives f_i for the singularity element

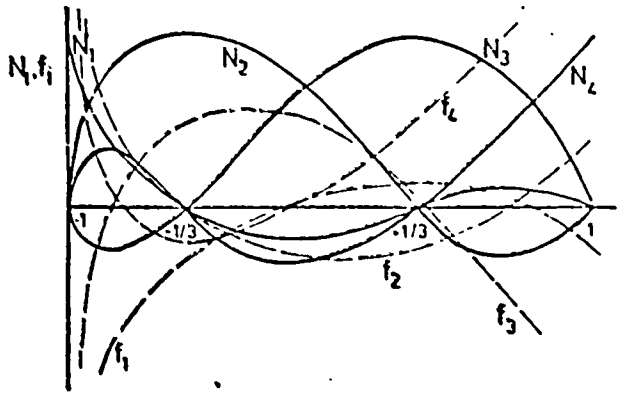

Fig. 3.7 Shape functions N_i and its derivatives f_i for the 4 node singularity element

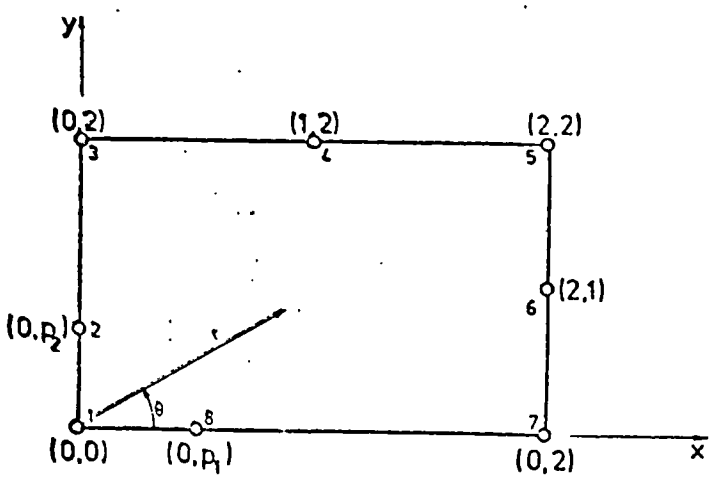

Fig. 3.8 2D 8 node isoparametric element

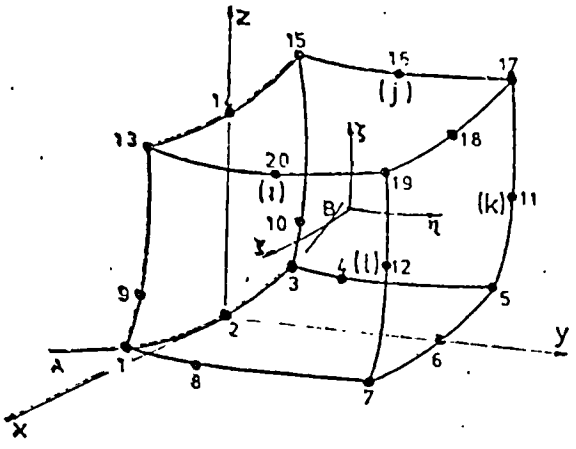

Fig. 3.9 3D 20 node singularity element

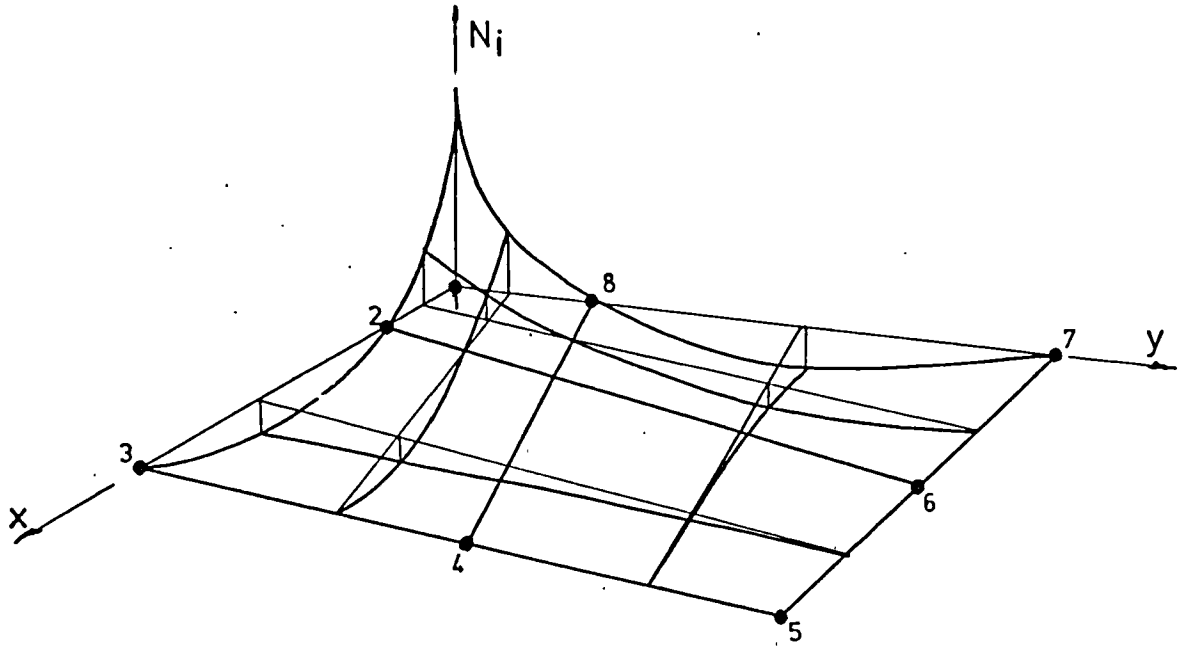

(a) Shape function N_1

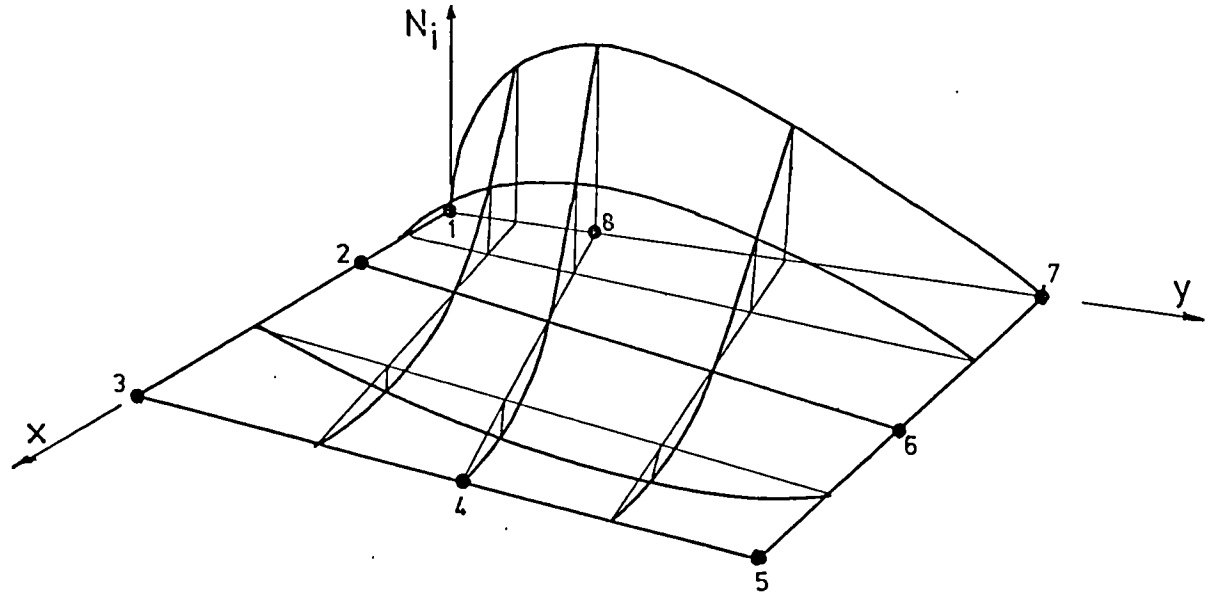

(b) Shape function N_8

Fig. 3.10 Two tipical shape functions for the 2D 8 node singularity element

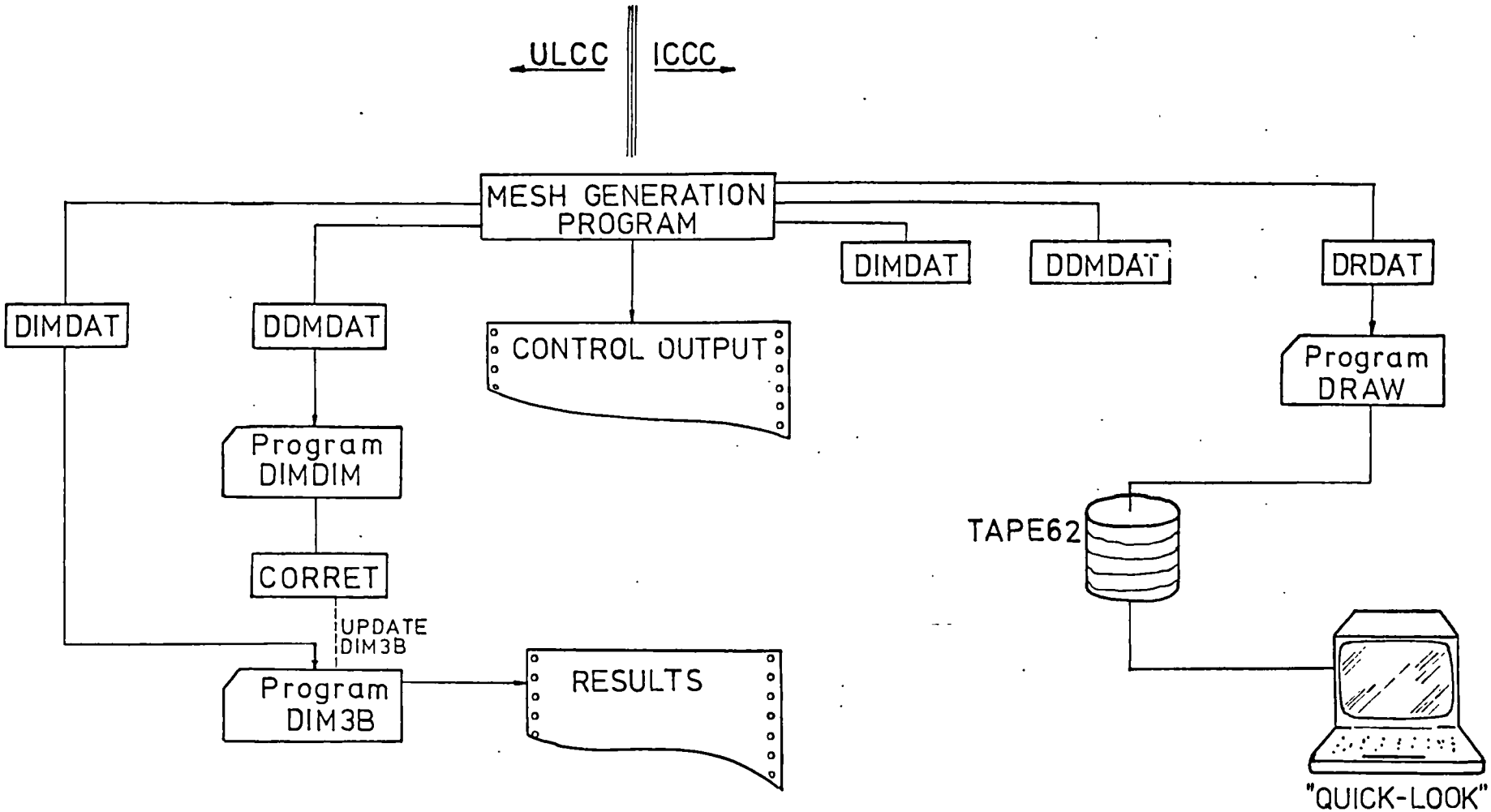

Fig. 3.11 Procedure for data generation and execution of DIM3B code

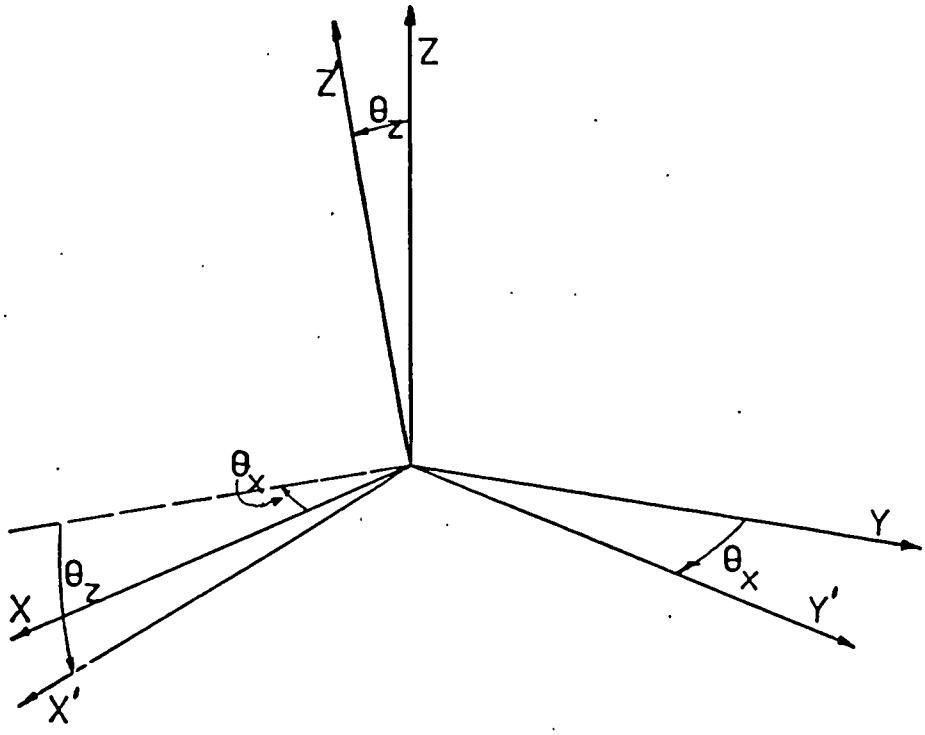

Fig. 3.12 Transformation of coordinates to obtain a prespective view of a finite element mesh

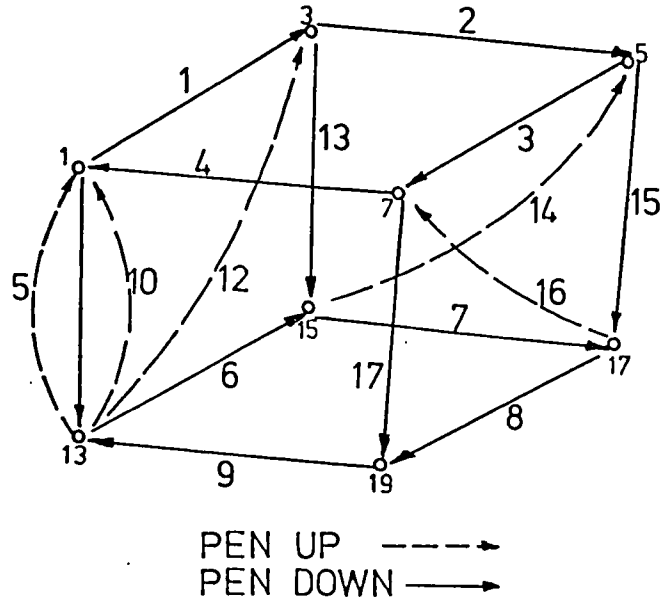

Fig. 3.13 Order of execution of logical functions 'Pen up','Pen down' in a hexahedron element

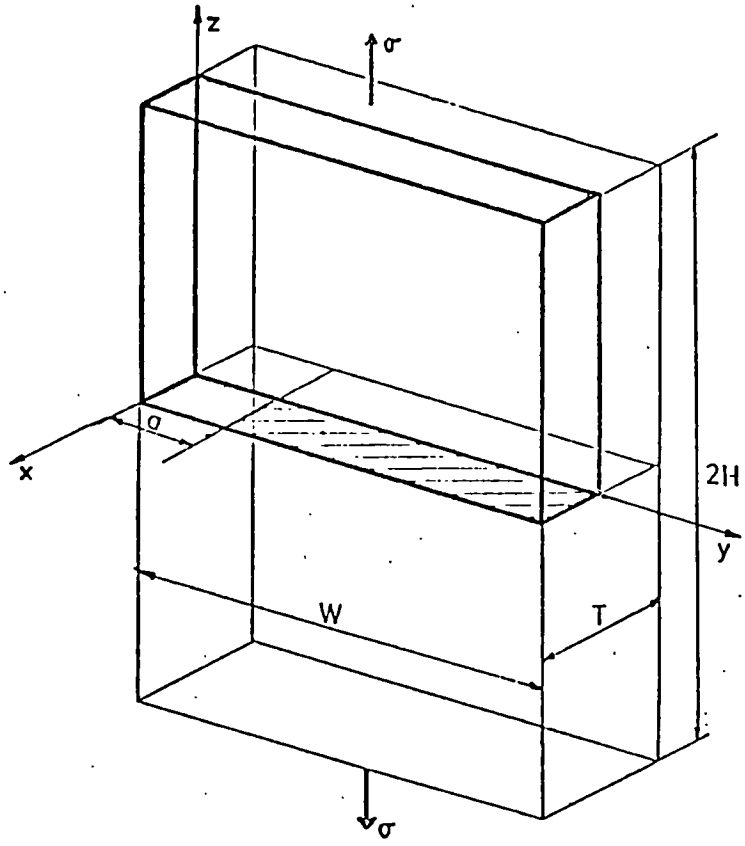

(a) Compact Tension Specimen

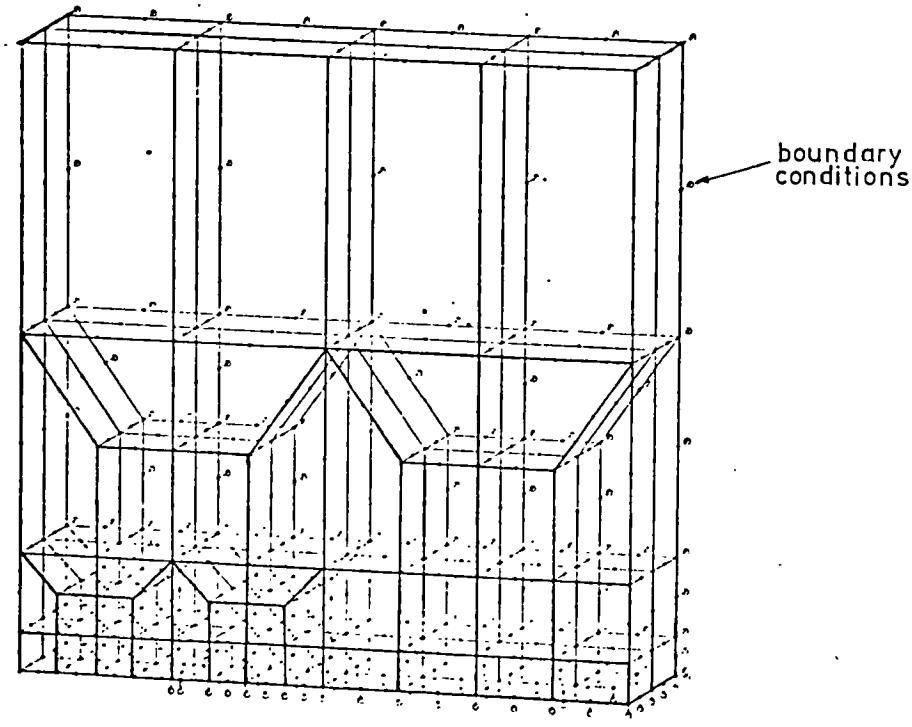

Fig. 3.14 Finite element mesh idealization for the CTS shown in figure 3.14 (a)

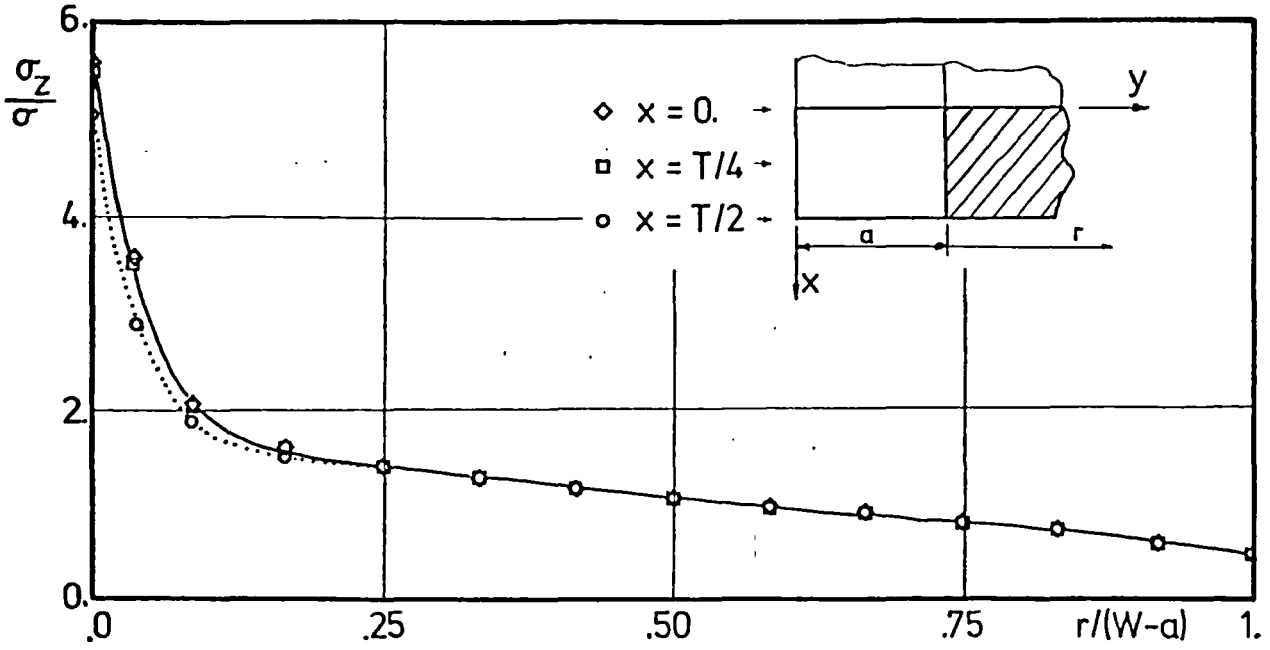

Fig. 3.15 Undistorted elements. Variation of σ_z stresses ahead of the crack front.

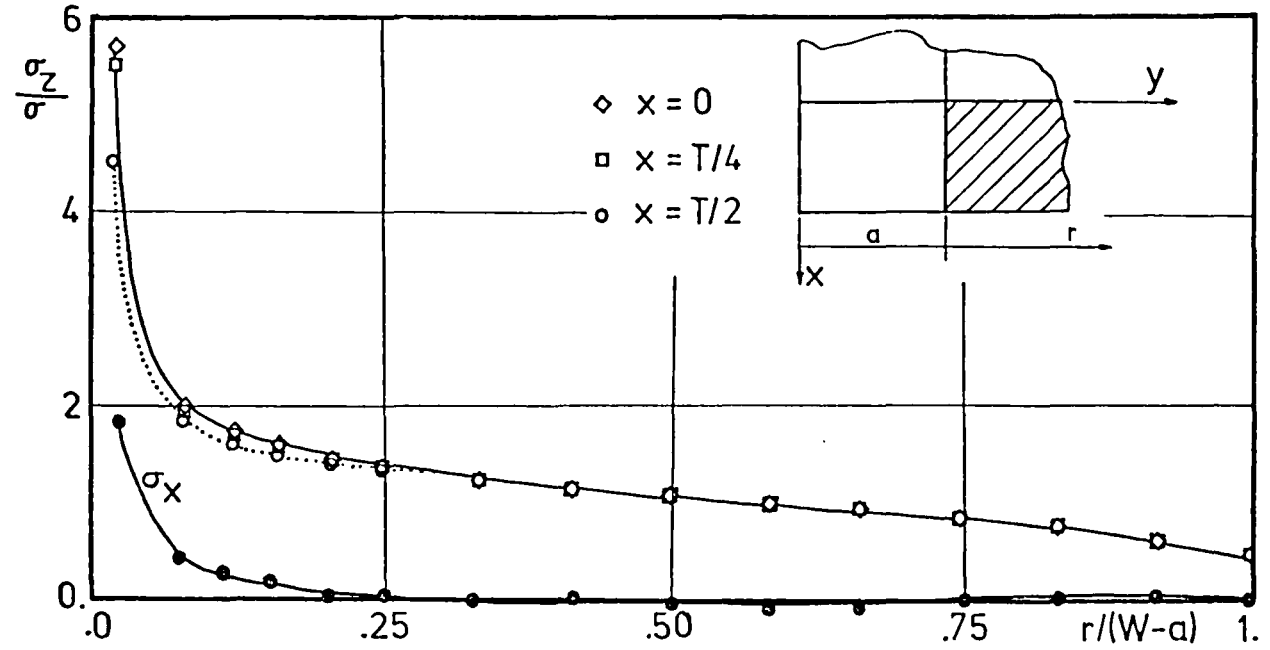

Fig. 3.16 Distorted elements. Variation of σ_x and σ_z stresses ahead of the crack front

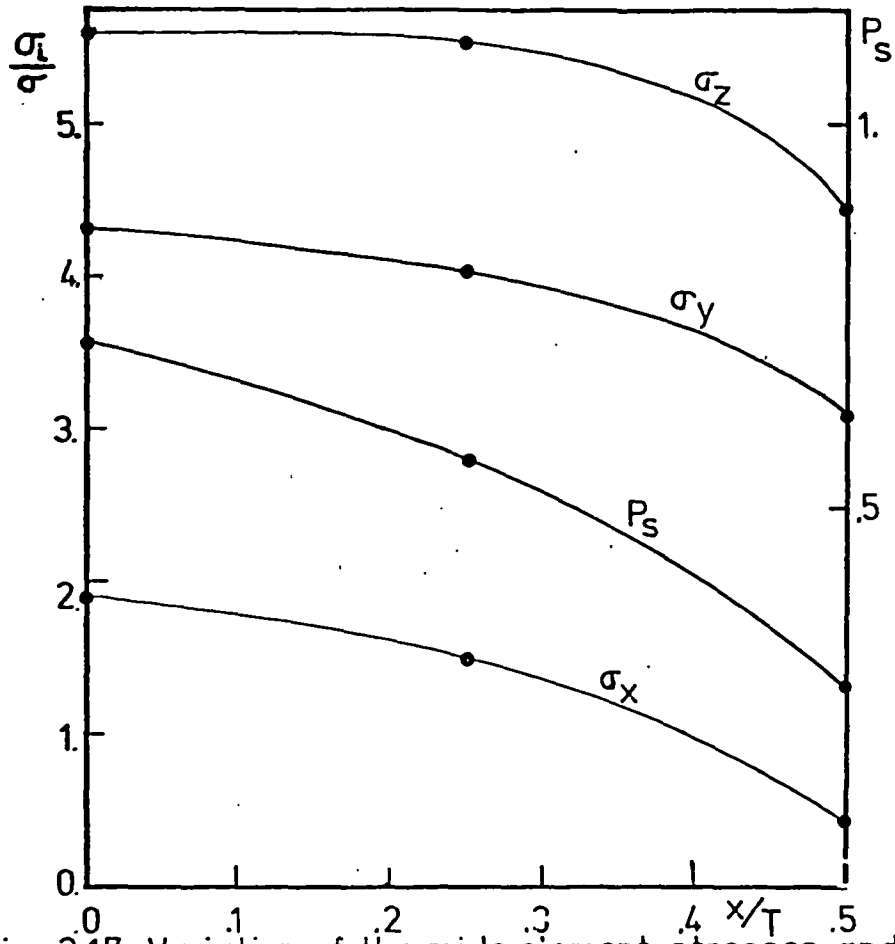

Fig. 3.17 Variation of the mide element stresses and the parameter P accross the thickness in the vicinity of the crack front

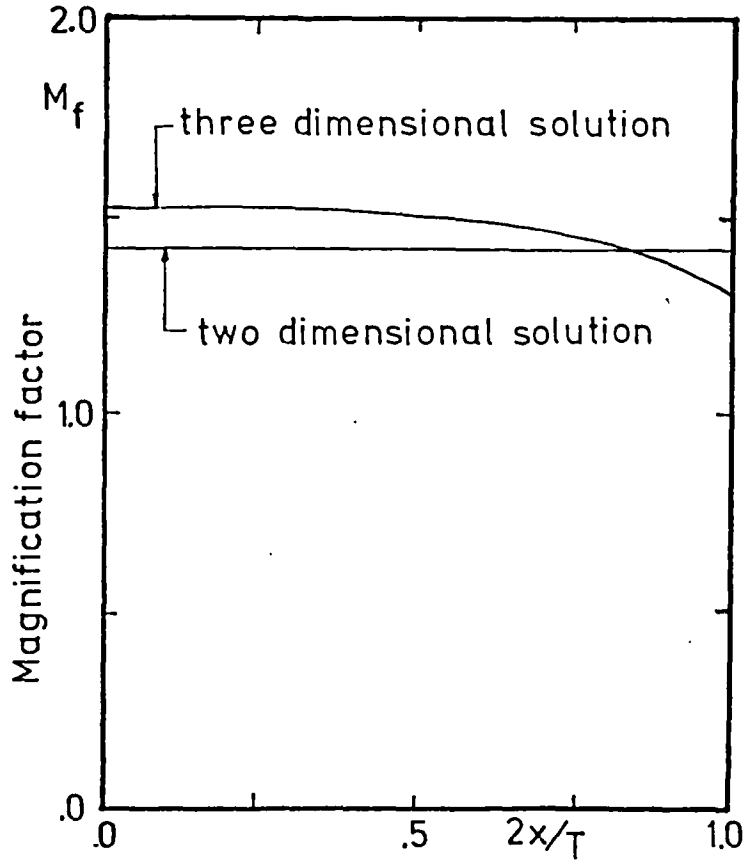

Fig. 3.18 Variation of the K factor obtained along the crack of a CTS by Yamamoto & Sumi, Ref. (86)

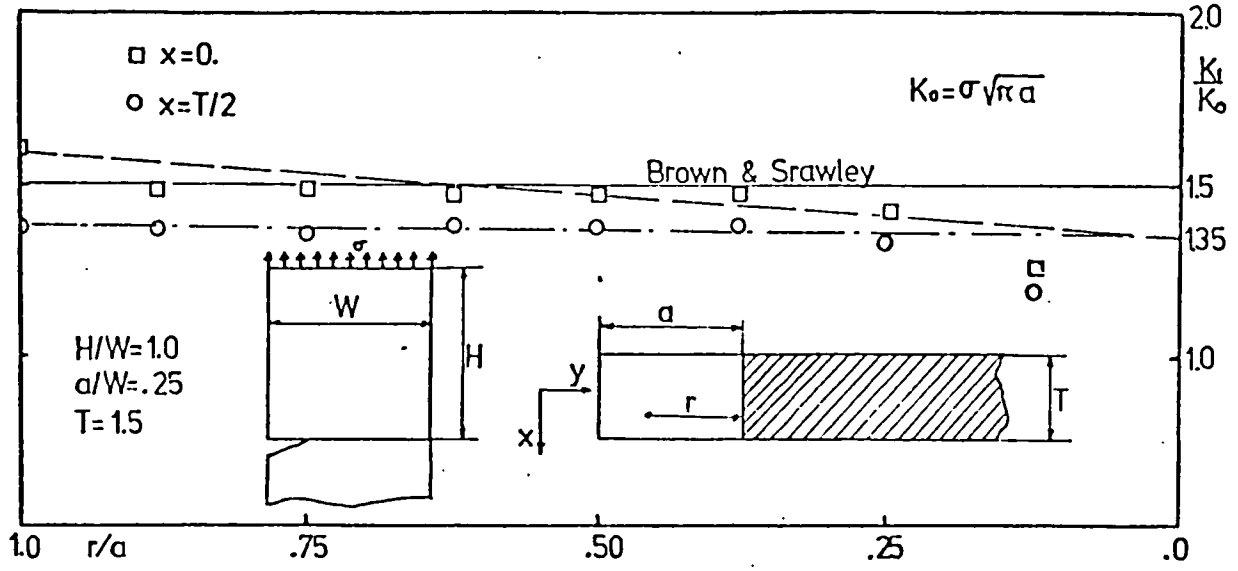

Fig. 3.19 Extrapolation procedure using undistorted elements

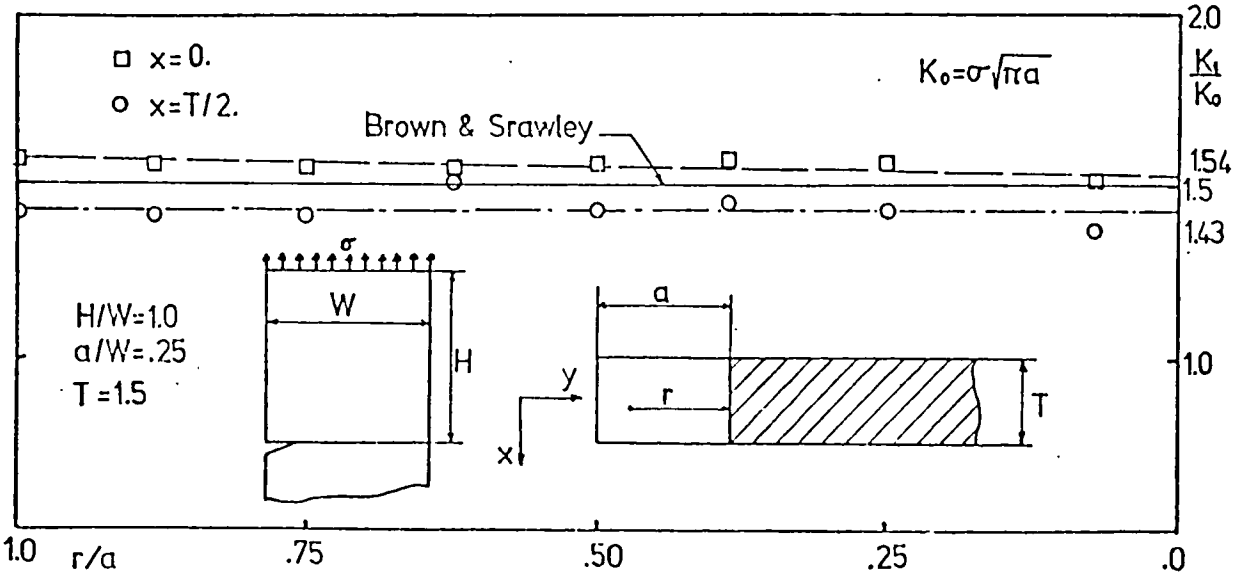

Fig. 3.20 Extrapolation procedure using distorted elements

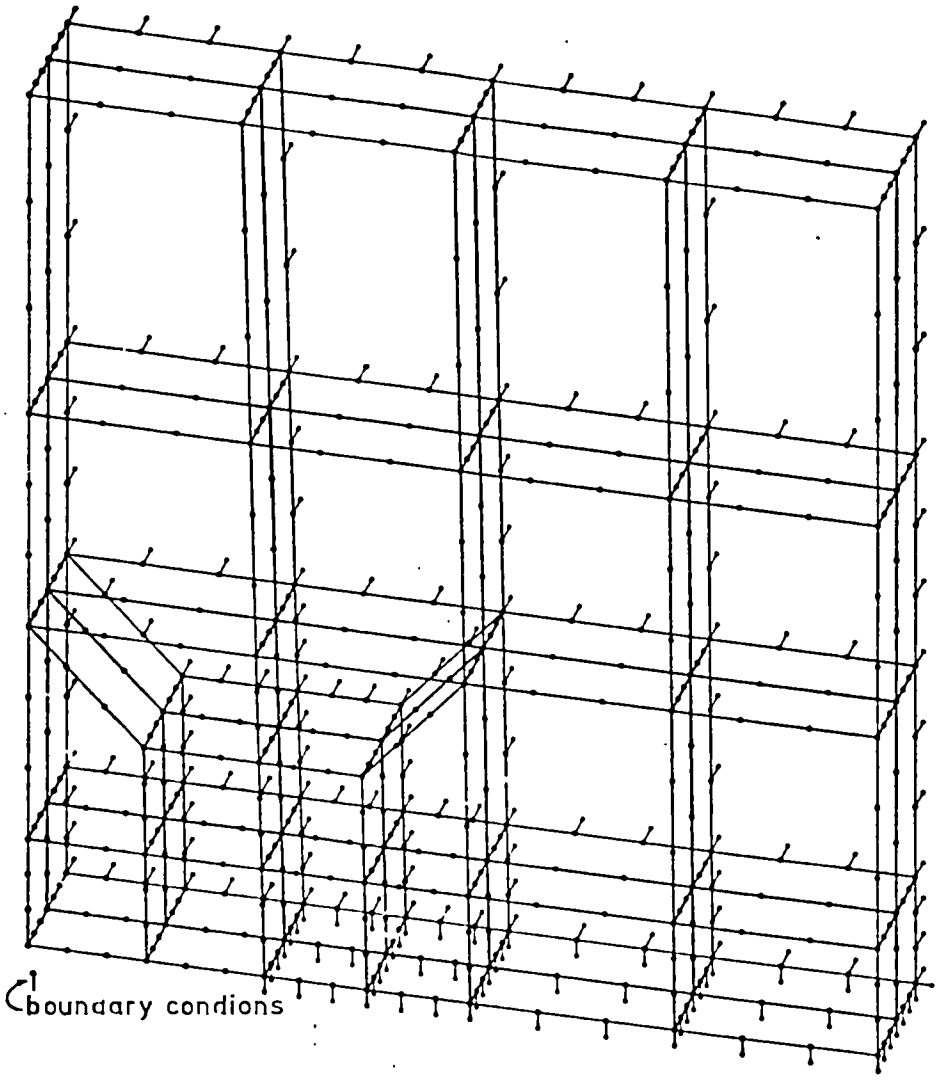

(a) Finite element mesh idealization of a CTS using 3D 32 node elements

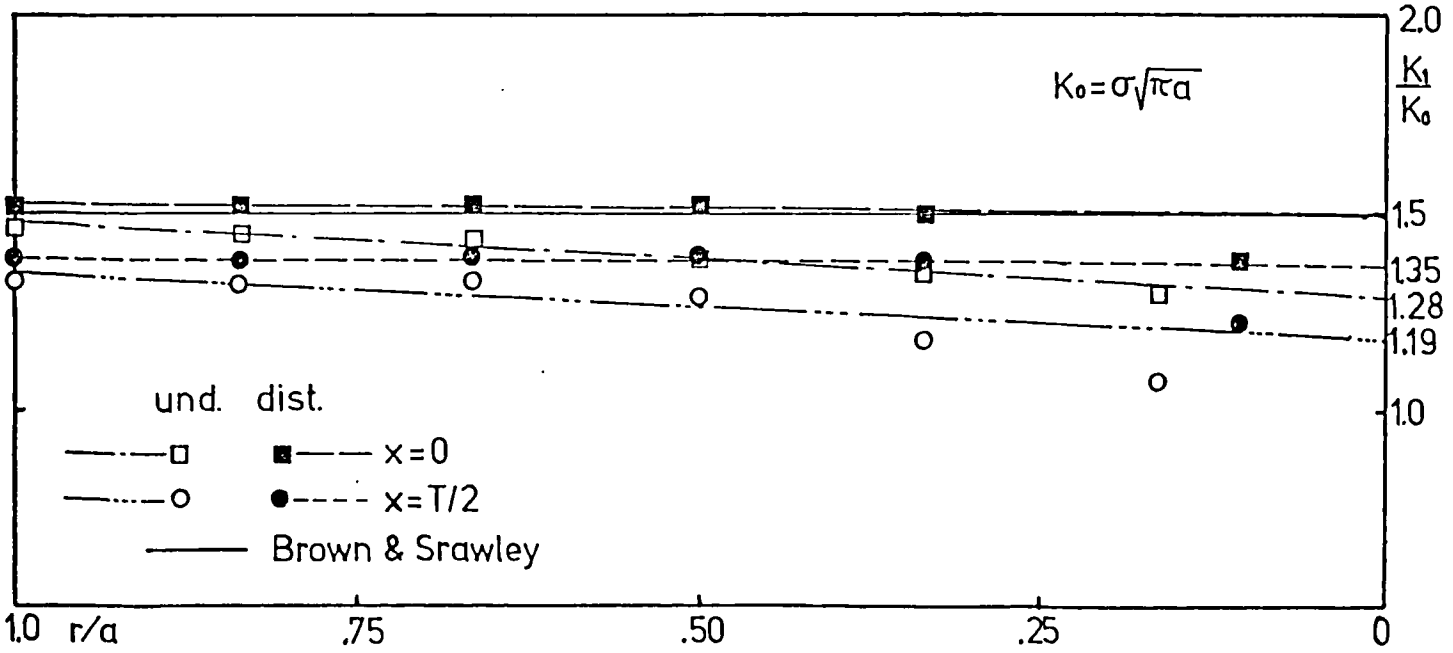

(b) Comparison of extrapolation procedures

Fig. 3.21 Singularity elements derived from 32 node isoparametric elements

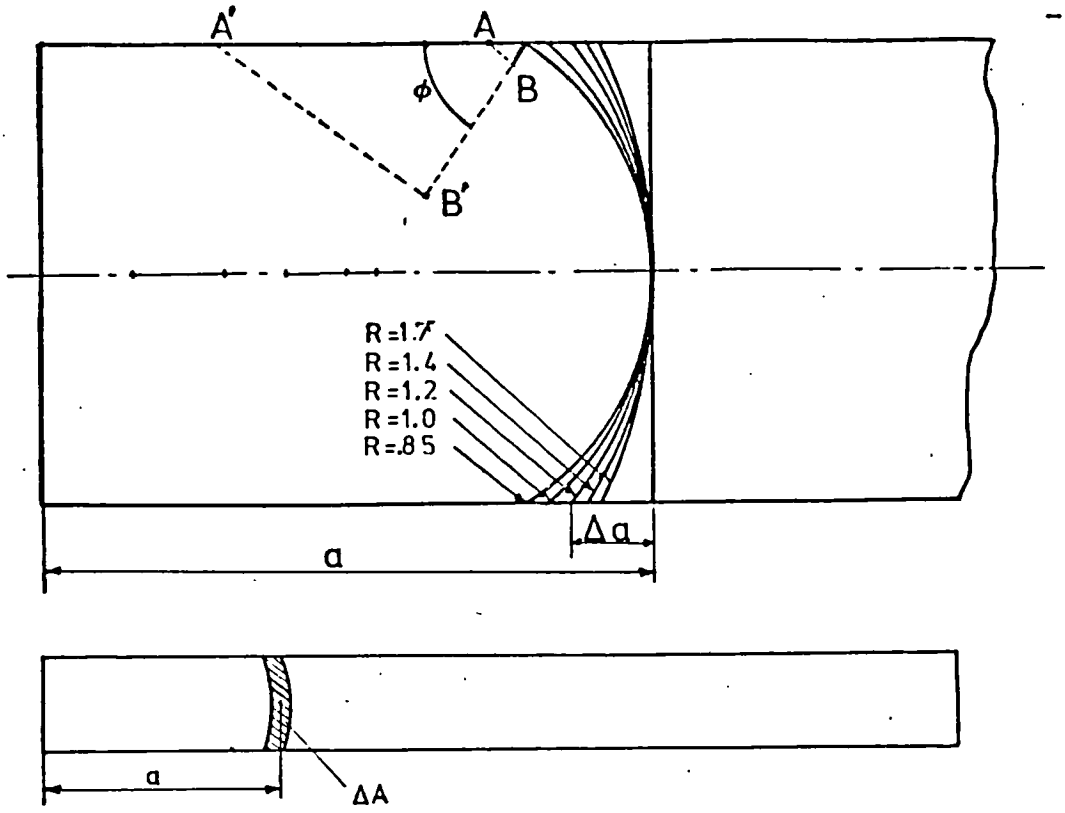

(a)

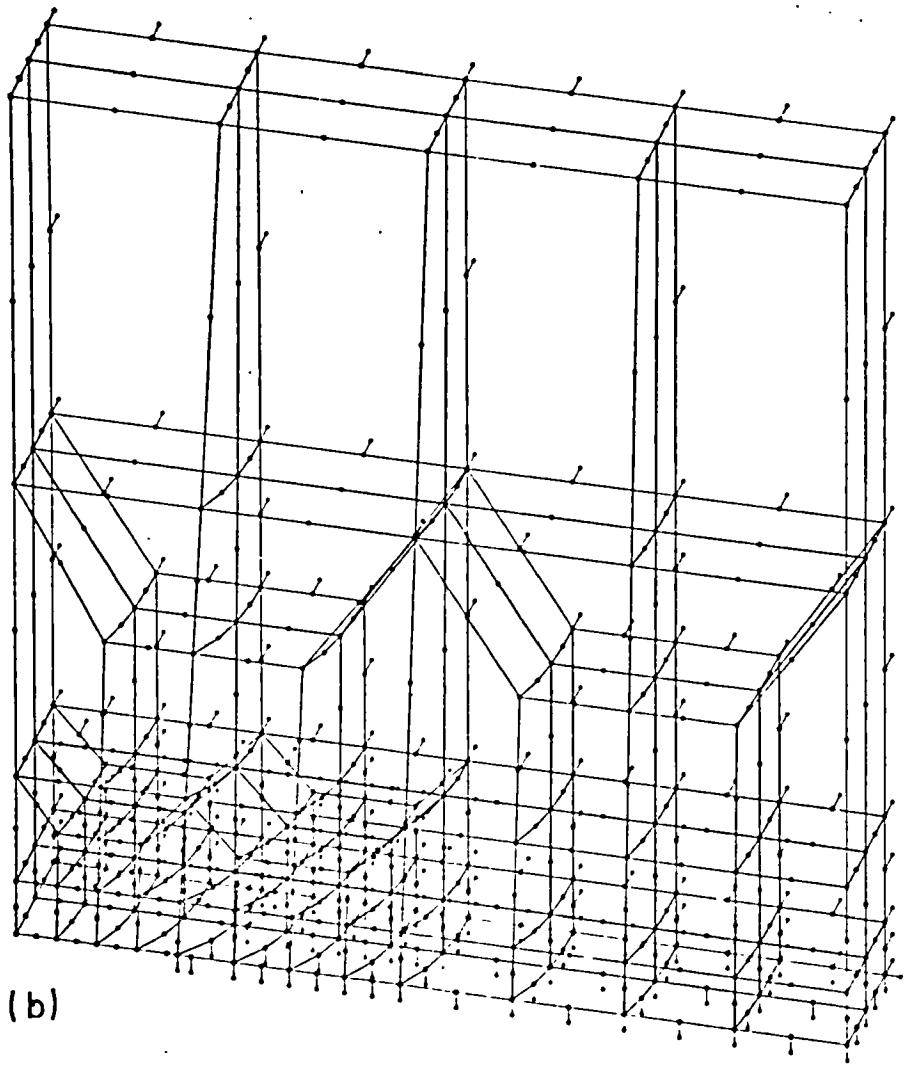

(b)

Fig. 3.22 CTS with curved crack front and its mesh idealization

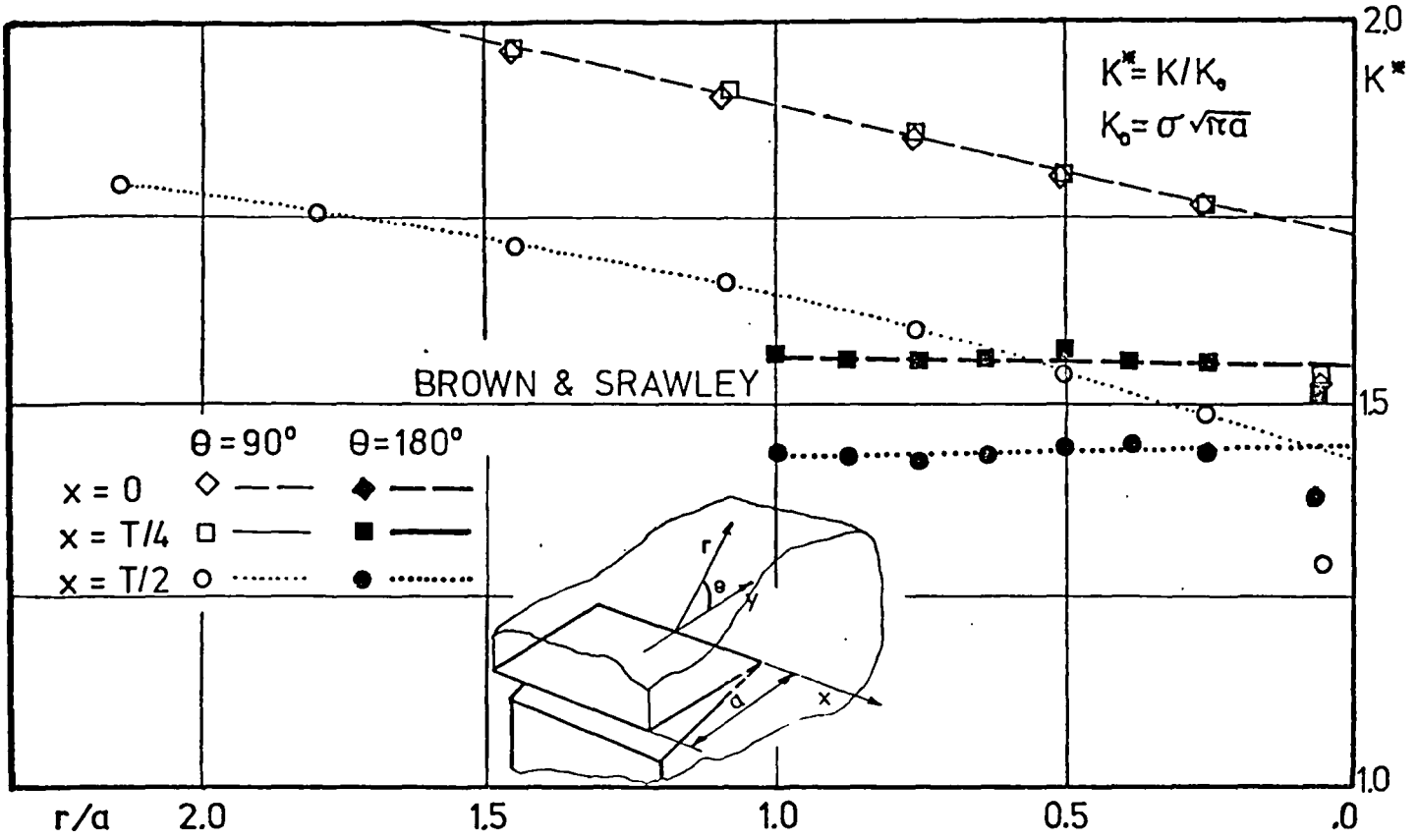

(a) straight crack front

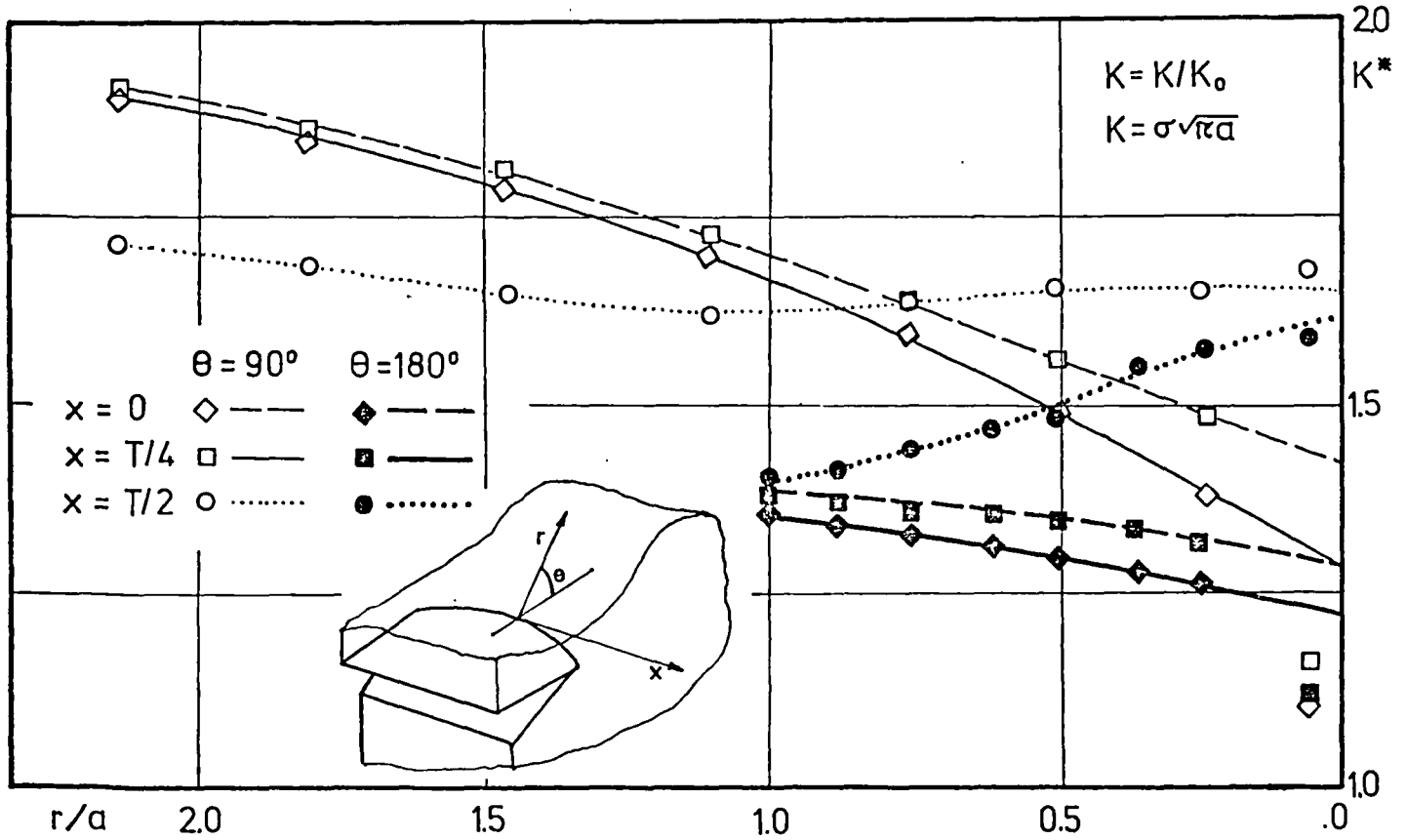

(b) curved crack front

Fig. 3.23 Comparison of extrapolation procedures using two directions of extrapolation, $\theta = \pi$ and $\theta = \pi/2$

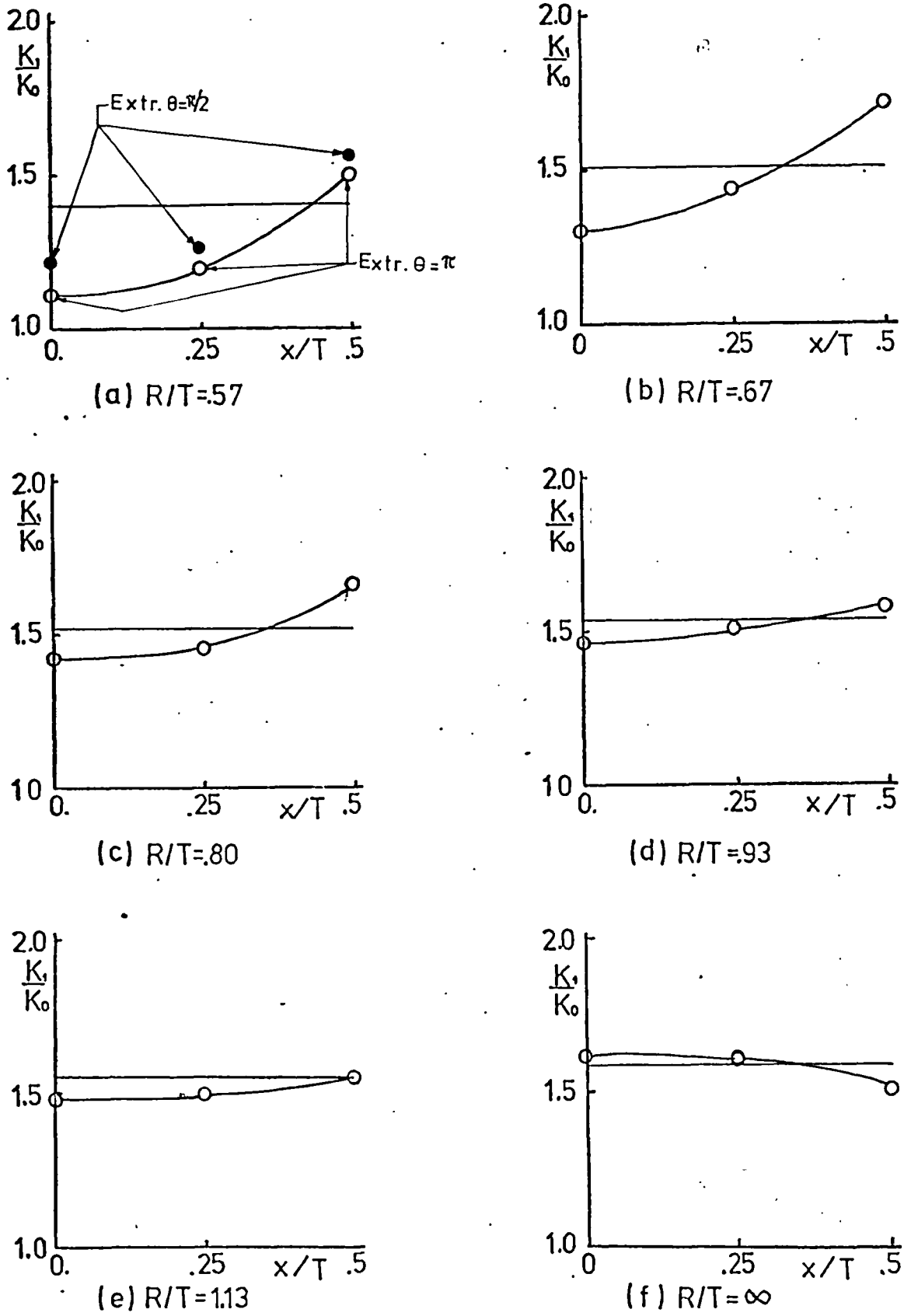

Fig. 3.24 CTSs with curved crack fronts of different curvature. Variation of K along crack front. The horizontal lines indicate, for each case, an averaged K calculated by the Global Energy Method

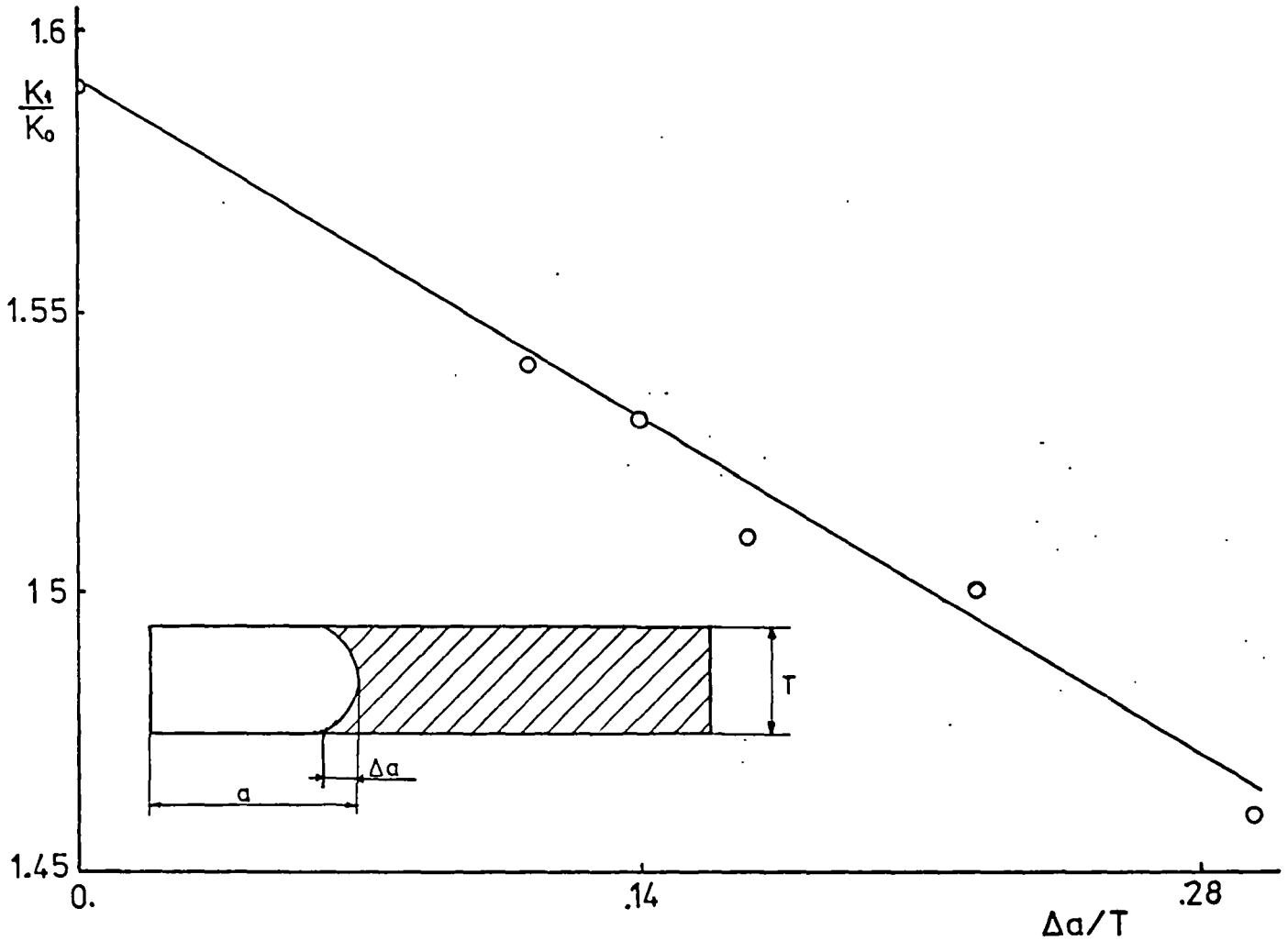

Fig. 3.25 CTS. Variation of the averaged K values (see fig.3.24) with a normalized parameter defining the crack front curvature

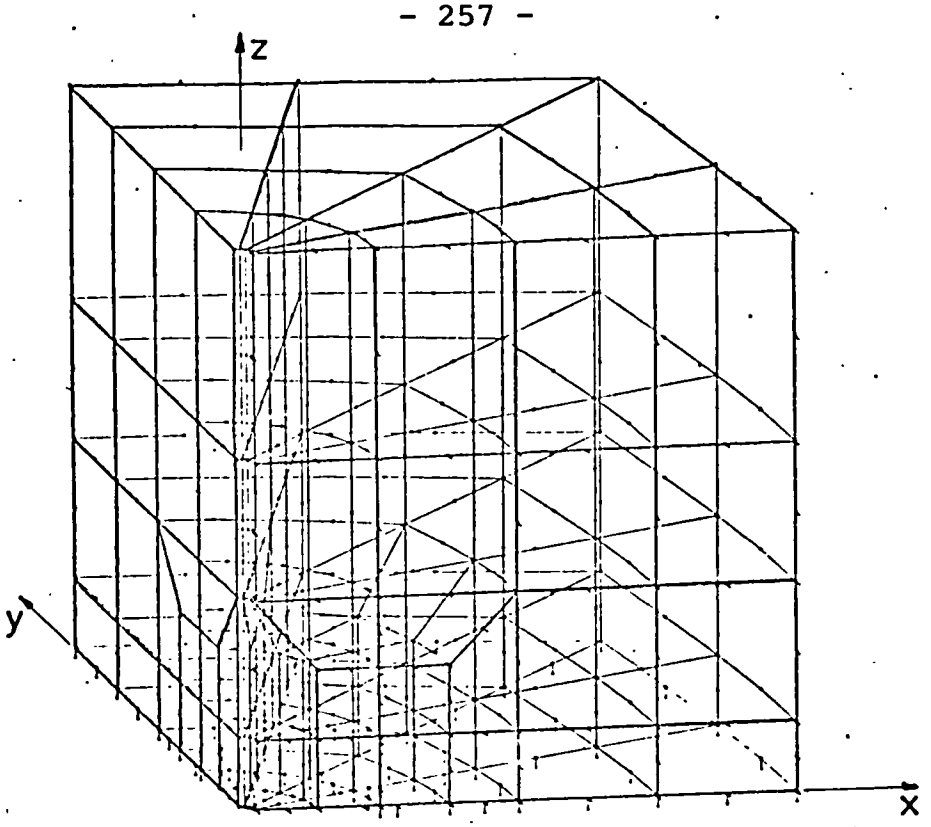

Fig. 3.26 Mesh idealization of corner crack specimen

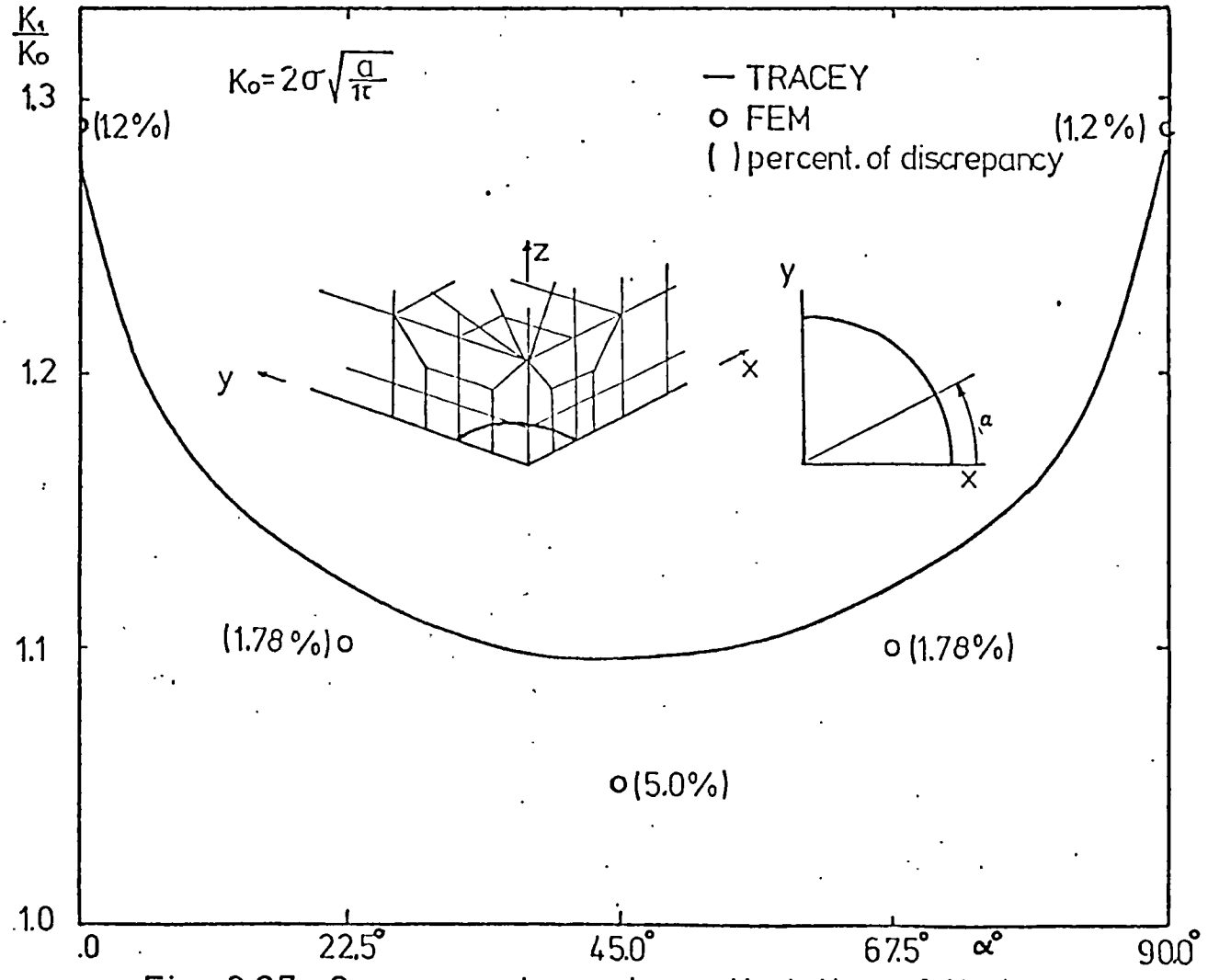

Fig. 3.27 Corner crack specimen. Variation of K along the crack front

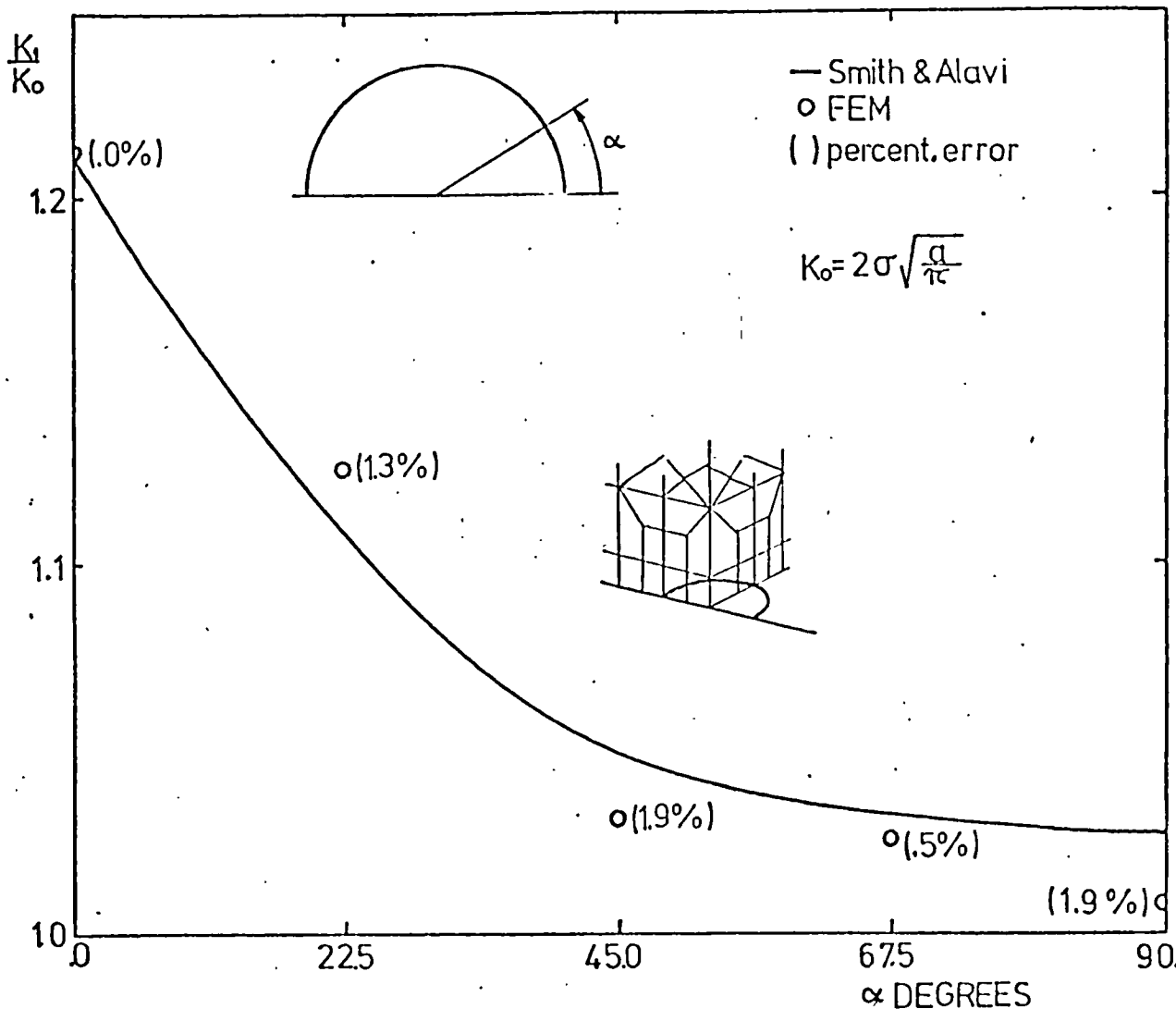

Fig. 3.28 Part-through semi-circular crack. Variation of K along the crack front

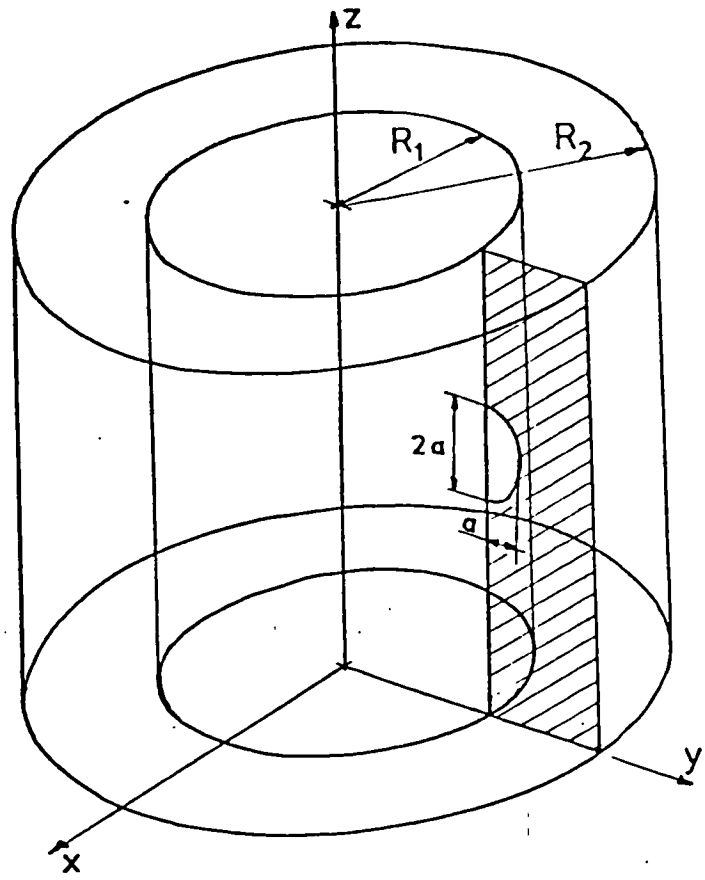

(a)

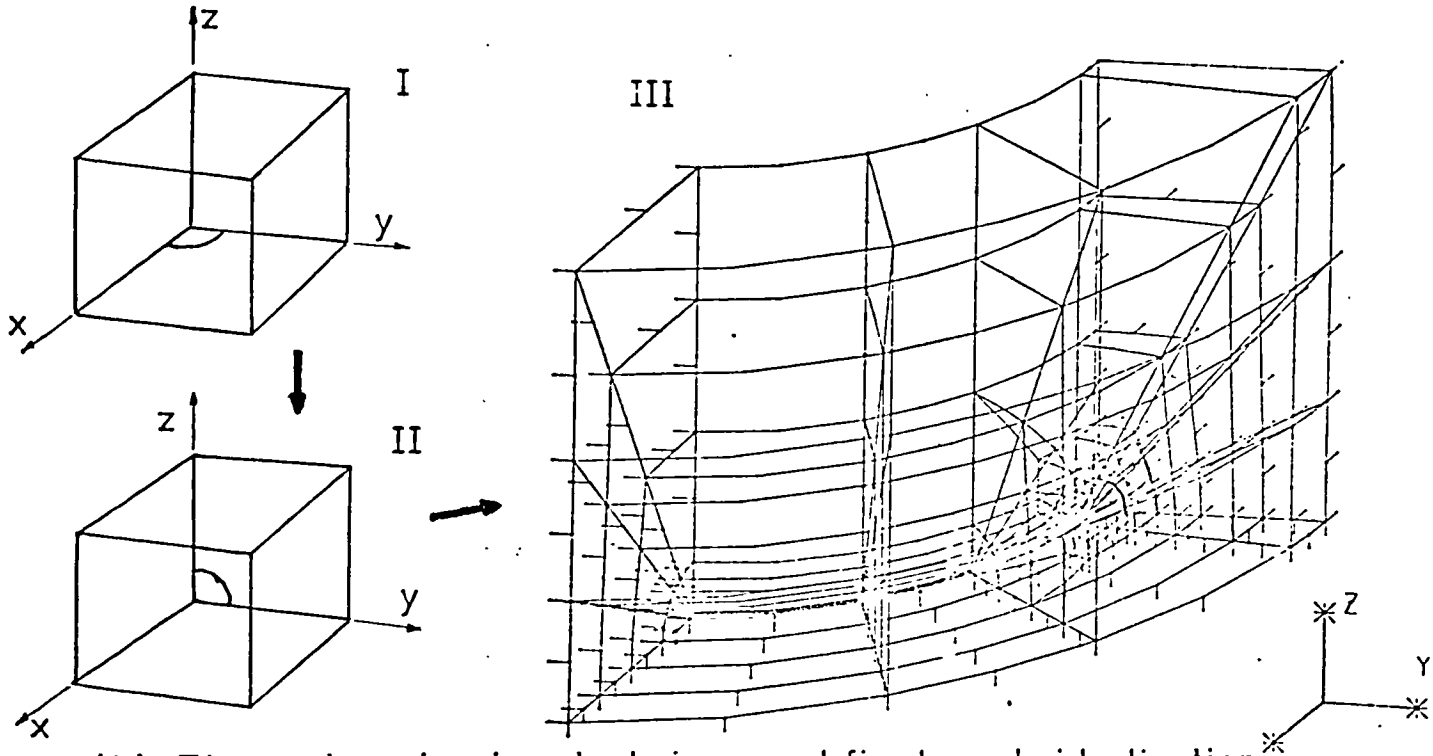

(b) Three step skewing technique and final mesh idealization

Fig. 3.29 Part-through semi-circular crack emanating from the inner surface of a thick-walled cylinder

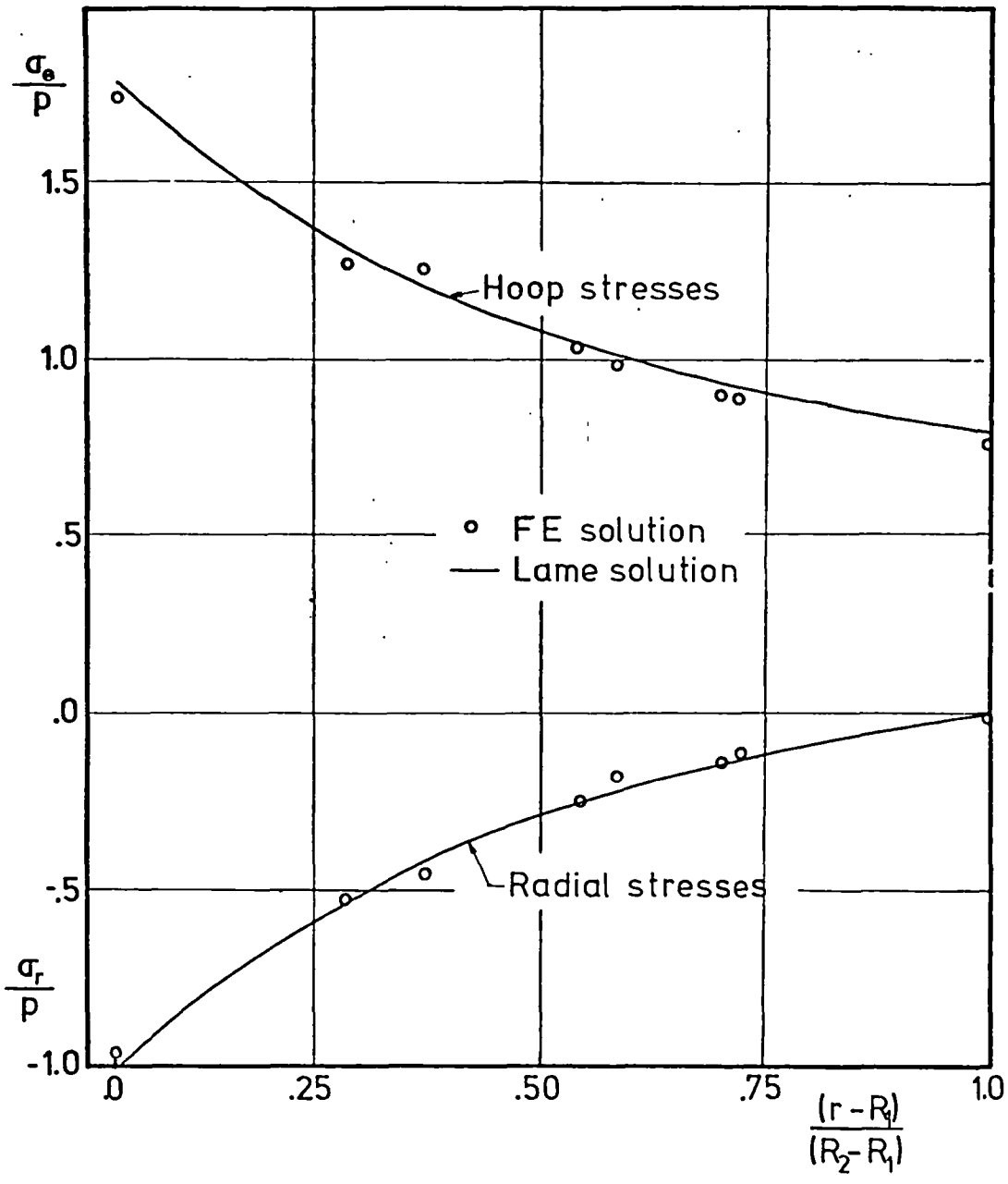

Fig. 3.30 Radial and hoop stresses obtained with the FEM in the radial section y=0 for the case CYL1

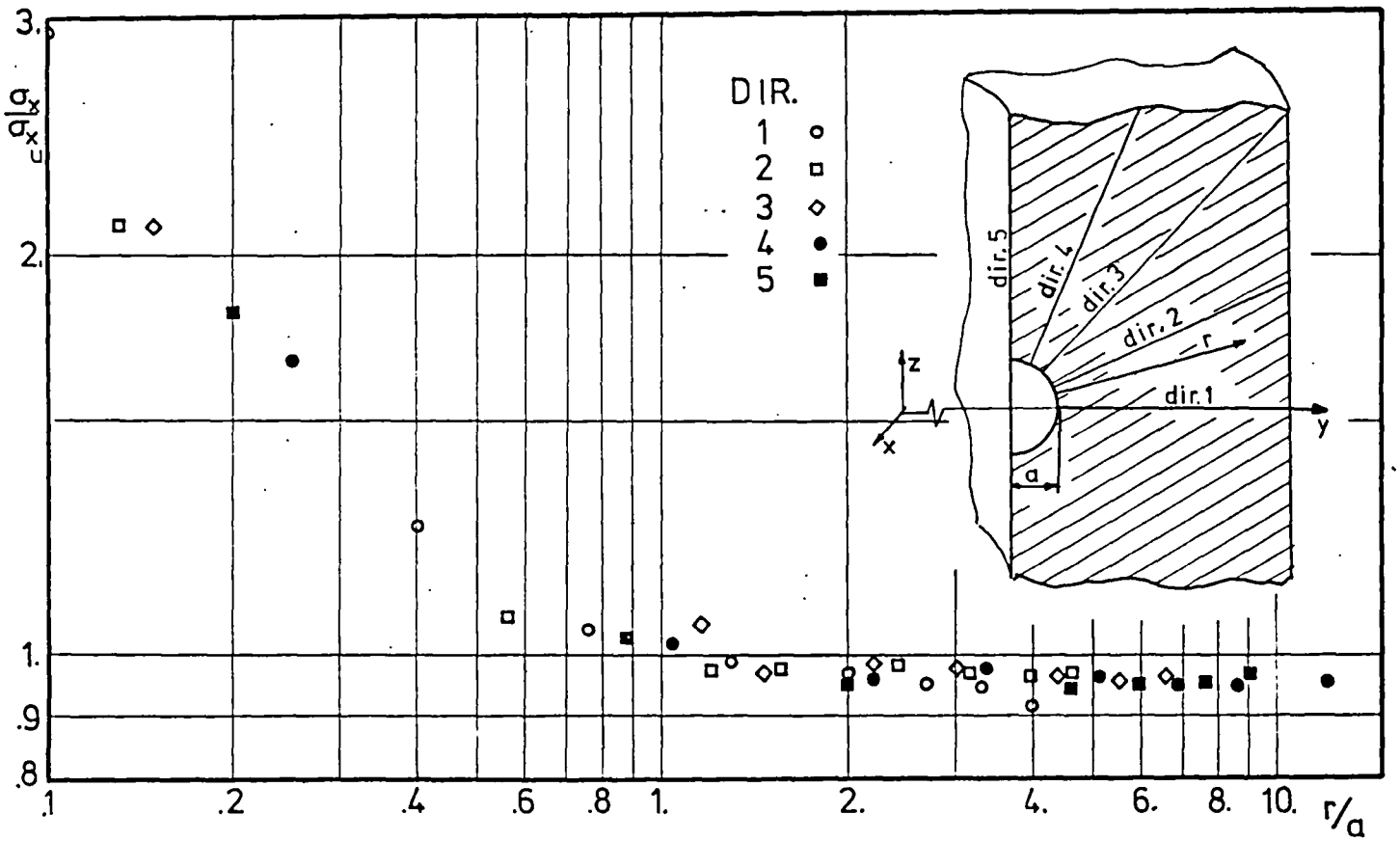

Fig. 3.31 CYL1 case. Hoop stresses, σ_x, ahead of the crack front in the plane x=0

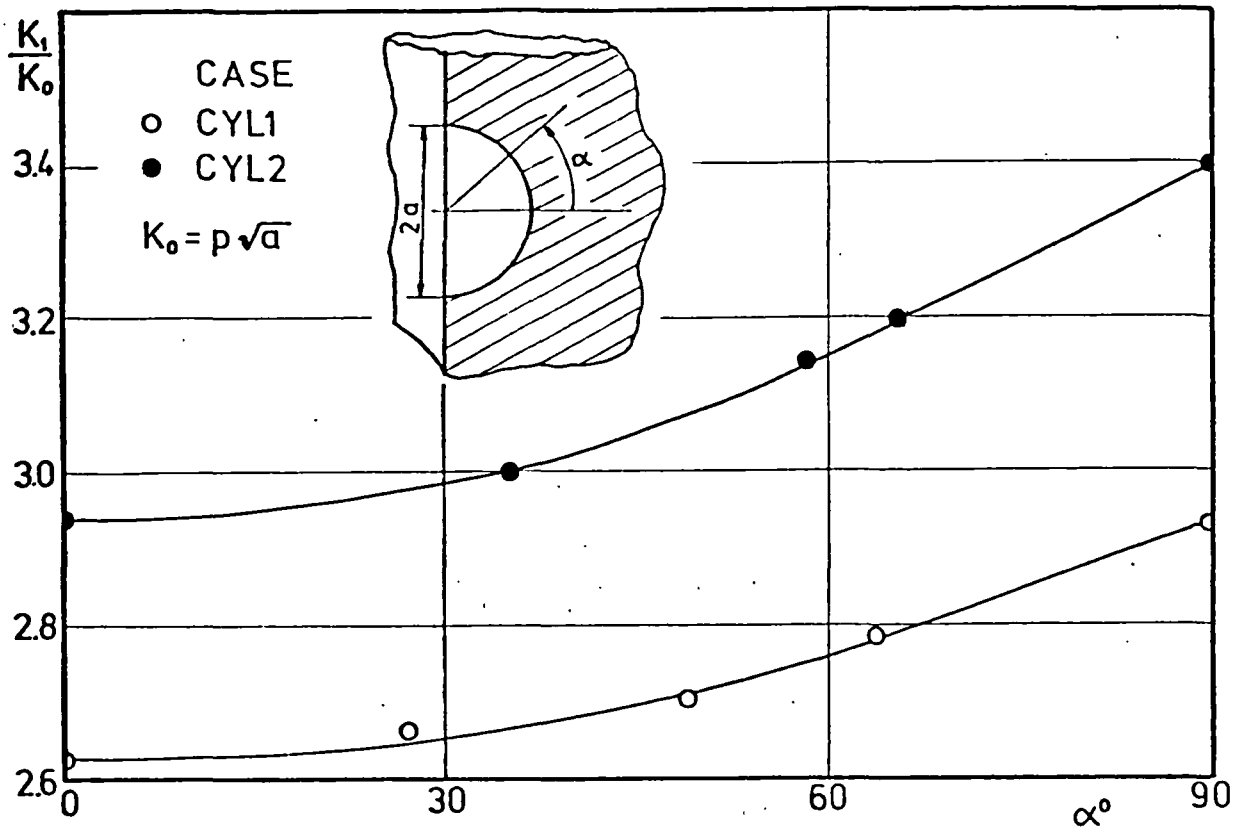

Fig. 3.32 CYL1 and CYL2 cases. Variation of K along the crack fronts

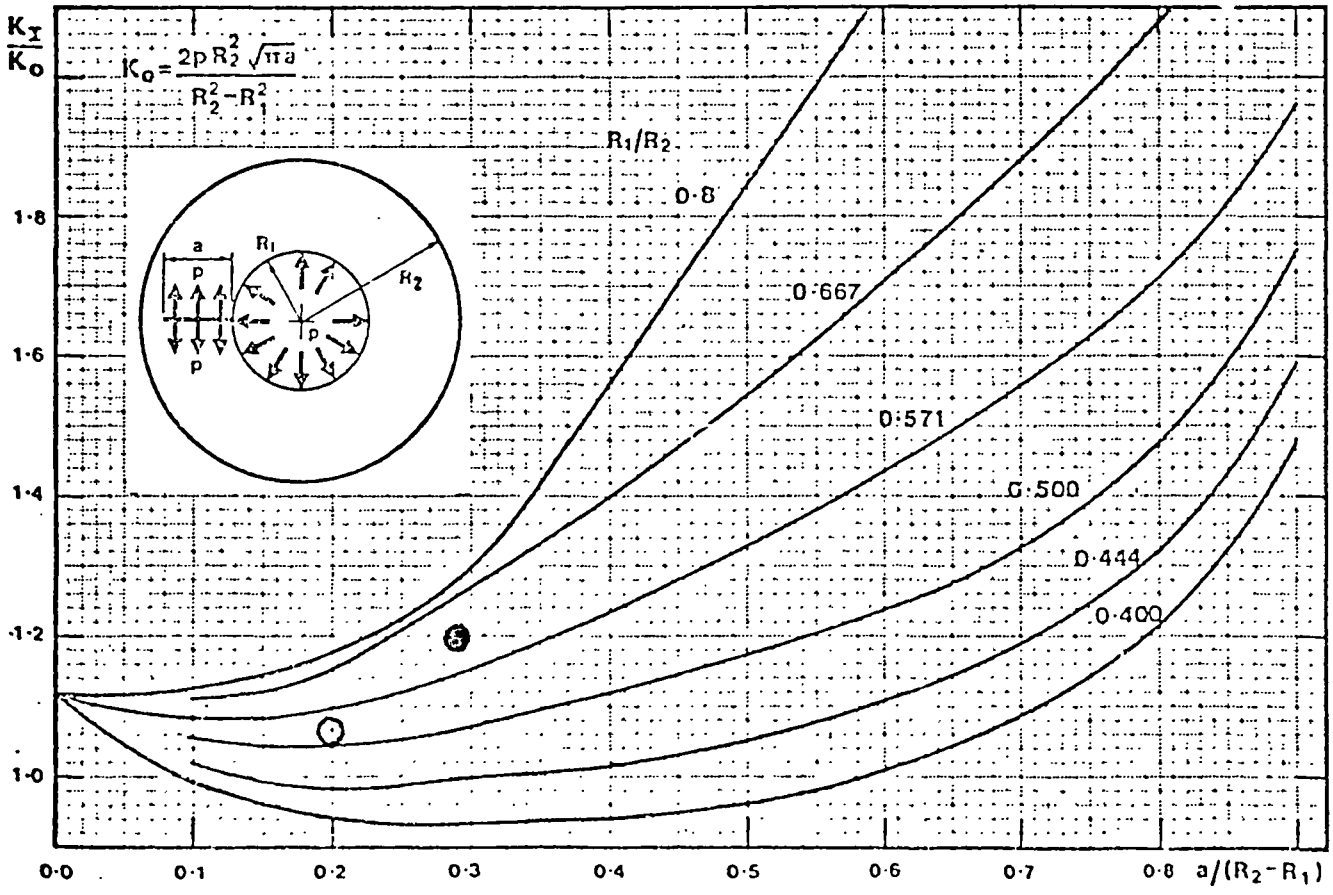

Fig. 3.33 K values for a pressurized internal radial edge crack in a tube subjected to a uniform internal pressure (from Ref. (30))

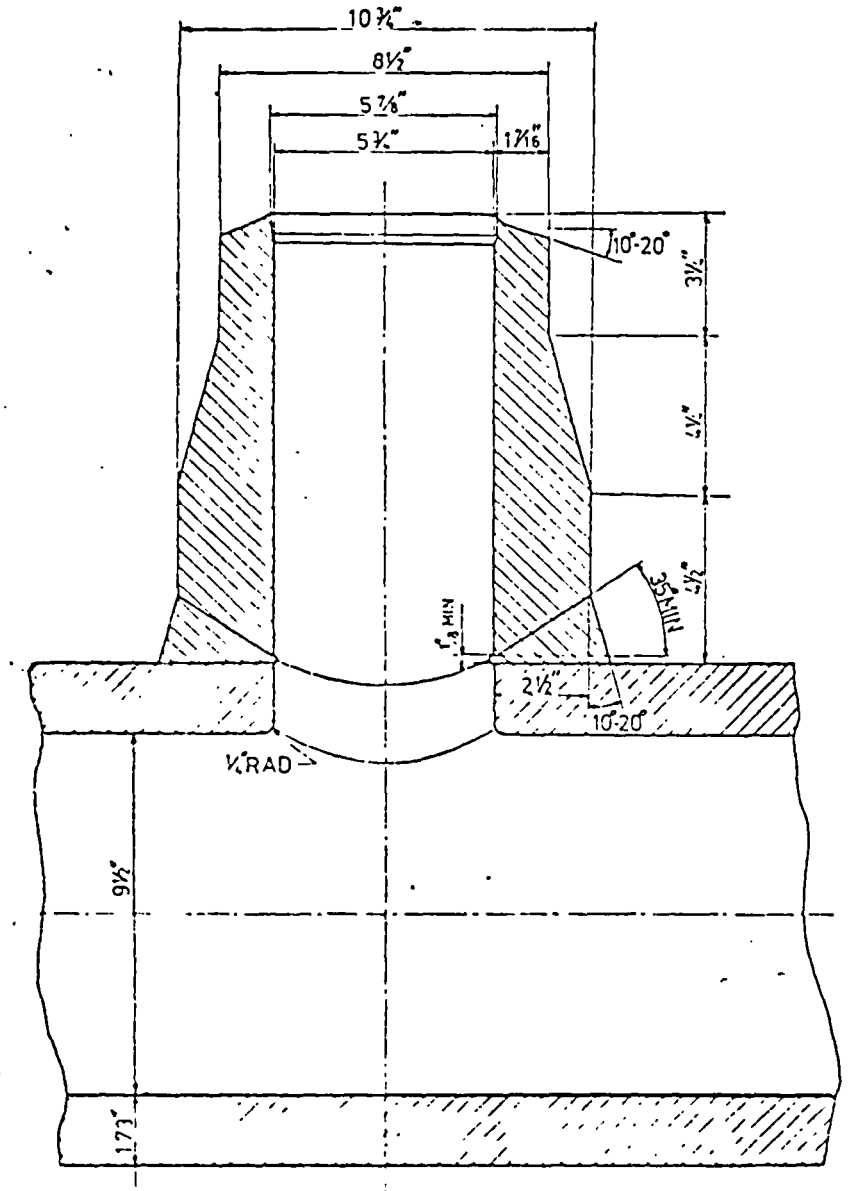

Fig. 4.1 Specification of geometric details of a main steam vent pipe "T-piece"

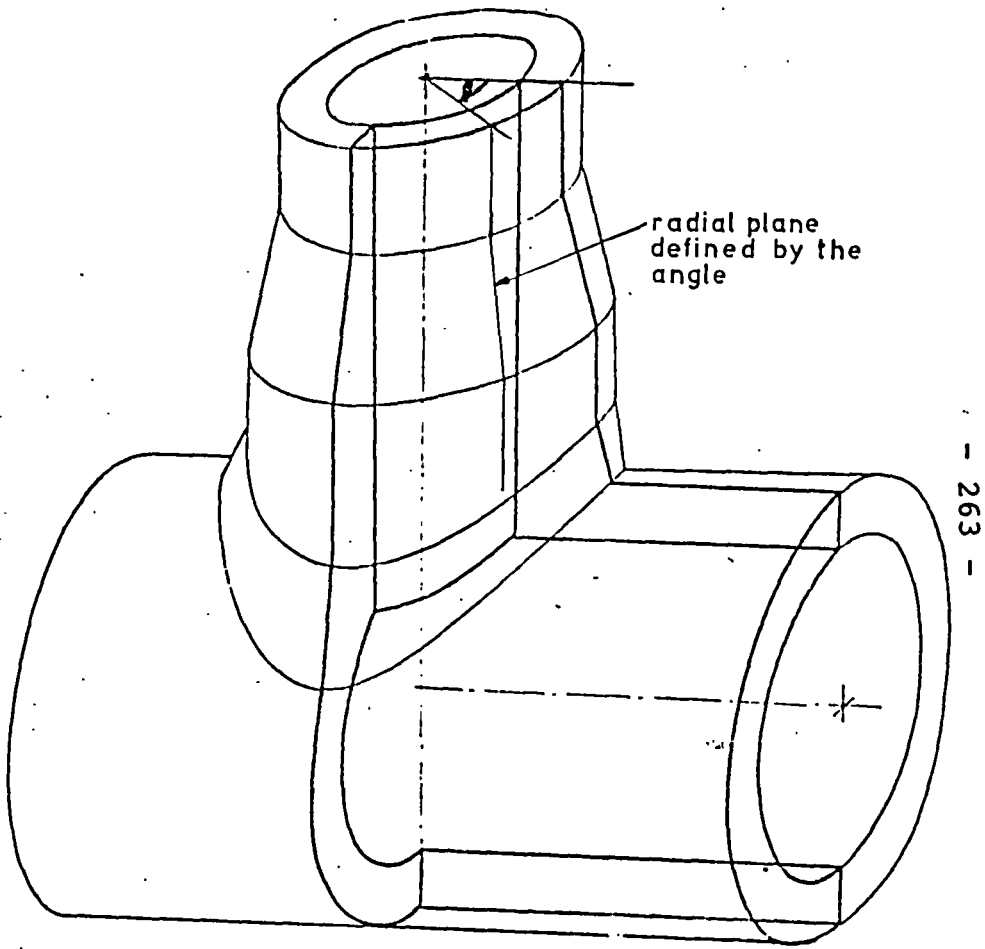

Fig. 4.2 Prespective view of the "T-piece"

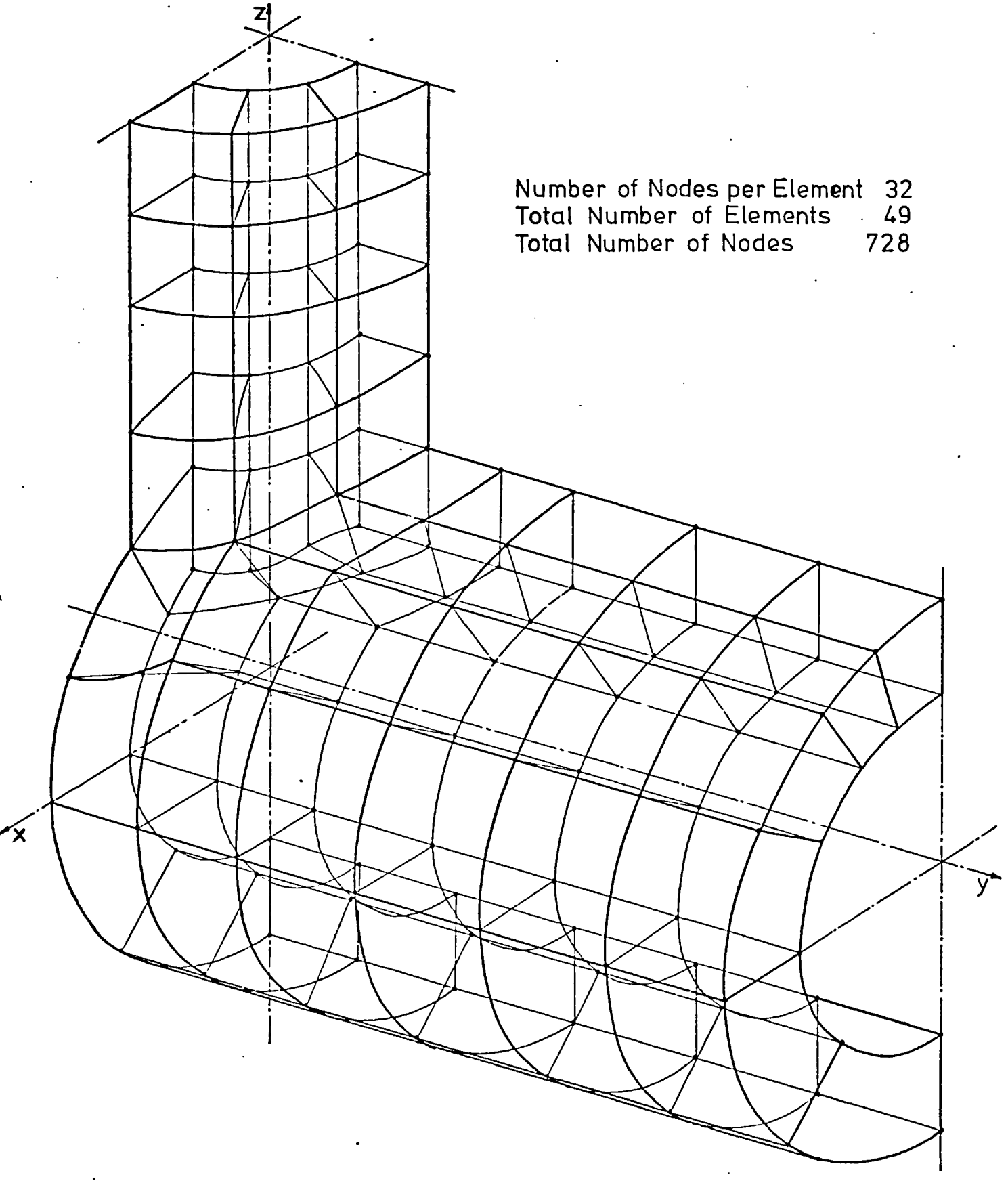

Fig. 4.3 TJUN1 case. 32 node element mesh idealization of a T-junction of thick walled cylinders

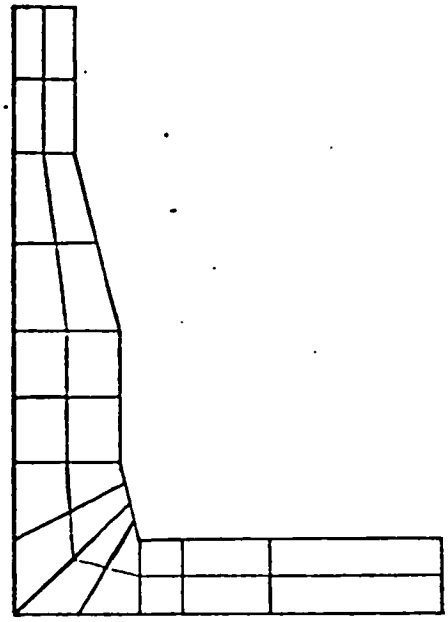

Fig. 4.4 Primary 2D mesh idealization for the section $\beta=0°$

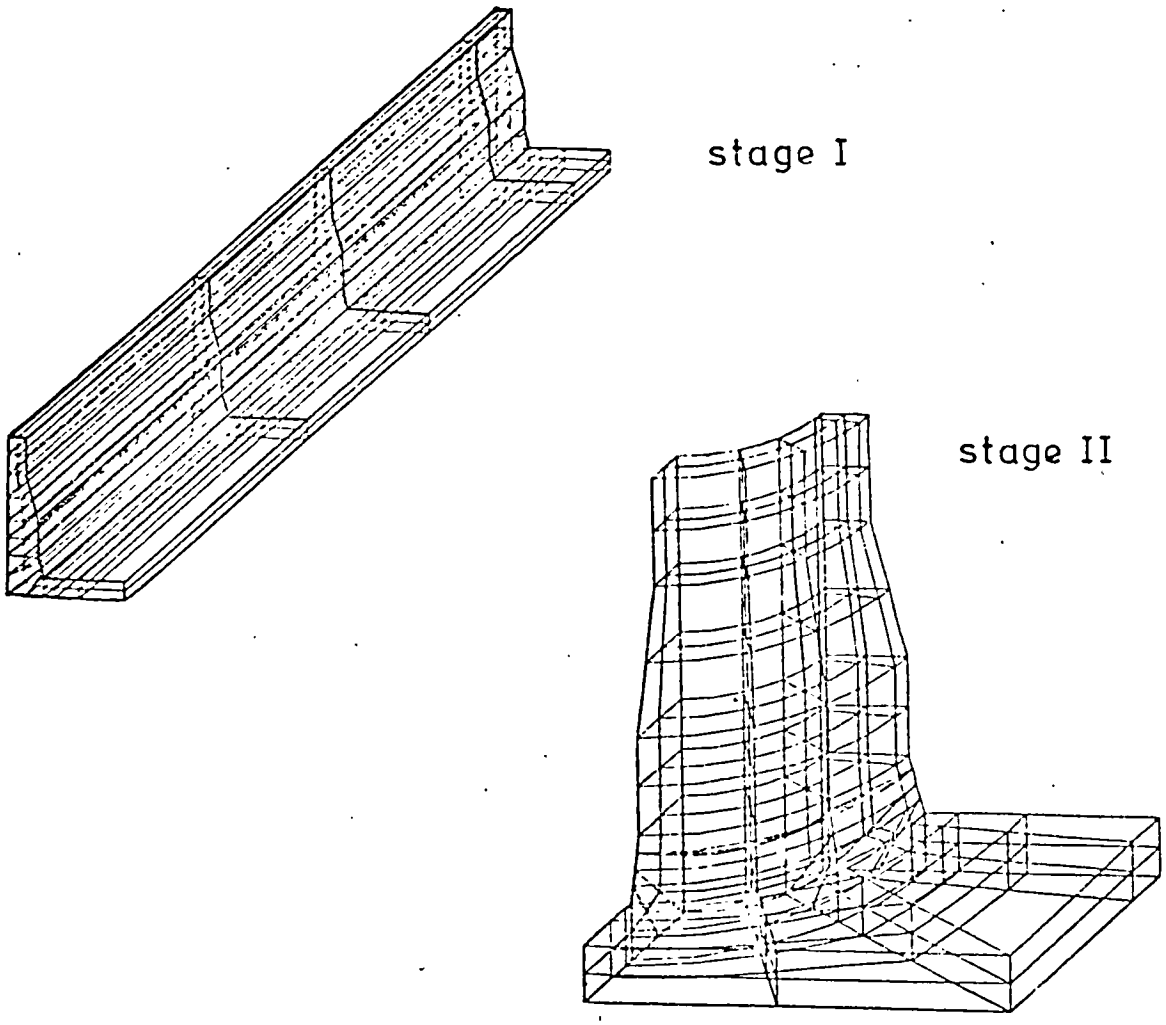

Fig. 4.5 Intermediate stages in the generation technique for the node element meshes

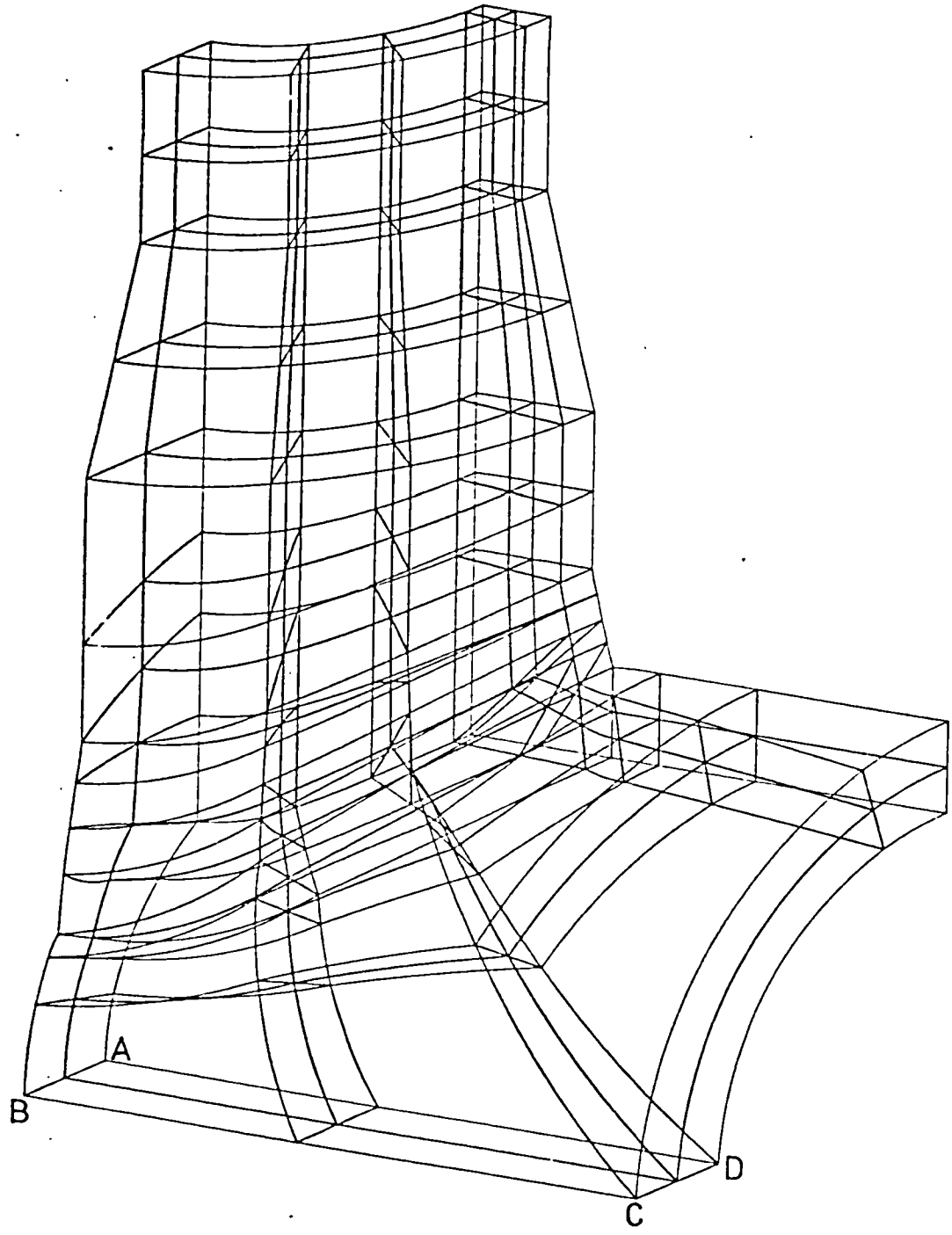

Fig. 4.6 TJUN2 case. 20 node element mesh idealization of a T-junction of thick walled cylinders

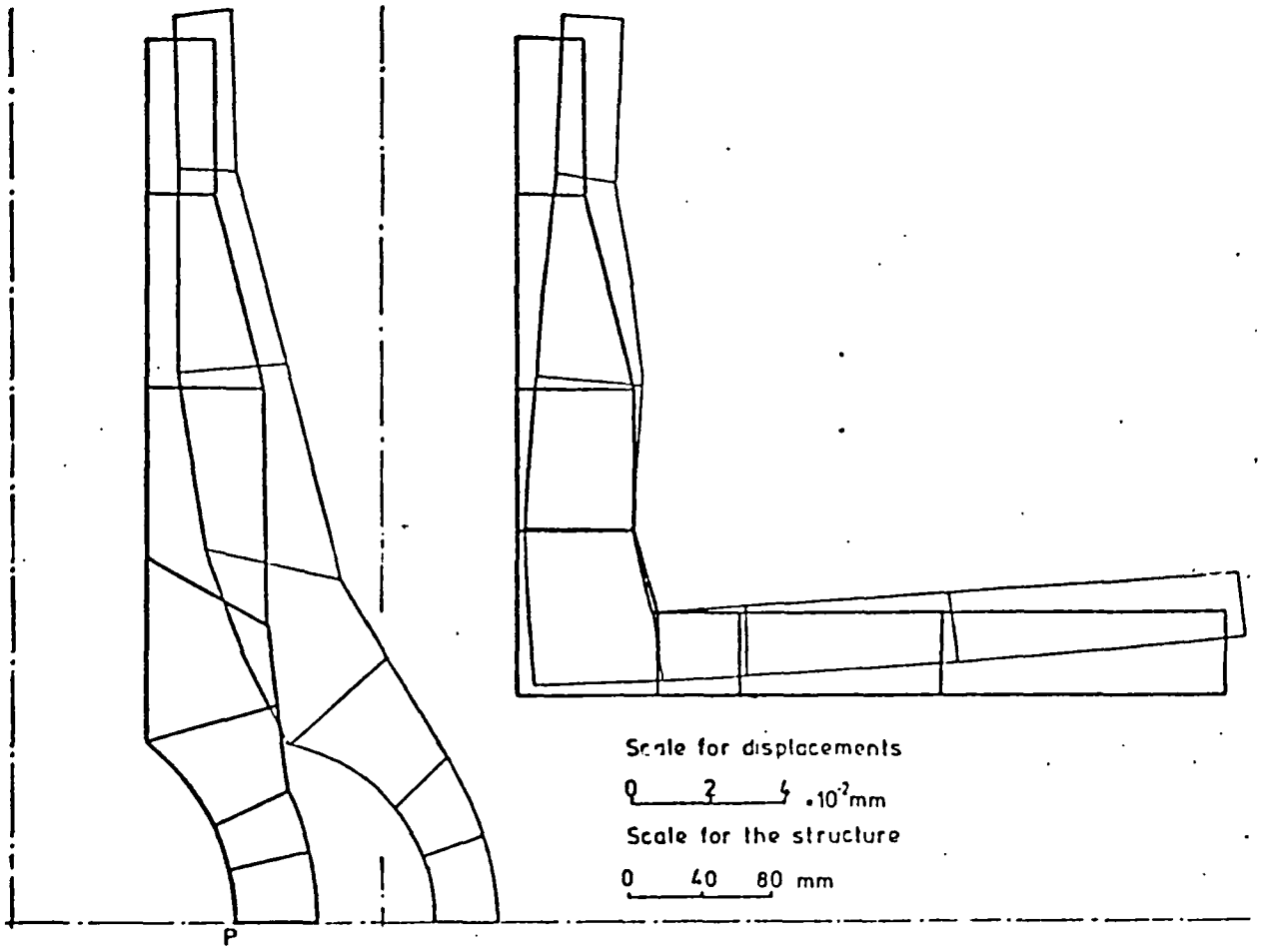

Fig. 4.7 Case TJUN2. Displacement solution for the cross sections $\beta = 0°$ and $\beta = 90°$

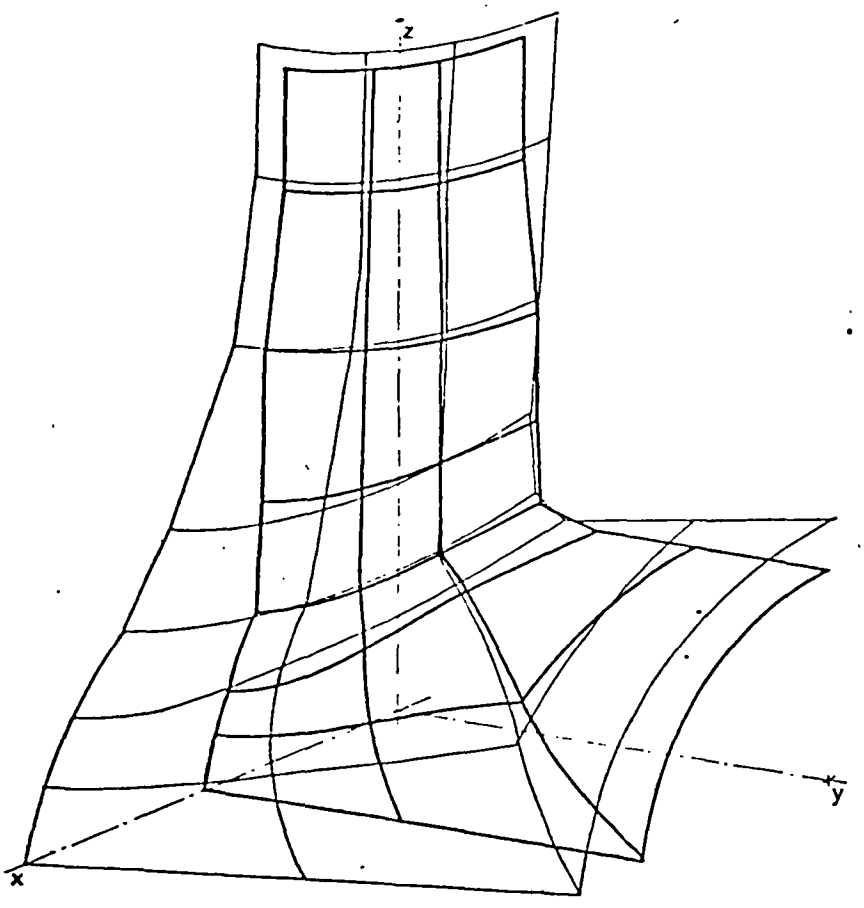

Fig. 4.8 Case TJUN2. Prespective view of the mid-surface of the structure and the correspondent displacement solution.

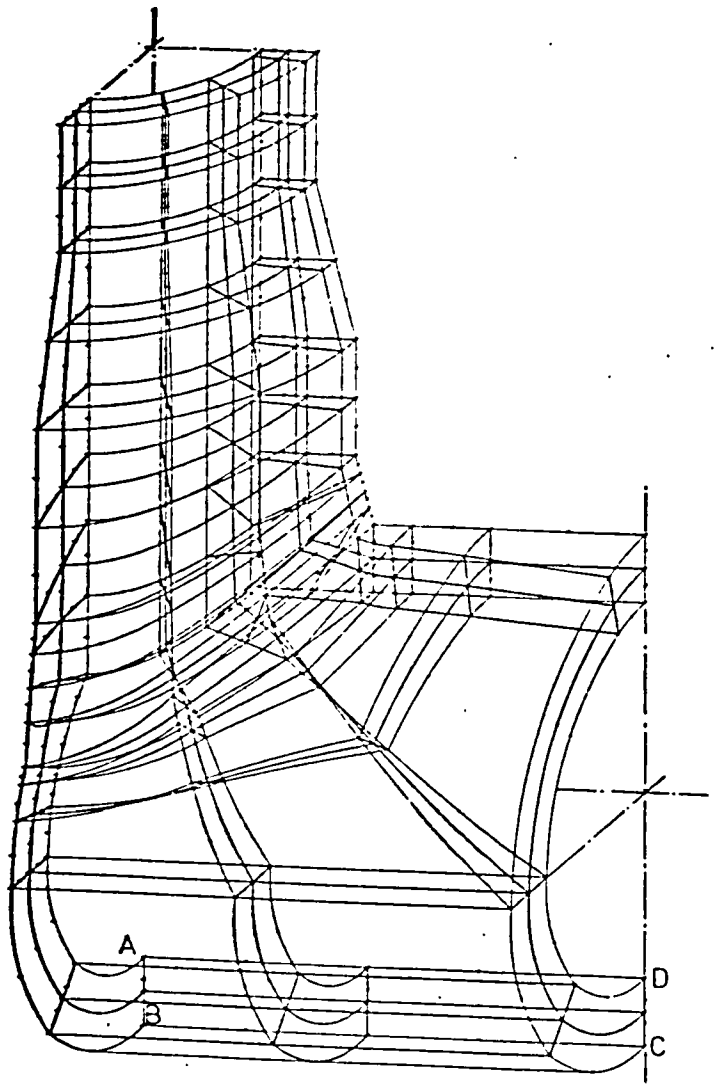

Fig. 4.9 Case TJUN3. Finite element mesh idealization of a T-junction of thick walled cylinders

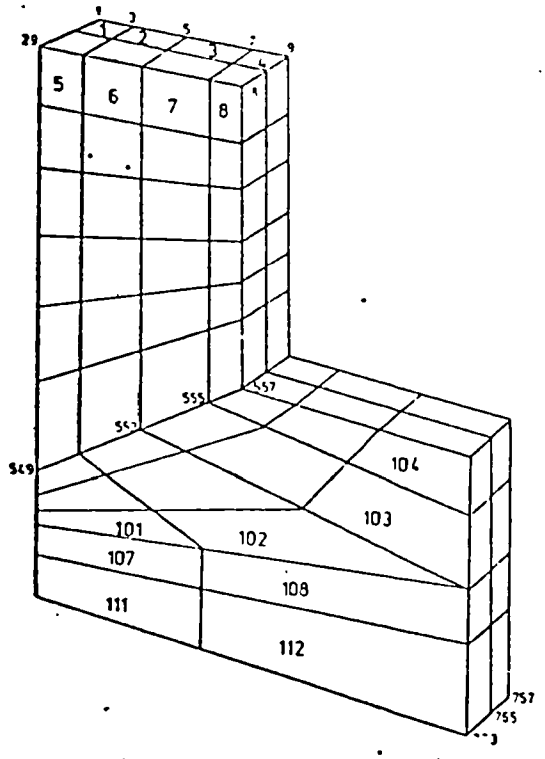

Fig. 4.10 Numbering scheme for elements and nodes of the mesh illustrated in figure 4.9

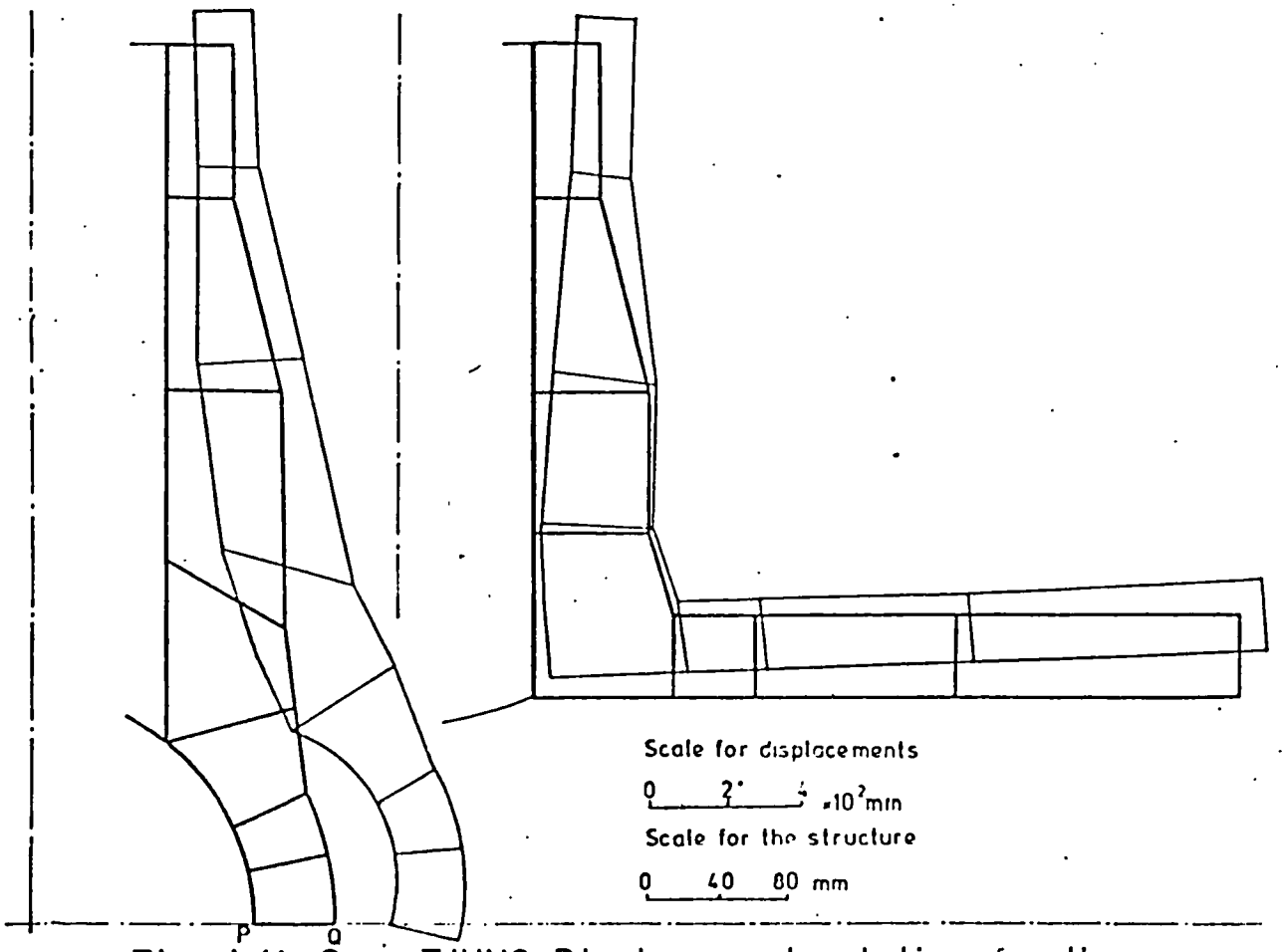

Fig. 4.11 Case TJUN3. Displacement solution for the cross sections $\beta=0°$ and $\beta=90°$

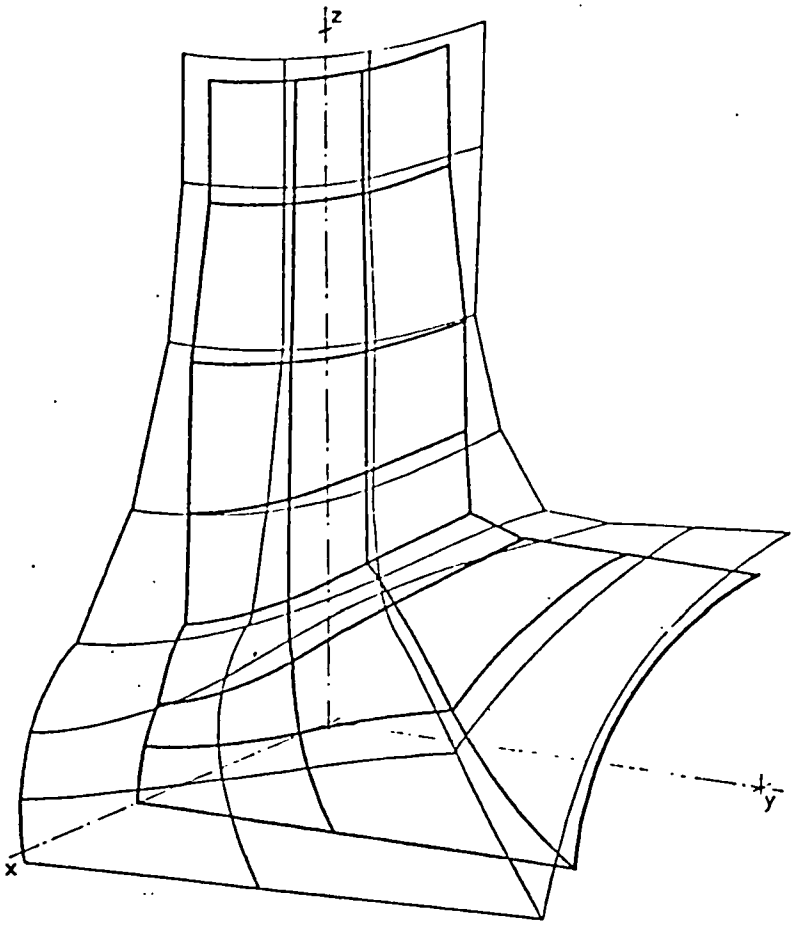

Fig. 4.12 Case TJUN3. Prespective view of the mid-surface of the structure and the correspondent displacement solution

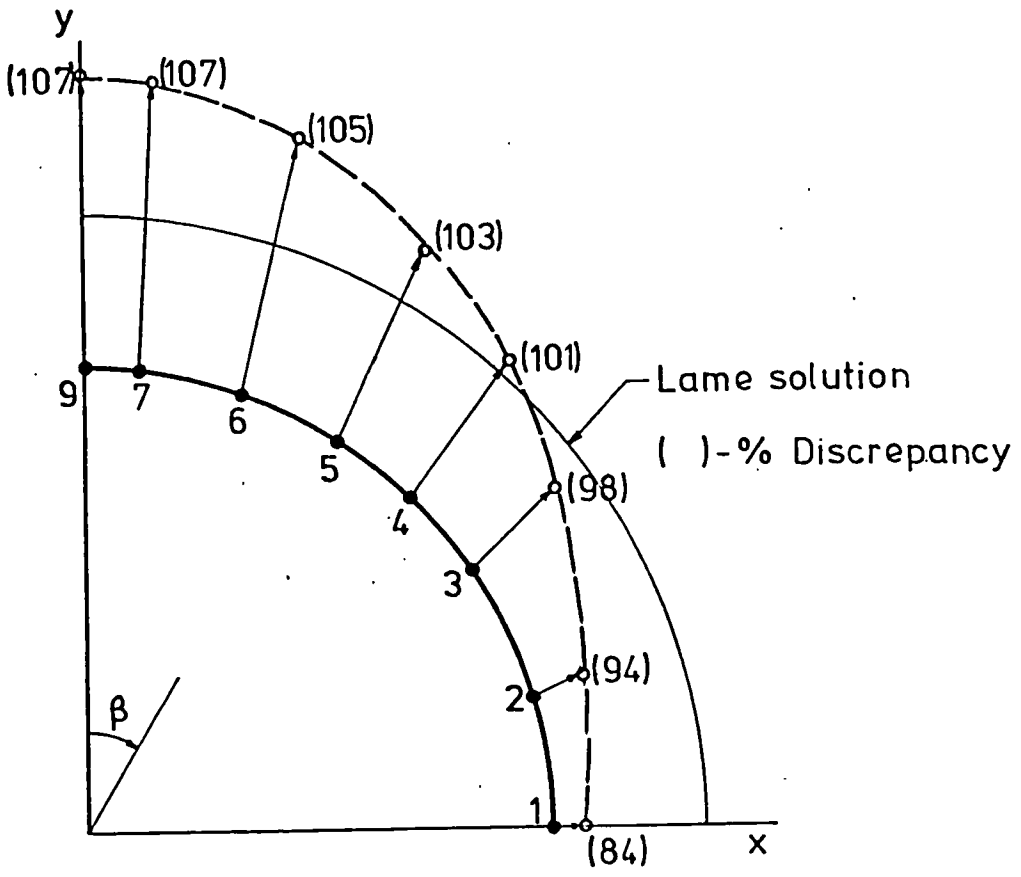

(a) Displacements of nodes in the inner surface

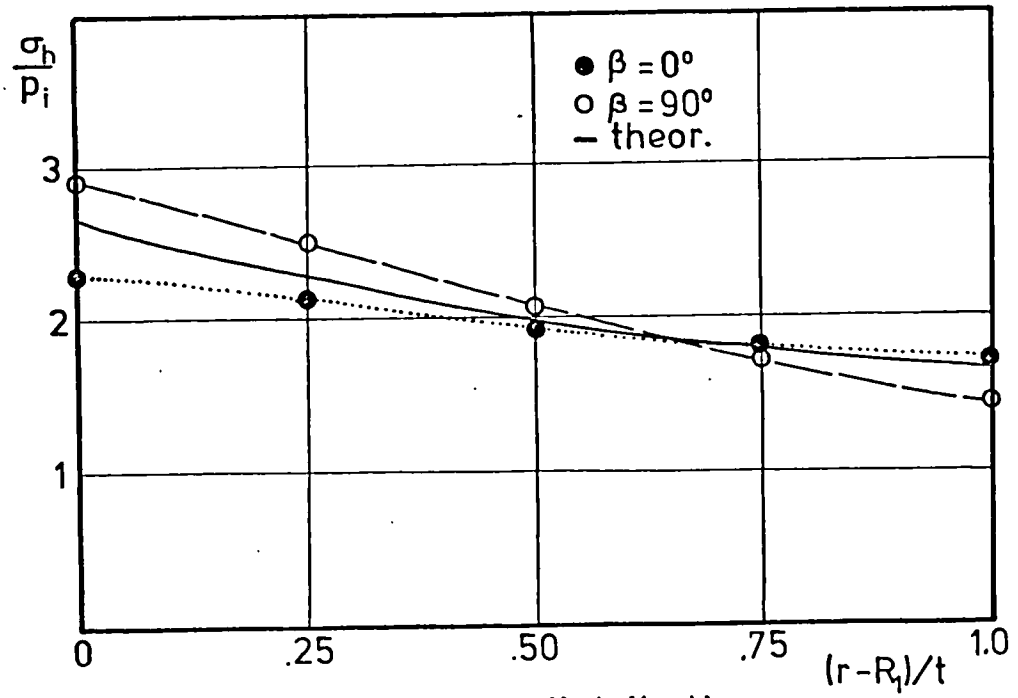

(b) Hoop stress distributions

Fig. 4.13 Ovalization effect in the end of the branch pipe

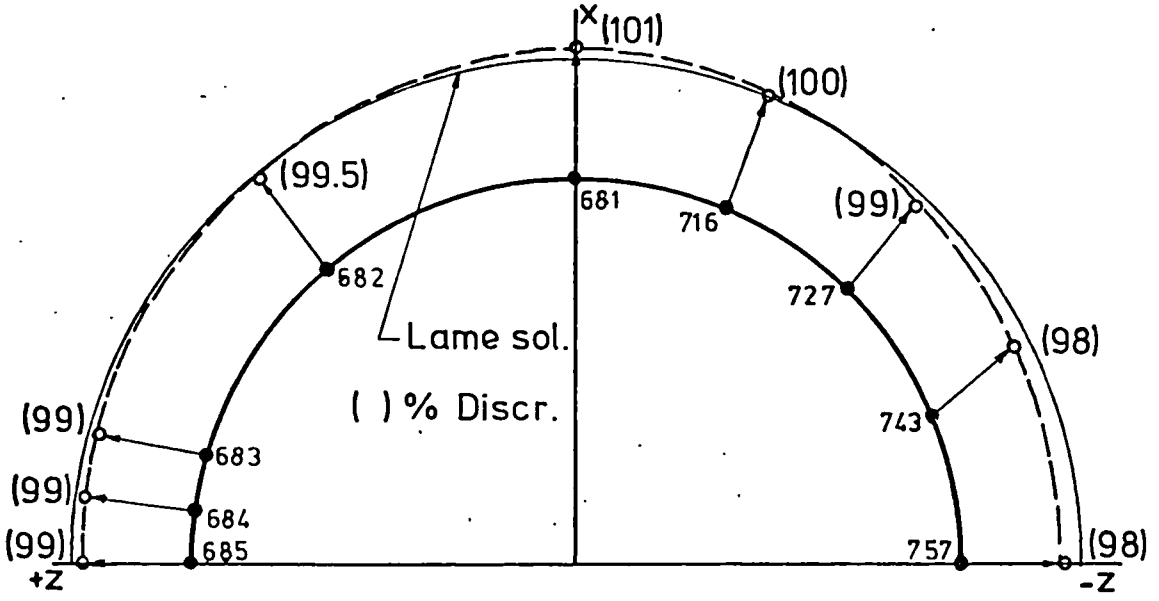

(a) Displacements of nodes in the inner surface

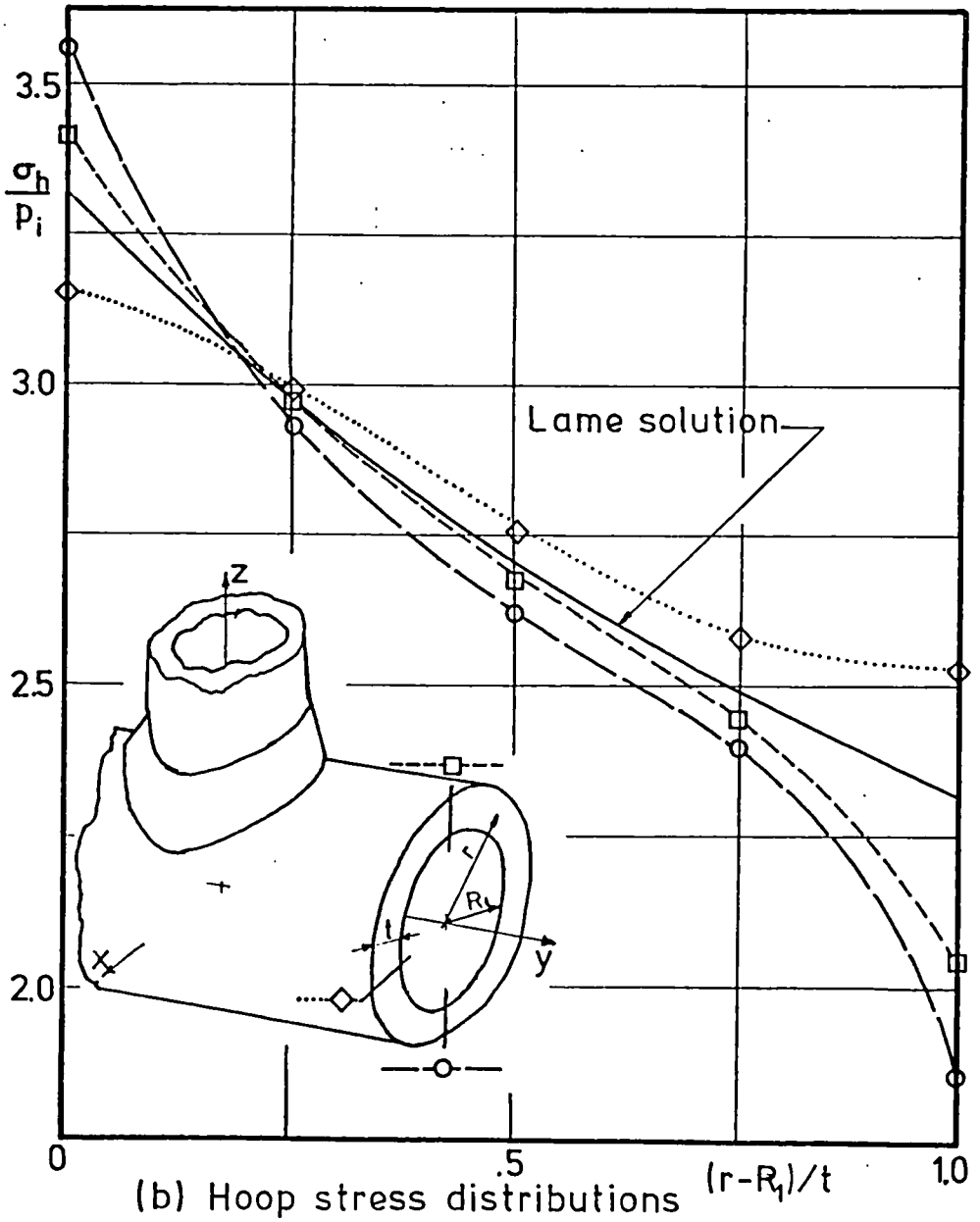

(b) Hoop stress distributions

Fig. 4.14 Ovalization effect in the end of the run pipe

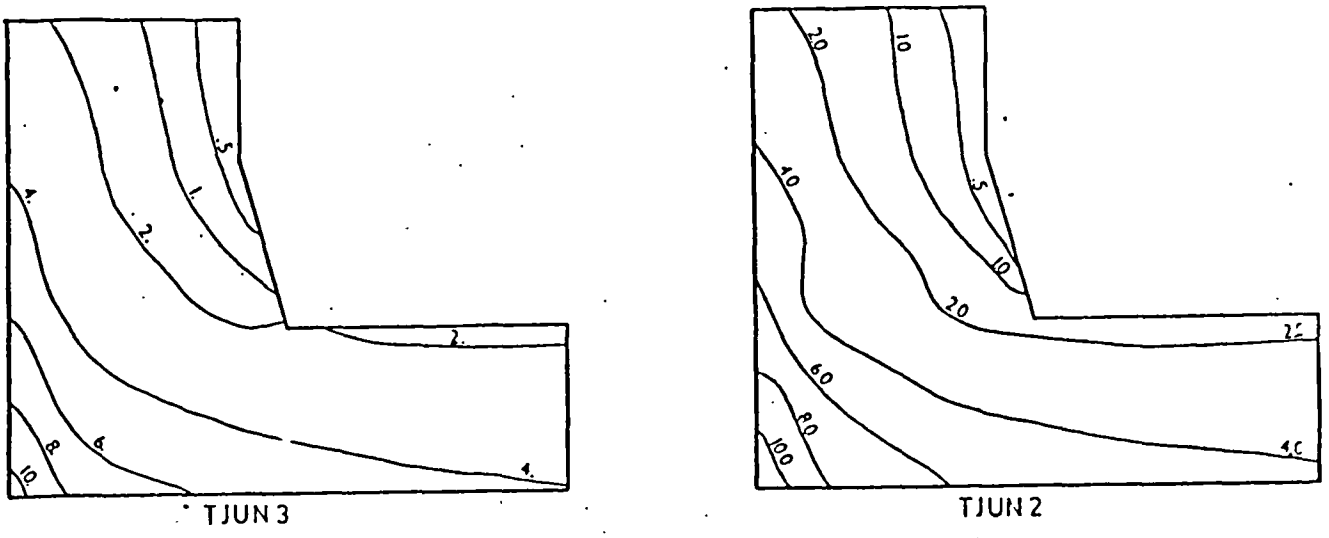

Fig. 4.15 Distribution of hoop stresses, σ_x / p_i, in the nozzle region for the cross sections $\beta = 0°$ of cases TJUN2 and TJUN3. The membrane stress in the run pipe is 2.75 times the internal pressure p_i

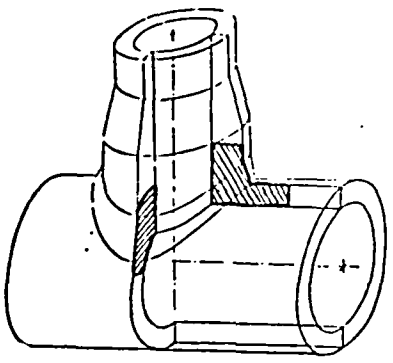

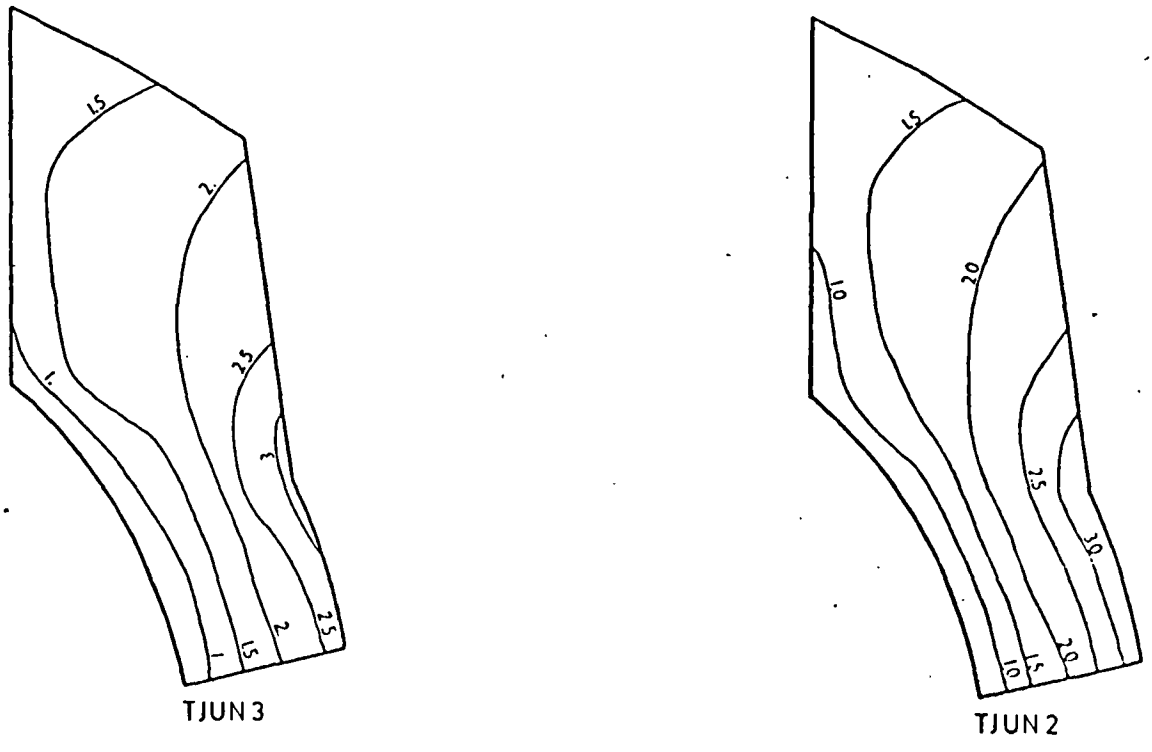

Fig. 4.16 Cases TJUN2 and TJUN3. Hoop stress distributions, σ_x / p_i, in the nozzle region for the cross sections $\beta = 90°$

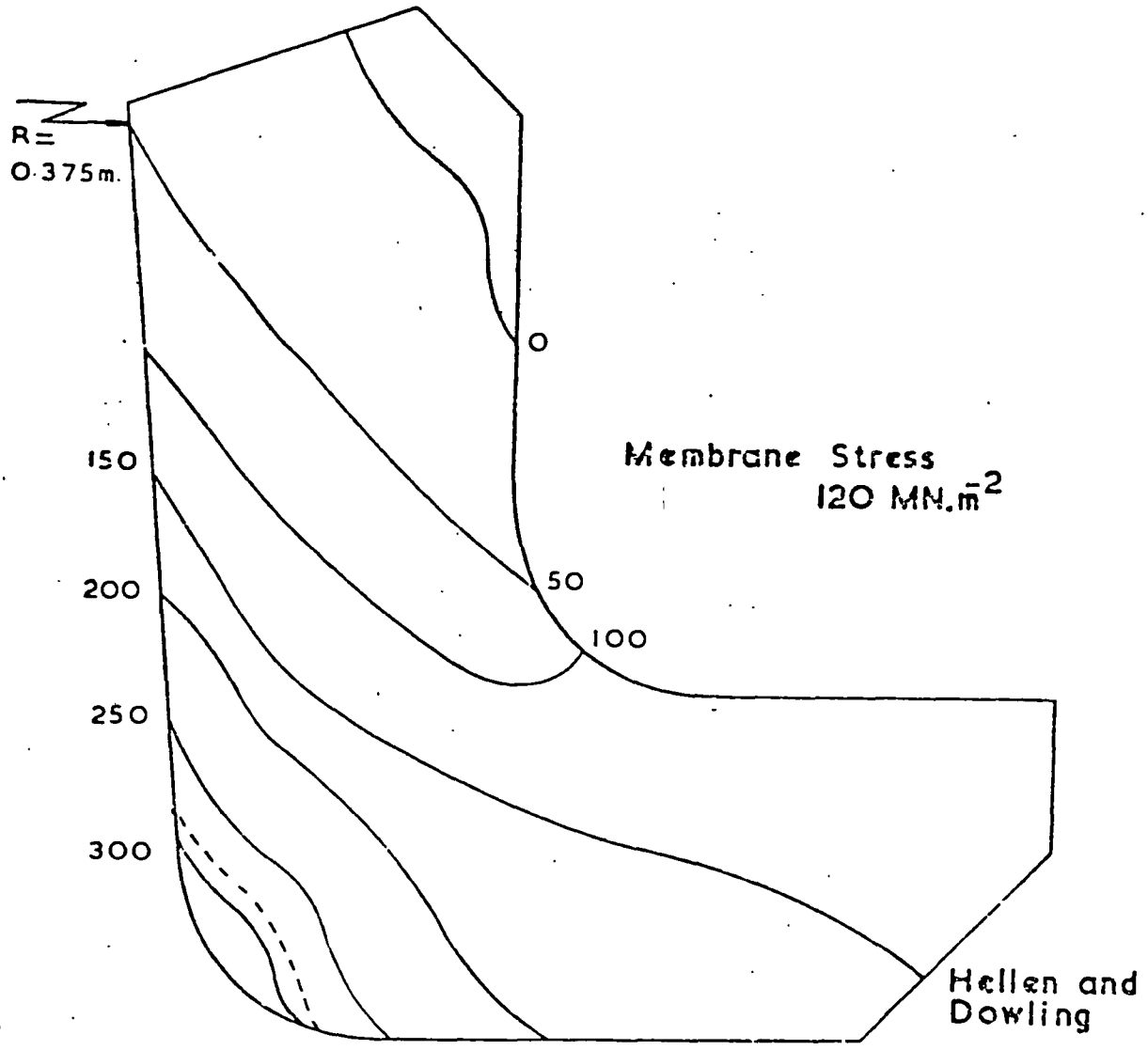

Fig. 4.17 Stress contour map of hoop stresses in the nozzle region of a BWR pressure vessel, Ref.(2)

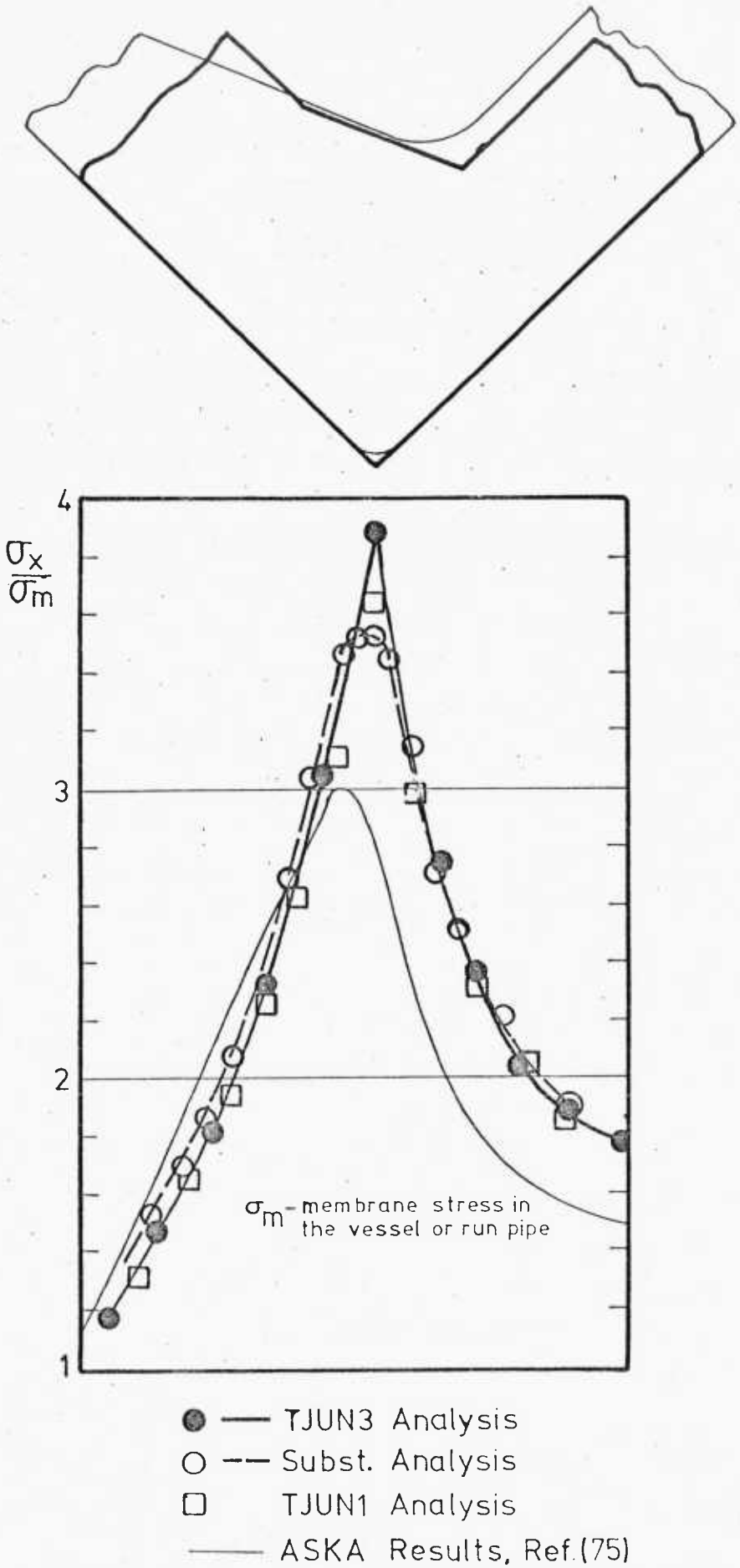

Fig. 4.18 Variation of hoop stresses along the inner surface in the crotch corner region

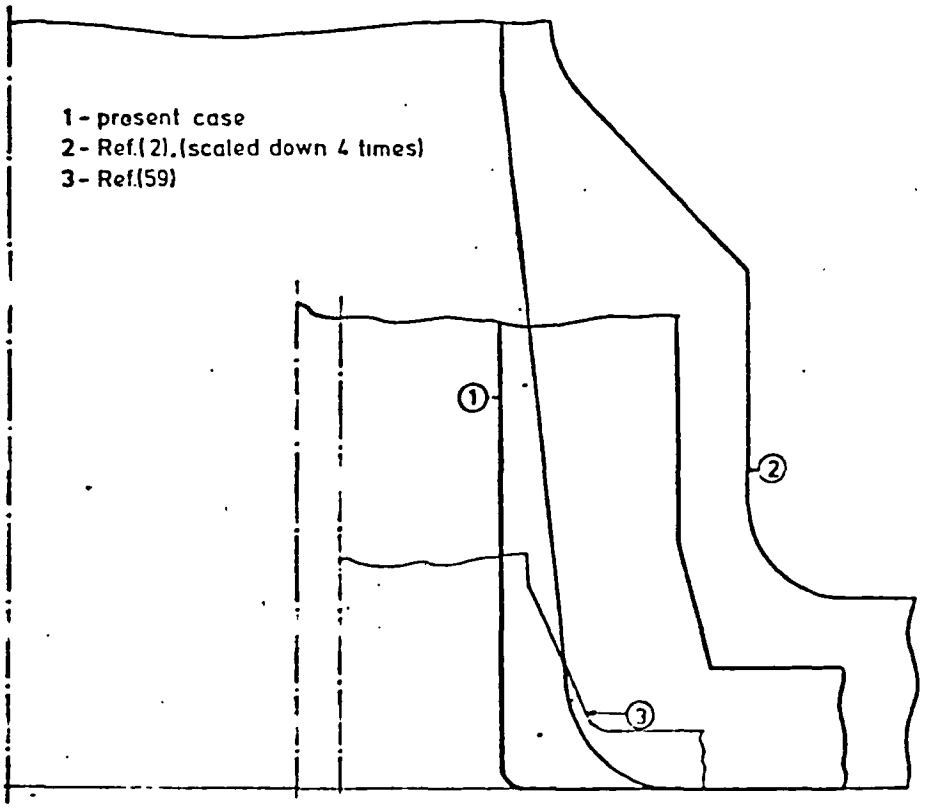

Fig. 4.19 Comparison of geometric details of three different nozzle configurations

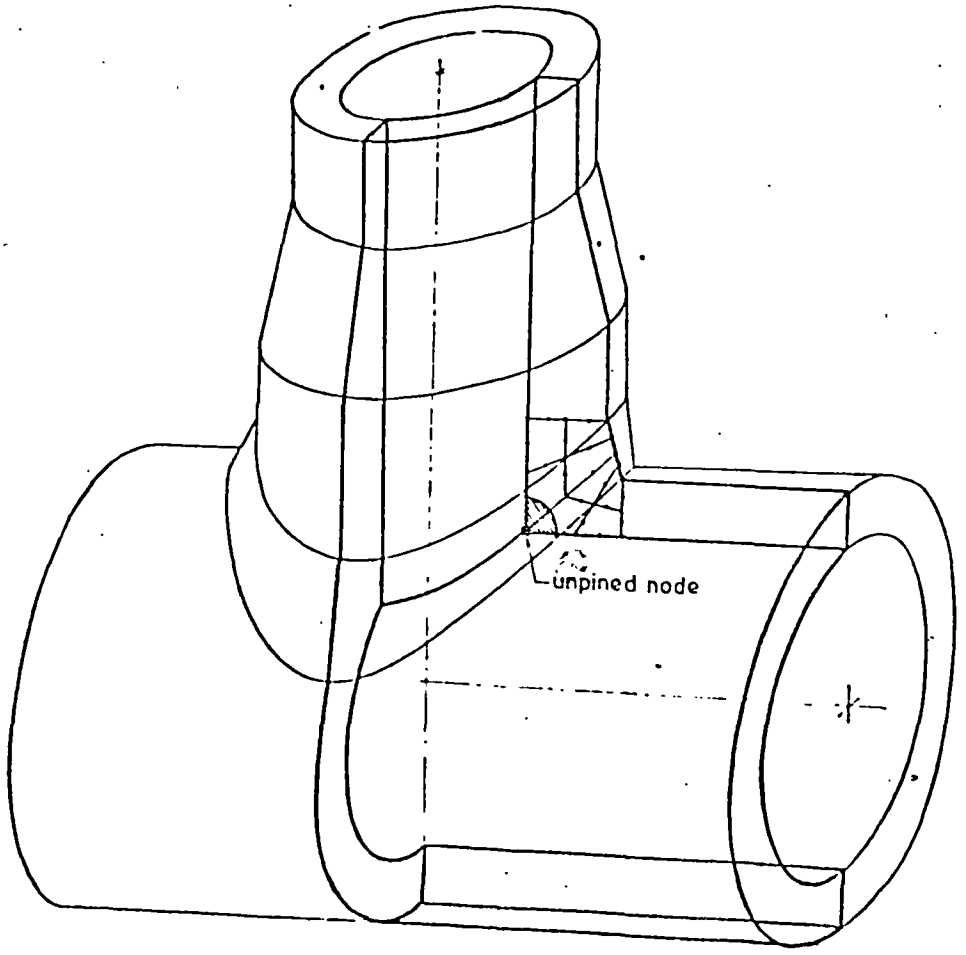

Fig. 4.20 Idealization of a corner crack using the TJUN3 finite element mesh

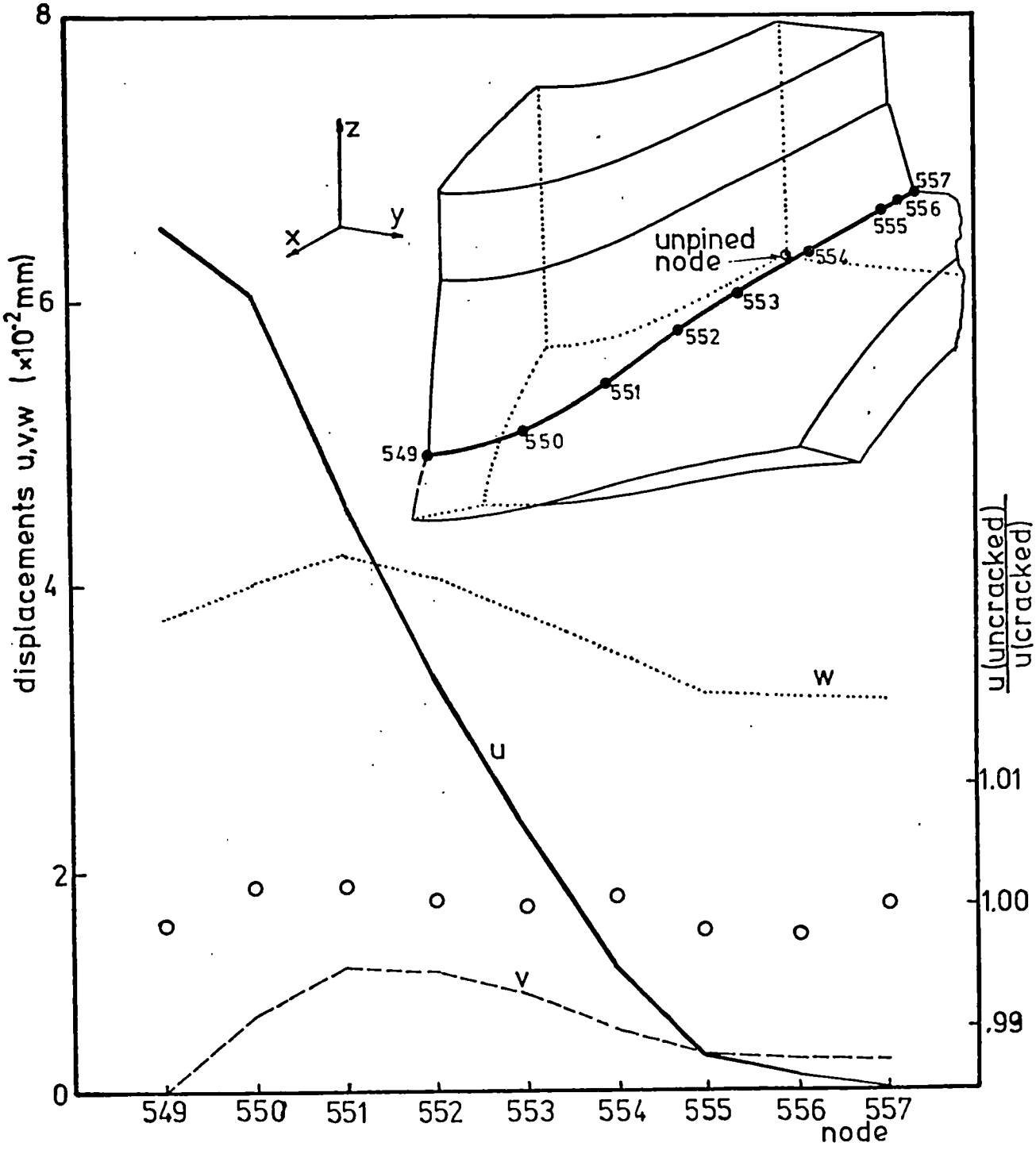

Fig. 4.21 Monitoring changes in nodal displacements when a crack is assumed to exist in the crotch region

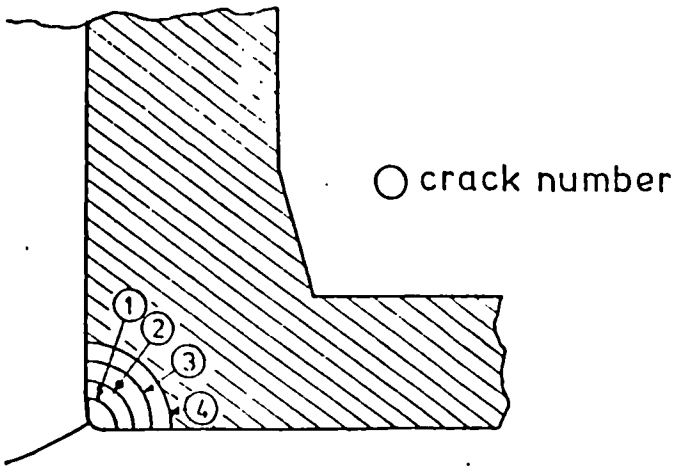

Fig. 4.22 Corner crack configurations 1, 2, 3 and 4

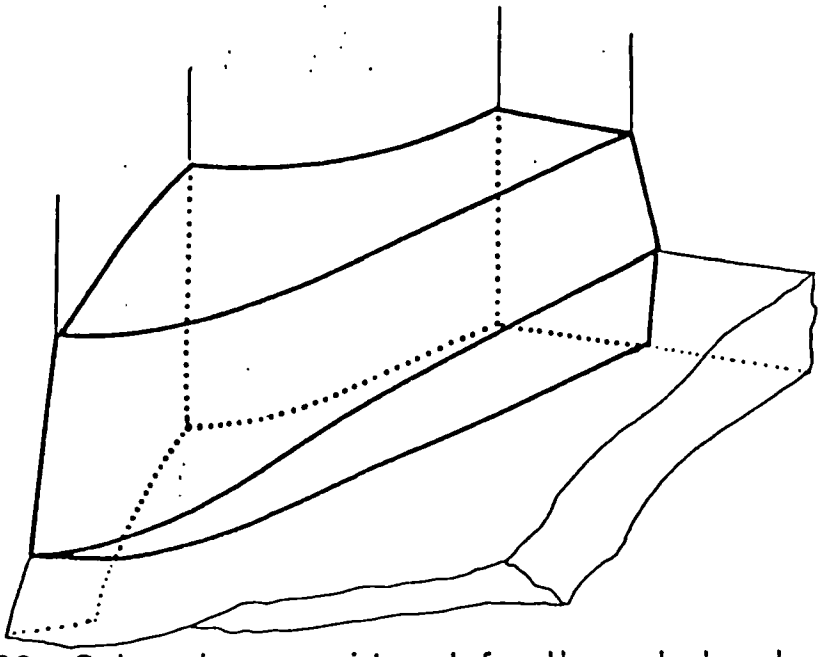

Fig. 4.23 Subregion considered for the substructuring scheme

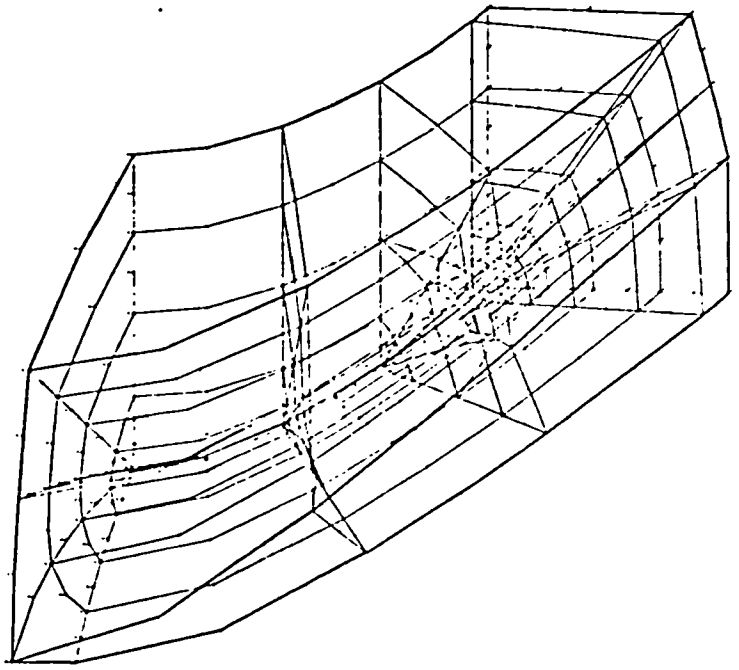

Fig. 4.24 Finite element mesh idealization of the subregion illustrated in figure 4.23

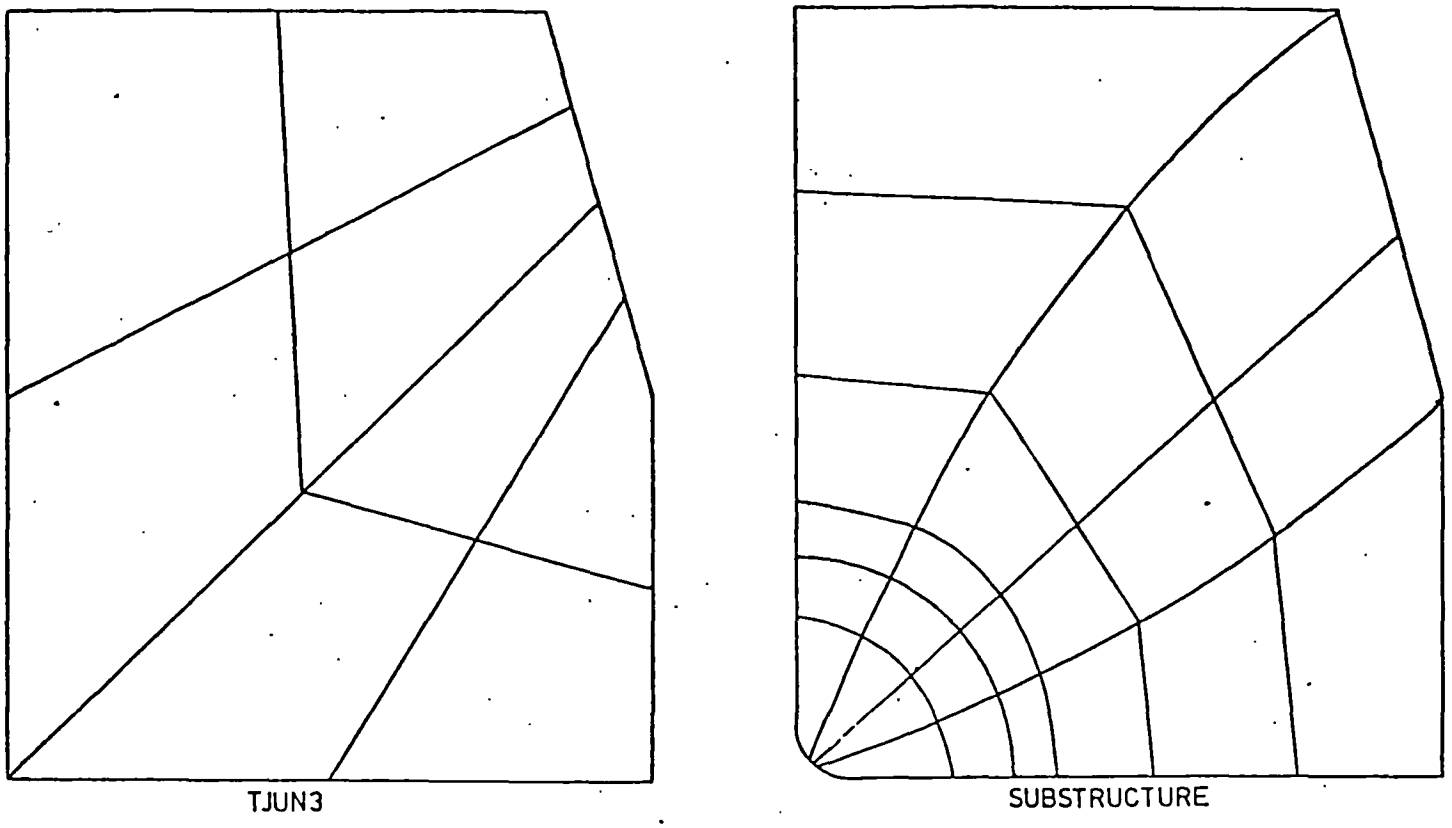

Fig. 4.25 Comparison of distribution of nodes in the nozzle region (cross section $\beta = 0°$)

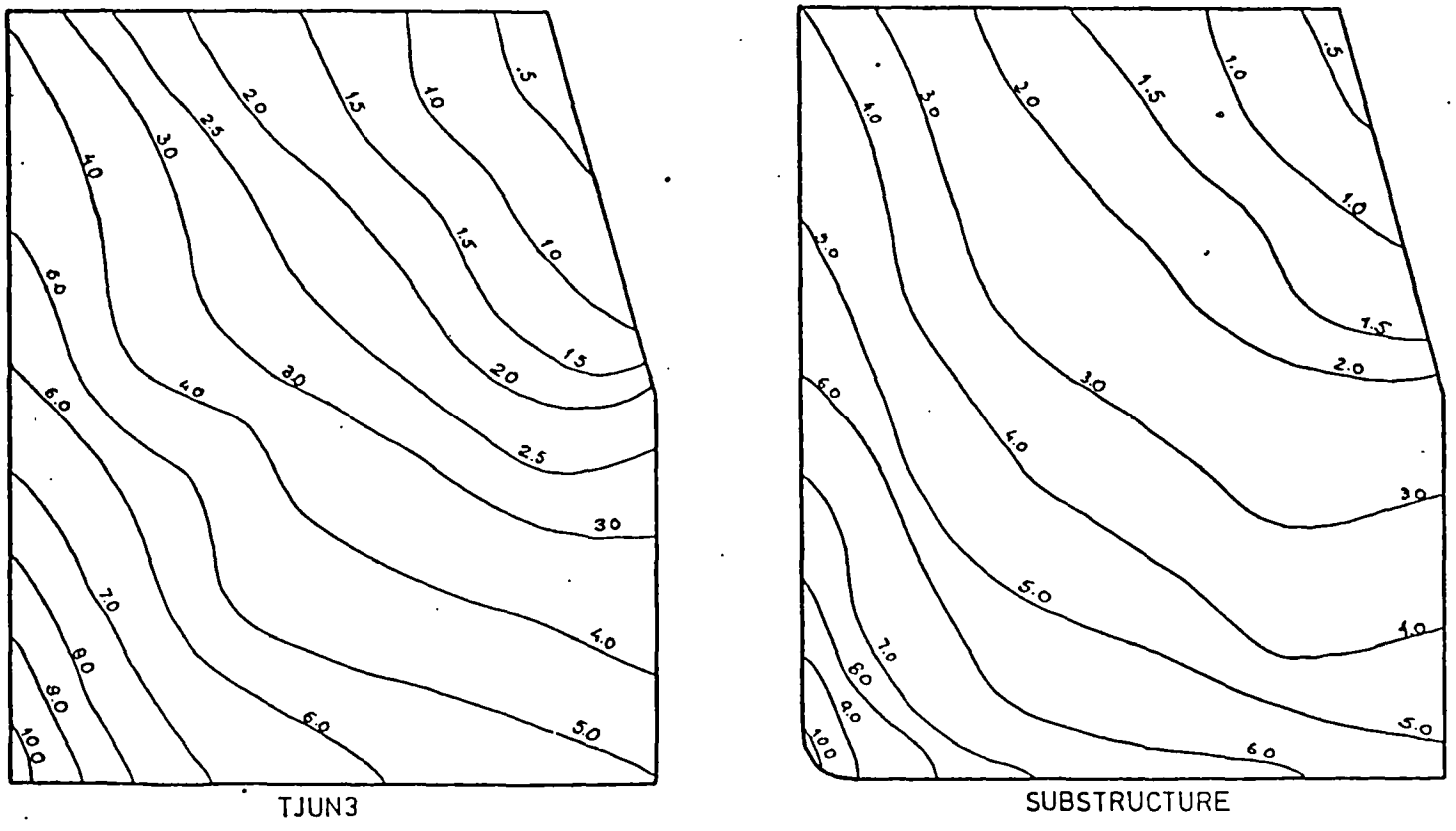

Fig. 4.26 TJUN3 and uncracked substructure analyses. Comparison of stress contour maps of hoop stresses, σ_x / p_i in the nozzle region (cross section $\beta = 0°$)

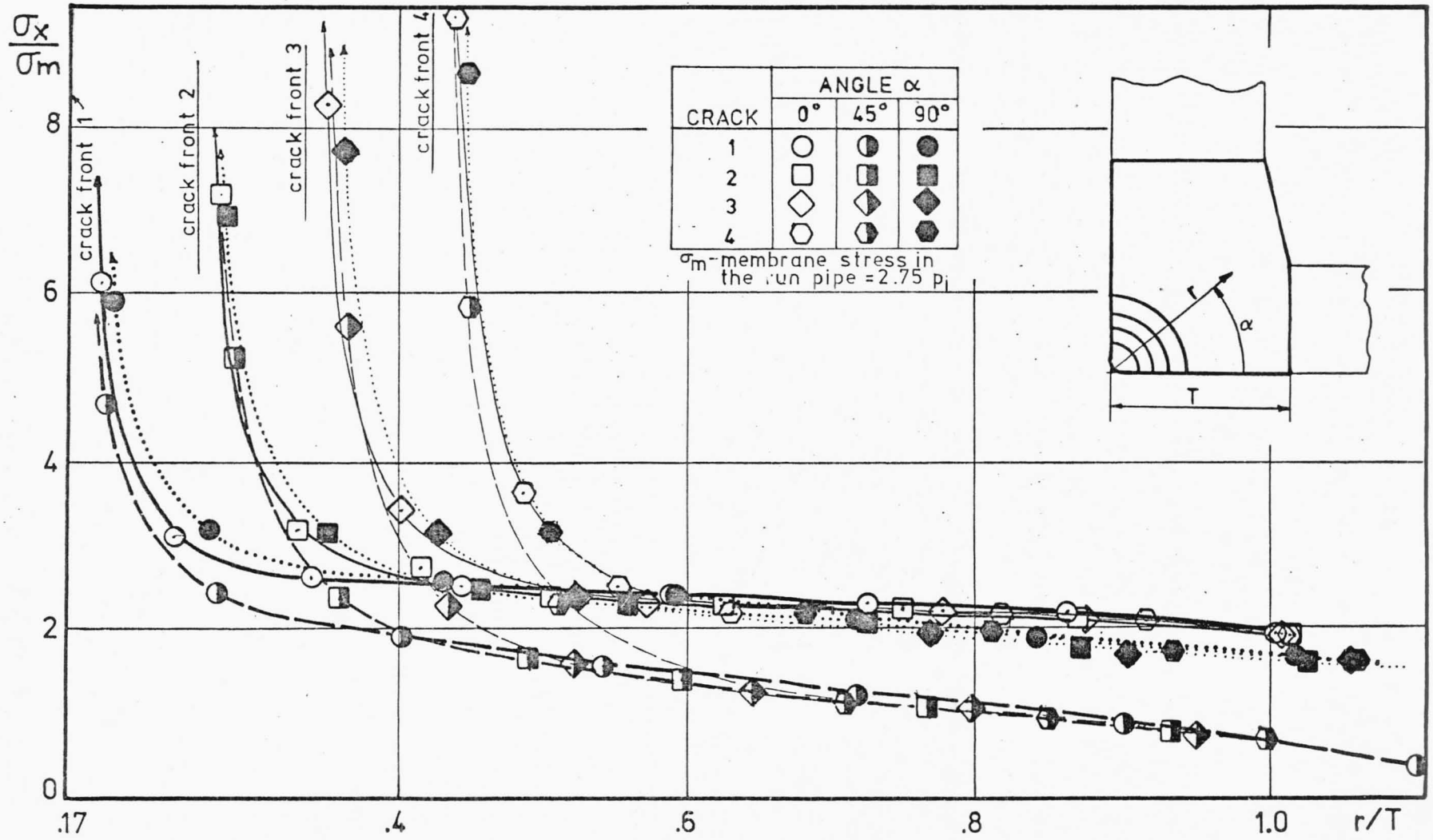

Fig. 4.27 σ_x stress distributions ahead of crack fronts 1, 2, 3 and 4

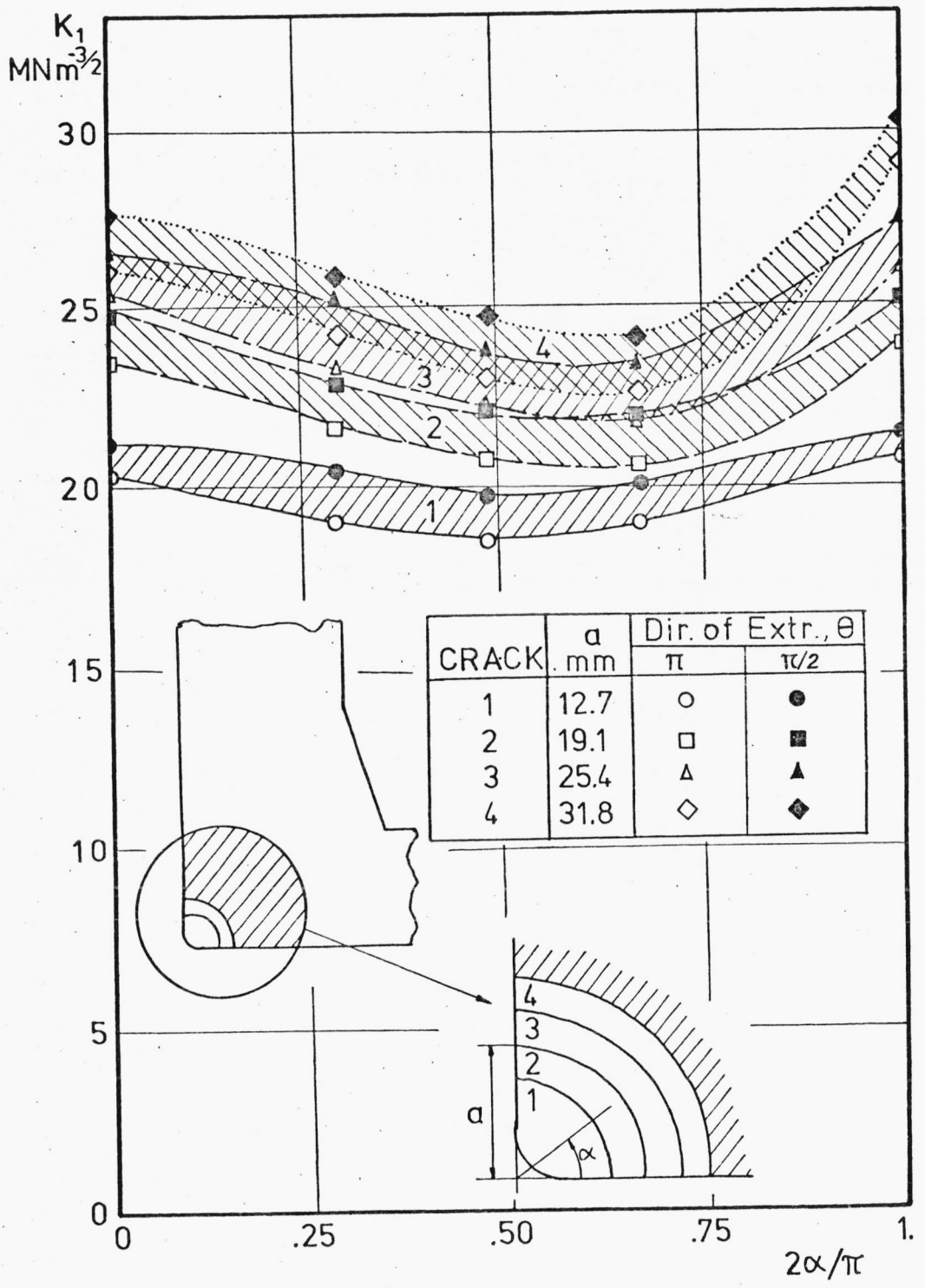

Fig. 4.28 Variation of K values along crack fronts 1, 2, 3 and 4

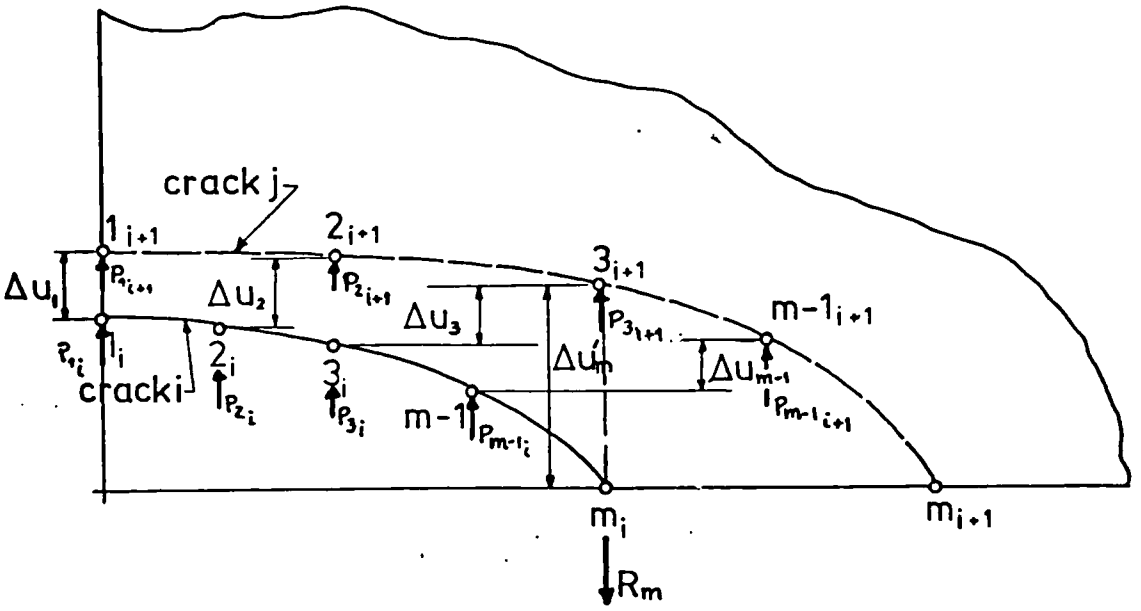

Fig. 4.29 Evaluation of K values by the Global Energy Method based on crack plane nodal point forces and displacements

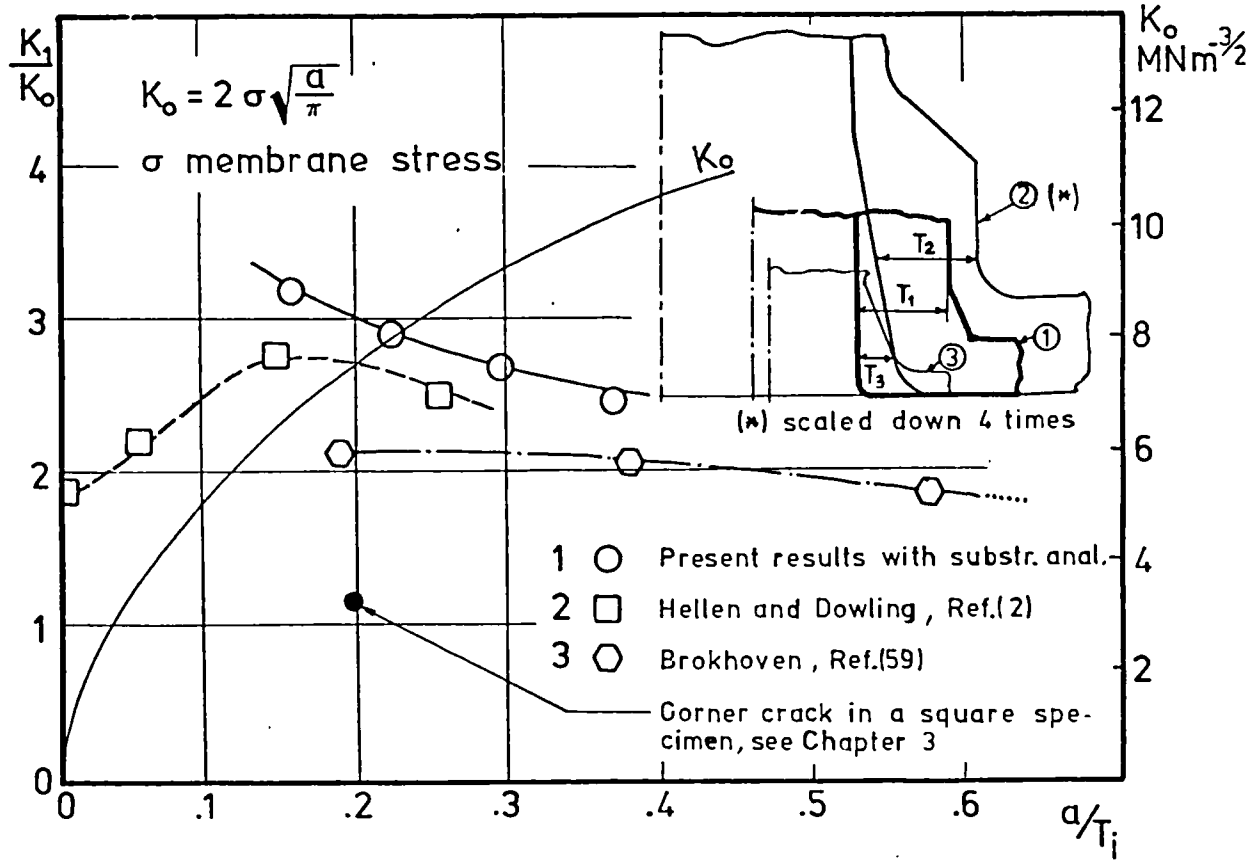

Fig. 4.30 Comparison of averaged K values of corner cracks emanating from the crotch corner of three different nozzle geometries